

A taxonomic monograph of the liphistiid spider genus *Heptathela*, endemic to Japanese islands

Xin Xu^{1,2}, Hirotsugu Ono³, Matjaž Kuntner^{2,4,5,6}, Fengxiang Liu², Daiqin Li⁷

1 College of Life Sciences, Hunan Normal University, 36 Lushan Road, Changsha 410081, Hunan Province, China **2** State Key Laboratory of Biocatalysis and Enzyme Engineering, Centre for Behavioural Ecology and Evolution, School of Life Sciences, Hubei University, 368 Youyi Road, Wuhan 430062, Hubei Province, China **3** Department of Zoology, National Museum of Nature and Science, 4-1-1 Amakubo, Tsukuba-shi, Ibaraki-ken, 305-0005, Japan **4** Evolutionary Zoology Laboratory, Department of Organisms and Ecosystems Research, National Institute of Biology, Ljubljana, Slovenia **5** Evolutionary Zoology Laboratory, Biological Institute ZRC SAZU, Ljubljana, Slovenia **6** Department of Entomology, National Museum of Natural History, Smithsonian Institution, Washington, DC, USA **7** Department of Biological Sciences, National University of Singapore, 14 Science Drive 4, 117543, Singapore

Corresponding authors: Xin Xu (xuxin_09@163.com); Daiqin Li (dbslidq@nus.edu.sg)

Academic editor: Jeremy Miller | Received 13 March 2019 | Accepted 5 September 2019 | Published 11 November 2019

<http://zoobank.org/B995C056-97EC-41A4-9012-B58F9D3AFDC1>

Citation: Xu X, Ono H, Kuntner M, Liu F, Li D (2019) A taxonomic monograph of the liphistiid spider genus *Heptathela*, endemic to Japanese islands. ZooKeys 888: 1–50. <https://doi.org/10.3897/zookeys.888.34494>

Abstract

Among the eight extant genera of primitively segmented spiders, family Liphistiidae, two are confined to East Asian islands, *Heptathela* Kishida, 1923 and *Ryuthela* Haupt, 1983. In this paper, a taxonomic revision of the genus *Heptathela* (Heptathelinae) from Kyushu and Ryukyu archipelago, Japan is provided. This study follows a multi-tier species delimitation strategy within an integrative taxonomic framework that is presented in a parallel paper, in which diagnosable lineages are considered as valid species. There, the initial hypothesis of species diversity (19) based on classical morphological diagnoses is tested with multiple species delimitation methods aimed at resolving conflict in data. This revision follows those analyses that converge on the species diversity of 20, which includes a pair of cryptic species that would have been undetected with morphology alone. After this revision, eight previously described species remain valid, two junior synonyms are proposed, and 12 new *Heptathela* species are described based on diagnostic evidence. To ease identification and to hint at putative evolutionary units, *Heptathela* is divided into three groups. The Kyushu group contains *H. higoensis* Haupt, 1983, *H. kikuyai* Ono, 1998, *H. kimurai* (Kishida, 1920), and *H. yakushimaensis* Ono, 1998; the Amami group contains *H. amamiensis* Haupt, 1983, *H. kanenoi* Ono, 1996, *H. kojima* **sp. nov.**, *H. sumiyo* **sp. nov.**, and *H. uken* **sp. nov.**; and the Ok-

inawa group contains *H. yanbaruensis* Haupt, 1983, *H. aba* sp. nov., *H. gayozan* sp. nov., *H. kubayama* sp. nov., *H. mae* sp. nov., *H. otoa* sp. nov., *H. shuri* sp. nov., *H. tokashiki* sp. nov., *H. unten* sp. nov., and *H. crypta* sp. nov. *Heptathela helios* Tanikawa & Miyashita, 2014 is not assigned to a species group. A combination of diagnostic tools augments the morphological diagnoses that, in isolation, would be prone to error in morphologically challenging groups of organisms.

Keywords

Heptathelinae, island endemism, Kyushu, Ryukyu archipelago, species delimitation, trapdoor spiders

Introduction

The spider family Liphistiidae is the sole extant lineage within the ancient suborder Mesothelae known to possess a combination of plesiomorphic traits, for example, abdominal tergites (Fig. 1A), as well as spinnerets that have a mid-venter position (Fig. 1B). Compared to its sister clade that comprises all other spider families, liphistiids are genus- and species-poor, containing eight genera restricted to Southeast and East Asia (Xu et al. 2015a, b; World Spider Catalog 2019). Only two of these genera are purely insular, both being restricted to Japanese islands, and we focus here on the taxonomy of the nominal genus *Heptathela* Kishida, 1923 (Heptathelinae) (Fig. 1A, B).

Taxonomic limits of *Heptathela* were recently redefined (Xu et al. 2015b) as its taxonomic history that we briefly summarise here had been inconclusive. Kishida (1923) named the genus *Heptathela* for *Liphistius kimurai* Kishida, 1920 because its female had seven spinnerets, unlike the expected eight as in other species of *Liphistius* Schiödte, 1849. Although originally placed in Liphistiidae, *Heptathela* was once considered a family rank taxon, Heptathelidae (Petrunkevitch, 1939), again stressing the spinneret number difference with Liphistiidae. Only later, it was clarified that the spinneret number is variable among *Heptathela* species and not suitable for high level taxonomic diagnosis, even if it is stable in *Liphistius* (Yoshikura 1955; Haupt 1983, 2003; Xu et al. 2015a, b). Nonetheless, the genus name remained to be used for many “non-*Liphistius*” liphistiid lineages until 1983 when the second genus, *Ryuthela* Haupt, 1983, was added to the family Heptathelidae (Haupt 1983). This major clade was subsequently stabilised as the liphistiid subfamily Heptathelinae (Ono 2000; Xu et al. 2015b), but with several additional genera. Both Ono (2000) and Haupt (2003) relimited *Heptathela* to apply only to the species inhabiting the Japanese island Kyushu as well as the northern Ryukyu archipelago. These authors agreed that the species from China and Vietnam belonged to distinct genera. They disagreed, however, in the details. While Ono (2000) placed the mainland heptathelines into three genera (*Abcathela*, *Vinathela*, and *Songthela*), Haupt (2003) rejected *Abcathela* and *Vinathela*, erected instead *Nanthela* and *Sinothela*, and proposed *Songthela* as a synonym of the latter. To complete the full circle of this complex taxonomic history, Schwendinger and Ono (2011) reverted to only two heptatheline genera. According to these authors, all

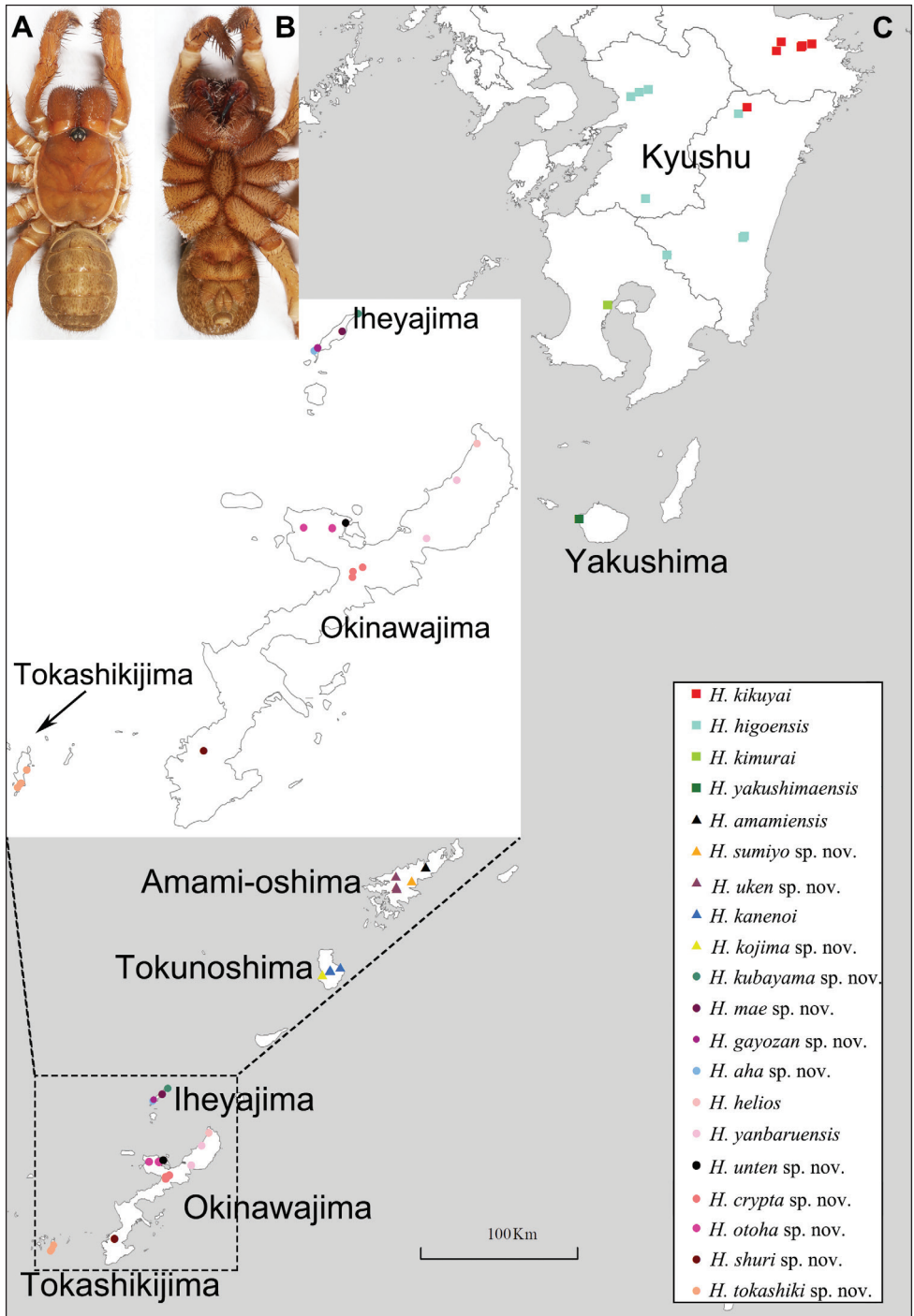


Figure 1. General somatic morphology of *Heptathela kimurai* (Kishida, 1920) **A** dorsal view **B** ventral view and map showing the sampling localities of *Heptathela* specimens from Kyushu to central Ryukyus (**C**).

Chinese, Vietnamese and some Japanese species (not *Ryuthela*) were within *Heptathela* sensu lato, and the names *Nanthela* and *Sinothela* became its synonyms. All the above hypotheses were based exclusively on morphology. Using combined molecular and morphological data, we recently showed *Heptathela* sensu lato to be paraphyletic, and redefined the genus to comprise only the species from Kyushu and from the Ryukyus (Xu et al. 2015a, b).

Heptathela therefore does not occur in continental Asia (Xu et al. 2015b); instead, its species are endemic to Kyushu (six known species) as well as the northern and central islands of the Ryukyu archipelago (Tanikawa and Miyashita 2014; World Spider Catalog 2019), two are known from Amamioshima and Tokunoshima, and another two from Okinawajima. As emphasised in the above overview, most known *Heptathela* species have been delimited solely morphologically. The study by Tanikawa and Miyashita (2014) is an exception as they discovered one species, *H. helios* Tanikawa & Miyashita, 2014, and delimited *H. yanbaruensis* Haupt, 1983 and *H. helios* from Okinawa using genetic distances. Our recent molecular data used to test biogeographical hypotheses within East Asian margins, on the other hand, suggested that over ten *Heptathela* species exist on these islands (Xu et al. 2016).

We follow this evidence with a thorough taxonomic revision of *Heptathela*. As is the case in other liphistiids, *Heptathela* females usually lack clear morphologically diagnostic characters and furthermore exhibit considerable intraspecific variation. While males are more readily diagnosable morphologically, they are very rarely collected (Haupt 2003; Schwendinger and Ono 2011; Tanikawa 2013; Tanikawa and Miyashita 2014; Xu et al. 2015c, 2017). A purely morphological revision would thus be preliminary, or even erroneous, and be an underestimation of true species diversity (Xu et al. 2017). Therefore, an integrative taxonomic revision of this genus is a preferred alternative. We first establish species hypotheses for all available *Heptathela* specimens using morphological diagnoses. We then use the evidence from a range of molecular species delimitation analyses from a parallel study (Xu et al. 2019) to test and further diagnose these species, and discuss the benefits of such taxonomic approaches.

Materials and methods

Specimen acquisition

Our original sampling, performed in the entire *Heptathela* range from Kyushu to the central Ryukyu archipelago, relied on the type locality information of each known *Heptathela* species, but also involved previously unexplored areas, focusing particularly on roadside habitats (Figs 1C, 2; for details of all specimens used in this study see Suppl. material 1: Table S1). We collected all specimens alive for initial check of their maturity status. We then fixed mature spiders in ethanol but retained all subadults alive to be reared to maturation. All mature specimens were subsequently preserved in 80% ethanol after being removed the right set of legs for the cryo-collection.

Morphological examination

Specimens were morphologically examined under an Olympus SZX16 stereomicroscope and an Olympus BX51 compound microscope. Their genitalia were cleared in boiling 10% KOH for a few minutes to dissolve soft tissues. Unless noted otherwise, left palps were imaged. All measurements are reported in millimetres. Leg and palp measurements are given in the following order: total length (femur + patella + tibia + metatarsus + tarsus). The value ranges for cheliceral groove denticles, spinnerets and measurements in taxonomic descriptions are based on all the examined specimens.

Taxonomic descriptions using morphological characteristics follow our established methodology (Xu et al. 2015c, 2017). We use the following abbreviations throughout:

ALE	anterior lateral eyes,	E	embolus,
AME	anterior median eyes,	OL	opisthosoma length,
BL	body length,	OW	opisthosoma width,
CL	carapace length,	PC	paracymbium,
Co	conductor,	PLE	posterior lateral eyes,
CT	contrategulum,	PME	posterior median eyes,
CW	carapace width,	RC	receptacular cluster,
D	depression,	T	tegulum.

Museum abbreviations:

CBEE	Centre for Behavioural Ecology and Evolution, School of Life Sciences, Hubei University, Wuhan, China;
NMNS	National Museum of Nature and Science, Japan;
NZMC	National Zoological Museum of China, Institute of Zoology, Chinese Academy of Sciences, Beijing, China;
MCZ	Museum of Comparative Zoology, Harvard University, Cambridge, USA;
ZMH	Zoological Museum Hamburg, Germany.

Voucher specimens are deposited at CBEE, and the type specimens will be deposited in NMNS and NZMC.

Integrative taxonomic framework

The integrative taxonomic framework considers diagnosable lineages as potentially valid species. Our taxonomic approach is based on morphological diagnoses that provide an initial species hypothesis (19 species). This is then further tested within a parallel, molecular species delimitation study (Xu et al. 2019). The parallel study amplified two molecular loci, the classical animal barcoding region (COI) as well as the nuclear ITS2 for most sampled specimens, and analysed those data using a multi-tier species

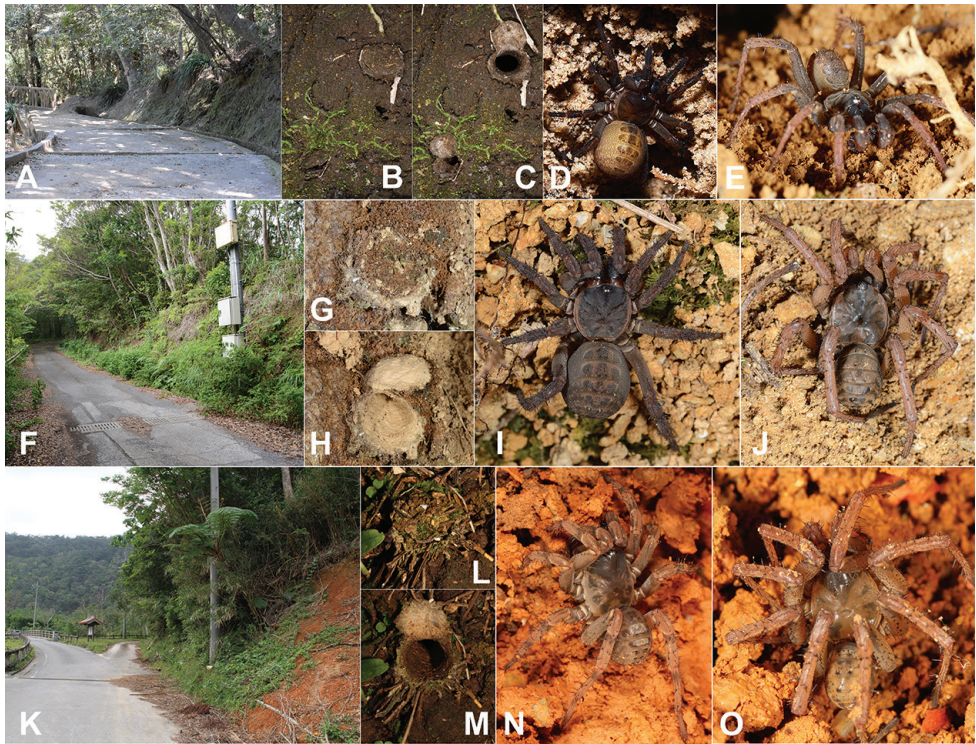


Figure 2. Microhabitats, trapdoors, and general somatic morphology of *Heptathela* Kishida, 1923 **A–E** Kyushu group: **A** microhabitat of *H. kimurai* (Kishida, 1920) at Shiroyama Park, Kyushu **B, C** open and closed trapdoor of *H. kimurai* **D** female *H. kimurai* **E** male *H. higoensis* (Haupt, 1983) **F–J** Amami group: **F** microhabitat of *H. sumiyo* sp. nov. at Sumiyo-cho, Amamioshima **G, H** open and closed trapdoor of *H. amamiensis* Haupt, 1983 **I** female *H. sumiyo* sp. nov. **J** male *H. sumiyo* sp. nov. **K–O** Okinawa group: **K** microhabitat of *H. yanbaruensis* Haupt, 1983 at Yona, Okinawajima **L, M** open and closed trapdoor of *H. yanbaruensis* **N** female *H. yanbaruensis* **O** male *H. yanbaruensis*.

delimitation strategy. In tier 1 analysis, six different sequence-based species delimitation methods using the full data matrix containing 180 samples are used to test the here proposed number of morphologically delimited species of *Heptathela*. The fully congruent species supported by all the methods are included within the final species counts, but only the conflicting species enter the tier 2 analysis in which more genetic markers are added for the samples that represent those conflicting lineages and multi-locus coalescent-based delimitation methods are used to test competing species models derived from tier 1 analysis. If conflict persists, our integrative approach re-evaluates DNA barcode gaps to delimit the competing species models derived from tier 2 analysis. The additional molecular diagnostic evidence, species specific nucleotide substitution information in the animal barcoding gene region (i.e. the standard alignment of COI) (Brower 2010; Cook et al. 2010; Planas and Ribera 2015), augments the morphological species diagnoses that in isolation would be prone to error.

The aligned DNA barcode gene COI is deposited in the Dryad Digital Repository.

Results and discussion

Of the total species diversity of 20, eight previously described species remain valid, two junior synonyms are proposed, and 12 new *Heptathela* species are discovered and described. This taxonomic revision thus represents a 137.5% increase in species diversity of the genus, drawing parallels with prior species richness underestimation found also in other liphistiid genera, e.g., *Ganthela* (Xu et al. 2015c) and *Ryuthela* (Xu et al. 2017).

To ease identification and to hint at putative evolutionary units, we divide *Heptathela* into the Kyushu, the Amami, and the Okinawa groups, each of which contains four, five, and ten species, respectively (Fig. 3). This division of groups is mostly based on species' morphology and geographical distributions, but also heeds the phylogeny. Hence, to avoid paraphyly of Okinawa group, we do not assign *H. helios* from northern Okinawajima to a group as it is sister to all the other *Heptathela* species (Fig. 3).

Taxonomy of *Heptathela*

Genus *Heptathela* Kishida, 1923

Type species. *Liphistius kimurai* Kishida, 1920: 235.

Diagnosis. *Heptathela* males differ from *Liphistius* males by lacking the tibial apophysis, and from males of all other Heptathelinae genera by possessing a leaf-shaped conductor (Fig. 4E, F, H), a wide and thumb-shaped embolus (Fig. 4F, I, K), and a wide tegulum with rugose margin (Fig. 4J, K). *Heptathela* females differ from *Liphistius* females by paired receptacular clusters, and from females of all other Heptathelinae genera by paired depressions on the ventro-lateral part of the genital atrium (Fig. 4C, D), and by the paired receptacular clusters with the main and secondary, lateral, irregular receptacular clusters (Fig. 4A–D).

General description. All the 20 species share the following characteristics: sternum narrow, longer than wide; a few short pointed hairs running over ocular mound in a longitudinal row; chelicerae robust with promargin of cheliceral groove with variable sized denticles (the number of denticles is presented under each species description); legs with strong hairs and spines, and male legs distinctly longer than female legs; opisthosoma with 12 tergites, and the fifth tergite is the largest in all the species except in *H. amamiensis*, *H. sumiyo* sp. nov., and *H. uken* sp. nov., in which the fourth tergite is the largest.

The Kyushu group

Diagnosis. The males of the Kyushu group differ from those of the other two groups by the nearly rectangular contrategulum whose two proximal thirds are serrated (Fig. 4H, I), whereas it is semi-elliptic in the others. The Kyushu group females resemble those

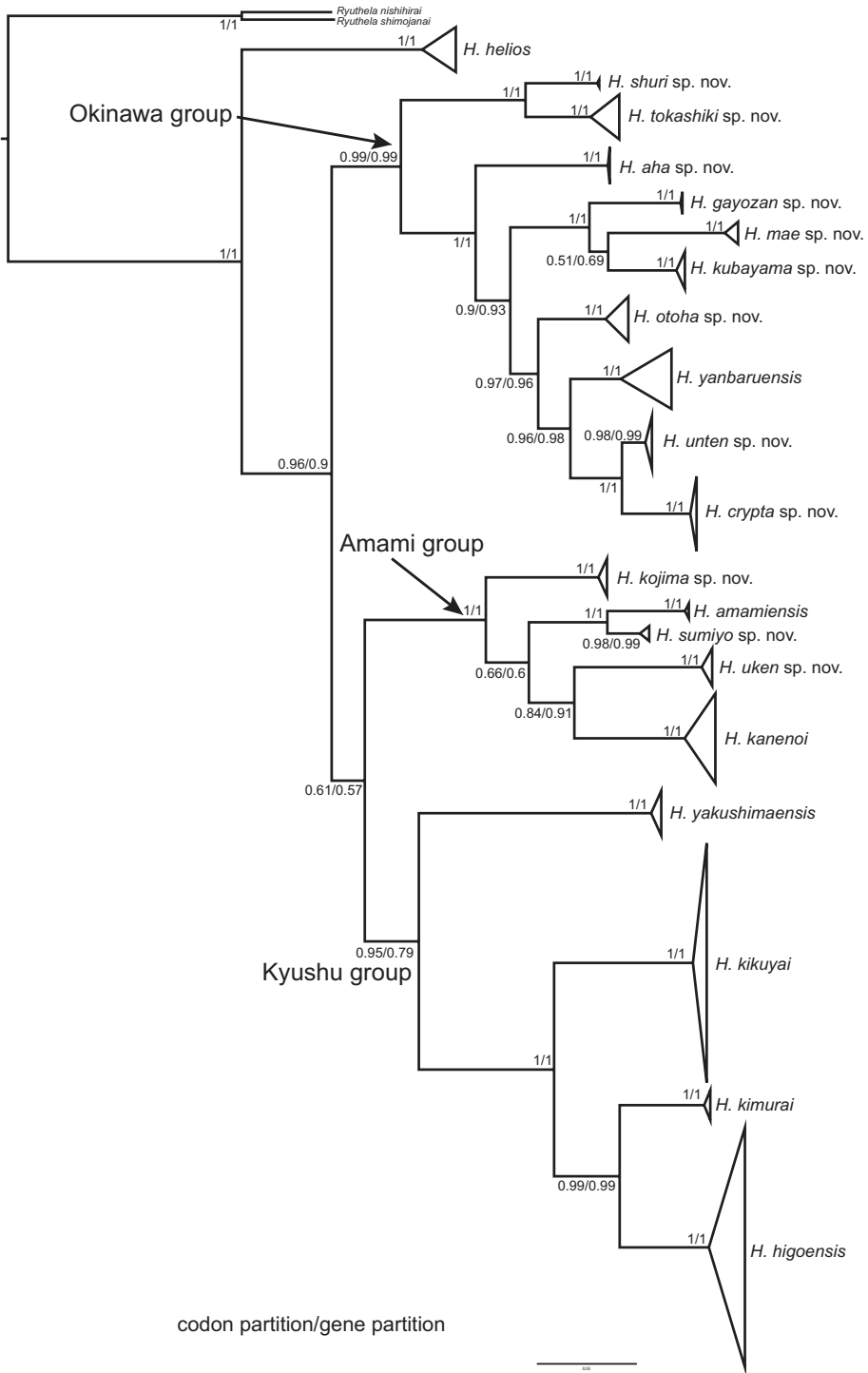


Figure 3. A simplified species-level phylogeny derived from the BI tree in the parallel paper (Xu et al. 2019) showing three species groups.

of the Okinawa group, but differ from those of the Amami group by distinctly paired depressions on the ventro-lateral part of the genital atrium (Fig. 4C, D).

Monophyly. The Bayesian analyses based on concatenated two genes and two partitions (for details, see Xu et al. 2019) inferred the same topology, which supports the Kyushu group monophyly (posterior probability, hereafter PP = 0.95/0.79) (Fig. 3).

Composition. *H. higoensis* Haupt, 1983, *H. kikuyai* Ono, 1998, *H. kimurai* (Kishida, 1920), and *H. yakushimaensis* Ono, 1998.

Distribution. Kyushu and Yakushima (Fig. 1C).

Heptathela higoensis Haupt, 1983

Figs 4, 5

Heptathela kimurai higoensis Haupt, 1983: 283 (holotype: male, from Kumamoto, Kyushu, Japan, collected by M. Yoshikura on 27 September 1973, deposited in MCZ, examined); Haupt 2003: 69. *Heptathela higoensis*: Ono 1998: 16; Ono 2009: 80; Ono and Ogata 2018: 26, 479.

Heptathela nishikawai Ono, 1998: 19 (holotype: female, from Hitoyoshi-shi, Kumamoto-ken, Kyushu, Japan, collected by H. Ono on 19 November 1996, deposited in NMNS, examined); Ono 2009: 83; syn. nov.

Heptathela yaginumai Ono, 1998: 20 (holotype: female, from Honjo, Kunitomi-cho, Higashimorokata-gun, Miyazaki-ken, Kyushu, Japan, collected by T. Yaginuma on 18 June 1949, deposited in NMNS, examined); Ono 2009: 81. syn. nov.

Diagnosis. Males of *H. higoensis* can be distinguished from those of *H. kikuyai* by one of the embolus peaks being longer than the other (Fig. 4H, I, K) and by the slightly blunt tegular marginal apophysis (Fig. 4J), and from those of *H. yakushimaensis* by the conductor with the weakly serrated prolateral margin (Fig. 4F, H, K). Females of *H. higoensis* can be distinguished from those of *H. kimurai* by the wide and flat dorso-posterior part of the genital area (Fig. 4A, B), and from those of *H. kikuyai* and *H. yakushimaensis* by the inner receptacular clusters that are larger than the outer ones (Fig. 4A–D). Moreover, *H. higoensis* differs from all other Kyushu group *Heptathela* species by the following unique nucleotide substitutions in the standard DNA barcode alignment: G (140), C (146), A (179), C (251), C (257), C (263), G (272), A (326), C (332), T (350), G (479), G (569), C (572), A (578), G (596), G (632), G (641).

Description. Males ($N = 11$). Carapace yellow brown; opisthosoma light brown, with dark brown tergites close to each other; cheliceral groove with 11–13 denticles; 7 or 8 spinnerets. Measurements: BL 8.80–11.00, CL 4.40–5.25, CW 4.10–4.90, OL 4.40–5.60, OW 2.90–3.40; ALE > PLE > PME > AME; leg I 11.75 (3.45 + 1.50 + 2.60 + 2.70 + 1.50), leg II 12.40 (3.40 + 1.60 + 2.50 + 3.10 + 1.80), leg III 13.30 (3.20 + 1.60 + 2.40 + 3.80 + 2.30), leg IV 16.80 (4.40 + 1.20 + 3.30 + 5.20 + 2.70).

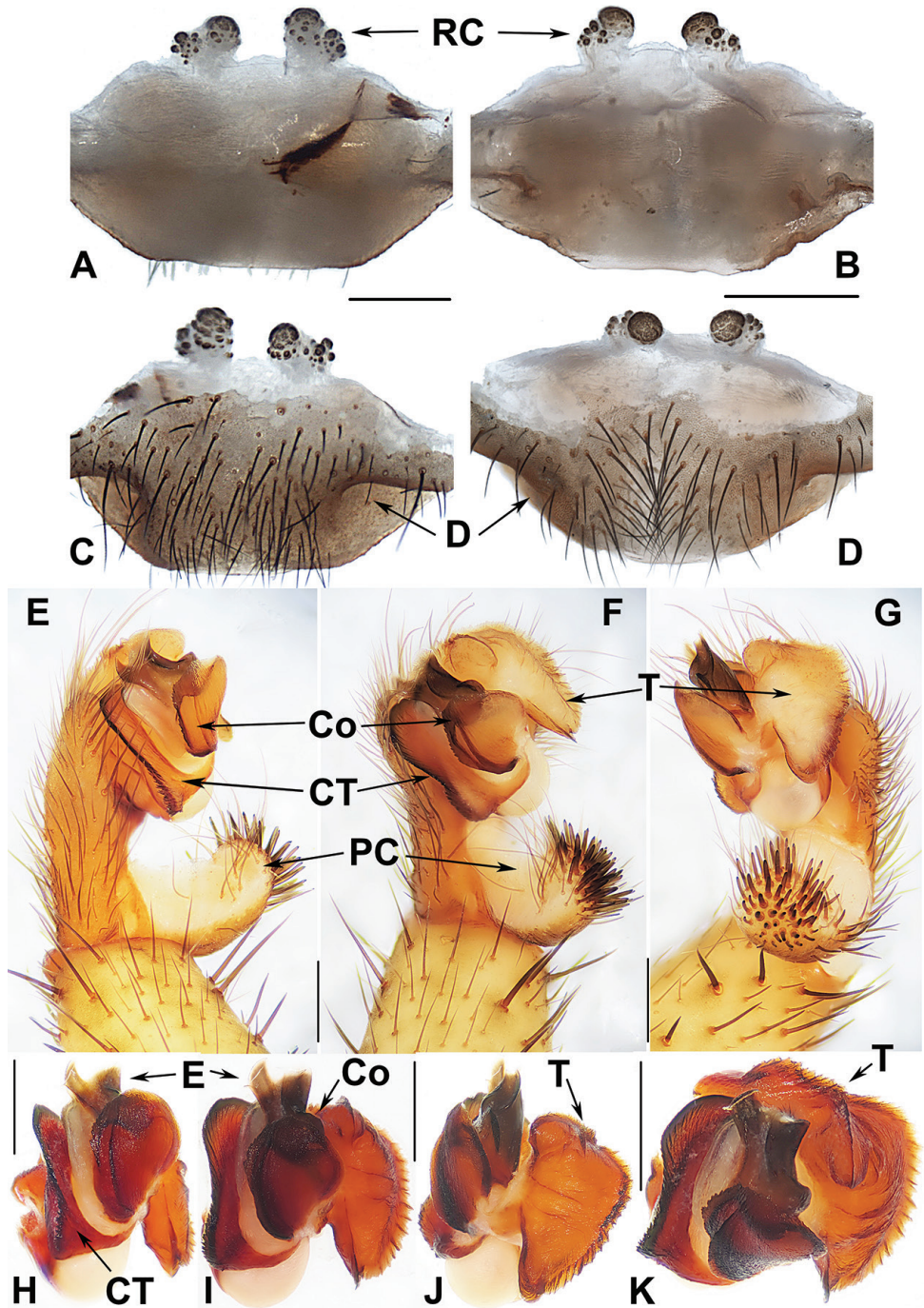


Figure 4. Male and female genital anatomy of *Heptatbela bigoensis* Haupt, 1983 **A, C** 3472 (short for XUX-2013-472) **B, D** 3435 **E-G** 3365 **H-K** 3381 **A, B** vulva dorsal view **C, D** vulva ventral view **E** palp pro-lateral view **F** palp ventral view **G** palp retrolateral view **H-K** palp distal view; 3365: Hitoyoshi Ruins Park, Kumamoto; 3472: Takachihokawara, Kagoshima; 3435: Mukoyama, Miyazaki; 3381: Kozomo, Kumamoto. Scale bar: 0.5 mm.

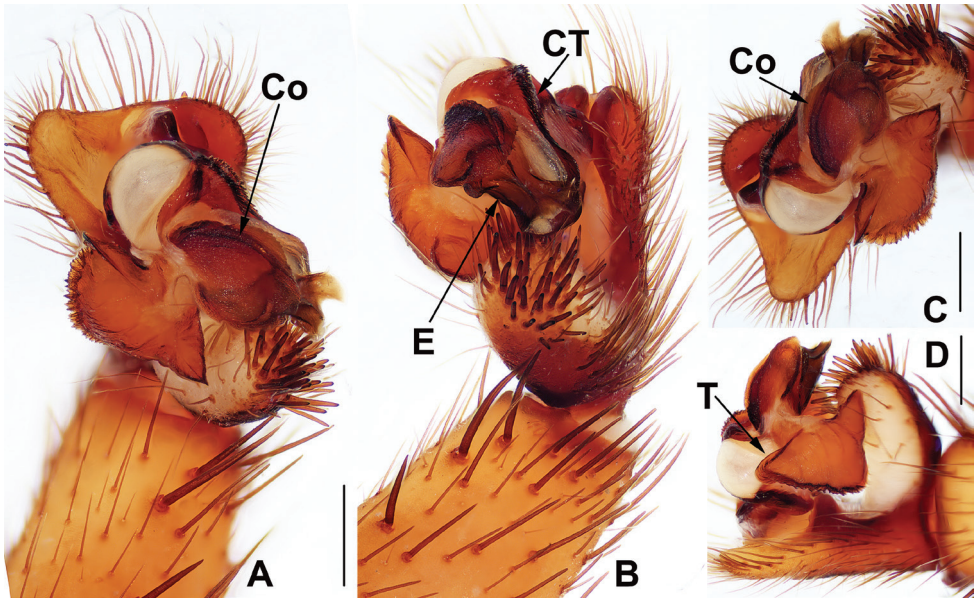


Figure 5. Male holotype genital anatomy of *Heptathela higoensis* Haupt, 1983 (MCZ 21751) **A** palp ventral view **B** palp retrolateral view **C, D** palp distal view. Scale bar: 0.5 mm.

Palp. Prolateral side of paracymbium unpigmented and unsclerotised, numerous setae and spines at the tip of paracymbium (Fig. 4E–G). Contrategulum with serrated margin proximally and smooth margin distally (Fig. 4I, K). Tegulum wide, the dorsal extension of terminal apophysis and marginal apophysis with a serrated margin retrolaterally (Fig. 4J, K). Conductor wide and with an apical tooth and a deep fold (Fig. 4H, K). Embolus with two peaks, one peak longer than the other, and with a curved margin retrolaterally (Fig. 4H–K).

Females ($N = 43$). Carapace and opisthosoma colour as in male; cheliceral groove with 11–16 pronounced denticles; tergites similar to male; 7–8 spinnerets. Measurements: BL 8.00–12.80, CL 4.30–6.10, CW 3.80–5.57, OL 4.10–6.50, OW 2.70–4.90; ALE > PLE > PME > AME; palp 8.20 (2.70 + 1.50 + 1.70 + 2.30), leg I 8.80 (2.80 + 1.75 + 1.70 + 1.55 + 1.00), leg II 8.93 (2.75 + 1.60 + 1.55 + 1.83 + 1.20), leg III 9.30 (2.70 + 1.60 + 1.50 + 2.20 + 1.30), leg IV 13.25 (3.65 + 1.80 + 2.40 + 3.40 + 2.00).

Female genitalia. A pair of depressions on the ventro-lateral part of genital atrium (Fig. 4C, D). Paired receptacular clusters along the anterior margin of bursa copulatrix, divided into two parts, the inner main part forming a large granulate tubercle, with short genital stalks, the outers with several small granules (Fig. 4).

Remarks. We examined the male holotype of *H. higoensis* (Fig. 5) and identified the species as *H. higoensis* even though the bulb of holotype male is relatively distorted compared to the specimens we collected. After we examined 11 males and 43 females collected at the type localities of *H. higoensis*, *H. nishikawai* and *H. yaginumai*, and compared the holotypes of *H. higoensis*, *H. nishikawai* and *H. yaginumai* with our specimens, we proposed synonymy of *H. nishikawai* and *H. yaginumai* with

H. higoensis based on their genital morphology, molecular species delimitation (Xu et al. 2019), and intraspecific genetic distances, 0–1.19% (K2P) and 0–1.18% (*p*-distance) among 43 specimens, although females exhibit a considerable intraspecific variation in genitalia.

Material examined. JAPAN · 1 ♂, 8 ♀♀; Kyushu, Kumamoto-ken, Hitoyoshi-shi, Fumotomachi, Hitoyoshi Ruins Park; 32.21N, 130.77E; alt. 140 m; 18 September 2013; D. Li and B. Wu leg.; XUX-2013-365 (♂ matured 19 July 2014 at CBEE), XUX-2013-360 to 364, 366 to 368 · 2 ♂♂, 5 ♀♀; Kyushu, Kumamoto-ken, Kumamoto-shi, Tatsutayama, Tatsuta National Park; 32.82N, 130.73E; alt. 60 m; 19 September 2013; D. Li and B. Wu leg.; XUX-2013-370 to 379 · 4 ♂♂, 4 ♀♀; Kyushu, Kumamoto-ken, Kumamoto-shi, Higashi-ku, Kozono 1-chome; 32.84N, 130.78E; alt. 100 m; 19 September 2013; D. Li and B. Wu leg.; XUX-2013-380 to 389 (XUX-2013-381, ♂ matured 2 August 2014 at CBEE) · 1 ♂, 3 ♀♀; Kyushu, Kumamoto-ken, Kumamoto-shi, Kasuga, Hanaokayama; 32.80N, 130.68E; alt. 120 m, 19 September 2013; D. Li and B. Wu leg.; XUX-2013-390 to 393 · 3 ♀♀; Miyazaki-ken, Nishiusuki-gun, Takachiho-cho, Mukoyama; 32.70N, 131.30E; alt. 320 m; 22 September 2013; D. Li and B. Wu leg.; XUX-2013-435 to 441 · 1 ♂, 3 ♀♀; Miyazaki-ken, Higashimorokata-gun, Kunitomi-cho, Honjo 11960-1; 32.00N, 131.34E; alt. 30 m; 23 September 2013; D. Li and B. Wu leg.; XUX-2013-456 (♂, matured 19 July 2014 at CBEE), XUX-2013-449 to 451 · 1 ♂, 12 ♀♀; Miyazaki-ken, Higashimorokata-gun, Kunitomi-cho, Honjo 4191; 31.98N, 131.33E; alt. 30 m; 23 September 2013; D. Li and B. Wu leg.; XUX-2013-457 to 467C · 1 ♀; Miyazaki-ken, Nishimorokata-gun, Takaharu-cho, Kamamoto, Lake Miike; 31.89N, 130.96E; alt. 360 m; 23 September 2013; D. Li and B. Wu leg.; XUX-2013-468 · 1 ♂, 4 ♀♀; 2 Kagoshima-ken, Kirishima-shi, Kirishima, Takachihokawara; 31.89N, 130.89E; alt. 960 m; 23 September 2013; D. Li and B. Wu leg.; XUX-2013-471 (♂, matured 8 June 2014 at CBEE), XUX-2013-472 to 474, 476.

Distribution. The species is known from the following prefectures on the Japanese island Kyushu: Kumamoto-ken (Hitoyoshi-shi and Kumamoto-shi), Miyazaki-ken (Nishiusuki-gun, Higashimorokata-gun and Nishimorokata-gun), Kagoshima-ken (Kirishima-shi) (Fig. 1C).

Heptathela kikuyai Ono, 1998

Fig. 6

Heptathela kikuyai Ono, 1998: 16 (holotype: male, from Mt. Gozaga-dake, 20 km south of Oita-shi, Oita-ken, Kyushu, Japan, collected by N. Kikuya on 13 September 1979, deposited in NMNS, examined); Ono 2009: 81; Schwendinger and Ono 2011: 613; Ono and Ogata 2018: 26, 479.

Diagnosis. Males of *H. kikuyai* differ from those of *H. higoensis* by the two embolus peaks of a similar height, and the hooked tegular marginal apophysis (Fig. 6J, K), and from those of *H. yakushimaensis* by only a weakly serrated prolateral margin of the con-

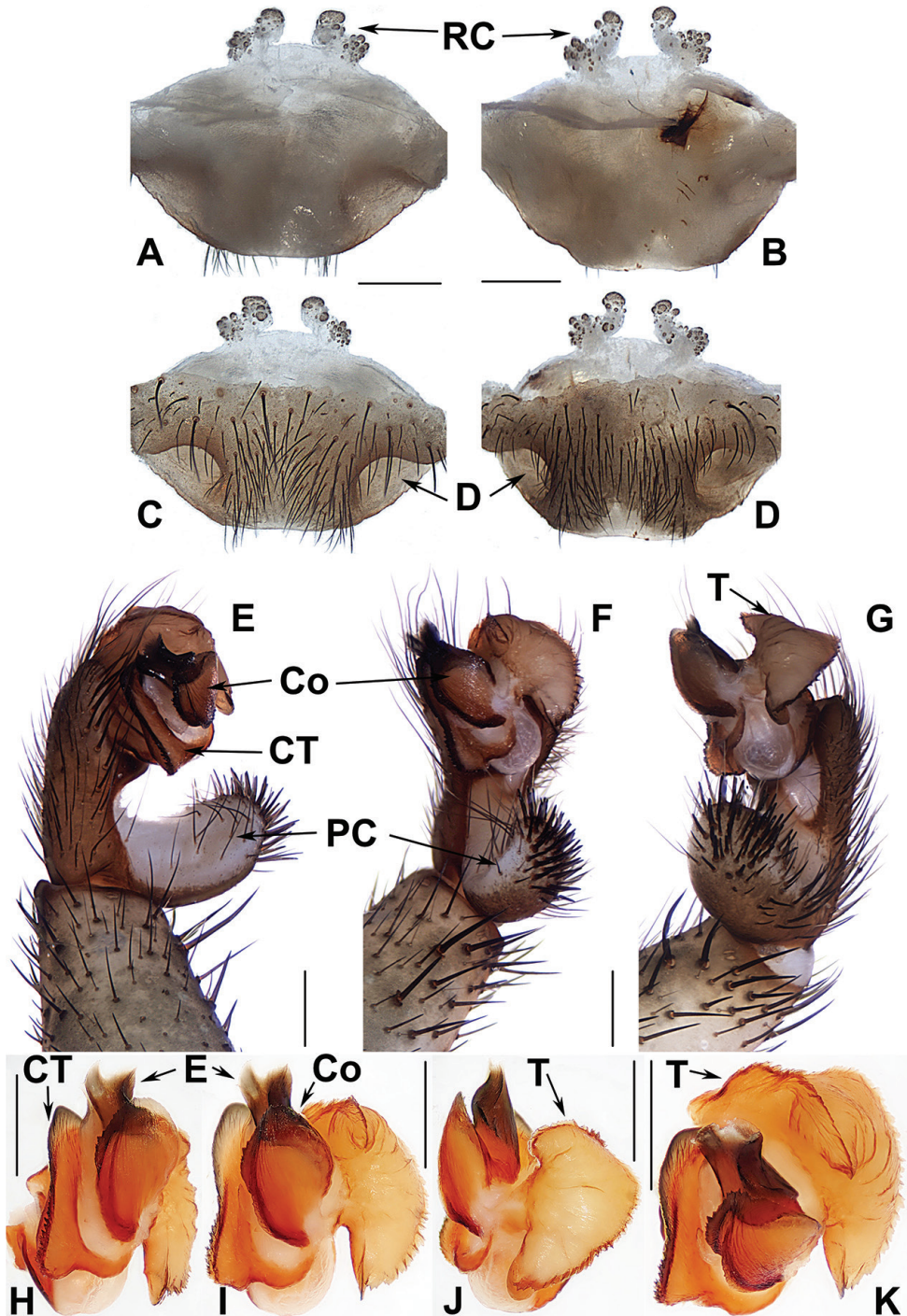


Figure 6. Male and female genital anatomy of *Heptathela kikuyai* Ono, 1998 **A, C** 3409 (short for XUX-2013-409) **B, D** 3401 **E-K** 3405 **A, B** vulva dorsal view **C, D** vulva ventral view **E** palp prolateral view **F** palp ventral view **G** palp retrolateral view **H-K** palp distal view; 3405, 3409: Mt. Gozaga-dake, Oita-ken; 3401: Onomachi, Oita-ken. Scale bar: 0.5 mm.

ductor (Fig. 6H, I). Females of *H. kikuyai* differ from those of all other Kyushu group *Heptathela* species by the inner receptacular clusters with longer and slender stalks (Fig. 6A–D). Moreover, *H. kikuyai* differs from all other Kyushu group *Heptathela* species by the following unique nucleotide substitutions in the standard DNA barcode alignment: G (11), A (33), C (41), C (59), C (68), A (83), A (89), C (116), T (194), A (212), T (222), A (239), A (251), C (260), T (276), T (287), C (305), C (329), A (345), T (365), C (470), G (491), T (546), T (578), T (581), G (635), C (656).

Description. Males ($N = 5$). Carapace and opisthosoma brown, with dark-spotted tergites; cheliceral groove with 10–12 denticles; 6 or 7 spinnerets. Measurements: BL 7.90–9.40, CL 4.00–5.05, CW 3.55–4.30, OL 3.90–4.60, OW 2.60–3.20; ALE > PLE > PME > AME; leg I 13.65 (3.90 + 1.90 + 2.75 + 3.30 + 1.80), leg II 13.35 (3.45 + 1.60 + 2.65 + 3.55 + 2.10), leg III 14.40 (3.30 + 1.50 + 2.75 + 4.45 + 2.40), leg IV 19.25 (4.85 + 1.90 + 3.35 + 6.00 + 3.15).

Palp. Prolateral side of paracymbium unpigmented and unsclerotised, numerous setae and spines at the tip of paracymbium (Fig. 6E–G). Contrategulum with serrated margin proximally and smooth margin distally (Fig. 6H, I, K). Tegulum wide, the dorsal extension of terminal apophysis and hooked marginal apophysis of tegulum with a serrated margin retrolaterally (Fig. 6J, K). Conductor wide and with an apical tooth and a deep fold (Fig. 6I, K). Embolus with two peaks at the slightly same level and a curved margin retrolaterally (Fig. 6H–K).

Females ($N = 30$). Carapace and opisthosoma as in male; cheliceral groove with 12–17 pronounced denticles; tergites similar to male; 6–8 spinnerets. Measurements: BL 8.55–15.10, CL 4.30–7.90, CW 3.80–6.70, OL 4.40–8.75, OW 2.80–6.10; ALE > PLE > PME > AME; palp 9.15 (3.25 + 1.60 + 1.90 + 2.40), leg I 10.30 (3.30 + 1.90 + 1.90 + 2.00 + 1.20), leg II 10.15 (3.10 + 1.80 + 1.85 + 2.10 + 1.30), leg III 10.80 (3.00 + 1.80 + 1.80 + 2.60 + 1.60), leg IV 15.80 (4.50 + 2.20 + 2.80 + 4.10 + 2.20).

Female genitalia. A pair of depressions on the ventro-lateral part of genital atrium. Paired receptacular clusters along the anterior margin of bursa copulatrix, indistinctly divided into two parts, with many small granules, inner ones with longer and slender genital stalks (Fig. 6A–D).

Material examined. JAPAN · 6 ♀♀; Oita-ken, Bungoono-shi, Totoki, Onomachi; 33.06N, 131.52E; alt. 240 m; 20 September 2013; D. Li and B. Wu leg.; XUX-2013-394 to 396, 399 to 401 · 2 ♂♂, 4 ♀♀; Oita-ken, Bungoono-shi, Onomachi-Ando, Mt. Gozaga-dake; 33.11N, 131.55E; alt. 630 m; 20 September 2013; D. Li and B. Wu leg.; XUX-2013-404, 405, 408, 409, 411, 412 (405, ♂ matured 2 May 2014 at CBEE) · 2 ♂♂, 6 ♀♀; Oita-ken, Usuki-shi, Takeyama; 33.10N, 131.72E; alt. 80 m; 20 September 2013; D. Li and B. Wu leg.; XUX-2013-414, 416 to 422 · 1 ♂, 8 ♀♀; Oita-ken, Usuki-shi, Inukai-machi Sasamuta; 33.09N, 131.67E; alt. 120 m; 21 September 2013; D. Li and B. Wu leg.; XUX-2013-424 to 430, 432, 433 · 6 ♀♀; Miyazaki-ken, Nishiusuki-gun, Takachiho-cho, Iwato; 32.73N, 131.35E; alt. 400 m; 22 September 2013; D. Li and B. Wu leg.; XUX-2013-442 to 444, 446 to 448.

Distribution. The species is known from the following prefectures on the Japanese island Kyushu: Oita-ken (Bungoono-shi and Usuki-shi) and Miyazaki-ken (Nishiusuki-gun) (Fig. 1C).

***Heptathela kimurai* (Kishida, 1920)**

Fig. 7

Liphistius kimurai Kishida, 1920: 362 (holotype: female, from Shiroyama, Kagoshima, Kyushu, Japan, collected by A. Kimura in October 1920, lost in the Science College Museum of the Tokyo Imperial University (Haupt, 1983); neotype: male, from the same locality as for the original type specimen, collected by J. Haupt on 21 March 1982, matured in August 1982, deposited in ZMH, but the neotype may be lost according to Dunlop et al. 2014).

Heptathela kimurai Kishida, 1923: 236; Bristowe 1933: 1030; Sawaguti and Ozi 1937: 116 (partly); Yaginuma 1954: 15; Yaginuma 1955: 35; Yaginuma 1960: 19; Yaginuma 1971: 19; Gertsch and Platnick 1979: 5; Yaginuma 1979: 1; Yaginuma 1980: 44; Haupt 1983: 283; Yoshikura 1983: 63; Haupt 1984: 163; Yaginuma 1986: 1; Yoshikura 1987: 148; Chikuni 1989b: 18; Ono 1998: 14; Yoo and Kim 2002: 27; Haupt 2003: 69; Ono 2009: 81; Schwendinger and Ono 2011: 614; Ono and Ogata 2018: 25, 479.

Diagnosis. Females of *H. kimurai* resemble *H. higoensis* females but differ by a slightly curved dorso-posterior margin of the genital area (Fig. 7A, B). Moreover, *H. kimurai* differs from all other Kyushu group *Heptathela* species by the following unique nucleotide substitutions in the standard DNA barcode alignment: C (26), T (98), G (191), G (194), G (206), C (215), T (251), T (278), G (293), C (362), T (366), G (443), T (449), C (452), G (506), G (521), C (527), G (548), T (572), C (599), A (615), C (638).

Description. Females ($N = 9$). Carapace yellow brown; opisthosoma brown, with brown tergites close to each other; cheliceral groove with 12–14 vestigial denticles; seven spinnerets. Measurements: BL 9.30–13.80, CL 4.88–6.30, CW 4.10–5.50, OL 4.80–7.30, OW 3.45–5.40; ALE > PLE > PME > AME; palp 7.77 (2.57 + 1.50 + 1.60 + 2.10), leg I 9.15 (2.85 + 1.70 + 1.75 + 1.65 + 1.20), leg II 8.88 (2.65 + 1.65 + 1.55 + 1.88 + 1.15), leg III 9.63 (2.70 + 1.70 + 1.60 + 2.30 + 1.33), leg IV 14.08 (3.88 + 1.90 + 2.50 + 3.60 + 2.20).

Female genitalia. A pair of depressions on the ventro-lateral part of genital atrium. Paired of receptacular clusters along the anterior margin of bursa copulatrix, divided into two parts, the inner main part forming a large granulate tubercle, the outer part with several small granules (Fig. 7A–D).

Male: unknown.

Remarks. We could not examine the presumably lost neotype male (Dunlop et al. 2014). The male is therefore unknown. The non-topotypical male described as *H. kimurai* by Ono (1998, 2009) is excluded here as we are not sure that the specimen was collected from the type locality although it was obtained in Kagoshima-shi.

Material examined. JAPAN · 9 ♀♀; Kagoshima-ken, Kagoshima-shi, Shiroyama-cho, Shiroyama Park; 31.60N, 130.55E; alt. 100 m; 18 September 2013; D. Li and B. Wu leg.; XUX-2013-349, 351, 352, 354 to 359.

Distribution. The species is known from the Kagoshima prefecture on the Japanese island Kyushu (Fig. 1C).

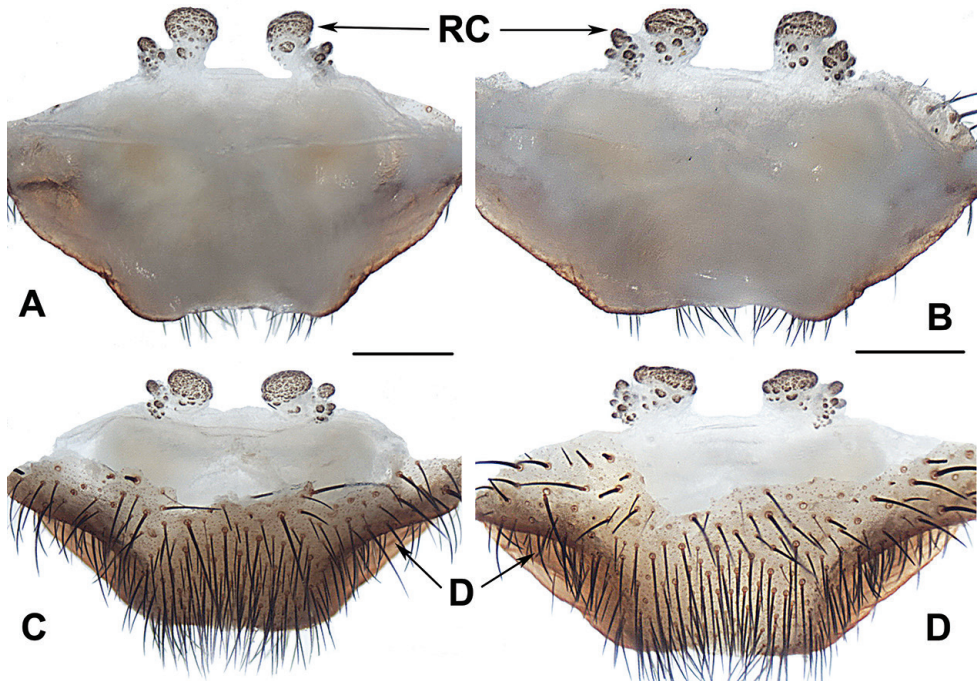


Figure 7. Female genital anatomy of *Heptathela kimurai* (Kishida, 1920) **A, C** 3351 (short for XUX-2013-351) **B, D** 3359 **A, B** vulva dorsal view **C, D** vulva ventral view. Scale bar: 0.5 mm.

Heptathela yakushimaensis Ono, 1998

Fig. 8

Heptathela yakushimaensis Ono, 1998: 23 (holotype: female, from Mt. Kunibaidake, Yakushima Island, Kagoshima-ken, Japan, collected by A. Tanikawa on 15 July 1990, deposited in NMNS, examined); Ono 2009: 83.

Heptathela kimurai yakushimaensis: Haupt 2003: 69.

Diagnosis. Males of *H. yakushimaensis* differ from those of all other Kyushu group *Heptathela* species by a strongly serrated prolater conductor margin (Fig. 8G, H, J, K), the tapered tegular marginal apophysis (Fig. 8L, M), and a larger tegular terminal apophysis (Fig. 8L, M). Females of *H. yakushimaensis* differ from those of *H. kimurai* and *H. bigoensis* by the finely granulated inner receptacular clusters that are smaller than the outer ones (Fig. 8A–F), and from those of *H. kikuyai* by the inner receptacular clusters lacking well defined stalks. *H. yakushimaensis* also differs from all other Kyushu group *Heptathela* species by the following unique nucleotide substitutions in the standard DNA barcode alignment: T (56), A (68), T (74), G (77), C (84), C (89), C (95), G (98), C (107), A (110), C (122), T (131), T (143), T (164), T (167), C (188), C (200), C (212), T (215), C (216), G (218), T (236), G (242), T (248), G (251), C (278), A (284), T (293), C (294), C (308), T (323), C (347), C (356), T (392), T (395), C (396), T (401), T (407),

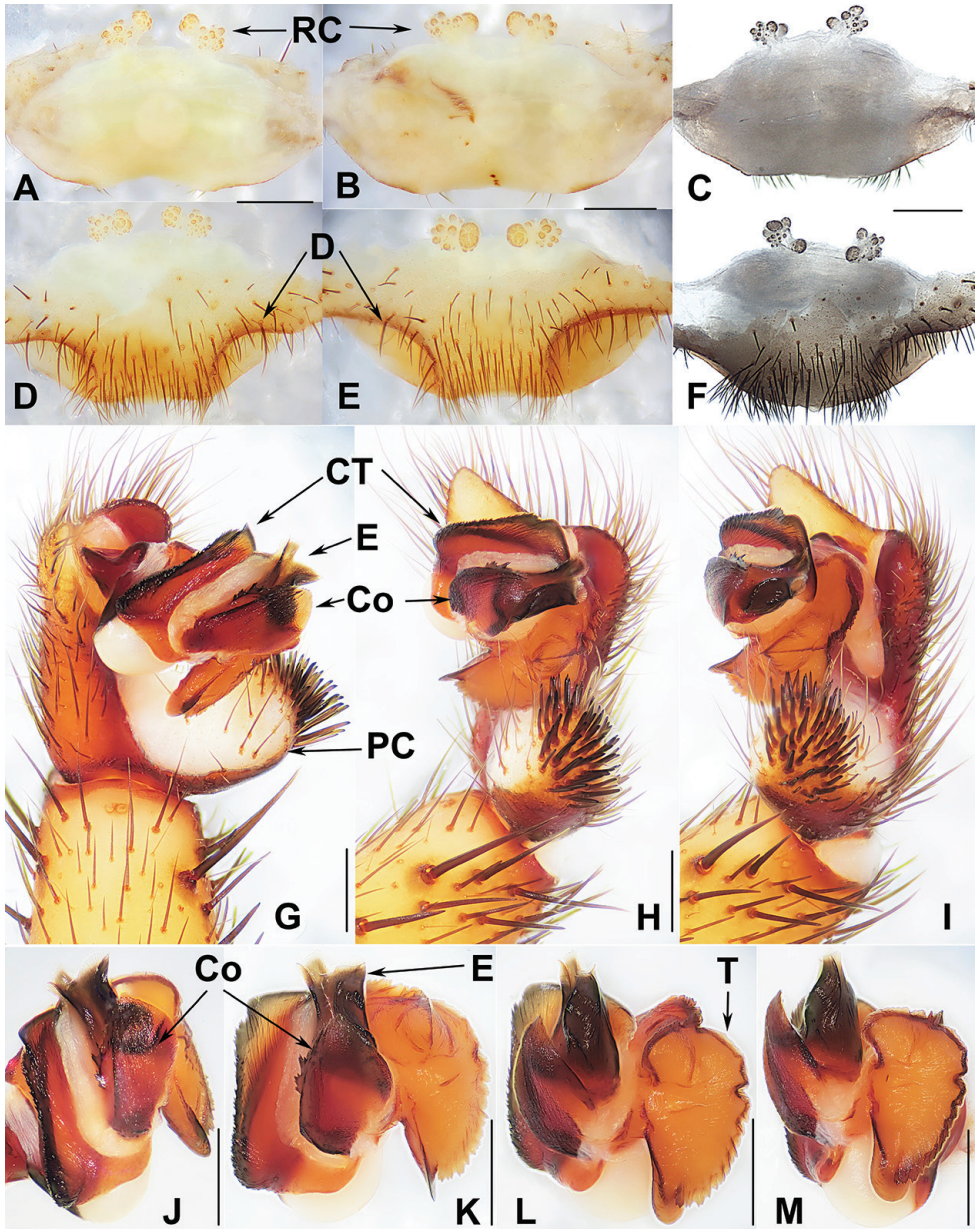


Figure 8. Male and female genital anatomy of *Heptathela yakushimaensis* Ono, 1998 **A, D** 3491 (short for XUX-2013-481) **B, E** 3495 **C, F** 3494 **G-M** 3500 **A-C** vulva dorsal view **D-F** vulva ventral view **G** palp prolateral view **H** palp ventral view **I** palp retrolateral view **J-M** palp distal view. Scale bar: 0.5 mm.

C (411), C (413), C (417), G (422), G (425), C (437), C (438), A (443), T (455), T (458), T (461), T (482), T (488), C (510), T (528), A (530), A (536), A (539), T (548), G (557), C (567), C (584), T (591), T (632), T (635), G (638), T (650), A (665).

Description. Males ($N = 2$). Carapace brown; opisthosoma light brown, with dark brown tergites close to each other; cheliceral groove with 10–13 denticles; 7 spinnerets. Measurements: BL 8.70–10.50, CL 4.27–5.50, CW 4.00–4.90, OL 3.80–6.10, OW 2.40–4.40; ALE > PLE > PME > AME; leg I 13.27 (3.70 + 1.60 + 2.72 + 3.50 + 1.75), leg II 13.71 (3.55 + 1.65 + 2.80 + 3.75 + 1.96), leg III 14.65 (3.52 + 1.65 + 2.78 + 4.50 + 2.20), leg IV 18.64 (4.35 + 1.70 + 3.72 + 6.20 + 2.67).

Palp. Prolateral side of paracymbium unpigmented and unscerotised, numerous setae and spines at the tip of paracymbium (Fig. 8G–I). Contrategulum with serrated margin proximally and smooth margin distally, and slightly curved at the proximal 2/3 of contrategulum (Fig. 8G, H, J, K). Tegulum with serrated margin, widest in the middle (Fig. 8K–M). Conductor prolateral margin strongly serrated (Fig. 8G, H, J, K). Embolus wide with two peaks (Fig. 8G–K).

Females ($N = 8$). Carapace and opisthosoma colour as in male; cheliceral groove with 12–15 pronounced denticles; tergites similar to male; 7 spinnerets. Measurements: BL 9.10–14.80, CL 4.50–6.80, CW 4.05–5.90, OL 4.70–8.60, OW 3.00–6.40; ALE > PLE > PME > AME; palp 9.72 (3.22 + 1.70 + 2.10 + 2.70), leg I 11.15 (3.45 + 1.90 + 2.05 + 2.35 + 1.40), leg II 9.61 (3.07 + 1.90 + 1.00 + 2.36 + 1.28), leg III 11.75 (3.25 + 1.95 + 2.05 + 2.80 + 1.70), leg IV 16.30 (4.25 + 2.25 + 2.90 + 4.40 + 2.50).

Female genitalia. A pair of depressions on the ventro-lateral part of genital atrium. A pair of receptacular clusters along the anterior margin of bursa copulatrix, divided into two parts, the inner part is similar or smaller than the outer part, on which there are several small granules (Fig. 8A–F).

Material examined. JAPAN · 2 ♂♂, 8 ♀♀; Kagoshima-ken, Kumage-gun, Yakushima-cho, Mt. Kankake-dake; 30.37N, 130.39E; alt. 170 m; 24 September 2013; D. Li and B. Wu leg.; XUX-2013-490, 491, 493 to 500 (500, ♂ matured 2 August 2014 at CBEE).

Distribution. The species is known from the Kagoshima prefecture on the Japanese island Yakushima (Fig. 1C).

The Amami group

Diagnosis. The males of the Amami group differ from those of the other two groups by the rugose conductor with a spiniform apex, the contrategulum with a strongly serrated margin whereas it is nearly rectangular in Kyushu group and weakly serrated in Okinawa group, and the embolus with a wide and flat opening (Fig. 9I–L). The females of the Amami group differ from those of the other two groups by indistinctly paired depressions on the ventro-lateral part of the genital atrium and the inner receptacular clusters without tubercula (Fig. 9A–E).

Monophyly. The Bayesian analyses based on concatenated two genes and two partitions (for details, see Xu et al. 2019) inferred the same topology, supporting the Amami group monophyly (PP = 1/1) (Fig. 3).

Composition. *H. amamiensis* Haupt, 1983, *H. kanenoi* Ono, 1996, *H. kojima* sp. nov., *H. sumiyo* sp. nov., and *H. uken* sp. nov.

Distribution. Amamioshima and Tokunoshima (Fig. 1C).

***Heptathela amamiensis* Haupt, 1983**

Fig. 9

Heptathela kimurai amamiensis Haupt, 1983: 283 (holotype: female, from Naze, Amami-oshima, Japan, collected by J. Haupt on 26 March 1980, deposited in ZMH, holotype presumably lost (Dunlop et al. 2014); Haupt 2003: 69. *Heptathela amamiensis*: Ono and Nishikawa 1989: 120; Ono 2009: 80; Ono and Ogata 2018: 27, 479.

Diagnosis. Males of *H. amamiensis* differ from those of *H. sumiyo* sp. nov. by the wider saddle-shaped embolus in the prolateral view, and the narrower conductor base in the ventral view (Fig. 9G, J–L); from those of *H. kanenoi* and *H. kojima* sp. nov. by the spiniform conductor apex (Fig. 9F, I, J). Females of *H. amamiensis* resemble those of other Amami group *Heptathela* species but can be distinguished from those of *H. kanenoi* by the tuberculate outer receptacular clusters (Fig. 9B–E). *H. amamiensis* can also be diagnosed from all other Amami group *Heptathela* species by the following unique nucleotide substitutions in the standard DNA barcode alignment: C (89), A (179), A (194), T (215), T (218), C (273), A (281), C (284), A (327), G (332), G (362), C (467), C (543), C (647).

Description. Male. Carapace brown; opisthosoma light brown, with dark brown tergites; cheliceral groove with 13 denticles; 8 spinnerets. Measurements: BL 12.85, CL 6.50, CW 5.98, OL 6.65, OW 4.00; ALE > PLE > PME > AME; leg I 18.25 (5.00 + 2.45 + 3.80 + 4.60 + 2.40), leg II 18.75 (4.85 + 2.40 + 3.75 + 5.00 + 2.75), leg III 20.10 (4.90 + 2.60 + 3.60 + 5.90 + 3.10), leg IV 25.30 (6.00 + 2.60 + 5.10 + 7.70 + 3.90).

Palp. Prolateral side of paracymbium unpigmented and unsclerotised, numerous setae and spines at the tip of paracymbium (Fig. 9F–H). Contrategulum with serrated margin (Fig. 9F, G, I, J). Tegulum wide, with dentate dorsal extension of terminal apophysis (Fig. 9H, L) and blunt terminal apophysis (Fig. 9H, K, L). Conductor sclerotised and rugose, with several folds and a spiniform apex (Fig. 9F–L). Embolus sclerotised, with a wide and flat opening, the distal part slightly sclerotised, and saddle-shaped in the prolateral view (Fig. 9F–L).

Females ($N = 5$). Carapace and opisthosoma colour as in male; cheliceral groove with 12–14 pronounced denticles; tergites similar to those of male; seven or eight spinnerets. Measurements: BL 11.08–16.90, CL 5.45–6.90, CW 4.70–6.20, OL 6.61–9.10, OW 4.70–7.38; ALE > PLE > PME > AME; palp 12.36 (4.12 + 2.11 + 2.75 + 3.38), leg I 14.12 (4.52 + 2.50 + 2.70 + 2.83 + 1.57), leg II 14.06 (4.25 + 2.37 + 2.61 + 3.15 + 1.68), leg III 15.13 (4.27 + 2.56 + 2.55 + 3.55 + 2.20), leg IV 21.86 (5.84 + 2.91 + 4.08 + 5.81 + 3.22).

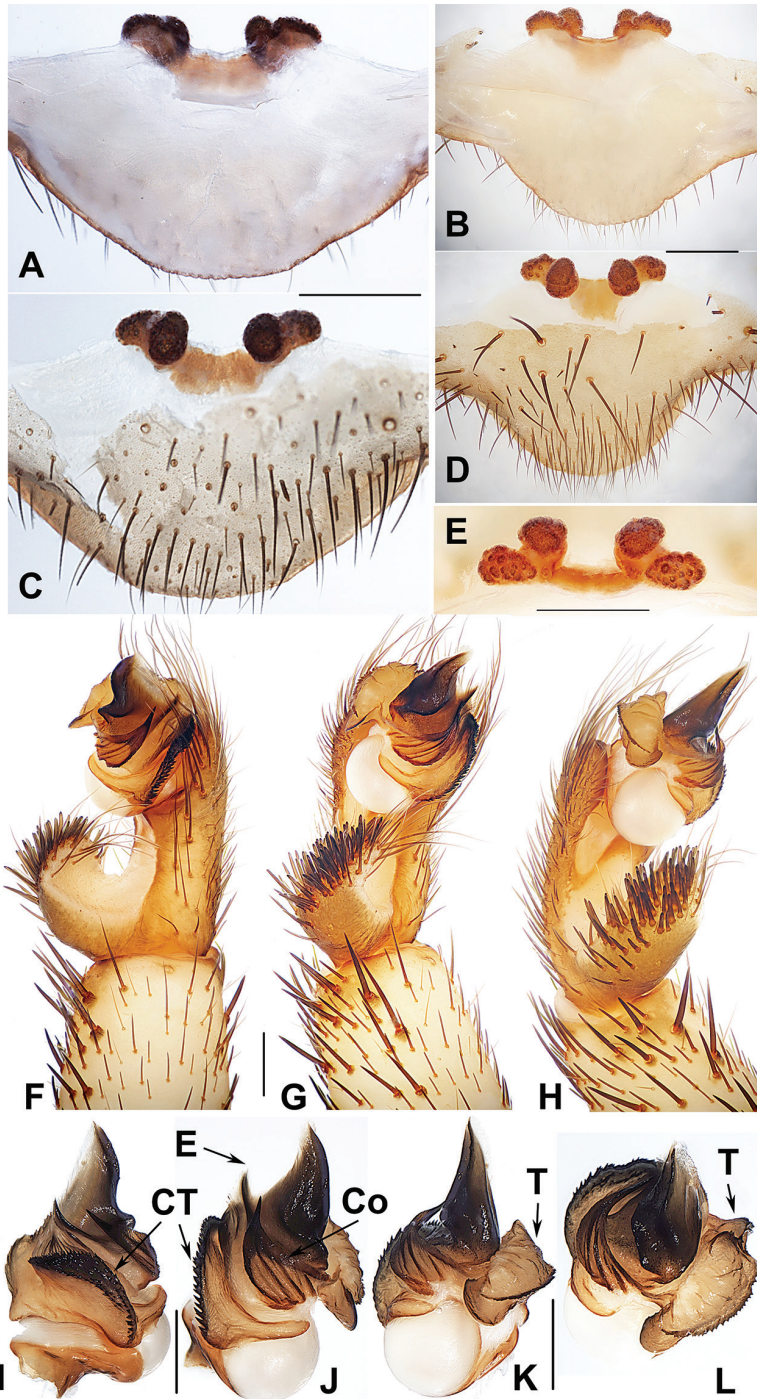


Figure 9. Male and female genital anatomy of *Heptathela amamiensis* Haupt, 1983 **A, C** 3278 (short for XUX-2013-278) **B, D, E** 3285 **F–L** 3283 **A, B** vulva dorsal view **C, D** vulva ventral view **E** vulva distal view **F** right palp prolateral view **G** right palp ventral view **H** right palp retrolateral view **I–L** left palp distal view. Scale bar: 0.5 mm.

Female genitalia. A pair of indistinct depressions on the ventro-lateral part of genital atrium (Fig. 9C, D). Paired receptacular clusters along the anterior margin of bursa copulatrix, divided into two parts, the inners ovate, the outers tuberculate, without genital stalks (Fig. 9A-E).

Material examined. JAPAN · 2 ♂♂, 5 ♀♀; Kagoshima-ken, Amami-Oshima, Amami-shi, Nazehirata-cho, Michinoshima Loop Bridge; 28.36N, 129.50E; alt. 60 m; 15 September 2013; D. Li and B. Wu leg.; XUX-2013-276, 278, 281 to 285.

Distribution. The species is known from the Japanese island Amamioshima (Fig. 1C).

Heptathela kanenoi Ono, 1996

Fig. 10

Heptathela kanenoi Ono, 1996: 158 (holotype: male, from Mikyo, Amagi-cho, Tokunoshima, Kagoshima-ken, Japan, collected by M. Owada and S. Kaneno on 2 November 1992, deposited in NMNS, examined); Ono 2009: 80.

Diagnosis. Males of *H. kanenoi* can be distinguished from those of all other Amami group *Heptathela* species by lacking a spiniform conductor apex (Fig. 10G, I). Females of *H. kanenoi* can be distinguished from those of all other Amami group *Heptathela* species by the inner receptacular clusters larger than the outers (Fig. 10B, C). *H. kanenoi* can also be diagnosed from all other Amami group *Heptathela* species by the following unique nucleotide substitutions in the standard DNA barcode alignment: A (35), G (38), C (71), C (125), C (224), G (278), T (281), C (288), T (332), G (359), C (396), C (410), G (443), T (449), A (512), C (533), G (557), C (560), C (623), T (641).

Description. Males ($N = 6$). Carapace yellow brown; opisthosoma brown, with dark-spotted tergites close to each other; cheliceral groove with 10–13 vestigial denticles; 7 spinnerets. Measurements: BL 9.80–11.60, CL 5.10–6.00, CW 4.60–5.40, OL 5.15–5.60, OW 4.00–4.85; ALE > PLE > PME > AME; leg I 17.85 (4.80 + 2.30 + 3.80 + 4.60 + 2.35), leg II 18.90 (4.90 + 2.30 + 3.80 + 5.20 + 2.70), leg III 20.80 (4.70 + 2.30 + 4.00 + 6.50 + 3.30), leg IV 26.00 (6.20 + 2.50 + 5.10 + 8.20 + 4.00).

Palp. Prolateral side of paracymbium unpigmented and unsclerotised, numerous setae and spines at the tip of paracymbium (Fig. 10D–F). Contrategulum with serrated margin (Fig. 10G–I). Tegulum with dentate dorsal extension of terminal apophysis (Fig. 10J) and blunt tegulum terminal apophysis (Fig. 10I, J). Conductor base wide and rugose, with several folds and each fold with an apical tooth (Fig. 10G–J). Embolus with a wide and flat opening, the distal part slightly sclerotised, and saddle-shaped in the prolateral view (Fig. 10H–I).

Females ($N = 11$). Carapace and opisthosoma colour as in male; cheliceral groove with 12–14 pronounced denticles; tergites similar to male; seven or eight spinnerets. Measurements: BL 8.30–12.90, CL 4.30–6.28, CW 3.60–5.40, OL 4.38–6.50, OW 3.70–6.20; ALE > PLE > PME > AME; palp 7.00 (2.50 + 1.35 + 1.55 + 1.60), leg

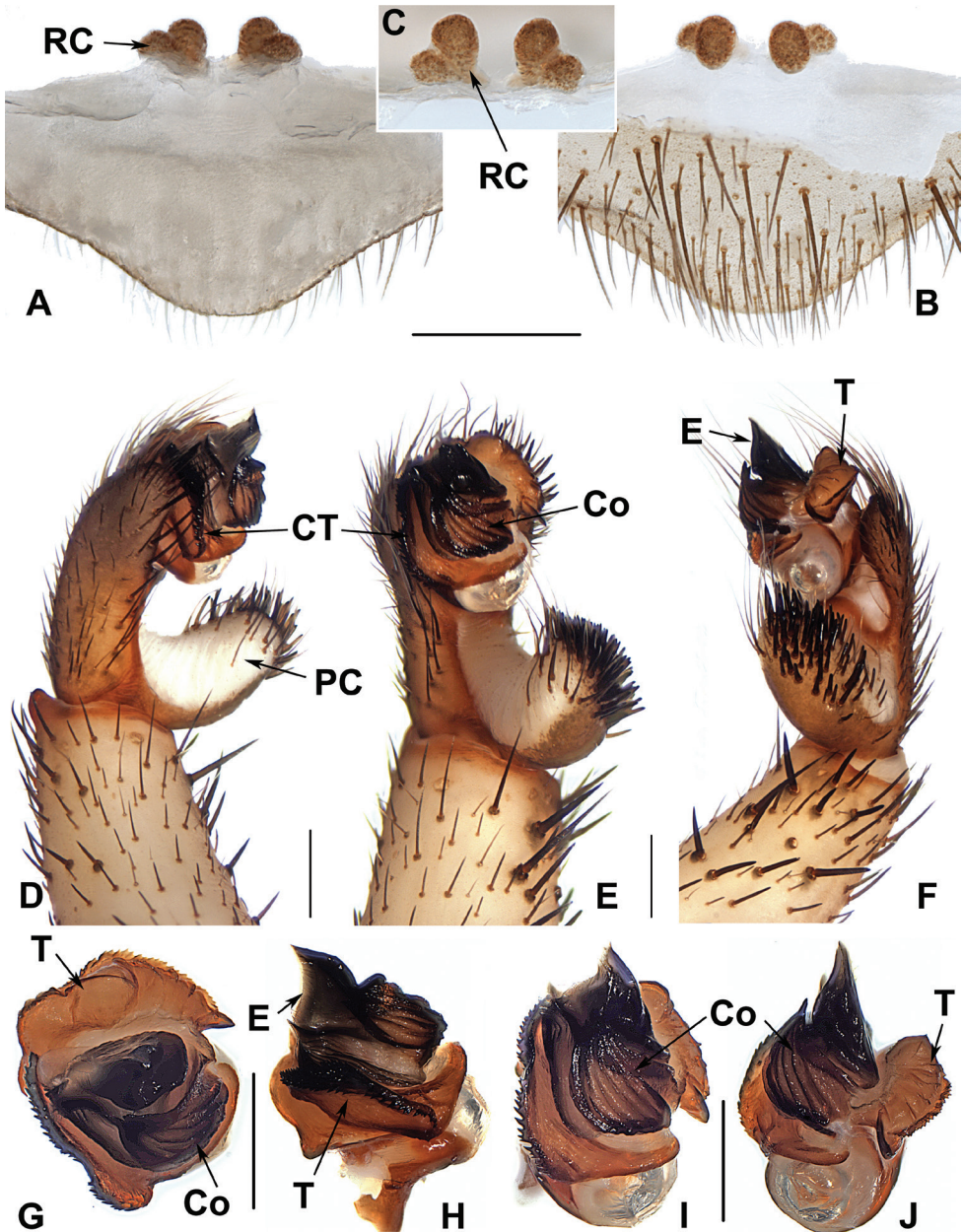


Figure 10. Male and female genital anatomy of *Heptathela kanenoi* Ono, 1996 **A–C** 3338 (short for XUX-2013-338) **D–J** 3334 **A** vulva dorsal view **B** vulva ventral view **C** vulva distal view **D** palp prolateral view **E** palp ventral view **F** palp retrolateral view **G–J** palp distal view. Scale bar: 0.5 mm.

I 7.75 (2.30 + 1.25 + 1.60 + 1.50 + 1.10), leg II 7.60 (2.60 + 1.10 + 1.50 + 1.50 + 0.90), leg III 8.35 (2.45 + 1.50 + 1.10 + 2.00 + 1.30), leg IV 12.15 (3.40 + 1.50 + 2.25 + 3.20 + 1.80).

Female genitalia. A pair of indistinct depressions on the ventro-lateral part of genital atrium. Paired receptacular clusters along the anterior margin of bursa copulatrix, divided into two parts, the inner ones larger than the outer ones, without genital stalks (Fig. 10A–C).

Material examined. JAPAN · 1 ♂, 1 ♀; Kagoshima-ken, Tokunoshima, Amagi-cho, Mikyo; 27.77N, 128.95E; alt. 180 m; 16 September 2013; D. Li and B. Wu leg.; XUX-2013-315 to 316 · 3 ♂♂, 7 ♀♀; Kagoshima-ken, Oshima-gun, Tokunoshima, Tokunoshima-cho, Tokuwase; 27.79N, 129.01E; alt. 150 m; 17 September 2013; D. Li and B. Wu leg.; XUX-2013-323 to 332 · 2 ♂♂, 3 ♀♀; Kagoshima-ken, Tokunoshima, Amagi-cho, Mikyo; 27.77N, 128.95E; alt. 130 m; 17 September 2013; D. Li and B. Wu leg.; XUX-2013-333 to 338.

Distribution. The species is endemic to the Japanese island Tokunoshima (Fig. 1C).

***Heptathela kojima* sp. nov.**

<http://zoobank.org/9330F719-A1B4-4169-9FBF-90D13CD49248>

Fig. 11

Type material. Holotype: JAPAN · ♂; Kagoshima-ken, Oshima-gun, Tokunoshima, Isen-cho, Kojima; 27.74N, 128.91E; alt. 160 m; 17 September 2013; D. Li and B. Wu leg.; XUX-2013-346 (matured 10 October 2013 at CBEE).

Paratypes: JAPAN · 2 ♂♂, 6 ♀♀; same data as for holotype; XUX-2013-339, 340, 342 to 345, 347, 348.

Diagnosis. Males of *H. kojima* sp. nov. differ from those of *H. amamiensis* and *H. kanenoi* by a wide leaf-shaped conductor (Fig. 11I, J), and a less dentate dorsal extension of the tegular terminal apophysis (Fig. 11G, J, K), from those of *H. sumiyo* sp. nov. by a shallow saddle-shaped in the prolateral view, and from those of *H. uken* sp. nov. by embolus with two longer peaks (Fig. 11I, J). Females of *H. kojima* sp. nov. resemble those of other Amami group *Heptathela* species but differ from those of other Amami group *Heptathela* species by paired receptacular clusters close to each other (Fig. 11B, D). *H. kojima* sp. nov. can also be diagnosed from all other Amami group *Heptathela* species by the following unique nucleotide substitutions in the standard DNA barcode alignment: C (44), C (56), C (128), A (131), C (134), C (137), C (155), G (158), G (176), T (230), T (245), C (269), T (320), C (357), C (377), A (378), A (443), C (446), G (464), A (479), C (518), G (521), T (554), A (560), C (608), C (611).

Description. Male (Holotype). Carapace brown; opisthosoma light brown, with dark brown tergites close to each other; cheliceral groove with eleven denticles; seven spinnerets. Measurements: BL 7.30, CL 3.60, CW 3.30, OL 3.60, OW 2.70; ALE > PLE > PME > AME; leg I 14.90 (4.20 + 1.65 + 3.15 + 4.00 + 1.90), leg II 16.10 (4.20 + 1.85 + 3.25 + 4.40 + 2.40), leg III 16.85 (4.25 + 1.90 + 3.20 + 5.00 + 2.50), leg IV 21.70 (5.50 + 2.00 + 4.20 + 6.90 + 3.10).

Palp. Prolateral side of paracymbium unpigmented and unsclerotised, numerous setae and spines at the tip of paracymbium (Fig. 11E–G). Contrategulum with serrated

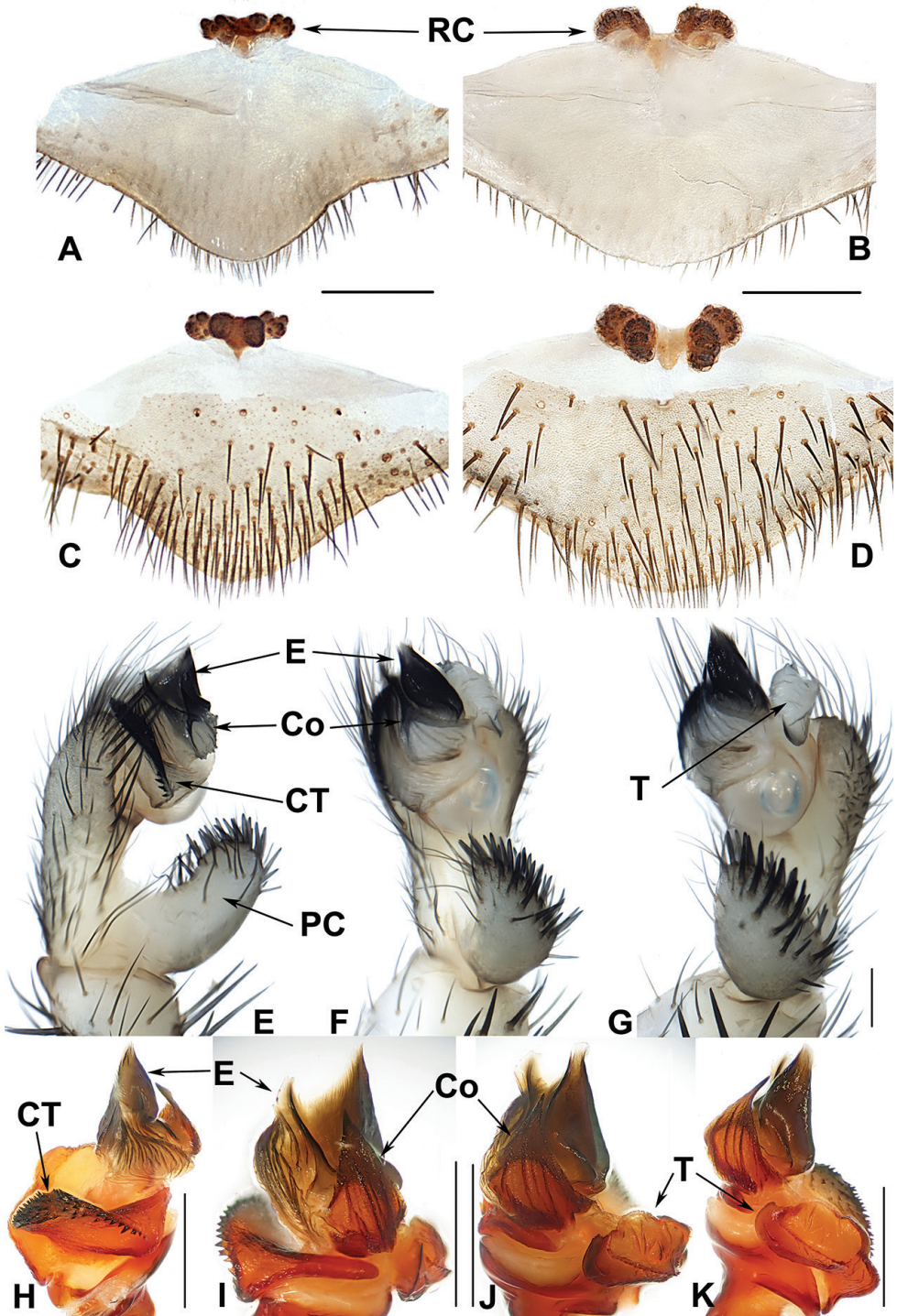


Figure 11. Male and female genital anatomy of *Heptathela kojima* sp. nov. **A, C** 3339 (short for XUX-2013-339) **B, D** 3340 **E-G** 3346 (holotype) **H-K** 3344 **A, B** vulva dorsal view **C, D** vulva ventral view **E** palp prolateral view **F** palp ventral view **G** palp retrolateral view **H-K** palp distal view. Scale bar: 0.5 mm.

margin (Fig. 11E, H, I). Conductor base wide, leaf-shaped and rugose, with several folds and gradually narrowing to a short spiniform apex (Fig. 11I, J). Embolus sclerotised, with a wide and flat opening (Fig. 11H–K).

Females ($N = 6$). Carapace and opisthosoma colour as in male; cheliceral groove with 13 pronounced denticles; tergites similar to male; 6–8 spinnerets. Measurements: BL 9.00–11.50, CL 4.90–6.15, CW 4.25–5.20, OL 4.30–6.10, OW 3.00–4.50; ALE > PLE > PME > AME; palp 9.05 (3.25 + 1.65 + 1.85 + 2.30), leg I 10.50 (3.35 + 1.80 + 2.00 + 2.10 + 1.25), leg II 10.05 (3.10 + 1.80 + 1.75 + 2.10 + 1.30), leg III 10.45 (2.90 + 1.95 + 1.65 + 2.40 + 1.55), leg IV 15.20 (4.40 + 2.20 + 2.60 + 4.00 + 2.00).

Female genitalia. A pair of indistinct depressions on the ventro-lateral part of genital atrium (Fig. 11C, D). Paired receptacular clusters separated from each other along the anterior margin of bursa copulatrix, or fused together, divided into two parts, without genital stalks (Fig. 11A–D).

Etymology. The species epithet, a noun in apposition, refers to the type locality.

Distribution. The species is endemic to the Japanese island Tokunoshima (Fig. 1C).

Heptathela sumiyo sp. nov.

<http://zoobank.org/BB1A7494-C5CD-4D69-BC49-67052BCF7E05>

Fig. 12

Type material. Holotype: JAPAN · ♂; Kagoshima-ken, Amami-Oshima, Amami-shi, Sumiyo-cho, Santaro-toge Pass; 28.28N, 129.42E; alt. 360 m; 15 September 2013; D. Li and B. Wu leg.; XUX-2013-293.

Paratypes: JAPAN · 4 ♂♂, 6 ♀♀; same data as for holotype; XUX-2013-287 to 292, 294 to 296B.

Diagnosis. Males of *H. sumiyo* sp. nov. can be distinguished from those of *H. kanenoi* by the spiniform conductor apex (Fig. 12A, E, F), from those of *H. amamiensis* by the narrow and deeper saddle-shaped embolus in the prolateral view (Fig. 12A, E, F). Females of *H. sumiyo* sp. nov. resemble those of the other Amami group *Heptathela* species but differ from those of *H. kanenoi* by the tuberculate lateral receptacular clusters that are equal in size, or slightly larger than the inner clusters (Fig. 12J, K). *H. sumiyo* sp. nov. also differs from all other *Heptathela* species of the Amami group by the following unique nucleotide substitutions in the standard DNA barcode alignment: G (92), C (218), A (227), G (281), C (308), A (363), T (647).

Description. Male (Holotype). Carapace brown; opisthosoma light brown, with dark brown tergites; cheliceral groove with eleven denticles; seven spinnerets. Measurements: BL 15.40, CL 7.70, CW 6.80, OL 8.00, OW 5.55; ALE > PLE > PME > AME; leg I 23.05 (6.05 + 3.10 + 4.90 + 6.10 + 2.90), leg II 24.46 (6.48 + 3.08 + 5.05 + 6.80 + 3.05), leg III 26.36 (6.10 + 3.20 + 5.05 + 8.20 + 3.81), leg IV 32.70 (8.00 + 3.50 + 6.75 + 9.70 + 4.75).

Palp. Prolateral side of paracymbium unpigmented and unsclerotised, numerous setae and spines at the tip of paracymbium (Fig. 12A–C). Contrategulum with

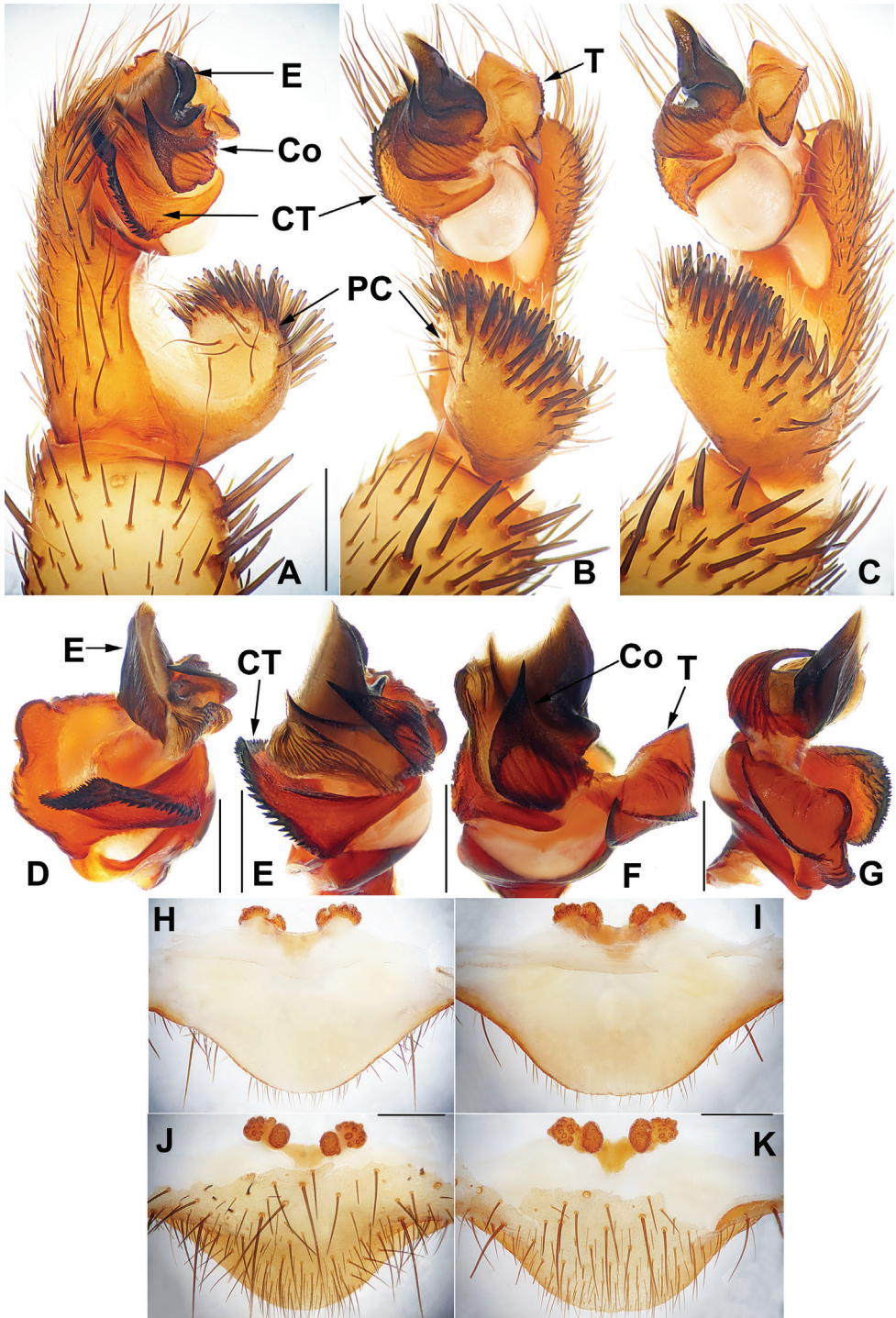


Figure 12. Male and female genital anatomy of *Heptathela sumiyo* sp. nov. **A–C** 3293 (holotype, short for XUX-2013-293) **D–G** 3292 **H, J** 3288 **I, K** 3296 **A** palp prolateral view **B** palp ventral view **C** palp retrolateral view **D–G** palp distal view **H, I** vulva dorsal view **J, K** vulva ventral view. Scale bar: 0.5 mm.

serrated margin (Fig. 12A, D, E). Tegulum wide with dentate dorsal extension of terminal apophysis (Fig. 12F, G) and blunt terminal apophysis (Fig. 12B, C, F, G). Conductor sclerotised and rugose, with several folds and a spiniform apex (Fig. 12A–B, E–F). Embolus largely sclerotised, with a wide and flat opening, the distal part slightly sclerotised, and narrow and deep saddle-shaped in the prolateral view (Fig. 12A, D–F).

Females ($N = 6$). Carapace and opisthosoma colour as in male; cheliceral groove with 13 or 14 pronounced denticles; tergites similar to those of male; seven or eight spinnerets. Measurements: BL 11.70–15.60, CL 6.25–7.55, CW 5.40–6.43, OL 5.40–8.80, OW 4.00–7.35; ALE > PLE > PME > AME; palp 12.90 (4.50 + 2.25 + 2.70 + 3.45), leg I 14.44 (4.55 + 2.68 + 2.55 + 3.08 + 1.58), leg II 13.93 (4.09 + 2.49 + 2.35 + 3.20 + 1.80), leg III 15.61 (4.40 + 2.70 + 2.68 + 3.80 + 2.03), leg IV 22.45 (6.20 + 3.20 + 4.15 + 6.10 + 2.80).

Female genitalia. A pair of indistinct depressions on the ventro-lateral part of genital atrium (Fig. 12J, K). Two pairs of receptacular cluster along the anterior margin of bursa copulatrix, the medians ovate, the laterals tuberculate, similar or slightly larger than inners, without genital stalks (Fig. 12H–K).

Etymology. The species epithet, a noun in apposition, refers to the type locality.

Distribution. The species is known from the Japanese island Amamioshima (Fig. 1C).

Heptathela uken sp. nov.

<http://zoobank.org/C538969C-60CB-4184-B388-E8958807AF33>

Fig. 13

Type material. Holotype: JAPAN · ♂; Kagoshima-ken, Amami, Uken-son, Oshima-gun, Road No. 85, Redsoil Park; 28.24N, 129.34E; alt. 260 m; 15 September 2013; D. Li and B. Wu leg.; XUX-2013-297.

Paratypes: JAPAN · 2 ♂♂, 2 ♀♀; same data as for holotype; XUX-2013-298, 301, 302, 304 · 3 ♂♂, 5 ♀♀; Kagoshima-ken, Amami, Yamato-son, Amami Forest Park; 28.31N, 129.33E; alt. 300 m; 17 September 2013; D. Li and B. Wu leg.; XUX-2013-305 to 314.

Diagnosis. Males of *H. uken* sp. nov. can be distinguished from those of *H. kane-noi* by the spiniform conductor apex (Fig. 13A, B, D, E), from those of *H. amamiensis* by the dorsal extension of regular terminal apophysis without dentation (Fig. 13F, G). Females of *H. uken* sp. nov. cannot be diagnosed from those of the other Amami group *Heptathela* species morphologically (Fig. 13H–M), only by the following unique nucleotide substitutions in the standard DNA barcode alignment: T (161), T (191), G (227), C (236), T (287), T (297), A (299), C (389), T (395), G (413), C (416), G (503), C (509), C (510), T (527), T (558), G (560), G (569), C (578), T (584), C (596), T (614), G (629), G (635), C (650), C (665).

Description. Male (Holotype). Carapace brown; opisthosoma light brown, with dark brown tergites; cheliceral groove with eight denticles; seven spinnerets. Measure-

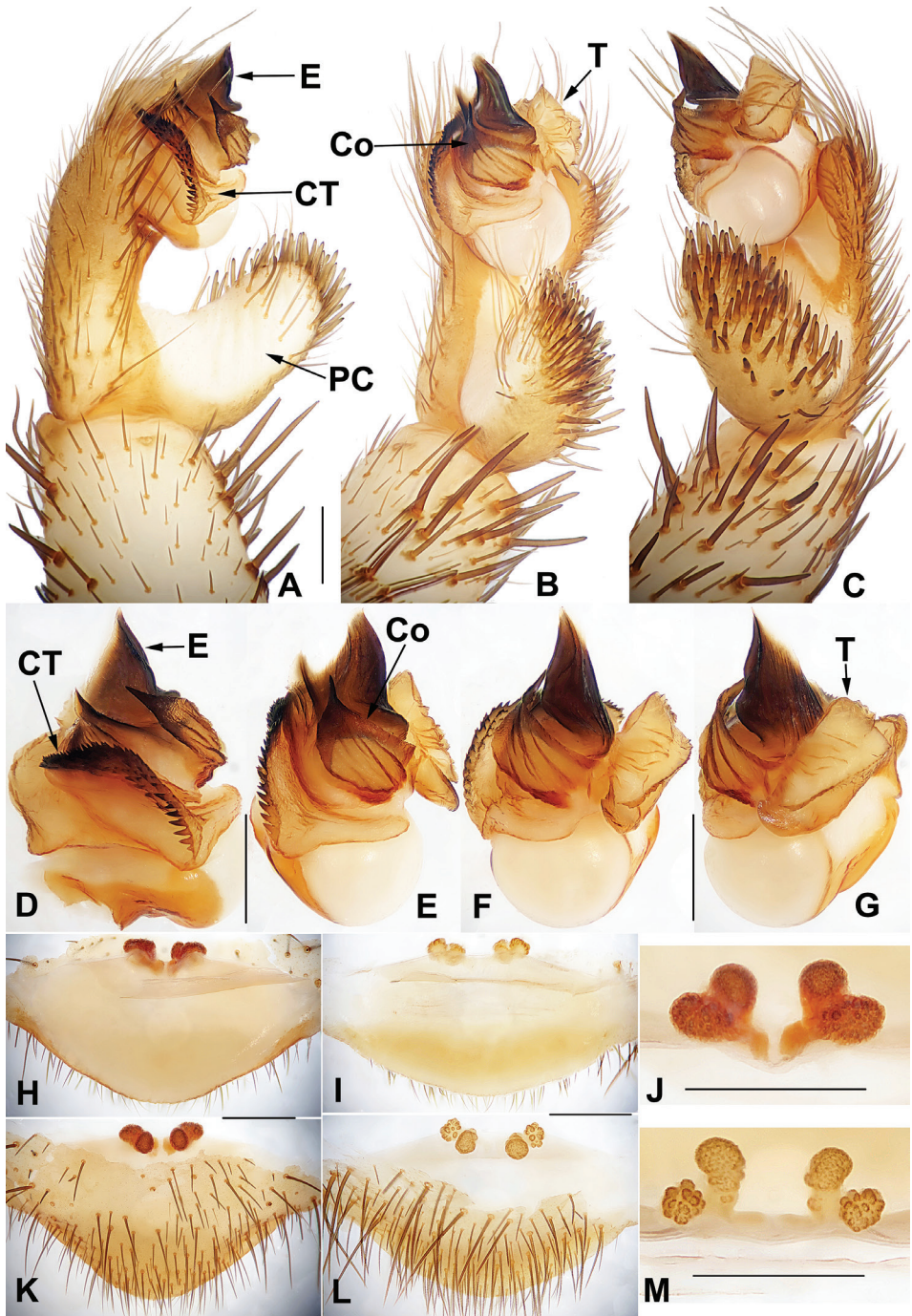


Figure 13. Male and female genital anatomy of *Heptatbela uken* sp. nov. **A–G** 3297 (holotype, short for XUX-2013-297) **H, K, J** 3301 **I, L, M** 3309 **A** palp prolateral view **B** palp ventral view **C** palp retrolateral view **D–G** palp distal view **H, I** vulva dorsal view **K, L** vulva ventral view **J, M** vulva distal view; 3297, 3301: Uken-son, Amamioshima; 3309: Yamato-son, Amamioshima. Scale bar: 0.5 mm.

ments: BL 11.60, CL 6.10, CW 5.60, OL 6.00, OW 4.30; ALE > PLE > PME > AME; leg I 17.47 (4.80 + 2.28 + 3.67 + 4.42 + 2.30), leg II 17.95 (4.65 + 2.30 + 3.60 + 4.90 + 2.50), leg III 18.80 (4.45 + 2.40 + 3.55 + 5.20 + 3.20), leg IV 23.60 (5.60 + 2.45 + 4.45 + 7.20 + 3.90).

Palp. Prolateral side of paracymbium unpigmented and unsclerotised, numerous setae and spines at the tip of paracymbium (Fig. 13A–C). Contrategulum with serrated margin (Fig. 13A, B, D, F). Tegulum with smooth dorsal extension of terminal apophysis (Fig. 13F, G). Conductor wide, sclerotised and rugose, with several folds and a spiniform apex (Fig. 13A, B, D, F). Embolus sclerotised, wide with a flat opening, and wide saddle-shaped in the prolateral view (Fig. 13A, B, D, E).

Females ($N = 8$). Carapace and opisthosoma colour as in male; cheliceral groove with 13–15 pronounced denticles; tergites similar to male; 7 or 8 spinnerets. Measurements: BL 11.80–16.00, CL 5.90–8.26, CW 5.20–7.20, OL 6.00–8.10, OW 4.60–6.00; ALE > PLE > PME > AME; palp 10.04 (3.05 + 1.89 + 2.30 + 2.80), leg I 12.05 (3.90 + 2.10 + 2.25 + 2.40 + 1.40), leg II 11.30 (3.55 + 2.05 + 1.80 + 2.45 + 1.45), leg III 12.42 (3.60 + 2.05 + 2.10 + 3.00 + 1.67), leg IV 18.33 (5.15 + 2.40 + 3.30 + 4.78 + 2.70).

Female genitalia. A pair of indistinct depressions on the ventro-lateral part of genital atrium (Fig. 13K). Two pairs of receptacular clusters along the anterior margin of bursa copulatrix, the inners almost globose, with short genital stalks in distal view, the laterals tuberculate, without genital stalks (Fig. 13H–M).

Etymology. The species epithet, a noun in apposition, refers to the type locality.

Distribution. The species is known from the Japanese island Amamioshima (Fig. 1C).

The Okinawa group

Diagnosis. The males of the Okinawa group differ from those of the Kyushu group by the semi-elliptic contrategulum (Fig. 14H–J), and from those of the Amami group by the contrategulum whose margin is only weakly serrated, is curved in the middle, and is proximally serrated and distally smooth (Fig. 14I, J). The females of the Okinawa group resemble those of the Kyushu group, but differ from those of the Amami group by distinctly paired depressions on the ventro-lateral part of the genital atrium (Fig. 14C, D).

Monophyly. The Bayesian analyses based on concatenated two genes and two partitions (for details, see Xu et al. 2019) suggested the Okinawa clades are paraphyly (Fig. 3). Therefore, in this study, Okinawa group includes all species from Okinawa except *H. helios*, which is sister to all the other *Heptathela* species (Fig. 3).

Composition. *H. yanbaruensis* Haupt, 1983, *H. aha* sp. nov., *H. gayozan* sp. nov., *H. kubayama* sp. nov., *H. mae* sp. nov., *H. otoa* sp. nov., *H. shuri* sp. nov., *H. tokashiki* sp. nov., *H. unten* sp. nov., and *H. crypta* sp. nov.

Distribution. Okinawajima, Iheyajima, Tokashikijima (Fig. 1C).

***Heptathela yanbaruensis* Haupt, 1983**

Fig. 14

Heptathela kimurai yanbaruensis Haupt, 1983: 284 (holotype: male, from Yona, Okinawa, Japan, collected by J. Haupt on 15 April 1977, deposited in ZMH, where the type may be lost (Dunlop et al. 2014); Haupt 1984: 166; Haupt 2003: 69. *Heptathela yanbaruensis*: Ono 2009: 80; Ono and Ogata 2018: 28, 480.

Diagnosis. Males of *H. yanbaruensis* can be distinguished from those of *H. helios* by the contrategulum that is distinctly curved in the middle (Fig. 14I, J), and from those of *H. unten* sp. nov. and *H. crypta* sp. nov. by the conductor that is longer than its width (Fig. 14I, J). Females of *H. yanbaruensis* can be distinguished from those of *H. shuri* sp. nov. by the wide and straight posterior margin of the genital atrium (Fig. 14A, C). *Heptathela yanbaruensis* can also be diagnosed from all other *Heptathela* species of the Okinawa group by the following unique nucleotide substitutions in the standard DNA barcode alignment: G (53), T (327), A (356), A (443).

Description. Males ($N = 3$). Carapace yellow brown; opisthosoma light brown, with dark-spotted tergites close to each other; cheliceral groove with 10–12 denticles; seven spinnerets. Measurements: BL 8.53–9.22, CL 4.21–4.57, CW 3.71–3.75, OL 4.20–4.48, OW 2.30–2.80; ALE > PLE > PME > AME; leg I 14.28 (4.15 + 1.70 + 3.05 + 3.56 + 1.82), leg II 15.15 (3.97 + 1.70 + 3.07 + 4.13 + 2.28), leg III 15.24 (4.00 + 1.68 + 3.08 + 4.10 + 2.38), leg IV 19.78 (4.75 + 1.37 + 3.91 + 6.45 + 3.30).

Palp. Prolateral side of paracymbium unpigmented and unsclerotised, numerous setae and spines at the tip of paracymbium (Fig. 14E–G). Contrategulum margin obviously curved in the middle, the contrategulum margin proximally serrated and distally smooth (Fig. 14H–J). Tegulum wide with a dentate dorsal extension of terminal apophysis (Fig. 14J, K), blunt terminal and marginal apophysis (Fig. 14J, K). Conductor oval, with weakly serrated margin, and a fold in prolateral view (Fig. 14H–J). Embolus sclerotised, with a wide opening, the distal margin slightly sclerotised, and with a wide saddle-shaped margin in the retrolateral view (Fig. 14I–K).

Females ($N = 15$). Carapace and opisthosoma colour as in male; cheliceral groove with 11–14 pronounced denticles; tergites similar to male; seven spinnerets. Measurements: BL 7.78–10.33, CL 3.90–5.10, CW 3.40–4.23, OL 3.90–6.00, OW 2.80–4.70; ALE > PLE > PME > AME; palp 8.70 (2.96 + 1.51 + 2.11 + 2.12), leg I 10.20 (3.12 + 1.75 + 1.93 + 2.12 + 1.28), leg II 9.97 (3.05 + 1.72 + 1.77 + 2.13 + 1.30), leg III 10.05 (2.91 + 1.78 + 1.48 + 2.47 + 1.41), leg IV 14.77 (4.08 + 2.10 + 2.51 + 3.97 + 2.11).

Female genitalia. A pair of depressions on the ventro-lateral part of the genital atrium (Fig. 14C, D). The posterior margin of genital atrium wide and straight (Fig. 14A–D). Paired receptacular clusters along the anterior margin of bursa copulatrix, divided into two parts, the size of inner ones similar to that of laterals, with several granules, with short genital stalks (Fig. 14A–D).

Material examined. JAPAN · 3 ♂♂, 9 ♀♀; Okinawa-ken, Kunigami-son, Yona, Tropical Biosphere Research Centre field station, University of the Ryukyus; 26.76N, 128.22E; alt. 20 m; 18 December 2012; D. Li, F.X. Liu and X. Xu leg.; XUX-2012-310

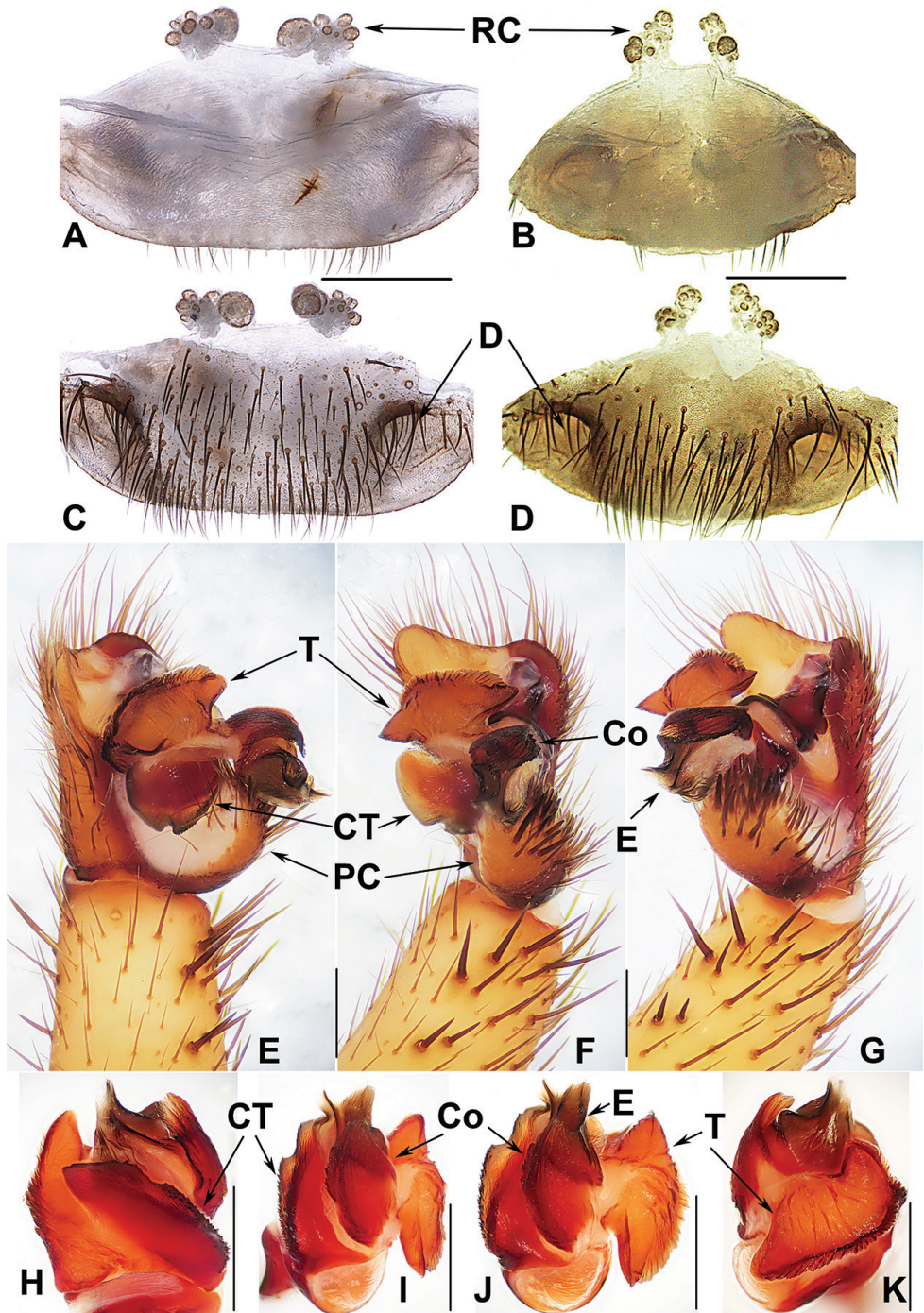


Figure 14. Male and female genital anatomy of *Heptathela yanbaruensis* Haupt, 1983 **A, C** 2315 (short for XUX-2012-315) **B, D** 2441 **E–G** 2322B **H–K** 2311, 2315, 2322B: Yona, Okinawajima; 2441: Taiho Dam, Okinawajima. Scale bar: 0.5 mm.

to 322B · 6 ♀♀; Okinawa-ken, Ogimi-son, Taiho Dam; 26.65N, 128.16E; alt. 80 m; 24 December 2012; D. Li, F.X. Liu and X. Xu leg.; XUX-2012-441 to 446.

Distribution. The species is endemic to the Japanese island Okinawajima (Fig. 1C).

***Heptathela aha* sp. nov.**

<http://zoobank.org/4F130218-5900-4688-AF57-F018C26E34C8>

Fig. 15

Type material. Holotype: JAPAN · ♀; Okinawa-ken, Iheyajima Island, Mt. Aha-dake; 27.02N, 127.93E; alt. 10 m; 26 December 2012; D. Li, F.X. Liu and X. Xu leg.; XUX-2012-502.

Paratypes: JAPAN · 6 ♀♀; same data as for holotype; XUX-2012-504 to 519.

Diagnosis. Females of *H. aha* sp. nov. cannot be distinguished morphologically from those of *H. gayozan* sp. nov. but can be distinguished from those of *H. kubayama* sp. nov. by the receptacular clusters without genital stalks; and from those of *H. mae* sp. nov. by the inner receptacular clusters similar to or larger than laterals (Fig. 15A–F). *Heptathela aha* sp. nov. can also be diagnosed from all other Okinawa group *Heptathela* species by the following unique nucleotide substitutions in the standard DNA barcode alignment: C (41), C (179), G (182), G (233), T (248), G (251), T (326), A (347), G (359), C (473), C (492), A (536), T (651).

Description. Female (Holotype). Carapace brown; opisthosoma brown, brown tergites with black plaques; cheliceral groove with 12 pronounced denticles; seven spinnerets. Measurements: BL 12.60, CL 5.55, CW 5.00, OL 6.82, OW 5.50; ALE > PLE > PME > AME; palp 9.90 (3.40 + 1.71 + 2.18 + 2.61), leg I 11.34 (3.31 + 2.05 + 2.31 + 2.35 + 1.32), leg II 11.65 (3.51 + 1.98 + 2.03 + 2.53 + 1.60), leg III 11.92 (3.30 + 1.90 + 2.05 + 2.97 + 1.70), leg IV 16.96 (4.88 + 2.22 + 2.98 + 34.45 + 2.43).

Female genitalia. A pair of depressions on the ventro-lateral part of the genital atrium (Fig. 15D–F). A pair of receptacular clusters along the anterior margin of bursa copulatrix, divided into two parts, both without genital stalks (Fig. 15A–F).

Male. Unknown.

Etymology. The species epithet, a noun in apposition, refers to the type locality.

Distribution. The species is endemic to the Japanese island Iheyajima (Fig. 1C).

***Heptathela gayozan* sp. nov.**

<http://zoobank.org/6DAC9A7B-50DD-4513-ACD6-B51AF264BBC2>

Fig. 16

Type material. Holotype: JAPAN · ♀; Okinawa-ken, Iheyajima Island, Mt. Gayozan; 27.02N, 127.97E; alt. 25 m; 27 December 2012; D. Li, F.X. Liu and X. Xu leg.; XUX-2012-511.

Paratypes: JAPAN · 2 ♀♀; same data as for holotype; XUX-2012-513, 515.

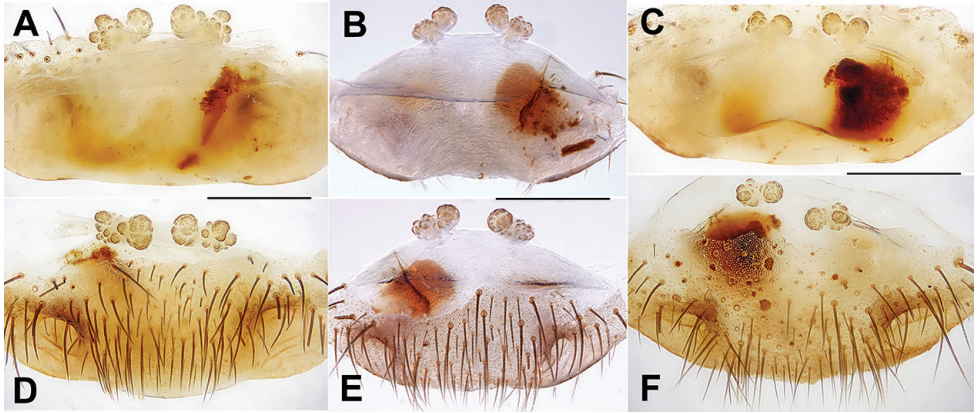


Figure 15. Female genital anatomy of *Heptathela aha* sp. nov. **A, D** 2502 (holotype, short for XUX-2012-502) **B, E** 2505 **C, F** 2506 **A–C** vulva dorsal view **D–F** vulva ventral view. Scale bar: 0.5 mm.

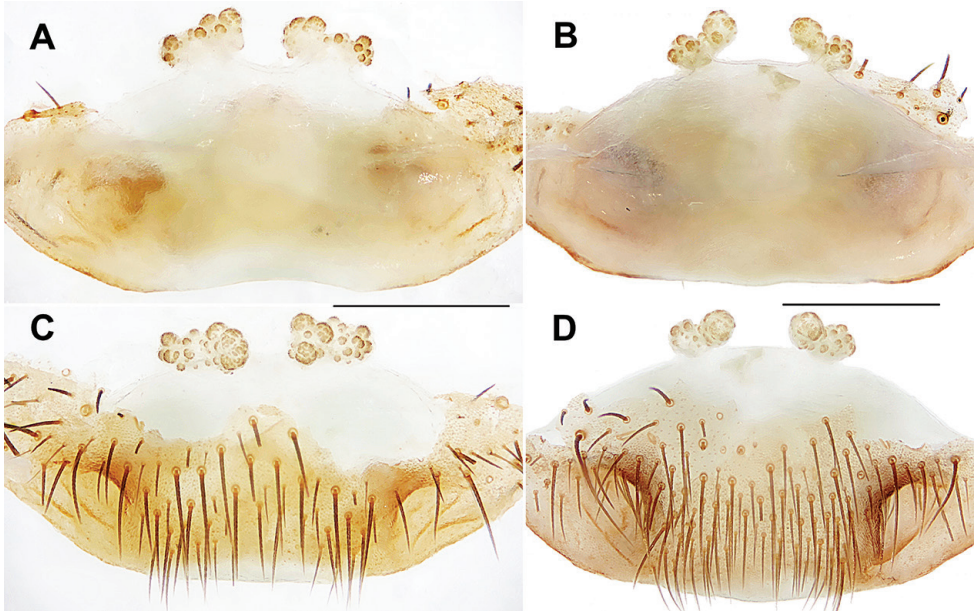


Figure 16. Female genital anatomy of *Heptathela gayozan* sp. nov. **A, C** 2511 (holotype, short for XUX-2012-511) **B, D** 2513 **A, B** vulva dorsal view **C, D** vulva ventral view. Scale bar: 0.5 mm.

Diagnosis. Females *H. gayozan* sp. nov. cannot be distinguished morphologically from those of *H. aha* sp. nov. but can be distinguished from those of *H. kubayama* sp. nov. by the receptacular clusters without genital stalks; and from those of *H. mae* sp. nov. by the inner receptacular clusters that are equal in size, or slightly larger than laterals (Fig. 16A–D). *H. gayozan* sp. nov. can be diagnosed from all other Okinawa group *Heptathela* species by the following unique nucleotide substitutions in the standard

DNA barcode alignment: G (38), G (41), G (122), C (203), C (365), C (452), C (470), T (518), C (527), C (533), T (560), T (653).

Description. Female (holotype). Carapace brown; opisthosoma light brown, with dark brown tergites close to each other; cheliceral groove with 12 denticles; seven spinnerets. Measurements: BL 10.00, CL 4.40, CW 3.88, OL 4.84, OW 3.48; ALE > PLE > PME > AME; palp 7.32 (2.72 + 1.50 + 1.80 + 1.30), leg I 9.61 (2.95 + 1.62 + 1.82 + 1.97 + 1.25), leg II 9.38 (2.80 + 1.58 + 1.71 + 2.07 + 1.22), leg III 9.60 (2.65 + 1.55 + 1.62 + 2.28 + 1.50), leg IV 13.89 (3.75 + 1.82 + 2.52 + 3.75 + 2.05).

Female genitalia. A pair of depressions on the ventro-lateral part of genital atrium (Fig. 16C, D). A pair of receptacular clusters along the anterior margin of bursa copulatrix, divided into two parts, with several granules, without genital stalks (Fig. 16).

Male. Unknown.

Etymology. The species epithet, a noun in apposition, refers to the type locality.

Distribution. The species is endemic to the Japanese island Iheyajima (Fig. 1C).

Heptathela kubayama sp. nov.

<http://zoobank.org/C8B09629-5191-447F-8C89-9953504F8E0D>

Fig. 17

Type material. Holotype: JAPAN · ♀; Okinawa-ken, Iheyajima Island, Mt. Kubayama Nature Conservation Area; 27.09N, 128.02E; alt. 85 m; 26 December 2012; D. Li, F.X. Liu and X. Xu leg.; XUX-2012-486.

Paratypes: JAPAN · 8 ♀♀; same data as for holotype; XUX-2012-479, 481 to 485, 487 to 488.

Diagnosis. Females of *H. kubayama* sp. nov. can be distinguished from those of *H. gayozan* sp. nov. and *H. mae* sp. nov. by paired receptacular clusters with short genital stalks (Fig. 17A–B). *Heptathela kubayama* sp. nov. can also be diagnosed from all other Okinawa group *Heptathela* species by the following unique nucleotide substitutions in the standard DNA barcode alignment: G (239), G (329), G (353), C (359), G (443), G (602), G (647).

Description. Female (Holotype). Carapace brown; opisthosoma light brown, with dark brown tergites close to each other; cheliceral groove with 12 pronounced denticles; six spinnerets. Measurements: BL 10.20, CL 4.89, CW 4.18, OL 4.90, OW 3.60; ALE > PLE > PME > AME; palp 8.25 (2.82 + 1.45 + 1.80 + 2.18), leg I 9.66 (3.10 + 1.70 + 1.81 + 1.90 + 1.15), leg II 8.90 (2.90 + 1.55 + 1.75 + 1.70 + 1.00), leg III 9.59 (2.81 + 1.65 + 1.60 + 2.13 + 1.40), leg IV 13.67 (4.25 + 2.00 + 2.00 + 3.54 + 1.88).

Female genitalia. A pair of depressions on the ventro-lateral part of the genital atrium (Fig. 17C, D). A pair of receptacular clusters along the anterior margin of bursa copulatrix, divided into two parts, with several granules; with short genital stalks (Fig. 17A–D).

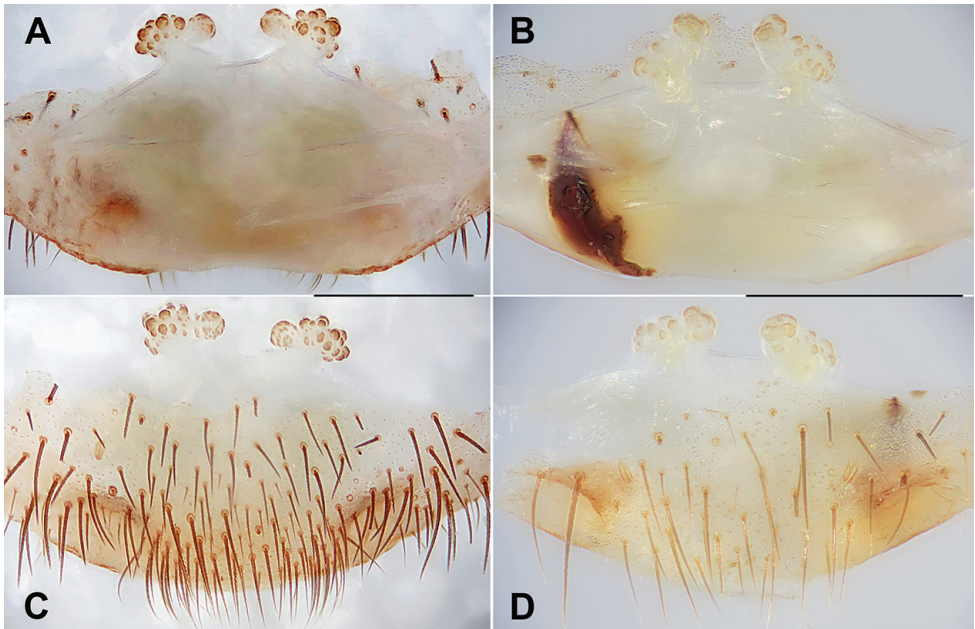


Figure 17. Female genital anatomy of *Heptathela kubayama* sp. nov. **A, C** 2486 (holotype, short for XUX-2012-486) **B, D** 2482 **A, B** vulva dorsal view **C, D** vulva ventral view. Scale bar: 0.5 mm.

Male. Unknown.

Etymology. The species epithet, a noun in apposition, refers to the type locality.

Distribution. The species is endemic to the Japanese island Iheyajima (Fig. 1C).

***Heptathela mae* sp. nov.**

<http://zoobank.org/45944FF0-D6B1-490B-ABCE-8CC5A933EDC3>

Fig. 18

Type material. *Holotype*: JAPAN · ♀; Okinawa-ken, Iheyajima Island, Mt. Mae-dake; 27.06N, 127.99E; alt. 10 m; 26 December 2012; D. Li, F.X. Liu and X. Xu leg.; XUX-2012-497.

Paratypes: JAPAN · 5 ♀♀; same data as for holotype; XUX-2012-494 to 496, 498, 500 · 3 ♀♀; Okinawa Prefecture, Iheyajima Island, Mt. Mae-dake; 27.06N, 127.99E; alt. 20 m; 10 May 2014; D. Li and B. Wu leg.; XUX-2014-079A to 079C.

Diagnosis. Females of *H. mae* sp. nov. can be distinguished from those of *H. aba* sp. nov. and *H. gayozan* sp. nov. by the lateral receptacular clusters being larger than the inner ones (Fig. 18B, D), and from those of *H. kubayama* sp. nov. by the receptacular clusters without short genital stalks (Fig. 18A–D). *Heptathela mae* sp. nov. can also be diagnosed from all other Okinawa group *Heptathela* species by the following unique nucleotide substitutions in the standard DNA barcode alignment: C (74), T (227), G (389), C (407), A (461), G (503), G (635).

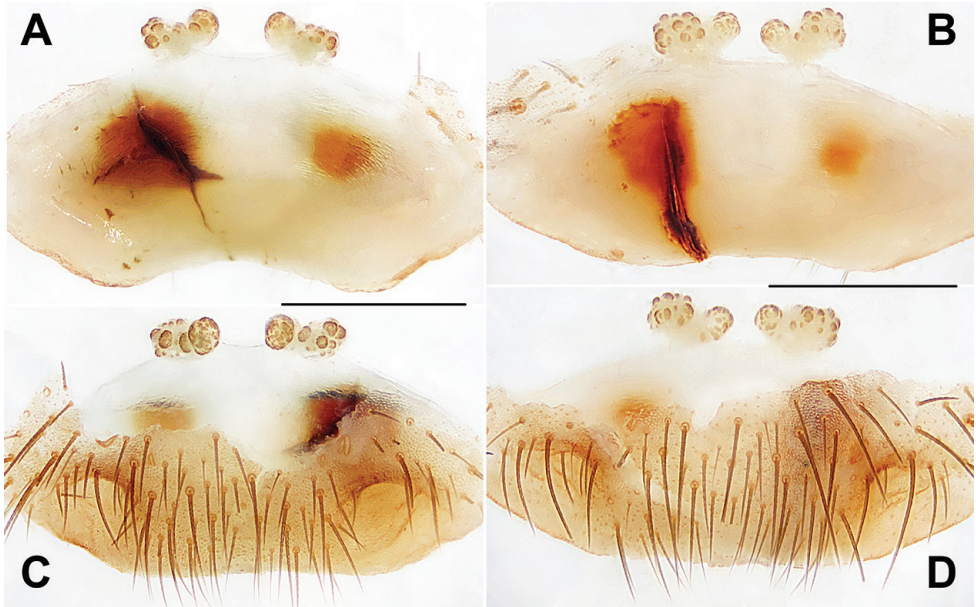


Figure 18. Female genital anatomy of *Heptathela mae* sp. nov. **A, C** 2497 (holotype, short for XUX-2012-497) **B, D** 4079B **A, B** vulva dorsal view **C, D** vulva ventral view. Scale bar: 0.5 mm.

Description. Female (Holotype). Carapace brown; opisthosoma brown, brown tergites with black plaques; cheliceral groove with 12 denticles; seven spinnerets. Measurements: BL 9.28, CL 4.48, CW 4.00, OL 5.12, OW 3.78; ALE > PLE > PME > AME; palp 7.80 (2.70 + 1.32 + 1.71 + 2.07), leg I 9.25 (3.00 + 1.52 + 1.80 + 1.78 + 1.15), leg II 8.55 (2.68 + 1.20 + 1.72 + 1.75 + 1.20), leg III 9.61 (2.75 + 1.60 + 1.55 + 2.31 + 1.40), leg IV 13.41 (3.90 + 1.70 + 2.31 + 3.60 + 1.90).

Female genitalia. A pair of depressions on the ventro-lateral part of the genital atrium (Fig. 18C, D). A pair of receptacular clusters along the anterior margin of bursa copulatrix, divided into two parts, with several granules, without genital stalks, the posterior part of genital area incurved (Fig. 18A–D).

Male. Unknown.

Etymology. The species epithet, a noun in apposition, refers to the type locality.

Distribution. The species is endemic to the Japanese island Iheyajima (Fig. 1C).

***Heptathela otoha* sp. nov.**

<http://zoobank.org/2C41220D-A64D-4750-9C99-D5F12FB4543E>

Fig. 19

Type material. Holotype: JAPAN · ♀; Okinawa-ken, Nakijin-son, Mt. Otoha-dake; 26.67N, 127.97E; alt. 80 m; 27 December 2012; D. Li, F.X. Liu and X. Xu leg.; XUX-2012-535.

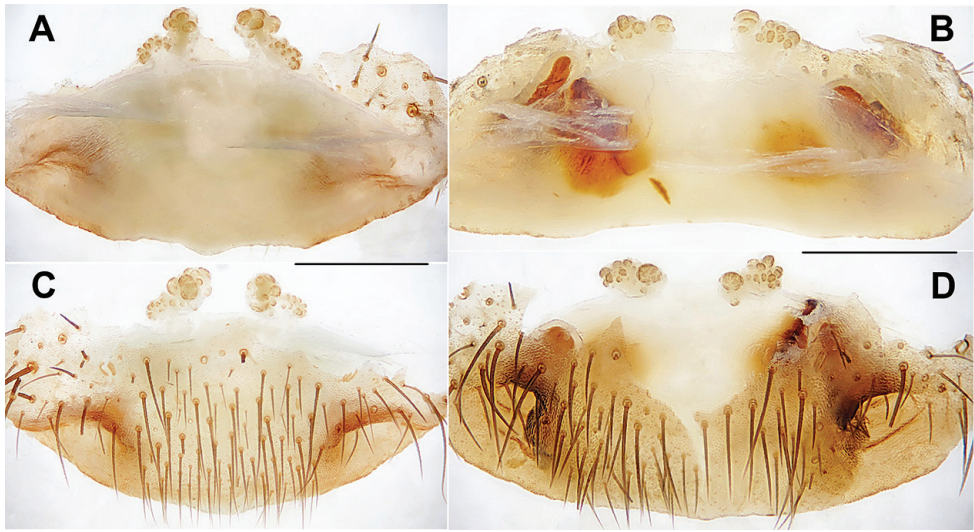


Figure 19. Female genital anatomy of *Heptathela otoa* sp. nov. **A, C** 2535 (holotype, short for XUX-2012-535) **B, D** 4094 **A, B** vulva dorsal view **C, D** vulva ventral view. Scale bar: 0.5 mm.

Paratypes: JAPAN · 3 ♀♀; Okinawa Prefecture, Motobu-cho, Yamazato; 26.67N, 127.91E; alt. 160 m; 11 May 2014; D. Li and B. Wu leg.; XUX-2014-094, 097, 099 · 3 ♀♀; Okinawa Prefecture, Nakijin-son, Mt. Otoa-dake; 26.67N, 127.97E; alt. 100 m; 11 May 2014; D. Li and B. Wu leg.; XUX-2014-101, 102, 103.

Diagnosis. Females of *H. otoa* sp. nov. can be distinguished from those of *H. yanbaruensis*, *H. unten* sp. nov., and *H. crypta* sp. nov. by the inner receptacular clusters with several granules, albeit these inner clusters are difficult to be separated from the laterals (Fig. 19A–D). *H. otoa* sp. nov. can also be diagnosed from all other Okinawa group *Heptathela* species by the following unique nucleotide substitutions in the standard DNA barcode alignment: G (83), G (206), G (488).

Description. Female (Holotype). Carapace yellow brown; opisthosoma light brown, with brown and black-spotted tergites; cheliceral groove with 13 pronounced denticles; seven spinnerets. Measurements: BL 10.92, CL 4.75, CW 4.35, OL 6.60, OW 4.90; ALE > PLE > PME > AME; palp 8.30 (2.78 + 1.39 + 1.90 + 2.23), leg I 9.80 (3.05 + 1.65 + 1.95 + 1.95 + 1.20), leg II 9.21 (2.90 + 1.50 + 1.81 + 1.90 + 1.10), leg III 9.84 (2.70 + 1.70 + 1.62 + 2.35 + 1.47), leg IV 14.74 (4.00 + 1.90 + 2.70 + 4.03 + 2.11).

Female genitalia. A pair of depressions on the ventro-lateral part of genital atrium (Fig. 19C, D). Paired receptacular clusters along the anterior margin of bursa copulatrix, divided into indistinct two parts, but difficulty to separate, both with several granules, with very short genital stalks (Fig. 19A–D).

Male. Unknown.

Etymology. The species epithet, a noun in apposition, refers to the type locality.

Distribution. The species is endemic to the Japanese island Okinawajima (Fig. 1C).

***Heptathela shuri* sp. nov.**

<http://zoobank.org/B74BEC88-F046-4583-80F3-E6BD2909BFAC>

Fig. 20

Type material. Holotype: JAPAN · ♀; Okinawa-ken, Naha, Shuri, Sueyoshi Park; 26.23N, 127.72E; alt. 45 m; 17 December 2012; D. Li, F.X. Liu and X. Xu leg.; XUX-2012-309.

Paratype: JAPAN · 1 ♀; same data as for holotype; XUX-2012-308.

Diagnosis. Females of *H. shuri* sp. nov. can be distinguished from those of *H. tokashiki* sp. nov. by paired receptacular clusters with larger granules (Fig. 20A–D). *Heptathela shuri* sp. nov. can also be diagnosed from all other Okinawa group *Heptathela* species by the following unique nucleotide substitutions in the standard DNA barcode alignment: G (89), G (131), C (134), C (396), C (510), C (512), A (524), T (641).

Description. Female (Holotype). Carapace yellow brown; opisthosoma brown, tergites with brown plaques; cheliceral groove with 12 pronounced denticles; seven spinnerets. Measurements: BL 10.78, CL 5.30, CW 4.12, OL 6.25, OW 4.40; ALE > PLE > PME > AME; palp 8.93 (3.15 + 1.43 + 2.03 + 2.32), leg I 10.91 (3.48 + 1.87 + 2.05 + 2.21 + 1.30), leg II 10.64 (3.18 + 1.85 + 1.86 + 2.28 + 1.47), leg III 11.26 (3.03 + 1.81 + 1.77 + 2.90 + 1.75), leg IV 17.02 (4.62 + 2.28 + 3.07 + 4.50 + 2.55).

Female genitalia. A pair of depressions on the ventro-lateral part of genital atrium (Fig. 20B, D). Paired receptacular clusters along the anterior margin of bursa copulatrix, divided into two parts, with several granules, the inner granules larger than laterals, both without genital stalks (Fig. 20A–D).

Male. Unknown.

Etymology. The species epithet, a noun in apposition, refers to the type locality.

Distribution. The species is endemic to the Japanese island Okinawajima (Fig. 1C).

***Heptathela tokashiki* sp. nov.**

<http://zoobank.org/A5A7B2B1-FE6F-4B42-AF06-48E7BDD937CB>

Fig. 21

Type material. Holotype: JAPAN · ♀; Okinawa-ken, Tokashikijima Island, Aharen; 26.19N, 127.37E; alt. 100 m; 8 May 2014; D. Li and B. Wu leg.; XUX-2014-062.

Paratypes: JAPAN · 25 ♀♀; same data as for holotype; XUX-2014-046 to 063D · 3 ♀♀; same data as for holotype; 27 December 2012; D. Li, F.X. Liu and X. Xu leg.; XUX-2012-417, 421, 425.

Diagnosis. Females of *H. tokashiki* sp. nov. can be distinguished from *H. shuri* sp. nov. by the long inner receptacular clusters with several granules (Fig. 21A–D). *Heptathela tokashiki* sp. nov. can also be diagnosed from all other Okinawa group

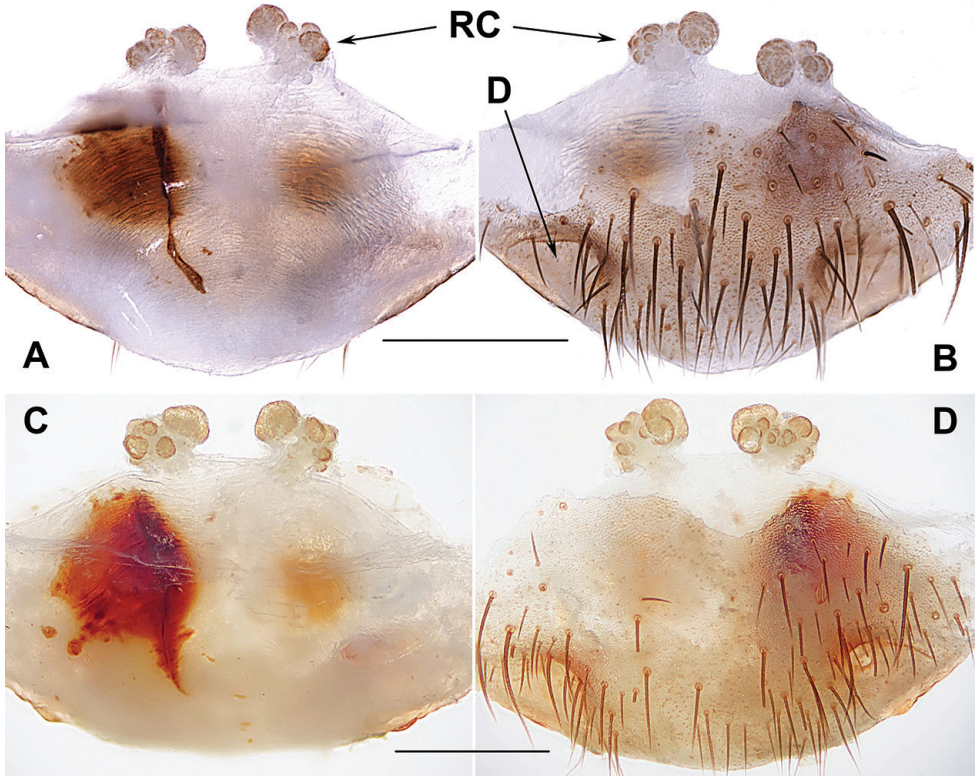


Figure 20. Female genital anatomy of *Heptathela shuri* sp. nov. **A, B** 2308 (short for XUX-2012-308) **C, D** 2309 (holotype) **A, C** vulva dorsal view **B, D** vulva ventral view. Scale bar: 0.5 mm.

Heptathela species by the following unique nucleotide substitutions in the standard DNA barcode alignment: T (68), A (200), C (290), A (362).

Description. Female (Holotype). Carapace brown; opisthosoma dark brown, with dark brown tergites close to each other; cheliceral groove with eleven pronounced denticles; seven spinnerets. Measurements: BL 11.80, CL 5.15, CW 4.10, OL 6.80, OW 5.10; ALE > PLE > PME > AME; palp 8.60 (3.05 + 1.50 + 1.95 + 2.10), leg I 10.50 (3.35 + 1.85 + 2.15 + 2.10 + 1.05), leg II 10.45 (3.40 + 1.75 + 2.00 + 2.20 + 1.10), leg III 10.95 (3.20 + 1.85 + 1.80 + 2.60 + 1.50), leg IV 15.70 (4.60 + 2.00 + 2.80 + 3.90 + 2.40).

Female genitalia. A pair of depressions on the ventro-lateral part of the genital atrium (Fig. 21B, D). Paired receptacular clusters along the anterior margin of bursa copulatrix, divided into two parts, the inners longer than the laterals, both with several granules, without genital stalks (Fig. 21A, B).

Male. Unknown.

Etymology. The species epithet, a noun in apposition, refers to the type locality.

Distribution. The species is endemic to the Japanese island Tokashikijima (Fig. 1C).

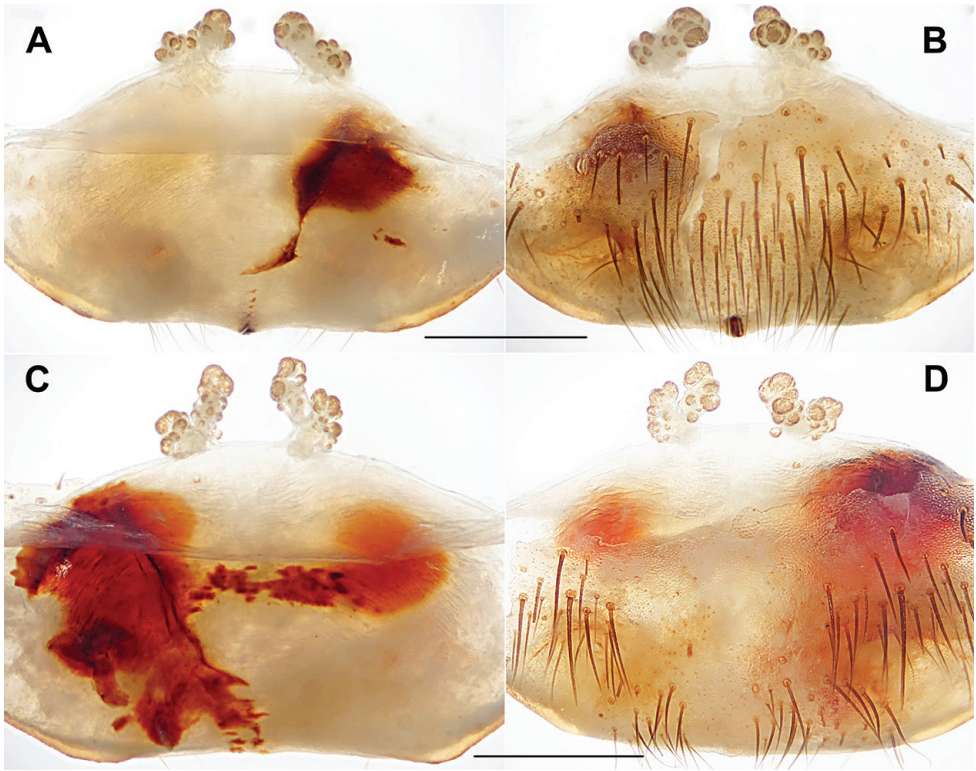


Figure 21. Female genital anatomy of *Heptathela tokashiki* sp. nov. **A, B** 4062 (holotype, short for XUX-2014-062) **C, D** 4063 **A, C** vulva dorsal view **B, D** vulva ventral view. Scale bar: 0.5 mm.

***Heptathela unten* sp. nov.**

<http://zoobank.org/65FF6B26-074B-4DC8-87F8-021268D23D87>

Figs 22, 23

Type material. Holotype: JAPAN · ♂; Okinawa-ken, Nakijin-son, Unten Port; 26.68N, 128.00E; alt. 25 m; 27 December 2012; D. Li, F.X. Liu and X. Xu leg.; XUX-2012-522.

Paratypes: JAPAN · 1 ♂, 2 ♀♀; same data as for holotype; XUX-2012-523, 527, 528A · 3 ♀♀; same data as for holotype; 10 May 2014; D. Li and B. Wu leg.; XUX-2014-083, 083A, 083B.

Diagnosis. Males of *H. unten* sp. nov. can be distinguished from those of *H. yanbaruensis* by the blunt tegular marginal apophysis (Fig. 22A, C, D); from those of *H. helios* by the conductor with serrated margin and small tegular marginal apophysis (Fig. 22A, C). Females of *H. unten* sp. nov. cannot be distinguished morphologically from those of *H. crypta* sp. nov. (Fig. 23A–L). However, *H. unten* sp. nov. can be diagnosed from all other Okinawa group *Heptathela* species by the following unique nucleotide substitutions in the standard DNA barcode alignment: G (482), C (635).

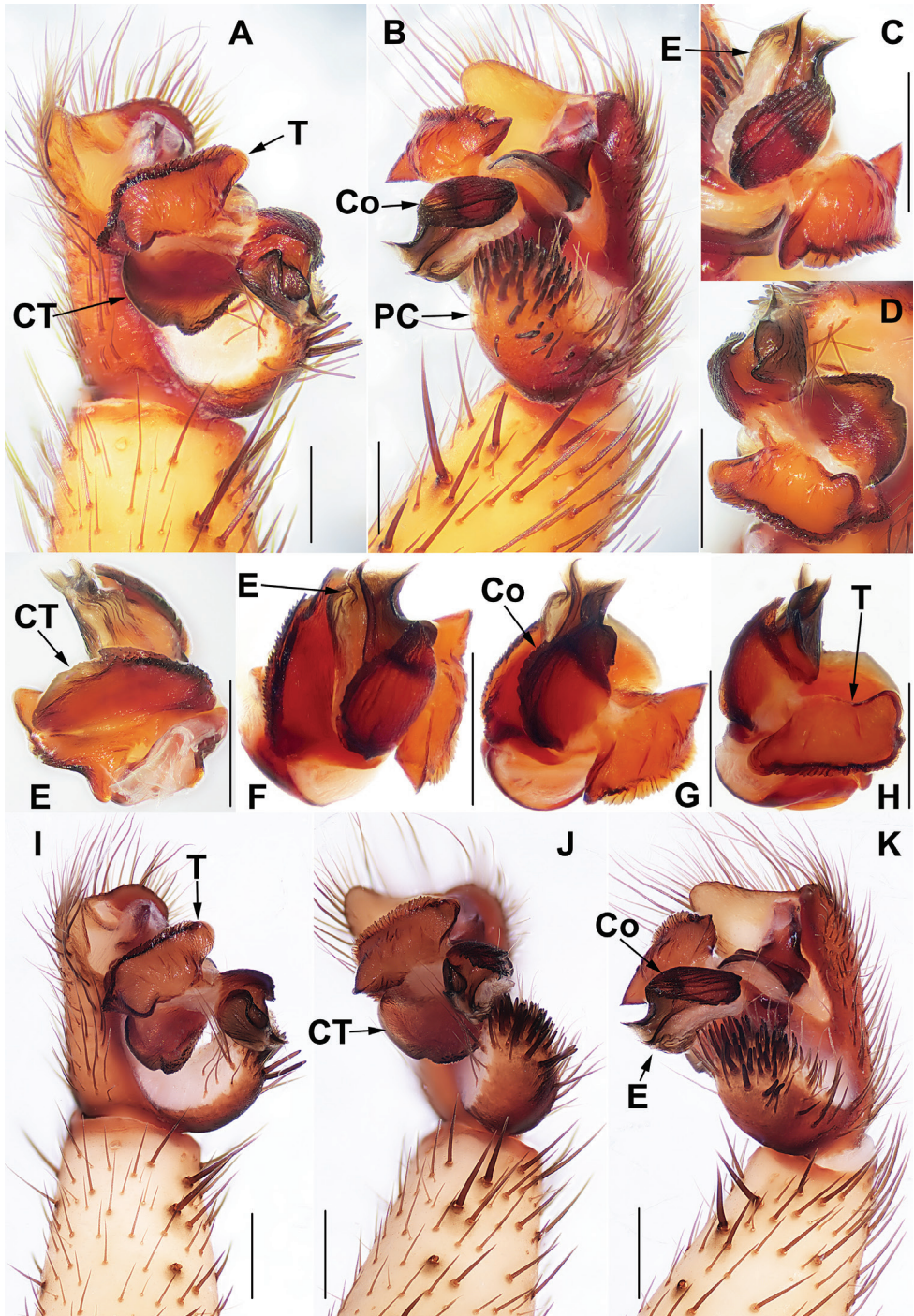


Figure 22. Male genital anatomy of *Heptathela unten* sp. nov. and *H. crypta* sp. nov. **A–D** *Heptathela unten* sp. nov., 2522 (holotype, short for XUX-2012-522) **E–K** *H. crypta* sp. nov. **E–H** 2328 (holotype) **I–K** 2460 **A, I** prolateral view **B, K** retrolateral view **J** ventral view **C–H** distal view; 2522: Unten Port, Okinawajima; 2328: Taira, Haneiji–Dam, Okinawajima; 2460: Yofuke, Okinawajima. Scale bar: 0.5 mm.

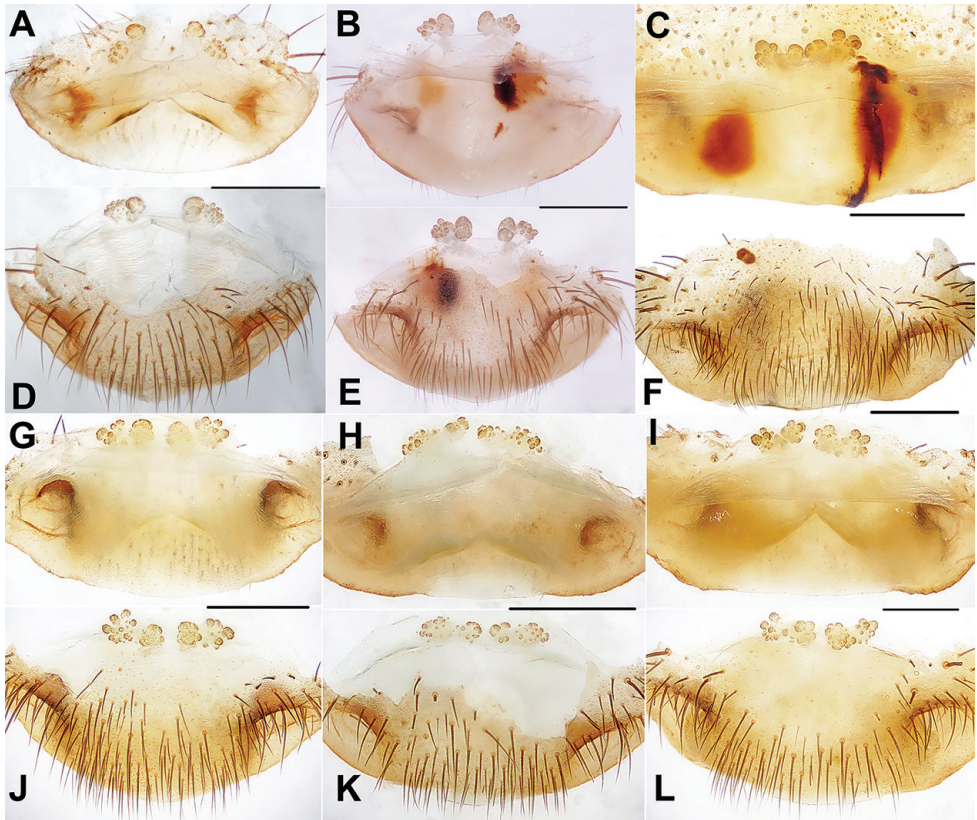


Figure 23. Female genital anatomy of *Heptathela unten* sp. nov. and *H. crypta* sp. nov. **A, D** 2527 **B, E** 4083A **C, F** 4027B **G, J** 2324 **H, K** 2327 **I, L** 2457 **A–C, G–I** dorsal view **D–F, J–L** ventral view; 2527, 4083A: Unten Port, Okinawajima; 4027B: Mt. Nago-dake, Okinawajima; 2324, 2327: Taira, Haneiji-Dam, Okinawajima; 2457: Yofuke, Okinawajima. Scale bar: 0.5 mm.

Description. Male (Holotype). Carapace yellow brown; opisthosoma brown, with dark brown tergites close to each other; cheliceral groove with ten denticles; seven spinnerets. Measurements: BL 10.00, CL 5.05, CW 4.60, OL 4.60, OW 2.90; ALE > PLE > PME > AME; leg I 15.71 (4.48 + 1.93 + 3.30 + 4.00 + 2.00), leg II 16.59 (4.45 + 1.90 + 3.37 + 4.62 + 2.25), leg III 18.29 (4.50 + 1.93 + 3.58 + 5.53 + 2.75), leg IV 23.40 (5.82 + 2.28 + 4.52 + 7.30 + 3.48).

Palp. Prolateral side of paracymbium unpigmented and unsclerotised, numerous setae and spines at the tip of paracymbium (Fig. 22A, B). Contrategulum margin incurved nearly in the middle and the contrategulum divided into proximally serrated and distally smooth margins (Fig. 22A, D). Tegulum with wide dorsal extension of terminal apophysis (Fig. 22C, D), blunt terminal and small marginal apophysis (Fig. 22A, C, D). Conductor sclerotised and ovate, prolateral conductor with one or two shallow folds, and with a serrated margin (Fig. 22B, C). Embolus sclerotised, with a wide opening, the distal margin slightly sclerotised, and with a saddle-shaped margin in the retrolateral view (Fig. 22B, C).

Females ($N = 5$). Carapace and opisthosoma colour as in male, dark brown tergites separated from each other; cheliceral groove with 12 or 13 pronounced denticles; seven or eight spinnerets. Measurements: BL 7.81–12.00, CL 3.60–4.55, CW 3.30–4.40, OL 4.10–7.60, OW 3.00–6.20; ALE > PLE > PME > AME; palp 6.64 (2.19 + 1.22 + 1.45 + 1.78), leg I 7.48 (2.47 + 1.35 + 1.22 + 1.52 + 0.92), leg II 7.40 (2.21 + 1.30 + 1.21 + 1.65 + 1.03), leg III 7.79 (2.11 + 1.38 + 1.20 + 1.90 + 1.20), leg IV 11.55 (3.20 + 1.55 + 2.10 + 3.05 + 1.65).

Female genitalia. A pair of depressions on the ventro-lateral part of genital atrium indistinct (Fig. 23D, E). Paired receptacular clusters along the anterior margin of bursa copulatrix, divided into two parts, the inners similar or smaller than the laterals, paired receptacular clusters tuberculate, inners with or without genital stalks (Fig. 23A, B, D, E).

Etymology. The species epithet, a noun in apposition, refers to the type locality, Unten Port.

Distribution. The species is endemic to the Japanese island Okinawajima (Fig. 1C).

***Heptathela crypta* sp. nov.**

<http://zoobank.org/62DDDCB8-8B43-4EFC-B42C-9BAA1E114A23>

Figs 22, 23

Type material. Holotype: JAPAN · ♂; Okinawa-ken, Nago-shi, Haneiji-Dam, Taira; 26.59N, 128.03E; alt. 100 m; 18 December 2012; D. Li, F.X. Liu and X. Xu leg.; XUX-2012-328.

Paratypes: JAPAN · 1 ♂, 3 ♀♀; same data as for holotype; XUX-2012-324, 326, 327, 333A · 2 ♂♂, 4 ♀♀; Okinawa Prefecture, Nago-shi, County Road 18 south, Nago/Yofuke; 26.57N, 128.01E; alt. 150 m; 24 December 2012; D. Li, F.X. Liu and X. Xu leg.; XUX-2012-457 to 462 · 3 ♀♀; Okinawa Prefecture, Nago-shi, Mt. Nago-dake; 26.58N, 128.01E; alt. 220 m; 06 May 2014; D. Li and B. Wu leg.; XUX-2014-027 to 027B.

Diagnosis. Males and females of *H. crypta* sp. nov. cannot be distinguished morphologically from *H. unten* sp. nov. (Figs 22A–K, 23A–L), but can be diagnosed from *H. unten* sp. nov. by the following unique nucleotide substitutions in the standard DNA barcode alignment: C (26), A (32), C (50), T (60), T (110), G (153), T (194), C (197), T (269), C (281), T (284), C (338), A (341), T (357), C (416), T (428), C (458), A (482), T (488), G (551), T (581), T (635), G (638), G (641), C (644), C (656), as well as from all other Okinawa group *Heptathela* species by the following unique nucleotide substitutions in the standard DNA barcode alignment: C (26), T (110), G (551), C (656).

Description. Male (Holotype). Carapace and opisthosoma description see *H. unten* sp. nov.; cheliceral groove with nine denticles of variable size; seven spinnerets. Measurements: BL 7.88, CL 4.01, CW 3.51, OL 4.23, OW 3.18; ALE > PLE > PME > AME; leg I 10.15 (3.60 + 1.50 + 2.38 + 1.00 + 1.67), leg II 13.08 (3.48 + 1.58 + 2.49 + 3.53 + 2.00), leg III 14.27 (3.38 + 1.55 + 2.65 + 4.30 + 2.39), leg IV 18.19 (4.45 + 1.63 + 3.50 + 5.50 + 3.11).

Palp. Prolateral side of paracymbium unpigmented and unsclerotised, numerous setae and spines at the tip of paracymbium (Fig. 22I–K). Contrategulum margin incurved nearly in the middle, and the contrategulum divided into proximally serrated and distally smooth (Fig. 22E, F, I, J). Tegulum with wide dorsal extension of terminal apophysis (Fig. 22G, H, J), blunt terminal and small marginal apophysis (Fig. 22H, I). Conductor sclerotised and ovate, prolateral conductor with one or two shallow folds, and with a serrated margin (Fig. 22F, G, K). Embolus sclerotised, with a wide opening, the distal margin slightly sclerotised, and with a saddle-shaped margin in the retrolateral view (Fig. 22F, G, K).

Females ($N = 10$). Carapace and opisthosoma description see *H. unten* sp. nov.; chelicerae with promargin of cheliceral groove with 13–14 pronounced denticles of variable size; seven spinnerets. Measurements: BL 8.35–16.50, CL 4.07–5.10, CW 3.30–4.80, OL 4.70–6.80, OW 3.00–5.20; ALE > PLE > PME > AME; palp 7.70 (2.87 + 1.13 + 1.68 + 2.02), leg I 9.57 (3.07 + 1.70 + 1.70 + 1.98 + 1.12), leg II 9.64 (2.95 + 1.68 + 1.61 + 2.08 + 1.32), leg III 9.60 (2.68 + 1.69 + 1.50 + 2.30 + 1.43), leg IV 14.21 (4.00 + 1.92 + 2.55 + 3.83 + 1.91).

Female genitalia. A pair of depressions on the ventro-lateral part of genital atrium indistinct (Fig. 23F, J–L). Paired receptacular clusters along the anterior margin of bursa copulatrix, divided into two parts, the inners similar or smaller than the laterals, paired receptacular clusters tuberculate, without genital stalks (Fig. 23C, G–L).

Etymology. The species epithet, a noun in apposition, refers to the cryptic nature of this species discovery.

Distribution. The species is endemic to the Japanese island Okinawajima (Fig. 1C).

Species not assigned to a group

Heptathela helios Tanikawa & Miyashita, 2014

Fig. 24

Heptathela helios Tanikawa & Miyashita, 2014: 68 (holotype: male (NSMT-Ar 12851), from Kunigami-son, Okinawajima, Japan, collected by A. Tanikawa on 26 May 2010, matured on 9 September 2012, deposited in NMNS, examined).

Diagnosis. Males of *H. helios* can be distinguished from those of all other Okinawa group *Heptathela* species by the serrated contrategulum margin and the hooked tegular marginal apophysis, the ovate, indistinctly rugose conductor with a poorly serrated margin (Fig. 24D–G). Females of *H. helios* can be distinguished from those of all other *Heptathela* species by the receptacular clusters with the inner ones being smaller than the laterals, and the laterals with numerous small granulate tubercula (Fig. 24H–M). *H. helios* can also be diagnosed from all other Okinawa group *Heptathela* species by the following unique nucleotide substitutions in the standard DNA barcode alignment: T (11), T (35), G (47), A (56), C (59), A (95), T (104), A (131), T (140), T (179),

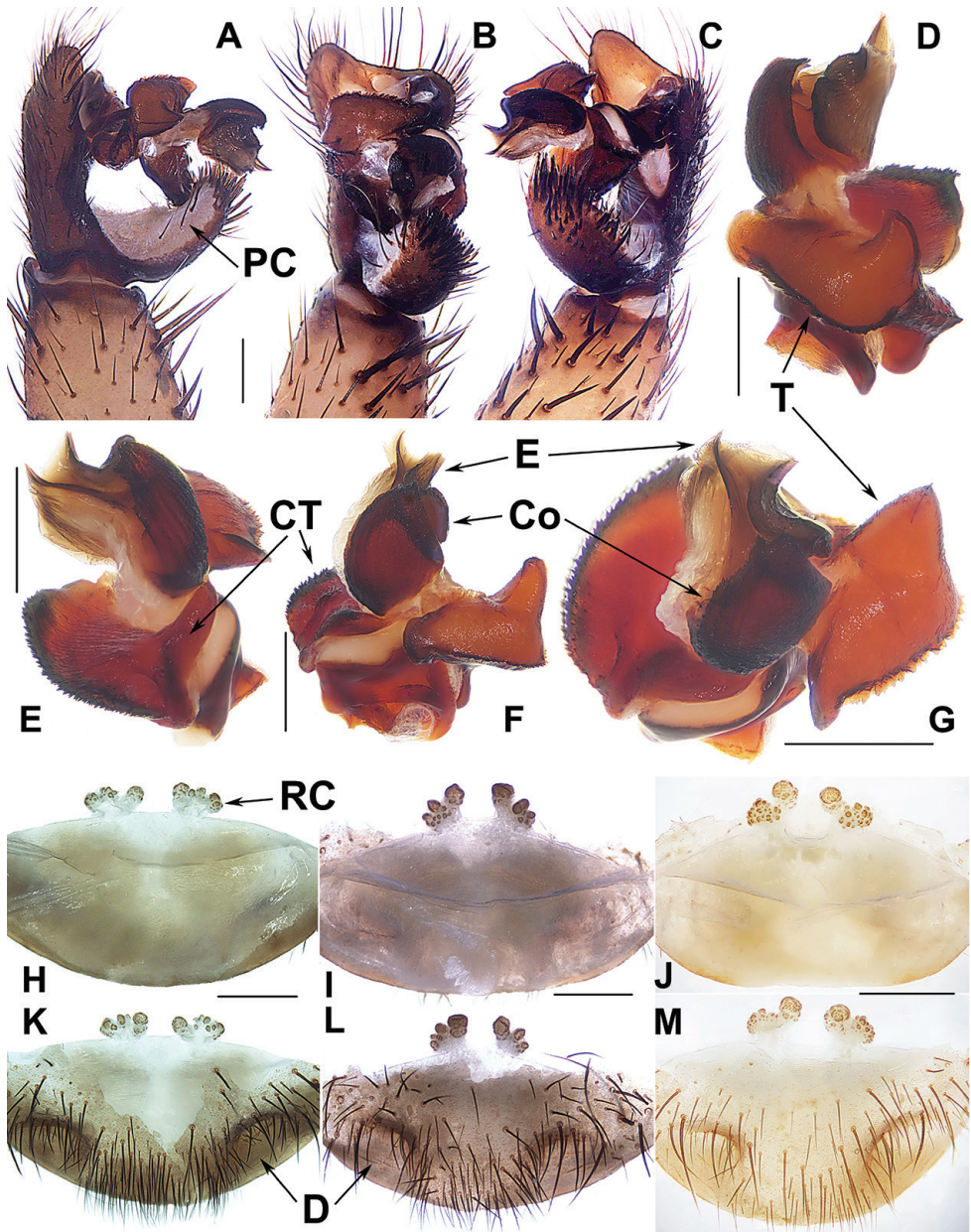


Figure 24. Male and female genital anatomy of *Heptathela helio* Tanikawa & Miyashita, 2014 **A-G** 2440A (short for XUX-2012-440A) **H, K** 2432 **I, L** 2434 **J, M** 2437 **A** palp prolateral view **B** palp ventral view **C** palp retrolateral view **D-G** palp distal view **H-J** vulva dorsal view **K-M** vulva ventral view. Scale bar: 0.5 mm.

C (188), C (215), G (221), C (242), C (266), C (273), C (299), C (300), C (304), T (359), G (380), T (413), A (422), T (425), T (431), G (479), G (480), G (491), G (506), C (543), T (546), G (548), C (551), C (596), T (662).

Description. Male. Carapace and opisthosoma brown, with dark brown tergites; cheliceral groove with 14 denticles; tergites closed to each other; seven spinnerets. Measurements: BL 9.88, CL 5.30, CW 4.81, OL 4.58, OW 2.92; ALE > PLE > PME > AME; leg I 16.56 (4.55 + 1.90 + 3.48 + 4.33 + 2.30), leg II 17.19 (4.50 + 2.00 + 3.34 + 4.68 + 2.67), leg III 18.35 (4.35 + 1.97 + 3.40 + 5.53 + 3.10), leg IV 23.37 (5.52 + 2.10 + 4.47 + 7.48 + 3.80).

Palp. The bulb of the two male specimens relatively distorted. Prolateral side of paracymbium unpigmented and unsclerotised, numerous setae and spines at the tip of paracymbium (Fig. 24A–C). Contrategulum with a serrated margin (Fig. 24E, G). Tegulum with a dentate dorsal extension of terminal apophysis (Fig. 24F, G), blunt terminal and hook-like marginal apophysis (Fig. 24D, F, G). Conductor sclerotised, ovate, and wide, with indistinct rugae (Fig. 24E–G). Embolus sclerotised, with a wide opening, the distal margin slightly sclerotised, and with a saddle-shaped margin in the retrolateral view (Fig. 24D–G).

Females ($N = 7$). Carapace and opisthosoma colour as in male; cheliceral groove with 12–14 pronounced denticles; opisthosoma with 12 well-separated tergites; seven spinnerets. Measurements: BL 11.70–14.45, CL 5.29–6.70, CW 4.29–5.81, OL 6.54–8.18, OW 4.70–6.63; ALE > PLE > PME > AME; palp 12.29 (4.20 + 2.03 + 2.63 + 3.43), leg I 14.31 (4.51 + 2.40 + 2.65 + 3.08 + 1.67), leg II 14.04 (4.25 + 2.35 + 2.53 + 3.11 + 1.80), leg III 13.75 (3.92 + 2.40 + 2.48 + 2.67 + 2.28), leg IV 21.77 (5.90 + 2.88 + 3.75 + 6.11 + 3.13).

Female genitalia. A pair of depressions on the ventro-lateral part of genital atrium (Fig. 24K–M). Paired receptacular clusters along the anterior margin of bursa copulatrix, divided into two parts, inner receptacular clusters smaller than laterals, laterals with several small tubercula, with short genital stalks (Fig. 24H–M).

Remarks. We identified the specimens collected from Ginama Dam, Okinawa, as *H. helios* based on evidence from morphology and COI barcode genetic distance compared with the male holotype and paratype (NSMT-Ar 12851, NSMT-Ar 12855) of *H. helios* in Tanikawa and Miyashita (2014). K2P and *p*-distances between Ginama Dam specimens and the holotype (NSMT-Ar 12851) were 3.2–3.4% and 3.1–3.3%, respectively, and those between Ginama Dam specimens and the paratype (NSMT-Ar 12855) were 1.8–2.1% and 1.7–2.1%, respectively.

Material examined. JAPAN · 2 ♂♂, 8 ♀♀; Okinawa-ken, Kunigami-son, Ginama Dam; 26.84N, 128.26E; alt. 150 m; 24 December 2012; D. Li, F.X. Liu and X. Xu leg.; XUX-2012-432 to 440C.

Distribution. The species is endemic to the Japanese island Okinawajima (Fig. 1C).

Acknowledgements

We thank Zoltán Korsós, Mamoru Toda, and Bo Wu for assistance in the field, and the staff of the Centre for Behavioural Ecology and Evolution (CBEE, Hubei University) for all their help and support throughout this study. We acknowledge constructive and

insightful comments on the manuscript from Ingi Agnarsson, Jason Bond, Rebecca Godwin, and Xiang Xu. We thank Gonzalo Giribet, Laura Leibensperger, Stefan Friedrich, Danilo Harms, and Jason A. Dunlop for information on the types and for facilitating loans. This study was supported in part by the grants from National Natural Sciences Foundation of China (NSFC-31601850; NSFC-31272324), the Hunan Provincial Natural Science Foundation of China (2017JJ3202), Singapore Ministry of Education AcRF Tier 1 grant (R-154-000-A52-114) to DL, the Japan Society of Promotion of Science (JSPS-21540487), the Slovenian Research Agency (P1-10236 and J1-6729), and the bilateral inter-governmental S&T exchange project between China and Slovenia (12-8).

References

- Bristowe WS (1933) The liphistiid spiders. With an appendix on their internal anatomy by J. Millot. Proceedings of Zoological Society of London 1932: 1015–1057. <https://doi.org/10.1111/j.1096-3642.1932.tb01575.x>
- Bao YH, Yin CM, Xu X (2003) A new species of the genus *Heptathela* from China (Araneae, Liphistiidae). Acta Zootaxonomica Sinica 28: 459–460.
- Bishop SC, Crosby CR (1932) A new species of the spider family Liphistiidae from China. Peking Natural History Bulletin 6(3): 5–7.
- Brower AVZ (2010) Alleviating the taxonomic impediment of DNA barcoding and setting a bad precedent: names for ten species of '*Astraptus fulgurator*' (Lepidoptera: Hesperidae: Eudaminae) with DNA-based diagnoses. Systematics and Biodiversity 8: 485–491. <https://doi.org/10.1080/14772000.2010.534512>
- Chen XE, Gao JC, Zhu CD, Luo ZM (1988) A new species of the genus *Heptathela* from China (Araneae: Heptathelidae). Sichuan Journal of Agricultural Science 1988: 78–81.
- Chen ZF, Zhang ZH, Zhu CD (1981) A new species of genus *Heptathela*. Journal of Hangzhou University 8: 305–308.
- Chikuni Y (1989) Pictorial Encyclopedia of Spiders in Japan. Kaisei-sha Publishing Co., Tokyo, 310 pp.
- Cook LG, Edwards RD, Crisp MD, Hardy NB (2010) Need morphology always be required for new species descriptions? Invertebrate Systematics 24: 322–326. <https://doi.org/10.1071/IS10011>
- Dunlop JA, Steffensen C, Ono H (2014) Mesothel spiders in the Museum für Naturkunde Berlin. Arachnologische Mitteilungen 47: 35–40. <https://doi.org/10.5431/aramit4705>
- Gertsch WJ (1967) A new liphistiid spider from China (Araneae: Liphistiidae). Journal of The New York Entomological Society 75: 114–118.
- Gertsch WJ, Platnick NI (1979) A revision of the spider family Mecicobothriidae (Araneae, Mygalomorphae). American Museum Novitates 2687: 1–32.
- Haupt J (1979) Lebensweise und Sexualverhalten der mesothelen Spinne *Heptathela nishihirai* n. sp. (Araneae, Liphistiidae). Zoologischer Anzeiger 202: 348–374.
- Haupt J (1983) Vergleichende Morphologie der Genitalorgane und Phylogenie der liphistiomorphen Webspinnen (Araneae: Mesothelae). I. Revision der bisher bekannten Arten.

- Zeitschrift Fur Zoologische Systematik Und Evolutionsforschung 21: 275–293. <https://doi.org/10.1111/j.1439-0469.1983.tb00296.x>
- Haupt J (1984) Comportement sexuel, morphologie génitale et phylogénèse des araignées liphistiomorphes. *Revue Arachnologique* 5(4): 161–168.
- Haupt J (2003) The Mesothelaeae – monograph of an exceptional group of spiders (Araneae: Mesothelaeae) (Morphology, behaviour, ecology, taxonomy, distribution and phylogeny). *Zoologica* 154: 1–102.
- Kishida K (1920) *Zoological Magazine*. Tokyo 32: 1–362. [no English title]
- Kishida K (1923) *Heptathela*, a new genus of liphistiid spiders. *Annotationes Zoologicae Japonenses* 10: 235–242.
- Ono H (1996) Two new species of the families Liphistiidae and Thomisidae (Araneae) from the Ryukyu Islands, southwest Japan. *Acta Arachnologica Tokyo* 45: 157–162. <https://doi.org/10.2476/asjaa.45.157>
- Ono H (1997) A new species of the genus *Heptathela* (Araneae: Liphistiidae) from Vietnam. *Acta Arachnologica* 46: 23–28. <https://doi.org/10.2476/asjaa.46.23>
- Ono H (1998) Spiders of the genus *Heptathela* (Araneae, Liphistiidae) from Kyushu, Japan. *Memoirs of the National Science Museum Tokyo* 30: 13–27.
- Ono H (1999) Spiders of the genus *Heptathela* (Araneae, Liphistiidae) from Vietnam, with notes on their natural history. *Journal of Arachnology* 27: 37–43. <https://doi.org/10.1080/096708799228085>
- Ono H (2010) Four new spiders (Arachnida, Araneae) of the families Liphistiidae, Ctenizidae, Araneidae and Ctenidae from Vietnam. *Memoirs of the National Museum of Nature and Science Tokyo* 46: 1–12.
- Ono H (2002) New and remarkable spiders of the families Liphistiidae, Argyronetidae, Pisauridae, Theridiidae and Araneidae (Arachnida) from Japan. *Bulletin of the National Museum of Nature and Science Tokyo (A)* 28: 51–60.
- Ono H (2009) The spiders of Japan with keys to the families and genera and illustrations of the species. Tokai University Press, Kanagawa, 739 pp.
- Ono H, Nishikawa Y (1989) Taxonomic revision of the heptathelid spider (Araneae, Mesothelaeae) from Amami-ôshima Island, the Ryukyus. *Memoirs of the National Science Museum Tokyo* 22: 119–125.
- Ono H, Ogata K (2018) Spiders of Japan, their natural history and diversity. Tokai University Press, Kanagawa, 714 pp.
- Planas E, Ribera C (2015) Description of six new species of *Loxosceles* (Araneae: Sicariidae) endemic to the Canary Islands and the utility of DNA barcoding for their fast and accurate identification. *Zoological Journal of the Linnean Society* 174: 47–73. <https://doi.org/10.1111/zoj.12226>
- Sawaguti Y, Ozi Y (1937) On *Heptathela kimurai* (Kishida, 1920). *Acta Arachnologica* 2: 115–123. <https://doi.org/10.2476/asjaa.2.115>
- Schenkel E (1953) Chinesische Arachnoidea aus dem Museum Hoangho-Peiho in Tientsin. *Boletim do Museu Nacional do Rio de Janeiro (N.S., Zool.)* 119: 1–108.
- Schiödte JC (1849) Om en afigende sloegt af spindlernes orden. *Naturhistorisk Tidsskrift* 2: 617–624.

- Schwendinger PJ, Ono H (2011) On two *Heptathela* species from southern Vietnam, with a discussion of copulatory organs and systematics of the Liphistiidae (Araneae: Mesothelae). *Revue suisse de Zoologie* 118: 599–637. <https://doi.org/10.5962/bhl.part.117818>
- Song DX, Haupt J (1984) Comparative morphology and phylogeny of liphistiomorph spiders (Araneae: Mesothelae) 2. Revision of new Chinese heptathelid species. *Verhandlungen des Naturwissenschaftlichen Vereins in Hamburg* 27: 443–451.
- Song DX, Wu KY (1997) On a new species of the genus *Heptathela* (Araneae: Liphistiidae) from Hong Kong, China. *Chinese Journal of Zoology* 32: 1–3.
- Tanikawa A (2013) Taxonomic revision of the spider genus *Ryuthela* (Araneae: Liphistiidae). *Acta Arachnologica* 62: 33–40. <https://doi.org/10.2476/asjaa.62.33>
- Tanikawa A, Miyashita T (2014) Discovery of a cryptic species of *Heptathela* from the northernmost part of Okinawajima Is., Southwest Japan, as revealed by mitochondrial and nuclear DNA. *Acta Arachnologica* 63(2): 65–72. <https://doi.org/10.2476/asjaa.63.65>
- Wang HZ, Jiao YC (1995) A new species of the family [sic] *Heptathela* in China. *Journal of Yunan Normal University* 15(1): 80–81.
- Wang JF (1989) A new species of spider of the genus *Liphistius* from south China (Araneae: Liphistiidae). *Acta Zootaxonomica Sinica* 14: 30–32.
- World Spider Catalog (2019) World Spider Catalog. Natural History Museum Bern. <http://wsc.nmbe.ch>, version 20.0. [accessed on 12 July 2019]
- Xu X, Liu FX, Cheng RC, Chen J, Xu X, Zhang ZS, Ono H, Pham DS, Norma-Rashid Y, Arnedo MA, Kuntner M, Li D (2015a) Extant primitively segmented spiders have recently diversified from an ancient lineage. *Proceedings of the Royal Society of London B* 282: 20142486. <https://doi.org/10.1098/rspb.2014.2486>
- Xu X, Liu FX, Chen J, Ono H, Li D, Kuntner M (2015b) A genus-level taxonomic review of primitively segmented spiders (Mesothelae: Liphistiidae). *ZooKeys* 488: 121–151. <https://doi.org/10.3897/zookeys.488.8726>
- Xu X, Liu FX, Chen J, Li D, Kuntner M (2015c) Integrative taxonomy of the primitively segmented spider genus *Ganthela* (Araneae: Mesothelae: Liphistiidae) – DNA barcoding gap agrees with morphology. *Zoological Journal of the Linnean Society* 175: 288–306. <https://doi.org/10.1111/zoj.12280>
- Xu X, Liu FX, Chen J, Ono H, Li D, Kuntner M (2016) Pre-Pleistocene geological events shaping diversification and distribution of primitively segmented spiders on East Asian Margins. *Journal of Biogeography* 43: 1004–1019. <https://doi.org/10.1111/jbi.12687>
- Xu X, Liu FX, Ono H, Chen J, Kuntner M, Li D (2017) Targeted sampling in Ryukyus facilitates species delimitation of the primitively segmented spider genus *Ryuthela* (Araneae: Mesothelae: Liphistiidae). *Zoological Journal of the Linnean Society* 181(4): 867–909. <https://doi.org/10.1093/zoolinlean/zlx024>
- Xu X, Kuntner M, Ono H, Liu FX, Li D (2019) A multi-tier species delimitation approach resolves conflicts in delineating the primitively segmented spider genus *Heptathela* endemic to Japanese islands. *bioRxiv*. <https://doi.org/10.1101/812214>
- Xu X, Yin CM (2001) A new species of the genus *Heptathela* from China (Araneae: Liphistiidae). *Acta Arachnologica Sinica* 10(1): 8–10.
- Yaginuma T (1954) Synopsis of Japanese spiders (1). *Atypus* 5: 13–24.

- Yaginuma T (1955) The development of araneology in Japan. Annual Report of the Otemon Gakuin University 1: 25–41.
- Yaginuma T (1960) Spiders of Japan in colour. Hoikusha, Osaka, 186 pp.
- Yaginuma T (1971) Spiders of Japan in colour (enlarged and revised edition). Hoikusha, Osaka (for 1969), 197 pp.
- Yaginuma T (1979) *Heptathela nishibirai* Haupt, 1979 from Okinawa. Atypus 75: 1–2.
- Yaginuma T (1980) A supplementary note on “*Heptathela nishibirai*” (Araneae: Heptathelidae). Atypus 76: 44–45.
- Yaginuma T (1986) *Spiders of Japan in color* (new edn.). Hoikusha Publishing Co., Osaka, 305 pp. [64 pls.]
- Yin CM (2001) A new species of the genus *Heptathela* and its variant type from China (Araneae: Liphistiidae). Acta Zootaxonomica Sinica 26: 297–300.
- Yin CM, Tang G, Xu X (2003) Two new species of the genus *Heptathela* from China (Araneae: Liphistiidae). Acta Arachnologica Sinica 12: 1–5.
- Yin CM, Tang G, Zhao JZ, Chen J (2002) Two new species of the genus *Heptathela* from China (Araneae: Liphistiidae). Acta Arachnologica Sinica 11: 18–21.
- Yoo JC, Kim JP (2002) Studies on basic pattern and evolution of male palpal organ (Arachnida: Araneae). Korean Arachnology 18: 13–31.
- Yoshikura M (1955) Embryological studies on the liphistiids spider *Heptathela kimurai*. Part II. Kumamoto Journal of Science B 2: 1–86.
- Yoshikura M (1983) Sexual characters in a liphistiid spider, *Heptathela kimurai* (Araneae: Heptathelidae). Heptathela 2: 63–73.
- Yoshikura M (1987) The biology of spiders. Japan Scientific Societies Press, Tokyo, 613 pp.
- Zhu CD, Wang YW (1984) A new species of genus *Liphistius* (Araneae: Liphistiidae). Journal of the Bethune Medical University 10: 251–253.

Supplementary material I

Table S1

Authors: Xin Xu, Hirotsugu Ono, Matjaž Kuntner, Fengxiang Liu, Daiqin Li

Data type: species data

Copyright notice: This dataset is made available under the Open Database License (<http://opendatacommons.org/licenses/odbl/1.0/>). The Open Database License (ODbL) is a license agreement intended to allow users to freely share, modify, and use this Dataset while maintaining this same freedom for others, provided that the original source and author(s) are credited.

Link: <https://doi.org/10.3897/zookeys.888.34494.suppl1>

Two new species of *Polydesmus* Latreille, 1802/1803 from northern Spain with reinstatements of two species, and a key to the Iberian *Polydesmus* species (Diplopoda, Polydesmida, Polydesmidae)

Per Djursvoll¹

¹ Department of Natural History, University Museum of Bergen, Allégaten 41, 5007 Bergen, Norway

Corresponding author: Per Djursvoll (per.djursvoll@uib.no)

Academic editor: D. Vanden Spiegel | Received 1 July 2019 | Accepted 26 September 2019 | Published 11 November 2019

<http://zoobank.org/C420CD3B-9C79-45D1-97CC-FA8C59D5D9EB>

Citation: Djursvoll P (2019) Two new species of *Polydesmus* Latreille, 1802/1803 from northern Spain with reinstatements of two species, and a key to the Iberian *Polydesmus* species (Diplopoda, Polydesmida, Polydesmidae). ZooKeys 888: 51–65. <https://doi.org/10.3897/zookeys.888.37816>

Abstract

Polydesmus biscayensis **sp. nov.** and *P. asturiensis* **sp. nov.** are described and figured based on material housed in the Museo Nacional de Ciencias Naturales in Madrid. The specimens were collected in six localities in the Asturias and Cantabria provinces, including four caves. In addition, *Polydesmus haroi* Mauriès & Vicente, 1977 and *Polydesmus racovitzaei* Brolemann, 1910 are transferred from *Propolydesmus* Verhoeff, 1895 to *Polydesmus* Latreille, 1802/1803 after examining the gonopod morphology. A key to the Iberian *Polydesmus* species is presented.

Keywords

Asturias, Cantabria, cave, millipede, *Propolydesmus*, taxonomy

Introduction

The Holarctic family Polydesmidae comprises of more than 240 occurring species, with 192 recorded in Europe (Kime and Enghoff 2011; Enghoff et al. 2015). Most species belong to the genera *Polydesmus* Latreille, 1802/1803 and *Brachydesmus* Heller,

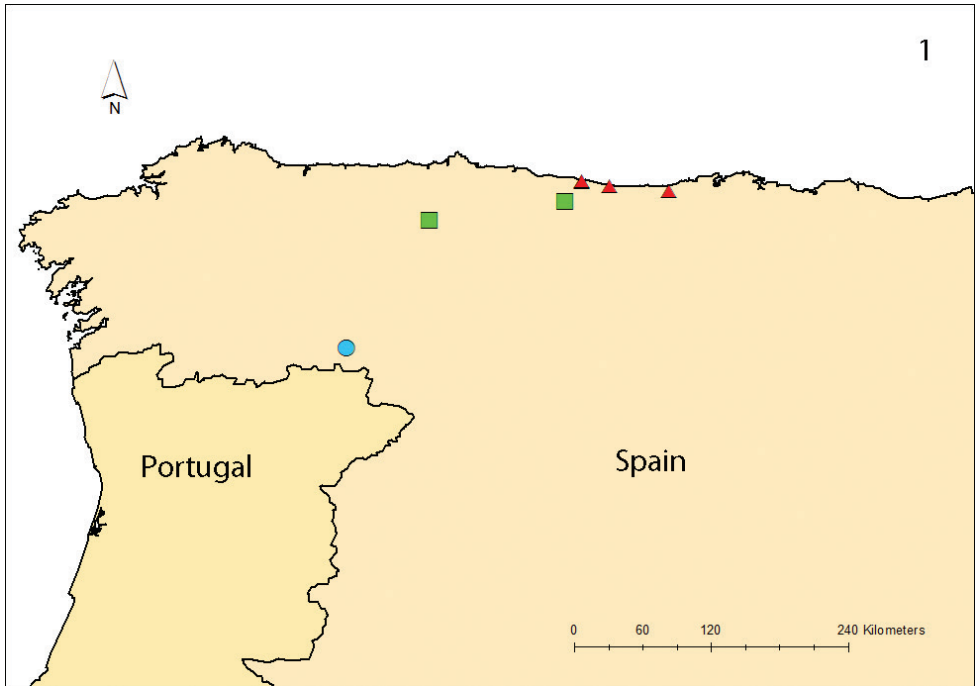


Figure 1. Records of *P. haroi* (Mauriès & Vicente, 1977), blue circle; *P. asturiensis* sp. nov., green square; *P. biscayensis* sp. nov., red triangle.

1858. However, new species are detected, even in Europe, particularly in the Mediterranean region and in caves (e.g., Mauriès 2013, 2014; Antić et al. 2013a, b; Gilgado et al. 2015). From the Iberian Peninsula, Azores, Madeira, Canary Islands, and Balearic Islands, 33 species in six genera, *Polydesmus* (10 spp.), *Propolydesmus* Verhoeff, 1895 (5 spp.), *Archipolydesmus* Attems, 1898 (9 spp.), *Schizomeritius* Verhoeff, 1931 (6 spp.), *Brachydesmus* (2 spp.) and *Tolosanius* Attems, 1952 (1 sp.) are recorded (see Table 1). Notably, most of them are endemic to the Iberian Peninsula.

Two new species of *Polydesmus* are described below, based on material housed in the Museo Nacional de Ciencias Naturales, Madrid. They were collected in northern Spain, from five localities in Asturias and one in Cantabria (Fig. 1).

Both species have strongly bifurcate gonopods, with well-developed endomere (endm) and exomere (exm) (see terminology in Djursvoll 2008). Based on the length and shape of the endomere and exomere, including the length and orientation of the seminal groove, the new species are placed in the genus *Polydesmus*, as diagnosed by Djursvoll et al. (2001). Some of these character states are also present in species considered by Enghoff and Golovatch (2003) to belong in the genus *Propolydesmus*, notably *Polydesmus haroi* Mauriès & Vicente, 1977 and *Polydesmus racovitzai* Brolemann, 1910. After an in-depth examination and comparison of the gonopod morphology, both species are transferred back to *Polydesmus* in the present paper.

Table 1. Species of Polydesmidae in Portugal and Spain and its known distribution.

Species	Portugal	Spain	Province/region
<i>Archipolydesmus altibaeticus</i> Gilgado, Enghoff, Tinaut & Ortuño, 2015		x	Granada
<i>Archipolydesmus bedeli</i> (Brolemann, 1902)		x	Segovia, Madrid and Guadalajara
<i>Archipolydesmus cordubaensis</i> Mauriès, 2013		x	Córdoba
<i>Archipolydesmus foliatus</i> Gilgado, Enghoff, Tinaut & Ortuño, 2015		x	Alicante
<i>Archipolydesmus giennensis</i> Mauriès, 2014		x	Jaén
<i>Archipolydesmus osellai</i> Ceuca, 1968		x	Huesca
<i>Archipolydesmus panteli</i> (Brolemann, 1900)		x	Cuenca, Tarragona and Lleida
<i>Archipolydesmus ribauti</i> (Brolemann, 1926)		x	Gerona
<i>Archipolydesmus terreus</i> (Attems, 1952)		x	Cádiz and Gipuzkoa
<i>Brachydesmus proximus</i> Latzel, 1889	x	x	Madeira, Azores, Canary Islands, Balearic Islands, Huesca, Malaga
<i>Brachydesmus superus</i> Latzel, 1884	x	x	Azores, Madeira, Lisbon, Balearic Islands, Canary Islands, Granada, Orense, Pontevedra, Zamora, Burgos, Madrid, Tarragona, La Rioja, Córdoba, Segovia, Navarra, Álava, Barcelona
<i>Polydesmus angustus</i> Latzel, 1884		x	Álava, Asturias
<i>Polydesmus asturiensis</i> sp. nov.		x	Asturias
<i>Polydesmus biscayensis</i> sp. nov.		x	Asturias, Cantabria
<i>Polydesmus coriaceus</i> Porat, 1871	x	x	Widely distributed in northern Iberia and adjacent islands
<i>Polydesmus geochromus</i> Attems, 1952		x	Jaén, Sevilla
<i>Polydesmus haroi</i> (Mauriès & Vicente, 1977)		x	Zamora
<i>Polydesmus incisus</i> Brolemann, 1921		x	Pyrenees, Girona, Huesca
<i>Polydesmus inconstans</i> Latzel, 1884	x	x	Navarra, Huesca, Madrid, Orense, Pontevedra, Viana do Castelo
<i>Polydesmus minutulus</i> Mauriès & Barraqueta, 1985		x	Viscaya
<i>Polydesmus racovitzaei</i> (Brolemann, 1910)		x	Gipuzkoa, Viscaya, Navarra
<i>Propolydesmus dissimilis</i> (Berlese, 1891)		x	Balearic Islands, Canary Islands, Valencia, Granada, Zamora, Huesca, Salamanca, Álava, Madrid, Segovia, Cuenca, Zaragoza, Toledo, Alicante, Guadalajara, Burgos
<i>Propolydesmus heroldi</i> (Schubart, 1931)		x	Sevilla
<i>Propolydesmus laevidentatus</i> (Loksa, 1967)	x	x	Canary Islands, Orense, Pontevedra, Minho, Azores, Madeira
<i>Propolydesmus miguelinus</i> (Attems, 1908)	x		Beira Litoral, Azores, Madeira
<i>Propolydesmus pectiniger</i> (Verhoeff, 1893)	x		Beira Litoral
<i>Schizomeritius phantasma</i> (Verhoeff, 1925)		x	Madrid and Ávila
<i>Schizomeritius andalusis</i> Djursvoll, 2008		x	Sevilla, Huelva and Cadis
<i>Schizomeritius armatus</i> (Machado, 1946)	x		Beira Litoral
<i>Schizomeritius esgrimidor</i> Djursvoll, 2008		x	Ávila
<i>Schizomeritius mauriesi</i> (Vicente, 1979)		x	Caceres
<i>Schizomeritius ortizi</i> Djursvoll, 2008		x	Toledo
<i>Tolosanius parvus</i> Attems, 1952		x	Gipuzkoa

Materials and methods

Preserved specimens were examined in 70 % ethanol using a Leica MZ Apo stereomicroscope. When making Scanning Electron Micrographs (SEM), structures such as gonopods and antennae were gently mounted on stubs using sticky tabs and the air-dried stubs were sputter coated with gold. A Zeiss Supra 55 UP field emission scan-

ning electron microscope used for observation and photographs. Photographs of tergal structures were made with an Olympus SC 50 camera mounted on an Olympus SZX 10 stereomicroscope using Olympus software.

Morphological terminology for this studied group follows Djursvoll (2008). Nonetheless, some names of the gonopod structures are specified here. **Endomere**, the main gonopod part which brings the seminal groove to the solenophore – surrounded with the pulvillus. The same part is identical to “solenomere” and “femorite”, occasionally used by other authors. **Acropodite**, a tooth that originates from the distal part of endomere, always distal to the solenophore/pulvillus. The same part is identical to “distofemoral process” occasionally used by other authors. Several acropodites may occur. **Exomere**, gonopod part that originates basally on endomere, usually lateral and sometimes with a marked sulcus, usually with outgrowth of several **teeth** (processes). Abbreviations: exm = exomere, endm = endomere, t = tooth on exomere, a = acropodite.

The type material is stored in the Museo Nacional de Ciencias Naturales, Madrid (MNCN). New material of *Polydesmus racovitzai* Brolemann, 1910 was mainly collected during a field trip in April 2009; participants were Karin Voigtländer, Hans Reip, Norman Lindner, Helen Read, Desmond Kime, Paul Richards, Steve Gregory, and Per Djursvoll. The new material of *Polydesmus racovitzai* is stored in the University Museum of Bergen (ZMBN) and Senckenberg Museum of Natural History Görlitz (SMNG).

Taxonomy

Polydesmus biscayensis sp. nov.

<http://zoobank.org/82FA05D9-FF77-4FC8-88E5-21FDF3F37A7D>

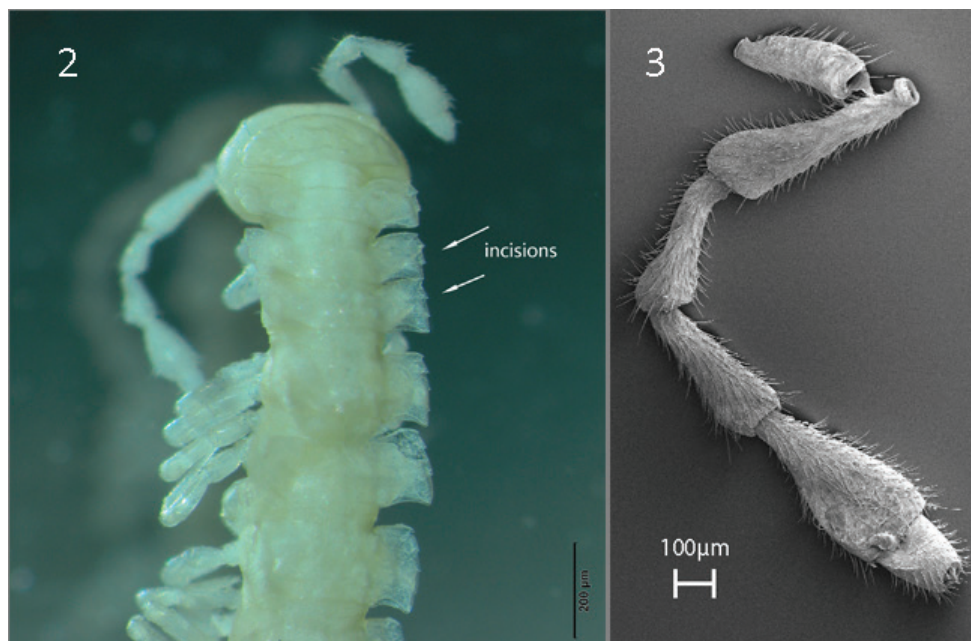
Figs 2–8

Type specimens. Spain, **Asturias province**; holotype ♂; Llanes, Cueva de la Coluvina; 1 Nov. 1969; E. Ortiz leg.; MNCN 20.07/1440 • paratype ♂; same data as holotype; MNCN 20.07/2020 • paratypes 2 ♂♂, 2 ♀♀ (fragments); Llanes, Bricia, La Cueva de Tebellin; C. Cardin leg.; date unknown; MNCN 20.07/1446 • paratype ♂ (fragments in three parts); Llanes, Piedra Llanes; 26 Jan. 1929; C. Cardin leg.; MNCN 20.07/1297. **Cantabria province** • paratypes ♂, ♀, 2 juveniles (fragments); Cueva de la Busta; 7 Aug. 1968; E. Ortiz leg.; MNCN 20.07/1320.

Etymology. Named after the Bay of Biscay.

Diagnostic characters. Differs from other *Polydesmus* species in having a well-developed twisted endomere together with the acropodites – a1 close to the solenophore and a hooked acropodite a2 at the distalmost end, a long, slender and curly exomere, together with the presence of a ventrolateral tooth t1 directed proximal just after main curvature point, and the placement of the distal t2 tooth distally.

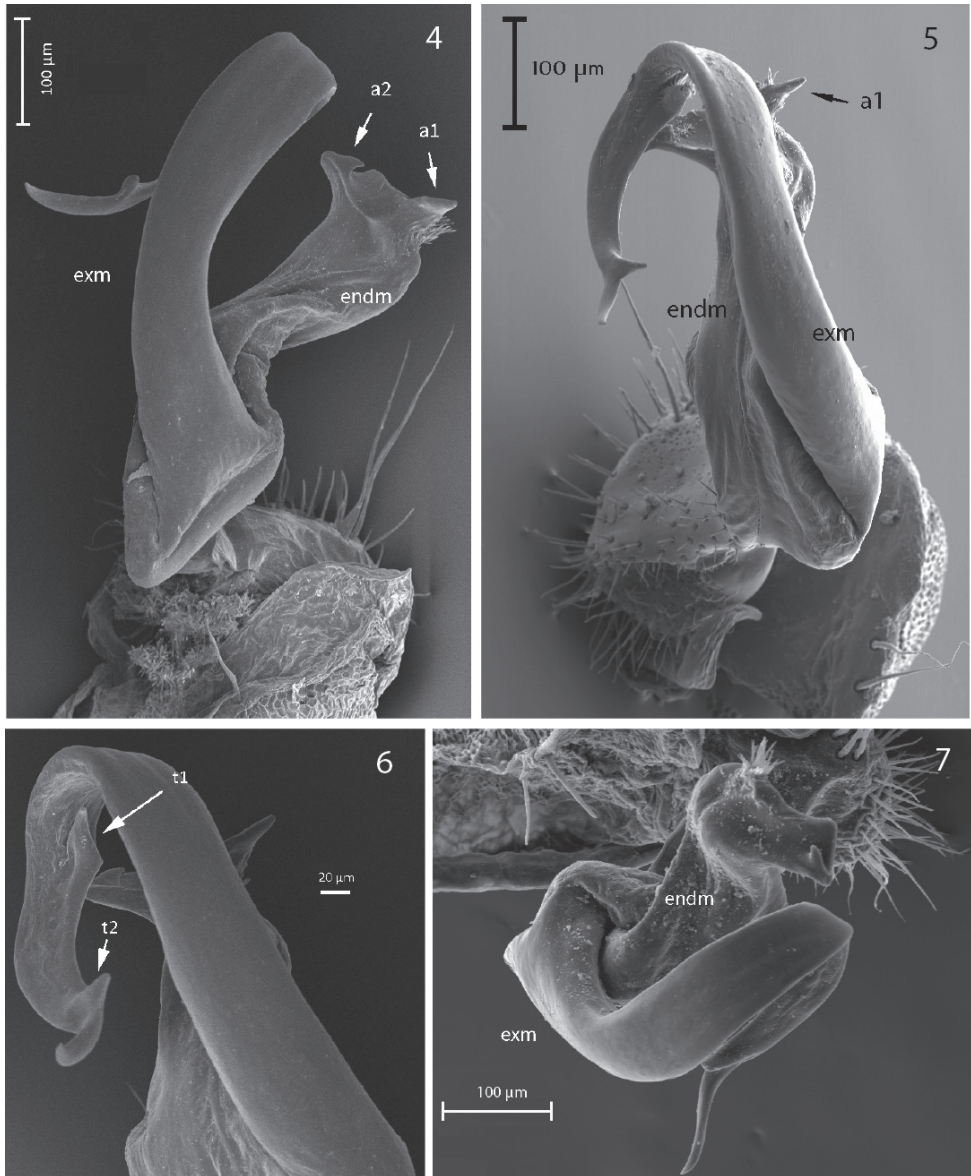
Description. With 20 body rings, total length 10–12 mm. Coloration whitish to pale yellow (longtime ethanol-preserved specimens only). Collum ovoid,



Figures 2–3. *P. biscayensis* sp. nov., male paratype **2** dorsal view of head and anterior body rings (MNCN 20.07/2020) **3** antenna (MNCN 20.07/1297).

narrower than head and the subsequent rectangular metatergum 2 which is approximately as wide as head, head > collum > metatergum 2 (Fig. 2). Antennae comparatively long, not surpassing body ring 3, antennomere 6 almost clavate and slightly longer than 4 and 5, $4 = 5 < 6 \gg 7$, with dorsoparabasal sensory knob on antennomere 7, sensillar area on antennomere 5–7 (Fig. 3). Metaterga rectangular, paraterga projected laterad, tergal sculpture (tuberculation) in three transverse rows, third row barely visible in metaterga 2–4. Setae clavi- to bacilliform, caudolateral part of paraterga with distinct keels especially from metaterga 4 and back. Ozopore located slightly inside caudolateral margin. Three distinct lateromarginal incisions in paratergum 2–4, four incisions on 5, incisions less distinct more posteriorly. Epiproct pointed apically. Male legs distinctly swollen, sphaerotrichomes present. Legs 1.5–2.0 times as long as midbody height, with single dorsal macrosetae on tibia.

Gonopod strongly bifurcate, including endomere and exomere, both parts twisted (curved). Endomere turns mesally crossing beneath oppositely directed exomere (Figs 4–7). Endomere stouter, bringing descending seminal groove to a mesad-directed solenophore-pulvillus surrounded with two small acropodites, a1 beside pulvillus, a2 hooked, and an excavation in between them (Fig. 4). Exomere originates from endomere with marked sulcus, very elongated and curly, descending to acute apex, with ventrolateral tooth t1 just after main curvature point directed backwards, t2 distally (Fig. 6). Prefemoral part densely setose. Lateral edge of coxite with two large macrosetae. Cannula tube-like and curved.



Figures 4–7. *P. biscayensis* sp. nov. **4** male paratype, right gonopod, dorsolateral view (MNCN 20.07/1297) **5** male holotype, right gonopod, dorsomesal view (MNCN 20.07/1440) **6** male paratype, right gonopod with ventrolateral tooth t1 on exomere (MNCN 20.07/1297) **7** male holotype, right gonopod, distal view (MNCN 20.07/1440).

Female with marked apophysis (tubercle) supporting the orifice of the gonopore on second coxae. Epigynal ridge poorly modified but with pin-shaped median process, with crevice inside (Fig. 8). Vulva relatively short, e.g., in lateral view less than 2× as long as high.

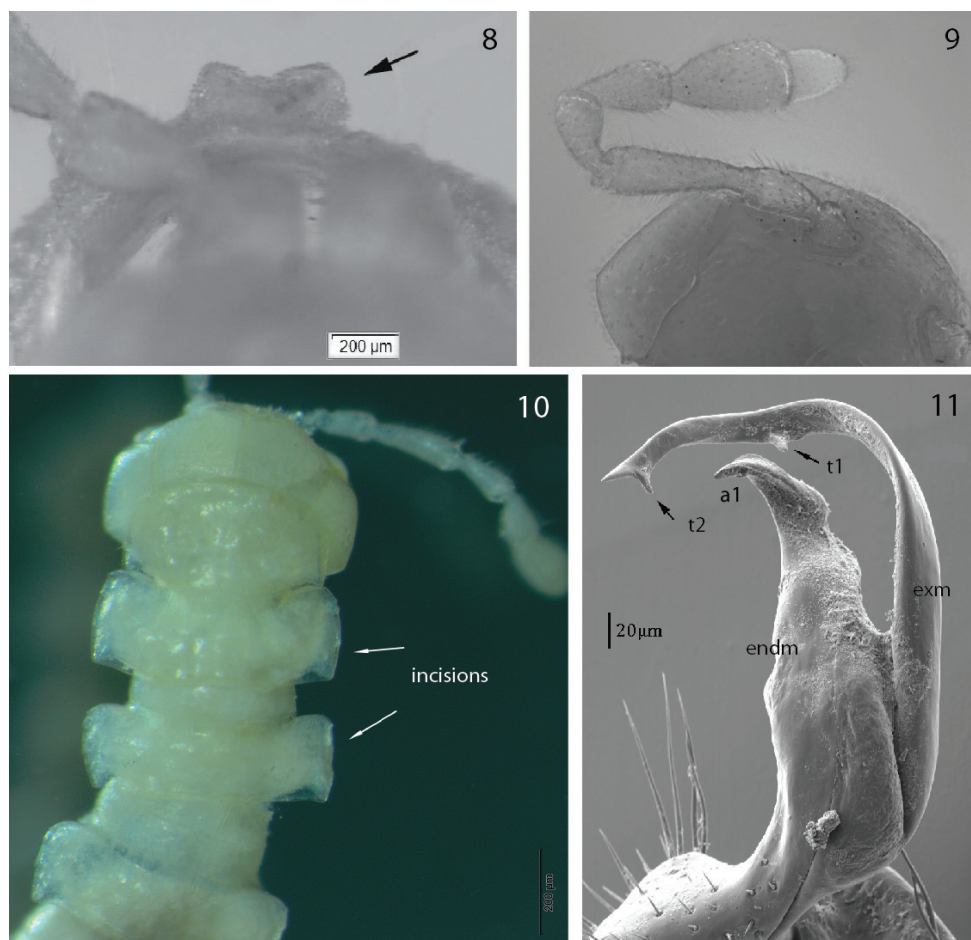
***Polydesmus asturiensis* sp. nov.**

<http://zoobank.org/91CCD20A-D879-4A5E-85FC-76550041F258>

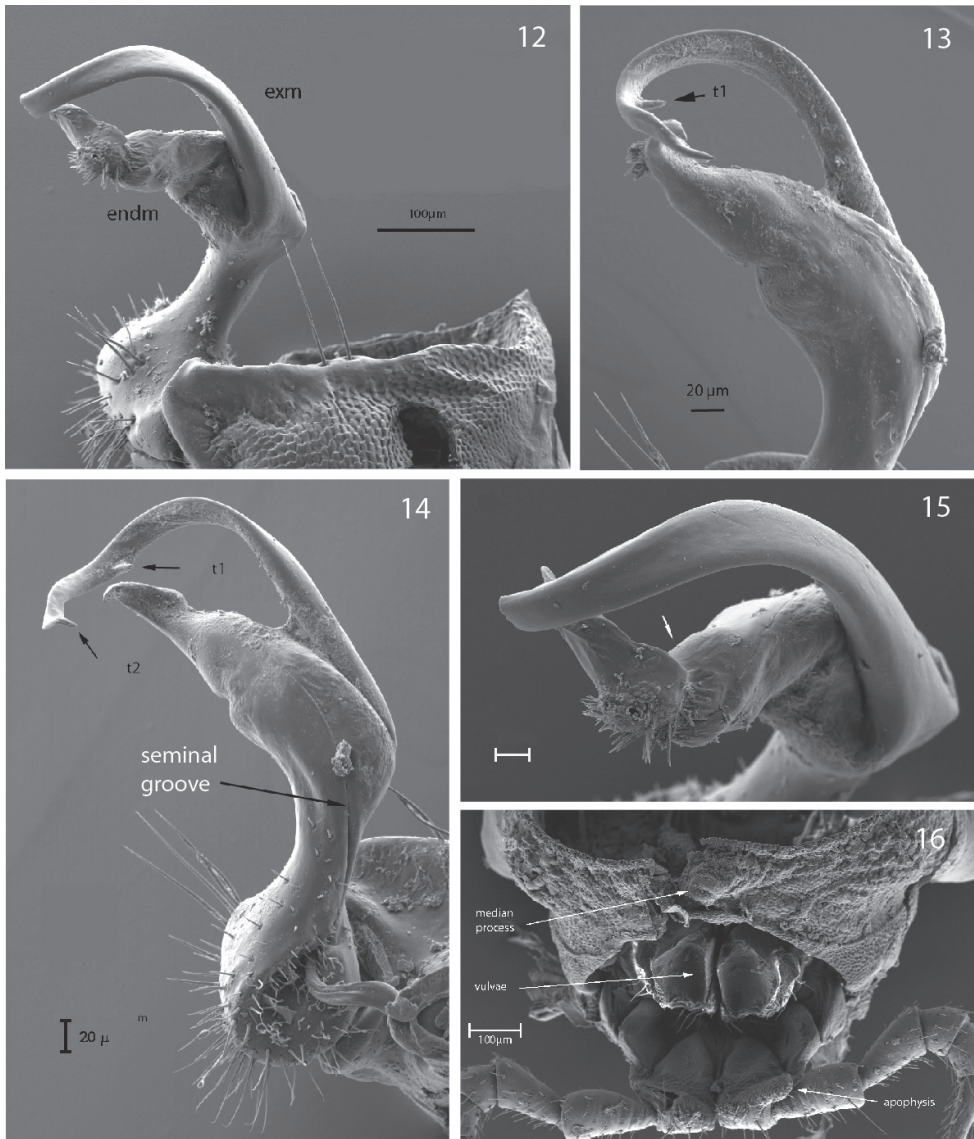
Figs 9–16

Type specimens. Spain, **Asturias province**; holotype ♂ (fragments); Teverga, Cueva de Huerta, 750 m a.s.l.; UTM 29TQH37; July. 1934; Bolivar col.; MNCN 20.07/1484 • paratype ♂; same data as holotype; MNCN 20.07/2021 • paratypes ♂, 2 ♀♀ (fragments); same data as holotype; MNCN 20.07/1481 • paratypes ♂, ♀ (fragments); Vega de Enol; ca. 1050 m a.s.l.; 2 Nov. 1969; E. Ortiz leg.; MNCN 20.07/1450.

Additional material. Two specimens in fragments, same locality data as holotype (MNCN 20.07/1484).



Figures 8–11. **8** *P. biscayensis* sp. nov., paratype, female epigyne (MNCN 20.07/1320) **9** *P. asturiensis* sp. nov., paratype, antenna (MNCN 20.07/1450) **10** *P. asturiensis* sp. nov., paratype, head and anterior body rings, dorsal view (MNCN 20.07/1481) **11** *P. asturiensis* sp. nov., male paratype right gonopod, mesal view (MNCN 20.07/1450).



Figures 12–16. **12** *P. asturiensis* sp. nov., male paratype, left gonopod, lateral view (MNCN 20.07/1481) **13–14** *P. asturiensis* sp. nov., male paratype, right gonopod, mesal view (MNCN 20.07/1450) **15** *P. asturiensis* sp. nov., male paratype, left gonopod, anterior view (MNCN 20.07/1481) **16** *P. asturiensis* sp. nov., paratype, female epigyne and vulva (MNCN 20.07/1481).

Etymology. Named after the province of Asturias.

Diagnostic characters. Differs from other *Polydesmus* species in having a twisted endomere with a distinct cleavage basad to the solenophore-pulvillus, with acute a1 distally. Exomere subfalcate, long and slender, with a ventrolateral right-angled tooth t1 just after main curvature point and together with the placement of the distal second tooth t2 close to apex.

Description. With 20 body rings, total length 7–10 mm. Coloration whitish to pale yellow (long-term ethanol-preserved specimens only). Tegument shiny. Collum ovoid, much narrower than head and metaterga 2, head >> collum << metatergum 2 (Fig. 10). Antennae comparatively long, not surpassing somite 3, antennomere 6 almost clavate, slightly longer than 4 and 5, $4 = 5 < 6 >> 7$. With dorsoparabasal sensory knob on antennomere 7, sensillar area on antennomere 5–7 (Fig. 9). Metaterga almost rectangular, tergal sculpture (tuberculation) in three transverse rows, third row barely visible in metaterga 2–4. Paraterga horizontal and rounded anterolaterally, paraterga 2–8 with barely visible lateromarginal incisions (not serrate), with gradually larger caudolateral projections from paraterga 5. Setae minute, barely visible. Ozopore located slightly inside caudolateral margin. Epiproct pointed apically. Male legs distinctly swollen, sphaerotrichomes present. Legs 1.5–2 times as long as midbody height, with single dorsal macrosetae on tibia.

Gonopod strongly bifurcate, including endomere and exomere (Figs 11–15). Endomere stouter, somewhat twisted, with descending seminal groove crossing beneath exomere to a distad-projecting solenophore-pulvillus, cleavage almost cut it into pieces behind solenophore-pulvillus, a1 distally smooth and pointed (Fig. 15). Exomere curved, originating from endomere with sulcus, with t1 and t2 tooth. Prefemoral part densely setose. Lateral gonocoxal edge with two large macrosetae.

Female with marked apophysis (tubercle) supporting the orifice of the gonopore on second coxae (Fig. 16). Epigynal ridge poorly modified but with pin-shaped median process, with crevice inside. Vulva relatively short, e.g., from lateral view less than 2× as long as high.

Polydesmus haroi Mauriès & Vicente, 1977

Fig. 20

Polydesmus haroi Mauriès & Vicente, 1977: 530.

Polydesmus (Hormobrachium) haroi Vicente, 1979: 23.

Propolydesmus haroi (Mauriès & Vicente, 1977): Enghoff and Golovatch (2003: 82), Kime and Enghoff (2011: 69), Djursvoll and Melic (2015: 8).

Notes. The species was figured and described in detail by Mauriès and Vicente (1977) based on material collected at Lago de Sanabria in Zamora province, with the main characters being the gonopod with two main gonopodal branches, exomere and endomere, and the seminal groove and solenophore-pulvillus extended onto endomere. These two characters differ from *Propolydesmus* but are in accordance with and support a phylogenetic relationship with the genus *Polydesmus* Latreille, 1802/03, and its type species *Polydesmus complanatus* Linnaeus, 1761.

It has similarities with *P. asturiensis* sp. nov. and *P. biscayensis* sp. nov. but differ in having a shorter exomere, the solenophore-pulvillus placed dorsally on the endomere and directed towards the exomere (Fig. 20), a wider space between the endomere and exomere, and in having a larger body size (length 17 mm). *Propolydesmus haroi* is here transferred back to *Polydesmus*.

***Polydesmus racovitzai* Brolemann, 1910**

Fig. 19

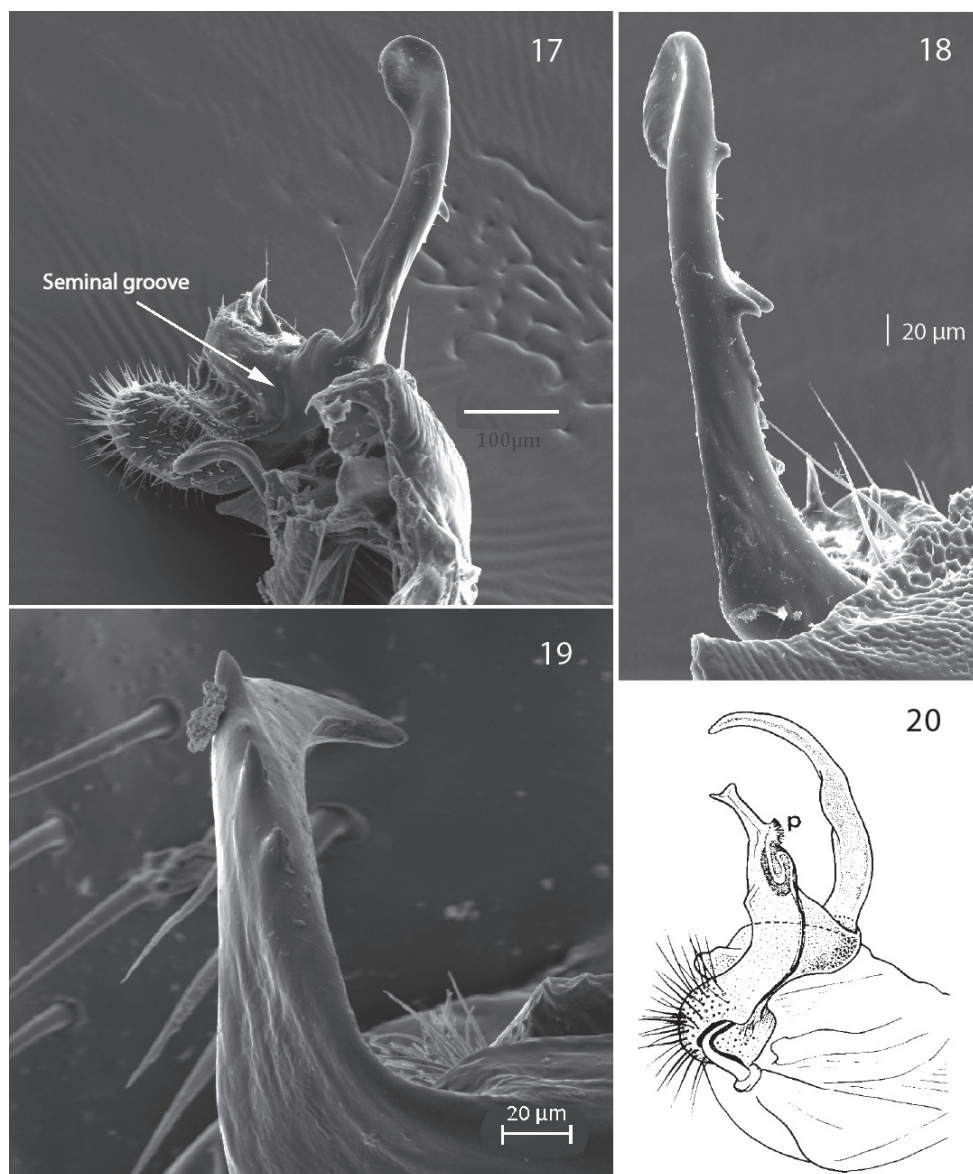
Polydesmus racovitzai Brolemann, 1910: 352; Attems 1927: 55, Demange 1981: 125, figs 170, 171.

Polydesmus (Hormobrachium) racovitzai Brolemann, 1910: Attems 1940: 48.

Propolydesmus racovitzai (Brolemann, 1910): Enghoff and Golovatch 2003: 82, Kime and Enghoff 2011: 69, Djursvoll and Melic 2015: 8.

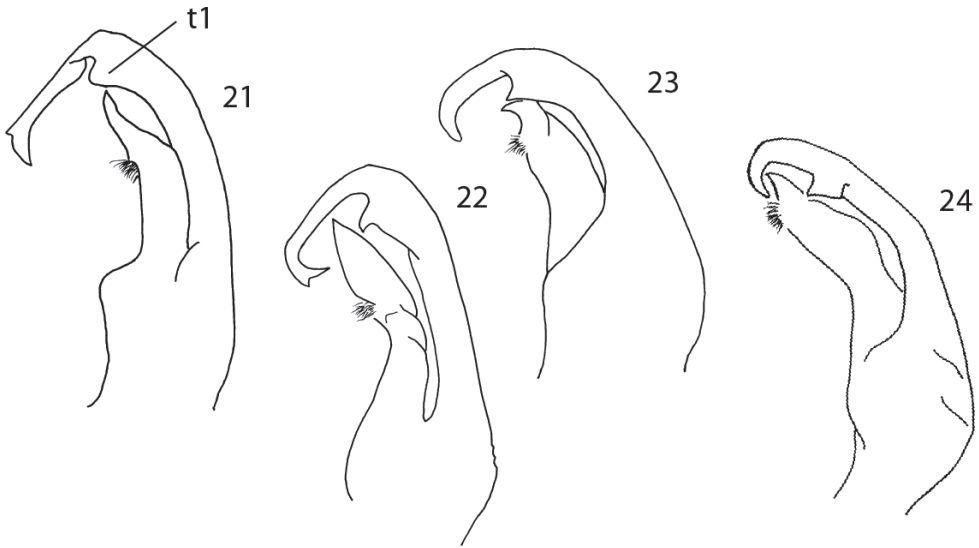
Material examined. SPAIN – **Viscaya province** • 1 ♂; 4 km s of Arrazua; pinewood; Desmond Kime leg.; 4.4.1978; ZMBN-ENT-PDESMID-49. – **Gipuzkoa province** • 1 ♂; Sierra de Aralar, Tolosa, 500 m south of Bedaio/Goikoa; 43.0494N, 2.04W; ca. 420 m a.s.l.; 21.4.2009; Helen Read leg.; farm buildings, under stones and logs; ZMBN-ENT-PDESMID-66 • 2 ♂♂; same collecting data as for preceding; 22.4.2009; Desmond Kime leg.; ZMBN-ENT-PDESMID-146, ZMBN-ENT-PDESMID-194) • 1 ♂; Sierra de Aralar, Beasain, road from Lazkao to Etxarri-Aranaz, west of the Pass Puerto de Lizarusti; 42.9572N, 2.1122W; ca. 550 m a.s.l.; 21.4.2009; Voigtlander, Reip & Lindtner leg.; forest of *Fagus*, in leaf litter; SMNG-14763. – **Navarra province** • 2 ♂♂, 2 juveniles; Leitza, Ariz Mendiak, between area “Ustarleku” and “Karobieta” above side stream to Gorritzaran; 43.0778N, 1.8775W; ca. 615 m a.s.l.; 20.04.2009; Per Djursvoll leg.; grove of *Castanea*, pollard trees on the slope with *Ranunculus ficaria*, *Daphne*, *Helleborus*, *Salvia*, *Rubus*, *Lathrea*, loamy and calcareous soil, under leaves and dead wood; ZMBN-ENT-PDESMID-133, ZMBN-ENT-PDESMID-135 • 1 ♂; Leitza, town area; 43.0788N, 1.9161W; ca. 470 m a.s.l.; 20.4.2009; Steve J. Gregory leg.; garden around casa rurale Aztieta; ZMBN-ENT-PDESMID-185 • 1 ♂, ♀; Lekunberri, local exit N-130 direction to Betelu, 43.011N, 1.902W; ca. 580 m a.s.l.; 20.4.2009; Per Djursvoll leg.; industrial area, synantropic, meadow with stones and brick waste, under stones; ZMBN-ENT-PDESMID-145 • 4 ♂♂, 1 juvenile; Sierra de Aralar, south Baraibar, on road NA-7510 to Santuario de San Miguel; 42.9762N, 1.9318W; ca. 670 m a.s.l.; 22.4.2009; Per Djursvoll leg; under stones, in *Corylus* litter; ZMBN-ENT-PDESMID-142 • 1 ♀, Sierra de Urbasa, Alava, under northern border, on road A-2128 south of Opakua, 42.821N, 2.3549W; ca. 740 m a.s.l.; 23.4.2009; Steve J. Gregory leg.; woodland of *Corylus*, *Quercus* and *Crategus*; ZMBN-ENT-PDESMID-181 • 1 ♀; Sierra de Urbasa, on top at southern cliff border, east of road NA-7182, 42.7989N, 2.1417W; ca. 930 m a.s.l.; 23.4.2009; Steve J. Gregory leg.; pasture on stony ground, some thorny bushes, occasional trees or groups of *Fagus*; ZMBN-ENT-PDESMID-176. FRANCE – **Pyrénées-Atlantiques** • 2 ♂♂, 1 ♀, 2 juveniles; Tarnos; 43.5203N, 1.4639E, ca. 30 m a.s.l.; 26.4.2009; Desmond Kime & Per Djursvoll leg. mixed deciduous forest; ZMBN-ENT-PDESMID-143.

Notes. The species was described by Brolemann (1910) and is distributed in the French Pyrenees, and in northern Spain. Body length is 13–16 mm, the gonopods may resemble those of *Polydesmus inconstans* Latzel, 1884 (see Demange 1981: 125, figs 170 – 171). It differs from *P. inconstans* in having a row of teeth dorsally on the endomere



Figures 17–20. **17** *Propolydesmus laevidentatus* (Loksa, 1967), from Madeira, right gonopod, medial view (ZMBN-ENT-PDESMID-342) **18** *Propolydesmus laevidentatus* (Loksa, 1967), from Madeira, right gonopod, lateral view (ZMBN-ENT-PDESMID-342) **19** *P. racovitzai* (Brolemann, 1910) right gonopod, lateral view (MNCN 20.07/1435) **20** *P. haroi* (Mauriès & Vicente, 1977) gonopod, redrawn after Mauriès and Vicente (1977).

and if this character was not observed, probably misidentified as *P. inconstans* (Fig. 19) in the literature. It differs from species of the genus *Propolydesmus* with the presence of the well-developed exomere and endomere – with seminal groove and solenophore-



Figures 21–24. **21** Sketch of the gonopod of *P. angustus* Latzel, 1884 **22** Sketch of the gonopod of *P. incisus* Brolemann, 1921 **23** Sketch of the gonopod of *P. inconstans* Latzel, 1884 **24** Sketch of the gonopod of *P. coriaceus* Porat, 1871.

pulvillus extended onto. These characters conform to those of the genus *Polydesmus* Latreille, 1802/03, and with its type species *Polydesmus complanatus* Linnaeus, 1761. *Propolydesmus racovitzai* is here transferred back to *Polydesmus*.

Key to the Iberian species of *Polydesmus*

- 1 With 19 body rings in both sexes ***P. minutulus* Mauriès & Barraqueta, 1985**
- With 20 body rings in both sexes **2**
- 2 Gonopod unipartite, as in *Brachydesmus* Heller, 1858 ***P. geochromus* Attems, 1952**
- Gonopod bifurcate – exomere and endomere distinct **3**
- 3 Exomere with a lateral tooth (t1) at main curvature point (Figs 21–24) **4**
- Exomere with a ventrolateral tooth (t1) at main curvature point (Figs 6, 11, 13–14) **9**
- 4 T1-tooth at main curvature point on exomere quadrangular or blade-like (Fig. 24) ***P. coriaceus* Porat, 1871**
- T1-tooth at main curvature point on exomere almost absent or triangular (Figs 21–23) **5**
- 5 Endomere and exomere branches widely separated ***P. haroi* Mauriès & Vicente, 1977**
- Endomere and exomere branches not widely separated **6**
- 6 Endomere apically stout and blunt, somewhat hooked (Figs 23–24) **7**
- Endomere apically pointed – a1, not hooked (Figs 21–22) **8**

- 7 With row of teeth dorsally on exomere (Fig. 19) *P. racovitzai* Brolemann, 1910
 – Without row of teeth dorsally on exomere *P. inconstans* Latzel, 1884
 8 Acropodite narrow and acute (Fig. 21) *P. angustus* Latzel, 1884
 – Acropodite broad, leaf-shaped, with acute apex (Fig. 22) ... *P. incisus* Brolemann, 1921
 9 Endomere with distinct cleavage, without acropodite a2 (Fig. 15)
 *P. asturiensis* sp. nov.
 – Endomere without distinct cleavage, with acropodites a1 and a2 (Fig. 4)
 *P. biscayensis* sp. nov.

Discussion

Enghoff and Golovatch (2003) redefined the small and solely southwestern European genus *Propolydesmus* Verhoeff, 1895, adding 12 species formerly placed in *Polydesmus* and adding one previously recognized *Propolydesmus* in synonymy, thus increasing the number of included species from four to 15. Consequently, the range of *Propolydesmus* has greatly expanded eastwards in Europe. Many of the species had been placed in subgenus *Hormobrachium* (Attems, 1940), that was synonymized with *Polydesmus* (s. str.) by Djursvoll et al. (2001). Later Djursvoll (2008) transferred *Propolydesmus mauriesi* (Vicente, 1979) to *Schizomeritius* Verhoeff, 1931. Without a species-level revision and a comprehensive analysis, the attributions of some of the species to *Propolydesmus* by Enghoff and Golovatch (2003) may be premature, as several of the species seem to have their affinities elsewhere.

Both Verhoeff (1895) and Djursvoll et al. (2001) in *Propolydesmus* diagnoses emphasized the character with particularly reduced endomere, while Enghoff and Golovatch (2003) stated “a relatively to very short/stout gonopod femorite”. This may have opened for the more extensive interpretation. However, Enghoff and Golovatch added for *Propolydesmus*, the important gonopodal character – presence of a seminal cavity, found in *Propolydesmus laevidentatus* (Loksa, 1967), in contrast to Verhoeff (1895) and Djursvoll et al. (2001). In particular, *Propolydesmus laevidentatus*, as illustrated by Enghoff and Golovatch (2003: 83, figs 4–7) differs from *Polydesmus* by having a strongly reduced endomere, and a slightly curved exomere with numerous teeth (Figs 18, 19). In addition, a looped seminal groove that does not extend onto the endomere branch, also in accordance with the type species *Propolydesmus pectiniger* (Verhoeff, 1893).

Acknowledgments

I am indebted to Dra. Begoña Sánchez Chillón, curator of arthropod collection at the Museo Nacional de Ciencias Naturales, Madrid, for the loan of the polydesmid material, to Egil Severin Erichsen at the ELMIR lab (UiB) for assistance with operating the scanning electron microscope. Thanks are due to Gunnar Kvitte and Trond Andersen (UiB) for comments on previous drafts. Special thanks to the reviewers Nesrine Akkari and Henrik Enghoff for constructive suggestions and useful comments.

References

- Antić DŽ, Ćurčić BPM, Mitic BM, Tomić VT, Lučić LR, Dudić BD, Stojanović DZ, Makarov SE (2013a) A new cave diplopod of the genus *Brachydesmus* Heller, 1858 from Southwest Serbia (Diplopoda: Polydesmida: Polydesmidae). Archives of Biological Sciences, Belgrade 65(2): 745–750. <https://doi.org/10.2298/ABS1302745A>
- Antić, DŽ, Ćurčić BPM, Tomić VT, Rada T, Rada B, Milinčić MA, Makarov SE (2013b) Two new species of *Brachydesmus* Heller, 1858 from the Balkan peninsula (Diplopoda: Polydesmida: Polydesmidae). Archives of Biological Sciences, Belgrade 65(3): 1233–1243. <https://doi.org/10.2298/ABS1303233A>
- Attems CG (1927) Über palaearktische Diplopoden. Archiv für Naturgeschichte 92(1–2): 1–256.
- Attems CG (1940) Myriapoda 3. Polydesmoidea III. Fam. Polydesmidae, Vanhoeffeniidae, Cryptodesmidae, Oniscodesmidae, Sphaerotrachopidae, Periodontodesmidae, Rhachidesmidae, Macellophidae, Pandiroidesmidae. Das Tierreich 70: 1–577. <https://doi.org/10.1515/9783111609645>
- Demange J-M (1981) Les Mille-Pattes, Myriapodes, Généralités, Morphologie, Écologie – Détermination des espèces de France. Société Nouvelle des Éditions Boubée, Paris, 284 pp.
- Djursvoll P (2008) Revision of the Iberian millipede genus *Schizomeritus* Verhoeff, 1931 (Diplopoda: Polydesmidae), with the description of three new species. International Journal of Myriapodology 1(1): 111–122. <https://doi.org/10.1163/187525408X316776>
- Djursvoll P, Melic A (2015) Orden Polydesmida. Revista IDE@, SEA 28: 1–11.
- Djursvoll P, Golovatch SI, Johanson KA, Meidell B (2001) Phylogenetic relationships within *Polydesmus sensu lato* (Diplopoda: Polydesmidae). Fragmenta Faunistica 43: 37–57.
- Enghoff H, Golovatch SI (2003) The millipede genus *Propolydesmus* Verhoeff, 1895 redefined, with a revision of the genus in the Canary Islands (Diplopoda, Polydesmida, Polydesmidae). Graellsia 59(1): 79–86. <https://doi.org/10.3989/graelisia>
- Enghoff H, Golovatch S, Short M, Stoev P, Wesener T (2015) Diplopoda – Taxonomic overview. In: Minelli A (Ed.) Treatise on Zoology – Anatomy, Taxonomy, Biology. The Myriapoda, Vol. 2. Brill, Leiden, 363–447. https://doi.org/10.1163/9789004188273_017
- Gilgado JD, Enghoff H, Tinaut A, Ortuno VM (2015) Hidden biodiversity in the Iberian Mesovoid Shallow Substratum (MSS): New and poorly known species of the millipede genus *Archipolydesmus* Attems, 1898 (Diplopoda, Polydesmidae). Zoologischer Anzeiger 258: 13–38. <https://doi.org/10.1016/j.jcz.2015.06.001>
- Kime RD, Enghoff H (2011) Atlas of European Millipedes (Class Diplopoda). Volume 1, Orders Polyxenida, Glomerida, Platydesmida, Siphonocryptida, Polyzoniida, Callipodida, Polydesmida. Co-published by Pensoft Publishers Sofia-Moscow and European Invertebrate Survey, Leiden, 282 pp.
- Mauriès JP (2013) Three new species of cavernicolous millipedes from Andalusia, Spain (Diplopoda: Polydesmida: Polydesmidae; Chordeumatida: Vandeumatidae, Opisthocheiridae). Trois espèces nouvelles de diplopedes cavernicoles de l'Andalousie (Espagne) (Diplopoda: Polydesmida: Polydesmidae; Chordeumatida: Vandeumatidae, Opisthocheiridae). Arthropoda Selecta 22(2): 97–112. <https://doi.org/10.15298/arthscl.22.2.01>

- Mauriès JP (2014) Four new species of cavernicolous millipedes from Andalusia, Spain (Diplopoda: Polydesmida: Polydesmidae; Chordeumatida: Chamaesomatidae, Opisthocheiridae). Quatre espèces nouvelles de Diplopodes cavernicoles de l'Andalousie (Espagne) (Diplopoda: Polydesmida: Polydesmidae; Chordeumatida: Chamaesomatidae, Opisthocheiridae). *Arthropoda Selecta* 23(1): 33–50. <https://doi.org/10.15298/arthsel.23.1.03>
- Mauriès JP, Vicente MC (1977) Myriapodes Diplopodes nouveaux ou peu connus des Pyrénées espagnoles, des monts Cantabriques et de Galice. *Bulletin du Muséum national d'Histoire naturelle*, 3^e série, Zoologie 315(452): 529–546.
- Verhoeff KW (1895) Aphorismen zur Biologie, Morphologie, Gattungs- und Art-Systematik der Diplopoden. *Zoologischer Anzeiger* 18: 203–211, 213–226, 237–244.
- Vicente MC (1979) Diplopodos polidesmidos de Zamora, Salamanca y Cáceres (España). Descripción de una nueva especie del género *Polydesmus* Latreille, 1802-3 (Diplopoda, Polydesmidae). *Miscelánea zoológica* 5: 21–23.

Description of a new leafhopper species of the genus *Longicornus* (Hemiptera, Cicadellidae, Deltocephalinae) from China, with a revised key to species

Yongqin Fang¹, Jichun Xing¹

¹ Institute of Entomology, Guizhou University, The Provincial Special Key Laboratory for Development and Utilization of Insect Resources, Guizhou University, Guiyang, 550025, China

Corresponding author: *Jichun Xing* (xingjichun@126.com)

Academic editor: *Mick Webb* | Received 23 March 2019 | Accepted 3 October 2019 | Published 11 November 2019

<http://zoobank.org/0D6DE308-9363-486F-802C-1765B69AA654>

Citation: Fang Y, Xing J (2019) Description of a new leafhopper species of the genus *Longicornus* (Hemiptera, Cicadellidae, Deltocephalinae) from China, with a revised key to species. *ZooKeys* 888: 67–73. <https://doi.org/10.3897/zookeys.888.34799>

Abstract

A new leafhopper species *Longicornus brevispinus* **sp. nov.** is described and illustrated from Yunnan Province, China. A key to distinguish all species of this genus is given, and a map showing the geographic distribution of all species is also provided. The type specimen of the new species is deposited in the Institute of Entomology, Guizhou University, Guiyang, China.

Keywords

distribution, Homoptera, leafhopper, morphology, taxonomy

Introduction

Li and Song (2008) established the genus *Longicornus* with *L. flavipuncatus* Li & Song, 2008 as its type species from China. This genus belongs to the tribe Scaphoideini of the subfamily Deltocephalinae based on the head being narrower than the pronotum, the frontoclypeus long and narrow, antennae long, and the forewing with one or more darkly pigmented reflexed veins in the vicinity of the outer anteapical cell (Zahniser

and Dietrich 2013). Recently, Fang and Xing (2018) reviewed this genus and added two new species: *L. furcatus* Fang & Xing and *L. biprocessus* Fang & Xing, and considered *L. flavipunctatus* Li & Song, 2008 as a senior synonym of *L. yunnanensis* Xing & Li, 2011. So far, this genus includes five species, all from China.

During a study of the Chinese Deltocephalinae, we discovered another new species *L. brevispinus* sp. nov. from Yunnan Province, China, which is described here. A key is also given to separate all five species of the genus. The type specimen of the new species is deposited in the Institute of Entomology, Guizhou University, Guiyang, China (GUGC).

Material and methods

Male specimens were used for the description and illustration. External morphology was observed under a stereoscopic microscope and characters were measured with an ocular micrometer. Color photographs were taken and stacked using a Nikon SMZ25 microscope. The genital segments of the specimens examined were macerated in 10% NaOH washed in distilled water and stored in glycerol. Male genital structures were drawn from preparations in glycerin jelly using a Leica MZ 12.5 stereomicroscope. Illustrations were scanned with a Canon CanoScan LiDE 200 and imported into Adobe Photoshop CS8 for labeling and plate composition.

Terminology of morphological and genital characters mainly follows Li et al. (2011) and Fang and Xing (2018). Absolute measurements, in millimeters (mm), are used for the body.

Taxonomy

Longicornus Li & Song

Longicornus Li & Song, 2008: 27; Li et al. 2011: 110; Zahniser and Dietrich 2013: 152; Fang and Xing 2018: 435.

Type species. *Longicornus flavipunctatus* Li & Song, 2008.

Remarks. For the relationship and diagnosis of *Longicornus* see Fang and Xing (2018: 436).

Distribution. China (Guizhou, Sichuan, Yunnan).

Checklist of species of *Longicornus*

L. biprocessus Fang & Xing, 2018: 440, figs 10–12; 34–40. China (Sichuan).

L. brevispinus sp. nov., Figs 1–11. China (Yunnan).

L. flavipunctatus Li & Song, 2008: 28, figs 1–8. China (Sichuan, Guizhou, Yunnan).

L. yunnanensis Xing & Li, 2011: 112, figs 5–102: 1–8 (in Li et al. 2011), synonymized by Fang and Xing 2018: 436.

L. furcatus Fang & Xing, 2018: 439, figs 7–9; 27–33. China (Sichuan).

L. longus Xing & Li, 2011: 112, figs 5–101: 1–7. China (Yunnan).

Key to species (males) of *Longicornus**

- 1 Aedeagal shaft with a pair of processes arising apically (Figs 8, 9; Fang and Xing 2018: figs 16,17, 23, 24) **2**
- Aedeagal shaft with pair of processes arising basally (Fang and Xing 2018: figs 30, 31, 37, 38)..... **4**
- 2 Aedeagal shaft processes longer than shaft (Fang and Xing 2018: figs 16, 17) ...
..... ***L. flavipuncatus***
- Aedeagal shaft processes shorter than shaft (Figs 8, 9; Fang and Xing 2018: figs 23, 24)..... **3**
- 3 Aedeagus long, and its apical processes approximately $\frac{3}{4}$ as long as shaft (Fang and Xing 2018: figs 23, 24) ***L. longus***
- Aedeagus short and stout, and its apical processes shorter than half length of aedeagal shaft (Figs 8, 9) ***L. brevispinus* sp. nov.**
- 4 Aedeagal shaft with pair of furcate processes arising from ventral margin near base (Fang and Xing 2018: figs 30, 31) ***L. furcatus***
- Aedeagal shaft with two pairs of processes medially on dorsal margin (Fang and Xing 2018: figs 37, 38) ***L. biprocessus***

***Longicornus brevispinus* sp. nov.**

<http://zoobank.org/267A75A3-4AEE-4D63-9F63-F117D095674D>

Figs 1–11

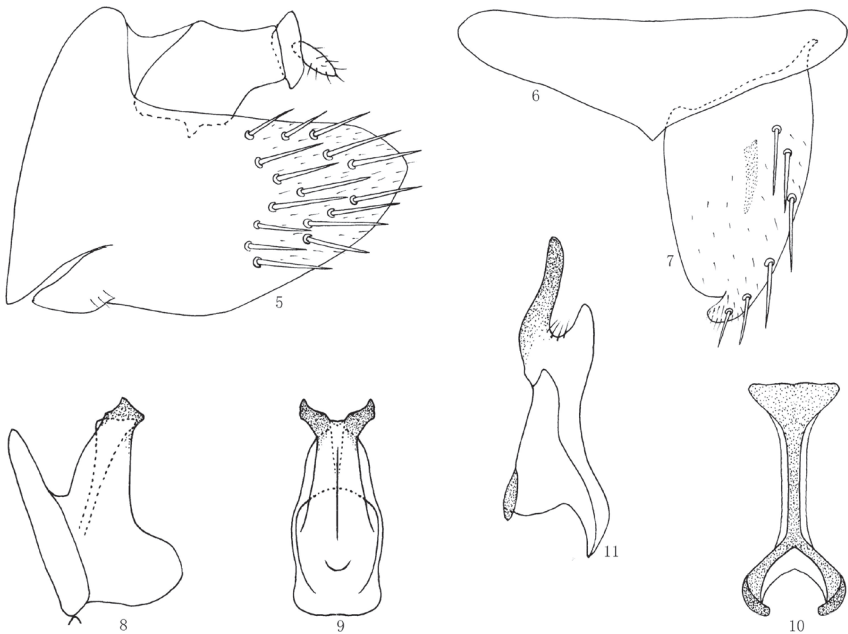
Description. Body robust, yellowish brown (Figs 1–4). Vertex with paired irregular dark brown short coalescing bands. Eyes black, ocelli pale yellow. Face marked with dark brown. Pronotum with irregular fuscous patches. Forewing brownish, with scattered hyaline areas, veins dark brown. Legs dark brown.

Head including eyes slightly narrower than pronotum. Vertex with fore margin produced roundly, median length distinctly shorter than width between eyes. Ocelli located on anterior margin of vertex. Frontoclypeus distinctly longer than wide, anteclypeus expanded apically. Antennae arising near lower corner of eye. Pronotum with anterior margin roundly produced and posterior margin concave, longer than vertex. Mesonotum triangular, slightly shorter than pronotum, with transverse su-

* Modified from Fang and Xing 2018



Figures 1–4. *Longicornus brevispinus* sp. nov., 1 ♂, dorsal view 2 ♂, lateral view 3 ♂, head and thorax, dorsal view 4 ♂, face, ventral view.



Figures 5–11. *Longicornus brevispinus* sp. nov., 5 male pygofer side, lateral view 6 valve, ventral view 7 subgenital plate, ventral view 8 aedeagus, lateral view 9 aedeagus, ventral view 10 connective, dorsal view 11 style, dorsal view.

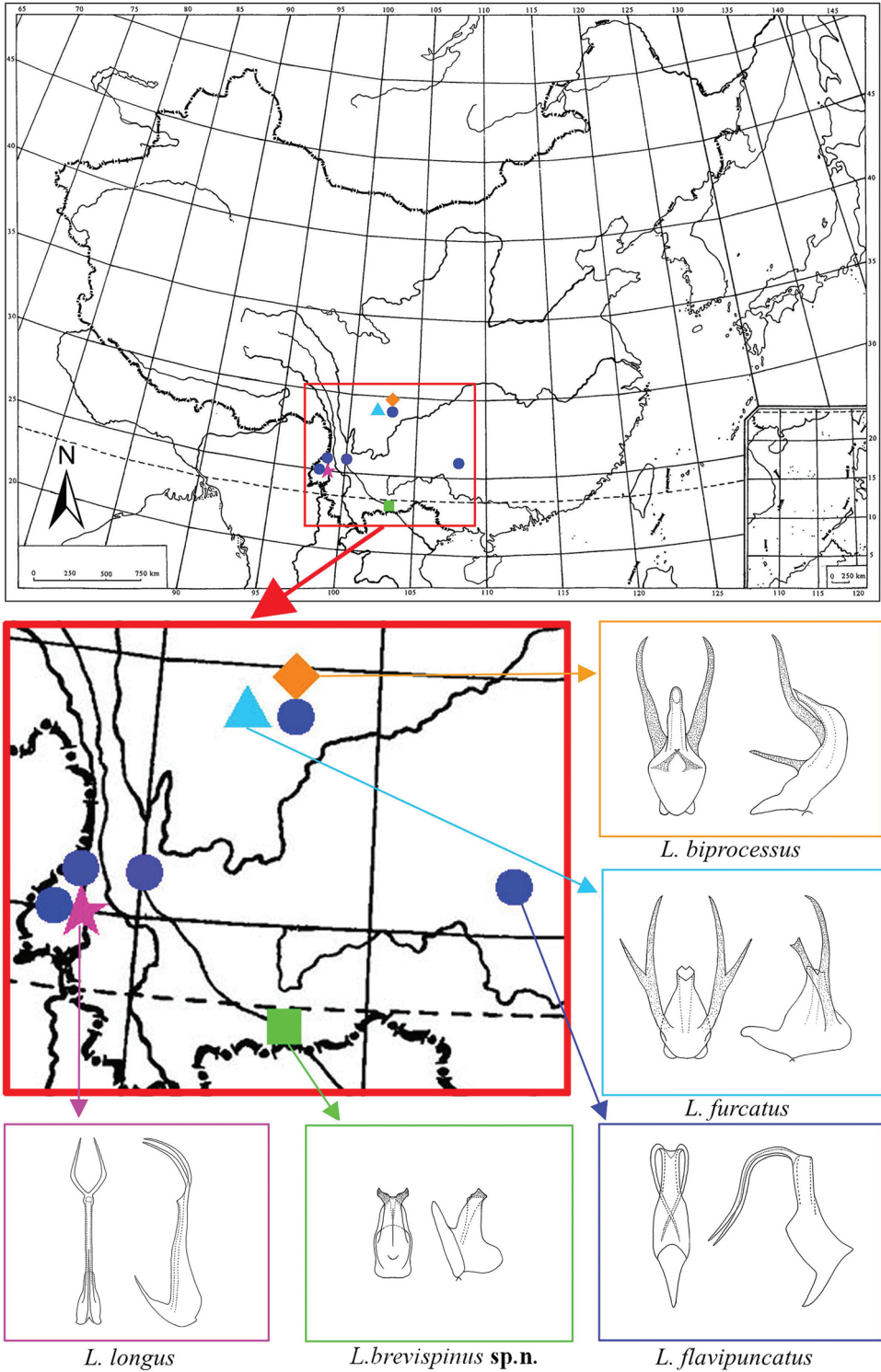


Figure 12. Geographic distribution of *Longicornus* species.

ture depressed. Forewing with four apical and three subapical cells, about 3 times as long as wide, appendix wide. Hind wing with three apical cells and two anteapical cells. Fore femur row IC with a row of short setae, row AM with 1 stout seta, 2 dorsoapical setae, and row AV with several short setae in basal half. Fore tibia with 4 macrosetae in row AD and numerous macrosetae decreasing in length toward the base in row AV. Hind femur broadened distally and slightly bowed, apical setal formula $2 + 2 + 1$. Hind tibia flattened and nearly straight, row PD with 12 macrosetae decreasing in length toward the base; row AD with 10 long stout setae and 1–4 shorter stout setae between each long seta; metabasitarsomere with 4 platellae and 2 setae on apical transverse row.

Male genitalia: Pygofer longer than broad in lateral view, with many long macrosetae in posterior half (Fig. 5). Valve subtriangular (Fig. 6). Subgenital plate with wide base, narrowed posteriorly, with 6 setae along lateral margin, and mesal margin deeply concave near apex (Fig. 7). Style relatively narrow, apical process acute, turned laterally (Fig. 11). Connective articulated with aedeagus, Y-shaped with stem long (Fig. 10). Aedeagus very short and stout with base broad in lateral view, gradually tapered to apex in lateral view, with a pair of short and robust apical processes with truncate apex, gonopore apical (Figs 8, 9).

Measurement. Length (including tegmen): ♂, 5.6 mm.

Type material. *Holotype* ♂, China: Yunnan Prov., Pingbian country, Daweishan, 22 May 2015, coll. Jiajia Wang (GUGC).

Distribution. China (Yunnan).

Remarks. The new species can be distinguished by the very short and stout aedeagus with a pair of short and robust apical processes with a truncate apex.

Etymology. The species name is derived from the Latin word “*brevis*” and “*spinus*”, referring to the short apical processes of the aedeagal shaft.

Discussion

Species of *Longicornus* are all very similar in coloration and difficult to distinguish externally, but the structure of aedeagus are markedly different. This genus now includes five species which can be divided into two types based on the structure of aedeagus: 1) aedeagus with one pair of apical processes (*L. brevispinus* sp. nov., *L. flavipuncatus* and *L. longus*); 2) aedeagus with paired basal processes (*L. furcatus* and *L. biprocessus*). *Longicornus furcatus* has one pair of furcate aedeagal processes arising from the ventral margin near the base and *L. biprocessus* has two pairs of aedeagal processes medially on the dorsal margin of the shaft.

All species of *Longicornus* are distributed in southwest China (Oriental Region) and the species without apical processes of the aedeagus are distributed in the north of the region (Fig. 12). So far, this genus has not been recorded in the Palearctic Region of China but it is highly likely that undiscovered species may be found there.

Acknowledgements

We thank Mick Webb (The Natural History Museum, London, U.K.) and Prof. C. A. Viraktamath (Department of Entomology University of Agricultural Sciences, GKVK, Bangalore, India) for reading the manuscript and making some suggestions. This work was supported by the National Natural Science Foundation of China (31660624, 31301909), the Science and Technology Project of Guizhou Province (Qian Ke He Platform Talent [2017]5788), Talent Fund Program of Guizhou University ([2014]15) and the Program of Science and Technology Innovation Talents Team, Guizhou Province (No. 20144001).

References

- Fang YQ, Xing JC (2018) Review of the leafhopper genus *Longicornus* Li & Song (Hemiptera: Cicadellidae: Deltocephalinae) with description of two new species. *Zootaxa* 4462(3): 435–442. <https://doi.org/10.11646/zootaxa.4462.3.9>
- Li ZZ, Dai RH, Xing JC (2011) Deltocephalinae from China (Hemiptera: Cicadellidae). *Popular Science Press*, Beijing, 336 pp. [in Chinese with English summary]
- Li ZZ, Song YH (2008) A new genus and species of Euecelinae (Hemiptera: Cicadellidae) from China. *Acta Zootaxonomica Sinica* 33(1): 27–28.
- Zahniser JN, Dietrich CH (2013) A review of the tribes of Deltocephalinae (Hemiptera: Auchenorrhyncha: Cicadellidae). *European Journal of Taxonomy* 45: 1–211. <https://doi.org/10.5852/ejt.2013.45>

Seven new species of *Trigonopterus* Fauvel (Coleoptera, Curculionidae) from the Tanimbar Archipelago

Raden Pramesa Narakusumo^{1,2}, Michael Balke³, Alexander Riedel¹

1 State Museum of Natural History Karlsruhe, Erbprinzenstr. 13, D-76133 Karlsruhe, Germany **2** Museum Zoologicum Bogoriense, Research Center for Biology, Indonesian Institute of Sciences (LIPI), Gd. Widiasatwalo, Jl. Raya Jakarta-Bogor km 46, Cibinong 16911, Indonesia **3** SNSB-Zoological State Collection (ZSM), Münchhausenstr. 21, D-81247 Munich, Germany

Corresponding author: *Alexander Riedel* (riedel@smnk.de)

Academic editor: *M. Alonso-Zarazaga* | Received 30 July 2019 | Accepted 8 October 2019 | Published 11 November 2019

<http://zoobank.org/6244FB2F-0BFE-4235-BADE-D25AEF147F39>

Citation: Narakusumo RP, Balke M, Riedel A (2019) Seven new species of *Trigonopterus* Fauvel (Coleoptera, Curculionidae) from the Tanimbar Archipelago. ZooKeys 888: 75–93. <https://doi.org/10.3897/zookeys.888.38642>

Abstract

Based on recent fieldwork, the hyperdiverse weevil genus *Trigonopterus* Fauvel is recorded for the first time from the Indonesian Tanimbar Archipelago, halfway between Australia and Western New Guinea. All seven species discovered on Tanimbar are new to science, and described here: *Trigonopterus atuf* **sp. nov.**, *T. kumbang* **sp. nov.**, *T. laratensis* **sp. nov.**, *T. porg* **sp. nov.**, *T. selaruensis* **sp. nov.**, *T. tanimbarensis* **sp. nov.**, and *T. triradiatus* **sp. nov.** The new species are authored by the taxonomists-in-charge, Raden Pramesa Narakusumo and Alexander Riedel. This fauna appears discordant and established by relatively recent dispersal from New Guinea and other Moluccan islands.

Keywords

Coleoptera; conservation; *cox1*; Cryptorhynchinae; DNA barcoding; endemism; hyperdiverse; integrative taxonomy; Moluccas; morphology; Southeast Asia; Tanimbar; turbo-taxonomy; Wallacea; weevils.

Introduction

Trigonopterus Fauvel is a genus of hidden snout weevils (Cryptorhynchinae) (Alonso-Zarazaga and Lyal 1999; Riedel et al. 2016). These beetles are flightless, yet the 444 species currently known cover a large geographic area, across the Indo-Australian Ar-

chipelago and into Oceania (Riedel et al. 2010, 2014; Riedel and Tänzler 2016; van Dam et al. 2016). Hundreds of additional species await discovery (Riedel et al. 2013b, 2014; Riedel and Tänzler 2016; Riedel and Narakusumo 2019; <https://species-id.net/wiki/Trigonopterus>; unpublished data). New Guinea is the center of *Trigonopterus* diversity (Tänzler et al. 2012, 2016, 2017).

The relatively rich *Trigonopterus* faunas of Sulawesi and Sundaland originated by dispersal from New Guinea and subsequent diversification (Tänzler et al. 2016). The fauna of the Moluccan Islands may have served as stepping stones, yet little is known about these islands. There is only one described species from Seram Island, i.e., *Trigonopterus ellipticus* (Pascoe) (Riedel 2011), though several undescribed species from Halmahera and Ternate Islands were included in the phylogeny of the genus published by Tänzler et al. (2016).

Here, we present the results of a recent survey of the Tanimbar Archipelago, or simply Tanimbar. Tanimbar is a cluster of islands located approximately halfway between Australia in the south (Darwin area, ca. 320 km distant) and Western New Guinea in the north (ca. 340 km). The island of Timor is ca. 380 km to the west, and the Kai and Aru Islands lie ca. 150 km and 240 km, respectively, to the northeast. The Tanimbar Islands are all low, i.e., below an elevation of 300 meters. The climate is relatively seasonal, and forest cover comprises of seasonal evergreen forest, dry deciduous forest and moist deciduous forest (Laumonier and Nasi 2018). Geologically, Tanimbar belongs to the outer non-volcanic Banda arc formed in the Quaternary (Hall 1998, 2002). Parts of the islands are covered with early Pleistocene marine deposits and quaternary reefs occur up to 200 m in altitude (De Smet et al. 1989; Charlton et al. 1991), indicating a very recent origin of ca. 1 Ma. During the Pleistocene, the Tanimbar Islands remained insular as they are not connected to the Sahul shelf (Voris 2000). Thus, Tanimbar has been used as a geological calibration point for a phylogenetic analysis of passerine birds (Jönsson et al. 2010).

Here we describe seven new species of *Trigonopterus* from Yamdena, Larat, and Selaru islands, the three biggest islands of the Tanimbar Archipelago. We follow the “fast-track” taxonomy approach that combines molecular and morphological systematics (Riedel et al. 2013a, b), including data release on open access websites, i.e., species-ID (<https://species-id.net/wiki/Trigonopterus>) and wikispecies (<https://species.wikimedia.org/wiki/Trigonopterus>).

Materials and methods

This study is based on 222 specimens of *Trigonopterus* collected on two field trips to the Tanimbar Islands by the first author. Specimens were collected by beating foliage in primary forest. Holotypes were selected from 44 DNA sequenced specimens. DNA was extracted nondestructively as described by Riedel et al. (2010), with proteinase K lysis so that the genitalia of most specimens did not require extra maceration after DNA-extraction and could be directly stained with an alcoholic Chlorazol Black solution and stored in glycerol in microvials attached to the pin of the specimens. Genitalia of collection specimens or specimens whose abdominal muscle tissue was not suffi-

ciently digested after DNA extraction were macerated in a 10% KOH solution and rinsed in diluted acetic acid before staining. Illustrations of habitus and genitalia were prepared from holotypes. Finally, type series were supplemented with specimens stored in ethanol and older material from the dry collection. Type depositories are cited using the following codens:

- MZB** LIPI Research Center of Biology, Division of Zoology, Museum Zoologicum Bogoriense, Widyasatwaloka, Cibinong, Indonesia;
SMNK Staatliches Museum für Naturkunde, Karlsruhe, Germany;
ZSM Zoologische Staatssammlung München, Germany.

The methods applied for DNA sequencing and sequence analysis are described by Riedel et al. (2010) and Tänzler et al. (2012). Morphological descriptions are limited to major diagnostic characters as outlined by Riedel et al. (2013a, b). Negative character states (i.e., the absence of a character) are only mentioned explicitly where it appears appropriate. In groups comprising hundreds of species enumerating the absence of rare character states leads to inflated descriptions that distract the reader from the important information, i.e., the diagnostic characters present in a given species.

The closest relatives of Tanimbar species were identified by creating an alignment of 1.154 *cox1* sequences representing ca. 1000 species and generating a maximum likelihood reconstruction using the program IQTREE (Nguyen et al. 2015, Trifinopoulos et al. 2016). Morphological terminology follows Beutel and Leschen (2005) and Leschen et al. (2009), i.e., the terms “mesoventrite” / “metaventrite” are used instead of “mesosternite” / “metasternite” and “mesanepisternum” / “metanepisternum” instead of “mesepisternum” / “metepisternum”; “penis” is used instead of “aedeagus” as the tegmen is usually without useful characters in *Trigonopterus* and therefore omitted from species descriptions. Specimens were examined with a Leica MZ16 dissecting microscope and a fluorescent desk lamp for illumination. Measurements were taken with the help of an ocular grid. The length of the body was measured in dorsal aspect from the elytral apex to the front of the pronotum. Legs were described in an idealized laterally extended position; there is a dorsal / ventral and an anterior / posterior surface. Habitus illustrations were compiled using a DFC495 camera with L.A.S. 4.8.0 software adapted to a Z6 APO (all from Leica Microsystems, Heerbrugg, Switzerland). Photographic illustrations of genitalia were made using a DFC450 camera with L.A.S. 4.8.0 software adapted to an Axio Imager M2 microscope (Carl Zeiss Microscopy), with 5×, respectively 10× A-Plan lenses; resulting image stacks were compiled using the Helicon Focus 6.7.1 Pro software (Helicon Soft Ltd). For photography genitalia were temporarily embedded in glycerol gelatin as described by Riedel (2005), with their longitudinal axis somewhat lifted caudally, to adequately illustrate structures of the curved down apex. All photographs were enhanced using the programs Adobe Photoshop CS2 and CS6. However, care was taken not to obscure or alter any features of the specimens illustrated. Sequence data were submitted to GenBank of NCBI (National Center for Biotechnology Information) and the accession numbers are provided under each species, e.g., as “(EMBL # MN322570)”.

Taxonomy

Trigonopterus Fauvel, 1862

Type species, by monotypy. *Trigonopterus insignis* Fauvel, 1862.

Diagnosis. Fully apterous genus of Cryptorhynchinae s. s. Length 1.5–6.0 mm. Rostrum in repose not reaching middle of mesocoxa. Scutellar shield completely absent externally. Mesothoracic receptacle deep, posteriorly closed. Metanepisternum completely absent externally. Elytra with nine striae (sometimes superficially effaced). Tarsal claws minute. Usually body largely unclothed, without dense vestiture. For additional information, see <http://species-id.net/wiki/Trigonopterus>.

Descriptions of species

Trigonopterus atuf Narakusumo & Riedel, sp. nov.

<http://zoobank.org/1367A851-B3E3-4A64-9463-73A828646D9B>

Diagnostic description. Holotype. Male (Fig. 1a). Length 2.65 mm. Color of antennae and legs ferruginous, remainder black. Body elongate subovate; profile dorsally convex; in dorsal aspect and in profile with weak constriction between pronotum and elytron. Eyes dorsally approximate. Rostrum with median carina and pair of submedian ridges, intervening furrows with suberect scales. Pronotum subglabrous, punctate. Elytra subglabrous, striae marked by rows of minute punctures and fine hairlines; along base towards humerus bordered by transverse row of deeper punctures; intervals subglabrous, with sparse minute punctures; subapically along ventral margin with row of white scales. Femora with distinct anteroventral ridge, edentate. Mesofemur and metafemur dorsally densely squamose with white scales. Metafemur with smooth dorso-posterior edge; subapically without stridulatory patch. Procoxa with patch of erect white scales. Abdominal ventrites 1–2 concave, medially subglabrous, laterally with sparse white scales; ventrite 5 with shallow impression, punctate, with sparse suberect scales. Penis (Fig. 1b) with sides subparallel, apex subtruncate, with sparse setae, medially with angulate extension; apodemes 3.0× as long as body of penis; transfer apparatus complex; ductus ejaculatorius without bulb. **Intraspecific variation.** Length 2.30–2.78 mm. Female rostrum subglabrous, punctate-rugose; in basal quarter with suberect scales. Female abdominal ventrite 5 flat.

Material examined. Holotype (MZB): MZB0014 (GenBank # MN322570), Indonesia, Maluku, Tanimbar, Yamdena Is, Lorulun, 07°48.788'S, 131°22.443'E to 07°48.137'S, 131°21.873'E, 140 m, beaten, 2-V-2017. **Paratypes** (MZB, SMNK): Indonesia, Maluku, Tanimbar: 13 exx, MZB0012 (EMBL # MN322578) MZB0013 (GenBank # MN322580) MZB0015 (GenBank # MN322569) same data as holotype; 3 exx, MZB0017 (GenBank # MN322568), MZB0018 (GenBank #

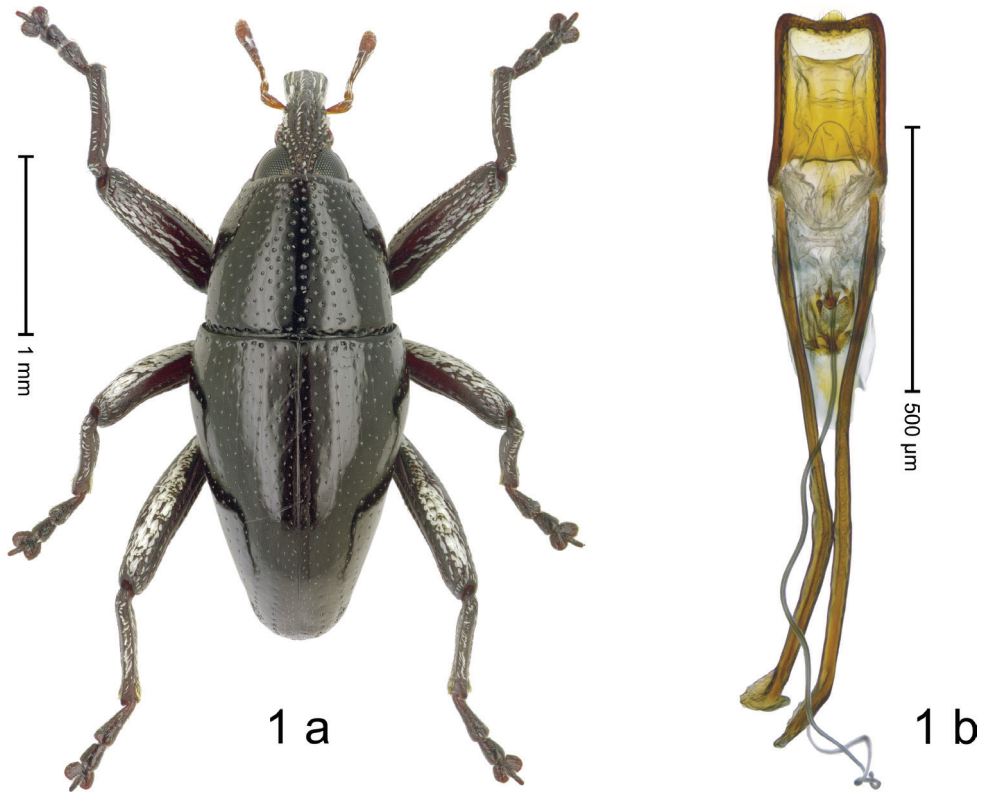


Figure 1. *Trigonopterus atuf* Narakusumo & Riedel, sp. nov., holotype **a** habitus **b** penis.

MN322567), MZB0024 (GenBank # MN322579), Selaru Is, Bangruti, 08°07.253'S, 131°02.947'E, 35 m, beaten, 22-IV-2018; 5 exx, MZB0031 (GenBank # MN322577), MZB0032 (GenBank # MN322576), MZB0040 (GenBank # MN322571), Yamdena Is, Lorulun, Jungle Camp, 07°46.46'S, 131°20.482'E, 110 m, beaten, 19-IV-2018; 1 ex, MZB0034 (GenBank # MN322574), Yamdena Is, Lorulun, Jungle track, 07°47.396'S, 131°20.849'E, 120 m, beaten, 19–20-IV-2018; 47 exx MZB0038 (GenBank # MN322573), MZB0039 (GenBank # MN322572), Yamdena Is, Lorulun, Jungle camp, 07°46.46'S, 131°20.482'E, 110 m, beaten, 24-IV-2018; 2 exx, MZB0033 (GenBank # MN322575), Yamdena Is, Lorulun, Jungle camp, 07°46.46'S, 131°20.482'E, 110 m, beaten, 27-IV-2018.

Distribution. Maluku Prov., Tanimbar (Yamdena Is, Selaru Is). Elevation: 35–120 m.

Biology. On foliage in lowland forest.

Etymology. The epithet is a noun in apposition. Atuf is a mythical warrior from the folklore of the Tanimbar people who defeated the sun.

Notes. This species is closely related to *Trigonopterus* species 773 from New Guinea, which differs by having a more distinct punctation and 15.1% p-distance of its *cox1* sequence.

***Trigonopterus kumbang* Narakusumo & Riedel, sp. nov.**

<http://zoobank.org/59F9DD00-C782-49EC-B32C-E53DD8F5ABB9>

Diagnostic description. Holotype. Male (Fig. 2a). Length 3.12 mm. Color of antennae ferruginous, remainder black. Body subovate; in dorsal aspect and in profile with weak constriction between pronotum and elytron. Eyes dorsally approximate. Rostrum in basal 1/2 dorsally weakly swollen, with median ridge, coarsely punctate, with dense white scales; in apical half flat, subglabrous, sparsely punctate. Pronotum subglabrous, sparsely punctate with small punctures, somewhat denser and larger along basal margin. Elytra subglabrous, with sparse minute punctures, laterally and subapically striae marked by sparse rows of small punctures; stria 8 along humerus with short row of seven deeper punctures. Femora with distinct anteroventral ridge, near middle with denticle. Mesofemur and metafemur dorsally densely squamose with white scales. Metafemur with smooth dorsoposterior edge; subapically without stridulatory patch. Mesocoxa with densely squamose patch. Abdominal ventrites 1–2 concave, subglabrous, laterally with sparse white scales; ventrite 5 flat, subglabrous, microreticulate, with minute punctures, laterally with coarse punctures and sparse white scales. Penis (Fig. 2b) with sides subparallel, apically subangulate. Transfer apparatus simple, dentiform. Apodemes 2.6× as long as body of penis; ductus ejaculatorius with indistinct bulb. **Intraspecific variation.** Length 3.12–3.53 mm. Female rostrum in apical 2/3 dorsally flat, subglabrous, with minute punctures; in basal 1/3 dorsally swollen, coarsely punctate. Female abdominal ventrites 1–2 flat.

Material examined. Holotype (MZB): MZB0002 (GenBank # MN322581), Indonesia, Maluku, Tanimbar, Yamdena Is, Lorulun, 07°48.788'S, 131°22.443'E to 07°48.82'S, 131°21.524'E, 140 m, beaten, 29-IV-2017. **Paratypes** (MZB, SMNK): Indonesia, Maluku, Tanimbar: 7 exx, MZB0001 (GenBank # MN322586), MZB0003 (GenBank # MN322585) same data as holotype; 1 ex, MZB0026 (GenBank # MN322582), Yamdena Is, Lorulun, Jungle Camp, 07°46.46'S, 131°20.482'E, 112m, beaten, 24-IV-2018; 3 exx, MZB0042 (GenBank # MN322584), Larat Is, Nature Reserve, 07°08.747'S, 131°49.092'E, 90 m, beaten, 25–26-IV-2018; 1 ex, MZB0019 (GenBank # MN322583), Larat Is, Nature reserve, 07°08.747'S, 131°49.092'E, 90 m, beaten, 26-IV-2018; 5 exx, Yamdena Is, Lorulun, 07°48.473'S, 131°22.266'E to 07°48.137'S, 131°21.873'E, 140 m, beaten, 02-V-2017.

Distribution. Maluku Prov., Tanimbar (Yamdena Is, Larat Is). Elevation 90–140 m.

Biology. On foliage in lowland forest.

Etymology. This epithet is the Indonesian word for beetle and a noun in apposition.

Note. This species is closely related to the undescribed *Trigonopterus* species 929 (*T. nasutus*-group) from the D'Entrecasteaux Islands from which it differs by its smaller body size, a subglabrous side of the pronotum, and a 12.3% p-distance of its *cox1* sequence.

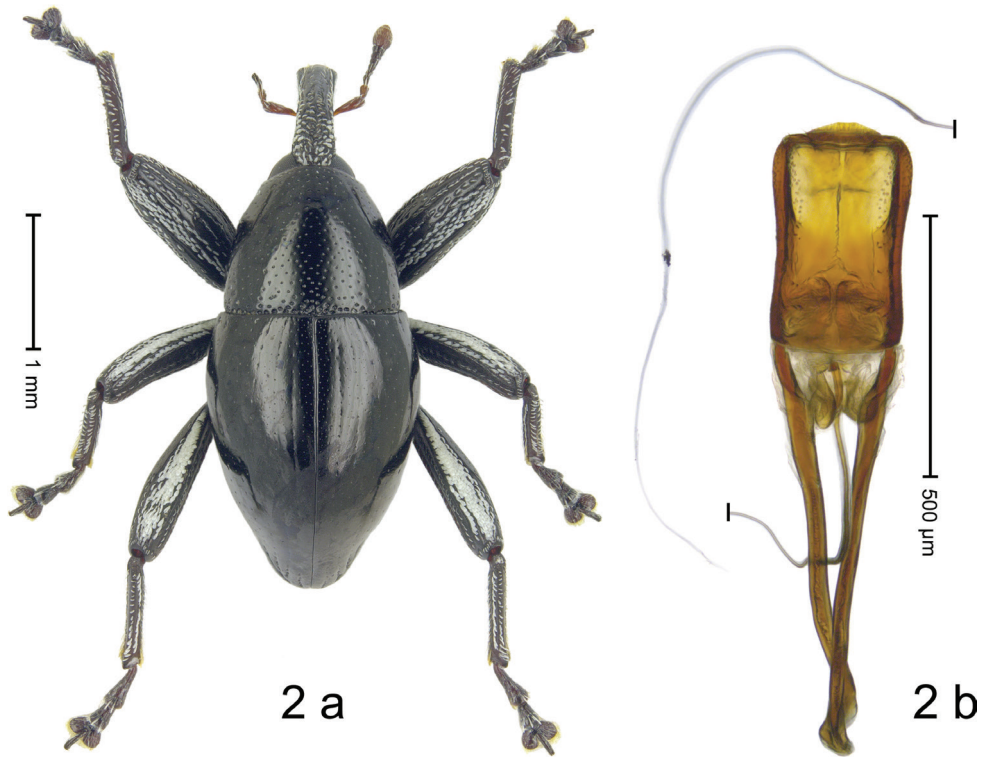


Figure 2. *Trigonopterus kumbang* Narakusumo & Riedel, sp. nov., holotype **a** habitus **b** penis.

***Trigonopterus laratensis* Narakusumo & Riedel, sp. nov.**

<http://zoobank.org/C27ED24F-2114-478D-AFBA-3256ECE4BD4B>

Diagnostic description. *Holotype: Male* (Fig. 3a). Length 2.53 mm. Color of head, femora and tibiae ferruginous; remainder black. Body subovate; in dorsal aspect almost without constriction between pronotum and elytron; profile dorsally convex. Rostrum in basal 1/2 with median costa and submedian ridges, intervening furrows with sparse, suberect scales. Pronotum subglabrous, sparsely punctate with small to minute punctures; anterolaterally with coarse punctures. Elytra subglabrous, punctate with minute punctures; striae marked by faint hairlines. Femora subglabrous weakly microreticulate, with minute punctures; with anteroventral ridge distinct, simple. Meso- and metafemur dorsally squamose with white scales. Mesotibia basally rounded; subapically with uncus and larger premucro. Metafemur subapically simple, without stridulatory patch; with uncus, without premucro. Abdominal ventrites 1–2 medially concave, subglabrous, microreticulate; ventrite 2 posteriorly projecting and forming edge; ventrite 5 almost flat, weakly concave, microreticulate. Penis (Fig. 3b) with side subparallel; apex symmetrical, with median triangular extension; transfer apparatus dentiform, apically bordered by pair of L-shaped sclerites; apodemes 3.0× as long as body of penis;

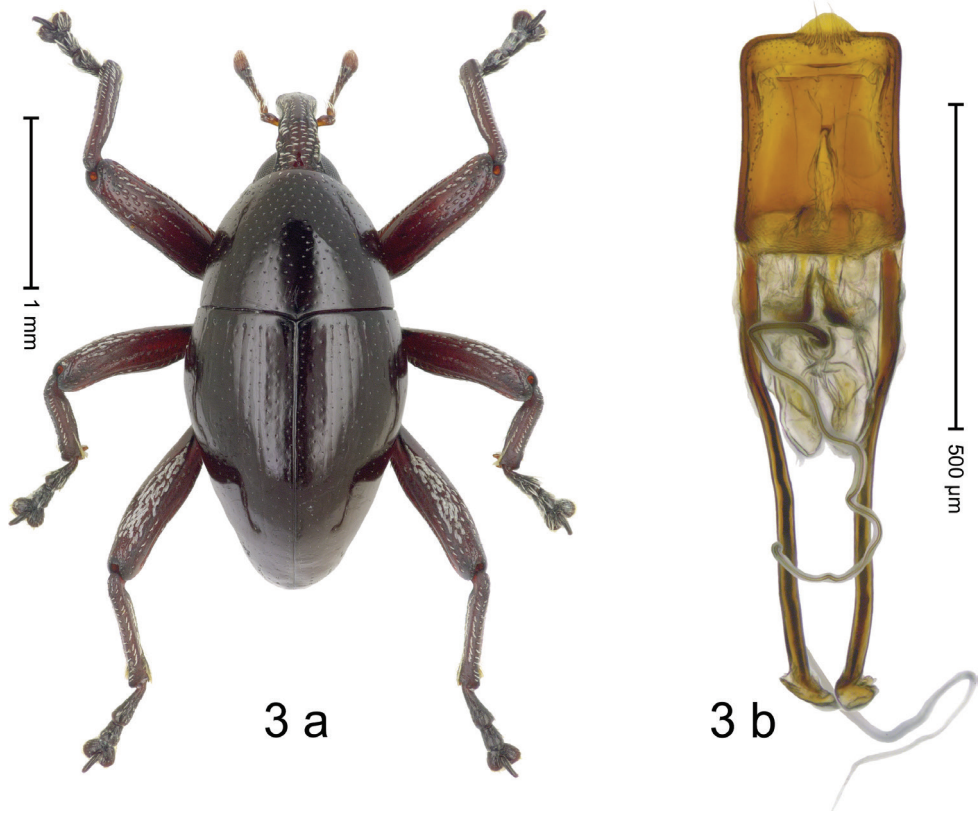


Figure 3. *Trigonopterus laratensis* Narakusumo & Riedel, sp. nov., holotype **a** habitus **b** penis.

ductus ejaculatorius with indistinct bulbus. **Intraspecific variation.** Length 2.48–2.53 mm. Female rostrum dorsally subglabrous, punctate; in basal 1/3 with median and submedian ridges. Female mesotibia subapically with uncus and minute premucro. Female abdominal ventrites 1–2 flat, with sparse punctures; ventrite 5 flat, subglabrous.

Material examined. Holotype (MZB): MZB0022 (GenBank # MN322587), Indonesia, Maluku, Tanimbar, Larat Is, Nature reserve, 07°08.747'S, 131°49.092'E, 85 m, beaten, 25–26-IV-2018. Paratype (SMNK): Indonesia, Maluku, Tanimbar: 1 ex, MZB0027 (GenBank # MN322588), Yamdena Is, Lorulun, Jungle Camp, 07°46.46'S, 131°20.482'E, 110 m, beaten, 24-IV-2018.

Distribution. Maluku Prov., Tanimbar (Yamdena Is, Larat Is). Elevation: 85–110 m.

Biology. On foliage in lowland forest.

Etymology. This epithet is based on the type locality Larat Island.

Notes. This species belongs to the *T. politus* group. It is most closely related to a clade comprising *T. allotopus* Riedel, *T. pseudallotopus* Riedel, and some undescribed species from New Guinea, but it has no close relationship to the clade of Australian species.

***Trigonopterus porg* Narakusumo & Riedel, sp. nov.**

<http://zoobank.org/96024735-BEC6-4650-BFB4-075551983D81>

Diagnostic description. Holotype. Male (Fig. 4a). Length 2.98 mm. Color of antennae, legs and elytra ferruginous, remainder black. Body elongate; in dorsal aspect and in profile with moderate constriction between pronotum and elytron. Rostrum in basal 2/3 with median carina, dorsal surface clothed with white scales; in apical 1/3 subglabrous, punctate-rugose, with suberect setae. Pronotum densely punctate, with large punctures, with subglabrous midline; anterolaterally with white scales. Elytra subglabrous with irregular small punctures; few striae faintly marked by hairlines. Femora with distinct anteroventral ridge, ending near middle with small tooth. Meso- and metafemur dorsally with silvery scales. Metafemur subapically with stridulatory patch. Abdominal ventrites 1–2 concave, subglabrous, posteriorly sparsely punctate, with sparse scales; ventrite 5 weakly concave with sparse setae. Penis (Fig. 4b) with sides subparallel, in apical 1/3 converging to subangulate apex; transfer apparatus denticulate; apodemes 1.6× as long as body of penis; ductus ejaculatorius with distinct bulbus. **Intraspecific variation.** Length 2.75–2.98 mm. Female rostrum with subglabrous median costa, laterally punctate-rugose, with short

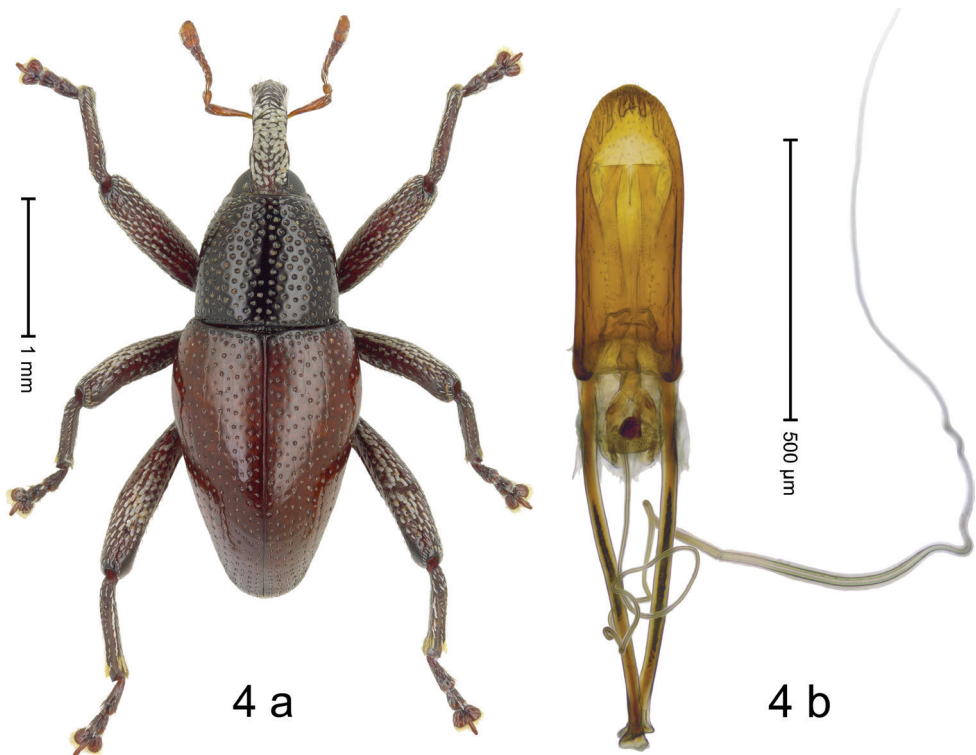


Figure 4. *Trigonopterus porg* Narakusumo & Riedel, sp. nov., holotype **a** habitus **b** penis.

setae. Female pronotum anterolaterally with scales transparent-yellowish. Female abdominal ventrites 1–2 concave, subglabrous with short setae. Female ventrite 5 flat.

Material examined. *Holotype* (MZB): MZB0043 (GenBank # MN322591), Indonesia, Maluku, Tanimbar, Larat Is, Nature reserve, 07°08.747'S, 131°49.092'E, 85 m, beaten, 25–26-IV-2018. *Paratypes* (MZB, SMNK): Indonesia, Maluku, Tanimbar: 4 exx, MZB0016 (GenBank # MN322590), MZB0044 (GenBank # MN322589) same data as holotype.

Distribution. Maluku Prov., Tanimbar (Larat Is). Elevation ca. 85 m.

Biology. On foliage in lowland forest.

Etymology. This epithet is a noun in apposition based on the fictional penguin-like character Porg in the Star Wars movies. This species inhabiting a remote island has the same color combination of black, orange and white.

Notes. This species is closely related to the undescribed species 437 from Kai Kecil Island from which it differs by the elytral color and a 13.6% p-distance of its *cox1* sequence.

***Trigonopterus selaruensis* Narakusumo & Riedel, sp. nov.**

<http://zoobank.org/A9B7F81C-432D-40A7-B99C-688C6F4BEA44>

Diagnostic description. *Holotype: Female* (Fig 6.a) Length 2.95 mm. Color of antennae ferruginous, head and legs dark ferruginous, remainder black. Body subovate; in dorsal aspect with weak constriction between pronotum and elytron; profile dorsally convex. Eyes dorsally approximate. Rostrum in basal 1/3 with median ridge and pair of submedian ridges; with suberect white scales; in apical half dorsally flattened, subglabrous, punctate Pronotum densely punctate with small punctures. Elytra subglabrous; striae marked by rows of minute punctures; intervals subglabrous and with row of even smaller punctures; along base and behind humerus bordered by row of deep punctures. Femora with distinct anteroventral ridge, near middle with denticle. Mesofemur and metafemur dorsally densely squamose with white scales. Metafemur with smooth dorsoposterior edge; subapically without stridulatory patch. Abdominal ventrites 1–2 flat, subglabrous, sparsely punctate, with sparse scales; ventrite 5 flat, punctate, sublaterally with suberect scales. Genitalia (Fig. 5b).

Material examined. Holotype (MZB): MZB0023 (GenBank # MN322592), Indonesia, Maluku, Tanimbar, Selaru Is, Bangruti, 08°07.253'S, 131°02.947'E, 35 m, beaten, 22-IV-2018.

Distribution. Maluku Prov., Tanimbar (Selaru Is). Elevation 35 m.

Biology. On foliage in lowland forest.

Etymology. This epithet is an adjective derived from the species' type locality, Selaru Island.

Notes. This species is closely related to the undescribed *Trigonopterus* species 436 from Kai Kecil Island, from which it differs by a larger body size and a more densely punctate pronotum and an 8.9% p-distance of its *cox1* sequence.

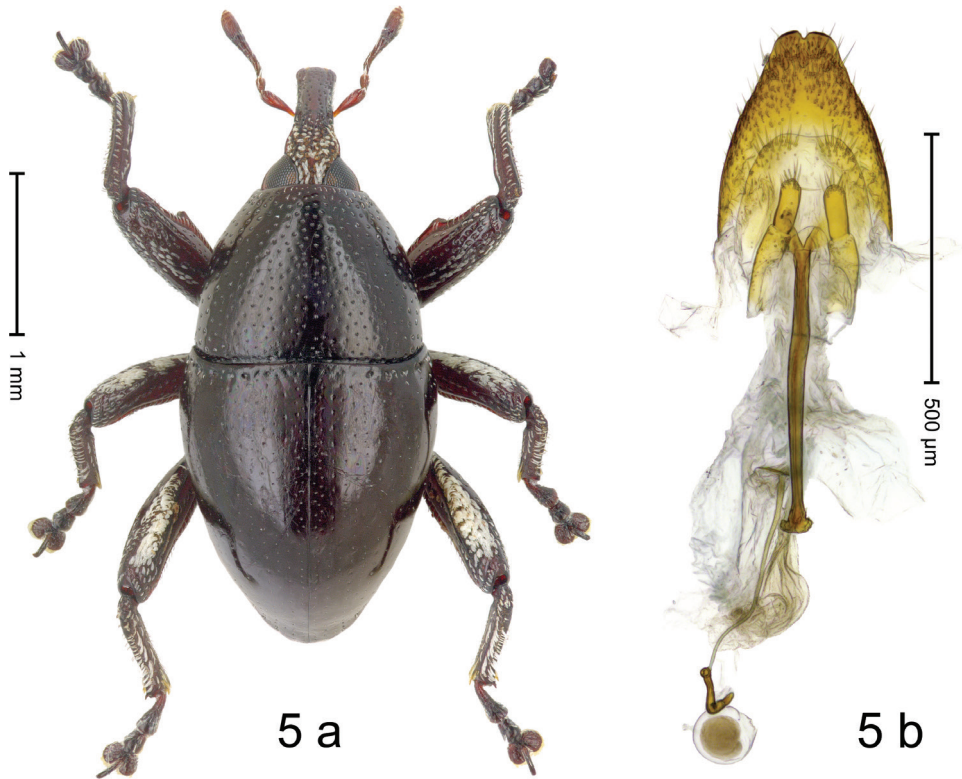


Figure 5. *Trigonopterus selaruensis* Narakusumo & Riedel, sp. nov., holotype **a** habitus **b** female genitalia.

***Trigonopterus tanimbarensis* Narakusumo & Riedel, sp. nov.**

<http://zoobank.org/D47905D5-2D81-4721-90E7-853F8714C52E>

Diagnostic description. Holotype. Male (Fig. 6a). Length 3.06 mm. Color of antennae and tarsi ferruginous, remainder black. Body slender subovate; profile dorsally convex; in dorsal aspect and in profile with weak constriction between pronotum and elytron. Rostrum dorsally with median ridge somewhat flattened at level of antennal insertion; with fine submedian ridges; in basal 1/2 with dense silvery scales, in apical 1/2 with suberect setae. Pronotum densely punctate; punctures becoming larger anterolaterad; each puncture containing short seta; with subglabrous midline. Elytra with striae marked by rows of small punctures and fine hairlines; basal margin bordered by transverse row of deeper punctures; intervals subglabrous, with interspersed minute punctures. Femora with anteroventral ridge weakly crenate, ending in apical half with small tooth. Metafemur dorsally with recumbent silvery scales; dorsoposterior edge indistinct, weakly denticulate-crenate, subapically with stridulatory patch. Abdominal ventrites 1–2 concave, coarsely punctate, at middle subglabrous; ventrite 5 with shallow impression, densely punctate, sparsely setose, laterally with sparse scale. Penis (Fig. 6b) with sides subparallel, apex subangulate, setose; transfer apparatus complex; sclerites of

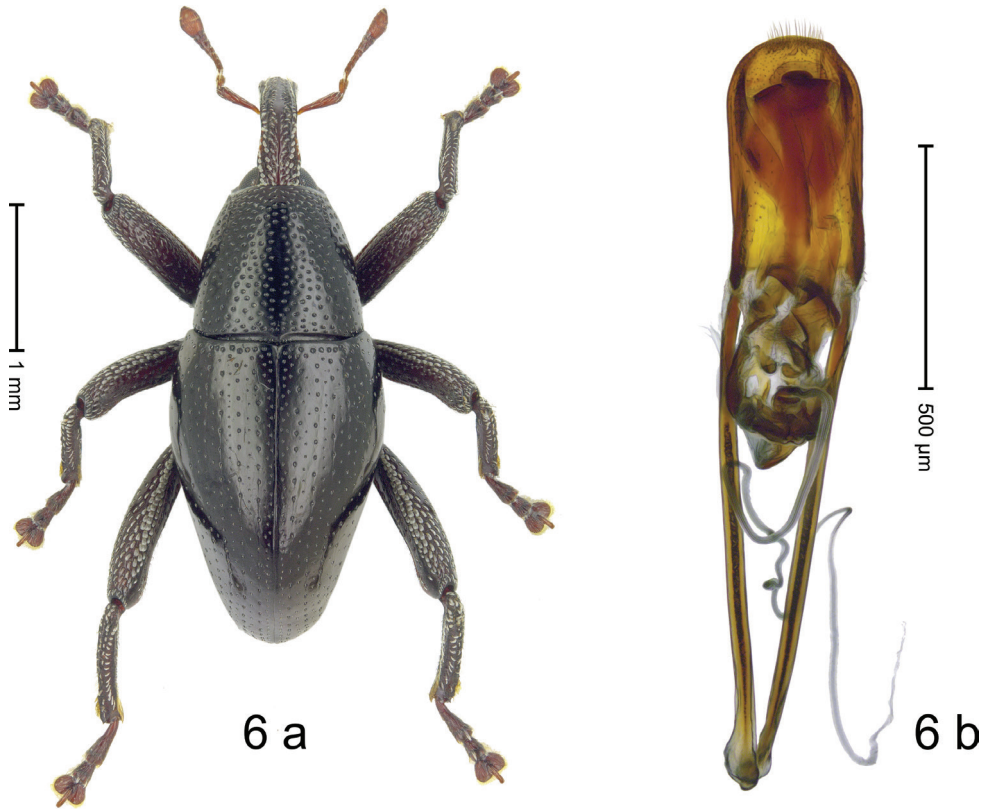


Figure 6. *Trigonopterus tanimbarensis* Narakusumo & Riedel, sp. nov., holotype **a** habitus **b** penis.

endophallus and orifice asymmetrical; apodemes 2.1× as long as body of penis; ductus ejaculatorius with indistinct bulbus. **Intraspecific variation.** Length 2.75–3.25 mm. Female rostrum slender, dorsally with subglabrous median costa, with sublateral rows of punctures, in basal 1/3 with sparse suberect scales. Female abdominal ventrites 1–2 flat. Female abdominal ventrite 5, punctate.

Material examined. **Holotype** (MZB): MZB0010 (GenBank # MN322598), Indonesia, Maluku, Tanimbar, Yamdena Is, Lorulun, 07°48.788'S, 131°22.443'E to 07°48.137'S, 131°21.873'E, 140 m, beaten, 02-V-2017. **Paratypes** (MZB, SMNK): Indonesia, Maluku, Tanimbar: 7 exx, MZB0008 (GenBank # MN322600), MZB0009 (GenBank # MN322599), MZB0011 (GenBank # MN322593), same data as holotype; 4 exx. MZB0035 (GenBank # MN322596), Yamdena Is, Lorulun, Jungle Camp, 07°46.46'S, 131°20.482'E, 110 m, beaten, 19-IV-2018; 53 exx. MZB0028 (GenBank # MN322597) MZB0037 (GenBank # MN322594), Yamdena Is, Lorulun, Jungle Camp, 07°46.46'S, 131°20.482'E, 110 m, beaten, 24-IV-2018; 1 ex., MZB0036 (GenBank # MN322595), Yamdena Is, Lorulun, Jungle Track, 07°47.396'S, 131°20.849'E, 120 m, beaten, 19–20-IV-2018.

Distribution. Maluku Prov., Tanimbar (Yamdena Is). Elevation 110–140 m.

Biology. On foliage in lowland forest.

Etymology. This epithet is an adjective derived from the Tanimbar Archipelago.

Notes. This species appears related to a species from New Guinea (species 959) from which it differs by 19.9% p-distance of its *cox1* sequence and many morphological characters.

***Trigonopterus triradiatus* Narakusumo & Riedel, sp. nov.**

<http://zoobank.org/4FE8402C-4899-4C13-AD16-B4DC50990282>

Diagnostic description. *Holotype*. **Male** (Fig. 7a). Length 3.03 mm. Color of antennae ferruginous, legs dark ferruginous, remainder black. Body subovate; in dorsal aspect and in profile with weak constriction between pronotum and elytron. Eyes dorsally approximate. Rostrum in basal 1/2 with median ridge and pair of sublateral ridge; intervening furrows with suberect scales; apical half subglabrous, punctate. Pronotum with disk subglabrous, with minute sculpture; in basal 1/3 laterally with indistinct edge lined with few coarse punctures; laterally anterior margin lined by few white scales, behind eye with row of coarse punctures. Elytra subglabrous, with minute punctures. Femora edentate; with distinct anteroventral ridge. Mesofemur and metafemur dorsally densely squamose with white scales. Metafemur with smooth dorsoposterior edge; subapically without stridulatory patch. Abdominal ventrites 1–2 medially concave, subglabrous, laterally with sparse white scales; ventrite 5 at middle with shallow impression, weakly punctate, with sparse short setae. Penis (Fig. 7b) with sides converging to slightly spatulate apex; transfer apparatus complex; endophallus with triradiate sclerites; apodemes 1.5× as long as body of penis; ductus ejaculatorius with distinct bulbus. **Intraspecific variation.** Length 2.68–3.53 mm. Female rostrum slender, subglabrous, sparsely punctate, in basal 1/4 with indistinct ridges and sparse suberect scale. Female abdominal ventrite 5 flat, subglabrous, with small punctures.

Material examined. *Holotype* (MZB): MZB0007 (GenBank # MN322604), Indonesia, Maluku, Tanimbar, Yamdena Is, Lorulun, 07°48.788'S, 131°22.443'E to 07°48.137'S, 131°21.873'E, 140 m, beaten, 2-V-2017. *Paratypes* (MZB, SMNK): Indonesia, Maluku, Tanimbar: 12 exx, MZB0004 (GenBank # MN322607), MZB0005 (GenBank # MN322606), MZB0006 (GenBank # MN322605) same data as holotype; 3 exx, Yamdena Is, Lorulun, 07°48.788'S, 131°22.443'E to 07°48.137'S, 131°21.873'E, 140 m, beaten, 28–29-V-2017; 7 exx, MZB0029 (GenBank # MN322601) MZB0030 (GenBank # MN322602) Yamdena Is, Lorulun, Jungle Camp, 07°46.46'S, 131°20.482'E, 110 m, beaten, 24-IV-2018; 1 ex, Yamdena Is, Lorulun, Jungle Camp, 07°46.46'S, 131°20.482'E, 110 m, beaten, 19-IV-2018; 1 ex, MZB0021 (GenBank # MN322608) Larat Is, margin of Nature reserve, 07°08.22'S, 131°49.49'E, 40 m, 25-IV-2018; 1 ex, MZB0041 (GenBank # MN322603) Larat Is, Nature reserve, 07°08.747'S, 131°49.092'E, 85 m, beaten, 25–26-IV-2018; 2 exx, MZB0025 (GenBank # MN322609), MZB0112 (GenBank # MN322610), Selaru Is, Bangruti, 08°07.253'S, 131°02.947'E, 40 m, beaten, 22-IV-2018.

Distribution. Maluku Prov., Tanimbar (Yamdena Is, Larat Is, Selaru Is). Elevation: 40–140 m.

Biology. On foliage in lowland forest.

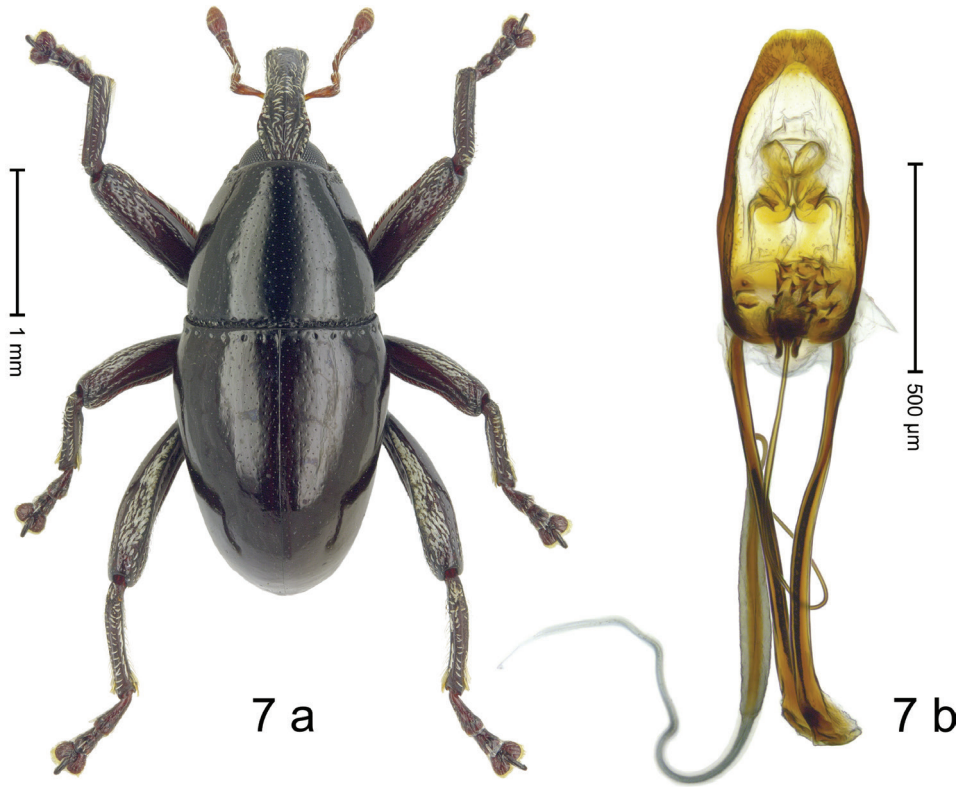


Figure 7. *Trigonopterus triradiatus* Narakusumo & Riedel, sp. nov., holotype **a** habitus **b** penis.

Etymology. This epithet is an adjective based on triradiate sclerites in the endophallus of the species.

Note. This species is closely related to *Trigonopterus* species 60 from Papua New Guinea from which it differs by the structure of the penis and a 17.8% p-distance of its *cox1* sequence.

Key to the *Trigonopterus* species of the Tanimbar Archipelago

- 1 Metafemur subapically with stridulatory patch. Pronotum densely punctate.....2
- Metafemur subapically without stridulatory patch. Pronotum subglabrous, sparsely punctate with small or minute punctures3
- 2 Elytra black. Basal half of rostrum and forehead with silvery scales not covering the surface. Side of pronotum anteriorly without scales..... ***T. tanimbarensis* sp. nov.**
- Elytra ferruginous. Basal half of rostrum and forehead almost covered by white scales. Side of pronotum anteriorly with white scales..... ***T. porg* sp. nov.**
- 3 Femora with simple anteroventral ridge; edentate.....4
- Femora with ventral denticle.....6

- 4 Eyes medially approximate; base of rostrum much wider than forehead between eyes. Apex of male mesotibia only with uncus **5**
- Base of rostrum subequal to forehead between eyes. Apex of male mesotibia with enlarged premucro ***T. laratensis* sp. nov.**
- 5 Body slender. Pronotum sparsely punctate. Elytral striae marked by rows of minute punctures and fine hairlines..... ***T. atuf* sp. nov.**
- Body wider. Pronotum subglabrous. Elytra subglabrous, without distinct striae ..
..... ***T. triradiatus* sp. nov.**
- 6 Elytral base bordered by row of deeper punctures. Apex of metatibia with supra-uncal denticle..... ***T. selaruensis* sp. nov.**
- Elytral base without deeper punctures (except row hidden behind humerus). Apex of metatibia dorsally of uncus rounded..... ***T. kumbang* sp. nov.**

Discussion

Trigonopterus had hitherto been recorded from Ceram Island (Riedel 2011), Flores of the Lesser Sunda Islands (Riedel et al. 2014), the Aru Islands (Pascoe 1885), Eastern Australia (Riedel and Tänzler 2016), and New Guinea (Riedel 2011, Riedel et al. 2013b). The newly discovered *Trigonopterus* fauna of the Tanimbar Islands fills a gap in the known distribution and is of special interest due to the isolated position and recent geological age of these islands. The islands of Sumba, Alor, Timor, and Wetar should be searched for additional undescribed species in future.

All the discovered species of Tanimbar *Trigonopterus* live on foliage, and no edaphic lineage could be found. This may be due to the relatively dry climatic conditions, which may be putting stress on species that depend on a layer of moist litter. Alternatively, it is possible, that edaphic species are present but have eluded discovery so far; sifting of leaf litter under the right conditions, e.g., after sufficient rainfalls, may bring them to light.

Morphologically the Tanimbar *Trigonopterus* species are very different from each other, a fact supported by the molecular dataset of their *cox1* sequences. Therefore, no closely related species pairs can be recognized, i.e., there is no indication for any autochthonous speciation on the Tanimbar Archipelago. Instead, the *Trigonopterus* fauna has been formed largely by repeated dispersal from neighboring regions, i.e., from Western New Guinea and the Moluccas. The sister species of *T. porg* sp. nov. (13.6% *p*-distance of *cox1*) and *T. selaruensis* sp. nov. (8.9% *p*-distance of *cox1*) were both found on Kai Kecil Island 190 km to the Northeast. *Trigonopterus triradiatus* sp. nov. is related to *Trigonopterus* species 60 from Papua New Guinea (17.8% *p*-distance of *cox1*). *Trigonopterus laratensis* sp. nov. belongs to a clade comprising *T. allotopus* Riedel, *T. pseudallotopus* Riedel, and some undescribed species from New Guinea (15.6% *p*-distance of *cox1*), but has no close relationship to the clade of Australian species of the *T. politus*-group. *Trigonopterus kumbang* sp. nov. belongs to the *T. nasutus*-group and appears most closely allied to *Trigonopterus* species 929 (12.3% *p*-distance of *cox1*)

from the D'Entrecasteaux Islands. *Trigonopterus atuf* sp. nov. is closely related to *Trigonopterus* species 773 (15.1% *p*-distance of *cox1*) from Papua New Guinea. *Trigonopterus tanimbarensis* sp. nov. appears related to a species from New Guinea (*Trigonopterus* species 959; 19.9% *p*-distance of *cox1*).

With its close proximity to Australia, stronger ties to the Australian fauna could be expected, but apparently this is not the case. An explanation could be that the Australian species are largely restricted to the Cape York Peninsula and the east coast of Queensland, which is quite distant from the Tanimbar Islands, and that the absence of *Trigonopterus* from the Northern Territory in Australia could be a real gap in the distribution of the genus and not just a sampling artifact, caused by environmental extremes.

All in all, the observed composition of the *Trigonopterus* fauna of the Tanimbar Archipelago is exactly what can be expected from the geological setting and what has been observed in other taxa (How and Kitchener 1997; Beck et al. 2006; Michaux 2010; Andersen et al. 2013): 1) a relatively recent origin that may not have allowed for local speciation and 2) an insular situation not compromised by periods of low sea level. This is quite different in the otherwise similar Aru Islands further east which were part of the continuous Sahul shelf during the Pleistocene. However, no focused fieldwork has ever been carried out on the Aru Islands, from which only *T. oblongus* Pascoe is known to date. Presumably, further collecting on these islands would discover additional species with stronger ties to the Southern Papuan fauna.

The rapid and ongoing anthropogenic activities in Tanimbar, i.e., agriculture and forestry, put pressure on the natural forests of the islands, which are the exclusive habitats of *Trigonopterus* species. The first author found the southern part of Yamdena Island to be extensively logged, and most areas of the eastern coast have been converted to agriculture and settlements. The forests of Larat Island are also severely affected by agriculture, with coconut plantations prevalent inside the wildlife conservation area. Finally, Selaru Island without any protected areas, has suffered worst from logging; its interior has already been turned into grassland and the remaining forests areas are fragmented on the sparse rocky soil that is almost useless for gardening. Such destructions of natural forest areas in Tanimbar threaten not only the endemic *Trigonopterus* species but also the remaining biodiversity of this fascinating archipelago.

Acknowledgements

We would like to thank the Indonesian Ministry of Environment and Forestry and Center for natural resources conservation (BKSDA) of Maluku for the permits to enter conservation areas and to collect wildlife. Specimens were exported as a loan from MZB. Thanks to Anang Setiawan Achmadi (MZB) and Ibnu Maryanto (MZB) for making it possible that RPN could join their expedition to the Tanimbar Archipelago. Special thanks to Wilhelmus Samangun (Tanimbar), Vera (Tanimbar), Mark O'Hara (Vienna), Berenica Mioduszewska (Vienna), and Tri Haryoko (MZB) in allowing

RPN to use their wonderful field station, Suprayitno (Denpasar) for the companionship during the first trip, and I Nyoman Sumerta (InaCC), Ruby Setiawan (InaCC), and the people of Lorulun, Adaut, and Keliobar for helping RPN during the fieldwork. Sequencing runs were done by A. Brachmann and G. Brinkmann of the LMU sequencing unit (Munich). This work was funded by the German Academic Exchange Service DAAD (91654661 to R.P.N.), pilot project funding from the laboratory of Michael Balke, DIPA KSK Pengembangan Database KEHATI PDII 2018 and the German Research Foundation DFG (RI 1817/3-4 to A.R.).

References

- Alonso-Zarazaga MA, Lyal CHC (1999) A world catalogue of families and genera of Curculionioidea (Insecta: Coleoptera) (excepting Scolytidae and Platypodidae). Entomopraxis, Barcelona, 315 pp.
- Andersen AN, Kohout RJ, Trainor CR (2013) Biogeography of Timor and Surrounding Wallacean Islands: Endemism in ants of the genus *Polyrhachis* Fr. Smith. Diversity 5: 139–148. <https://doi.org/10.3390/d5010139>
- Beck J, Kitching IJ, Linsenmair KE (2006) Wallace's line revisited: has vicariance or dispersal shaped the distribution of Malesian hawkmoths (Lepidoptera: Sphingidae)? Biological Journal of the Linnean Society 89(3): 455–468. <https://doi.org/10.1111/j.1095-8312.2006.00686.x>
- Beutel RG, Leschen RAB (2005) Handbook of Zoology, Vol. IV, Part 38, Coleoptera, Beetles. (Vol. 1). Morphology and Systematics (Archostemata, Adephaga, Myxophaga, Polyphaga partim). Walter de Gruyter, Berlin, 567 pp. <https://doi.org/10.1515/9783110904550>
- Charlton TR, De Smet MEM, Samodra H, Kaye SJ (1991) The stratigraphic and structural evolution of the Tanimbar islands, eastern Indonesia. Journal of Southeast Asian Earth Sciences 6(3–4): 343–358. [https://doi.org/10.1016/0743-9547\(91\)90080-H](https://doi.org/10.1016/0743-9547(91)90080-H)
- De Smet MEM, Fortuin AR, Tjokrosapoetro S, Van Hinte JE (1989) Late Cenozoic vertical movements of non-volcanic islands in the Banda Arc area. Netherlands Journal of Sea Research 24(2–3): 263–275. [https://doi.org/10.1016/0077-7579\(89\)90153-1](https://doi.org/10.1016/0077-7579(89)90153-1)
- Hall R (1998) Biogeographic implications of the Tertiary palaeogeographic evolution of Sulawesi and Borneo. Biogeography and geological evolution of SE Asia. Backhuys Publishers, Leiden, 133–163.
- Hall R (2002) Cenozoic geological and plate tectonic evolution of SE Asia and the SW Pacific: computer-based reconstructions, model and animations. Journal of Asian Earth Sciences 20: 353–431. [https://doi.org/10.1016/S1367-9120\(01\)00069-4](https://doi.org/10.1016/S1367-9120(01)00069-4)
- How RA, Kitchener DJ (1997) Biogeography of Indonesian snakes. Journal of Biogeography 24(6): 725–735. <https://doi.org/10.1046/j.1365-2699.1997.00150.x>
- Jönsson KA, Bowie RC, Moyle RG, Christidis L, Norman JA, Benz BW, Fjeldså J (2010) Historical biogeography of an Indo-Pacific passerine bird family (Pachycephalidae): different colonization patterns in the Indonesian and Melanesian archipelagos. Journal of Biogeography 37(2): 245–257. <https://doi.org/10.1111/j.1365-2699.2009.02220.x>

- Laumonier Y, Nasi R (2018) The last natural seasonal forests of Indonesia: Implications for forest management and conservation. *Applied vegetation science* 21(3): 461–476. <https://doi.org/10.1111/avsc.12377>
- Leschen RAB, Beutel RG, Lawrence JF, Slipinski A (2009) Handbook of Zoology, Vol. IV, Part 38, Coleoptera, Beetles (Vol. 2). Morphology and Systematics (Elateroidea, Bostrichiformia, Cucujiformia partim). Walter de Gruyter, Berlin 786 pp.
- Michaux B (2010) Biogeology of Wallacea: geotectonic models, areas of endemism, and natural biogeographical units. *Biological Journal of the Linnean Society* 101(1): 193–212. <https://doi.org/10.1111/j.1095-8312.2010.01473.x>
- Nguyen L-T, Schmidt HA, von Haeseler A, Bui QM (2015) IQ-TREE: A Fast and Effective Stochastic Algorithm for Estimating Maximum-Likelihood Phylogenies. *Molecular Biology and Evolution* 32(1): 268–274. <https://doi.org/10.1093/molbev/msu300>
- Pascoe FP (1885) List of the Curculionidae of the Malay Archipelago collected by Dr. Odoardo Beccari, L. M. D'Albertis, and others. *Annali del Museo Civico di Storia Naturale di Genova* 22: 201–332.
- Riedel A (2005) Digital imaging of beetles (Coleoptera) and other three-dimensional insects. In: Häuser C, Steiner A, Holstein J, Scoble MJ (Eds) *Digital Imaging of Biological Type Specimens – A Manual of Best Practice. Results from a study of the European Network for Biodiversity Information*, Stuttgart, 222–250.
- Riedel A (2011) The weevil genus *Trigonopterus* Fauvel (Coleoptera, Curculionidae) and its synonyms – a taxonomic study on the species tied to its genus-group names. *Zootaxa* 2977: 1–49. <https://doi.org/10.11646/zootaxa.2977.1.1>
- Riedel A, Daawia D, Balke M (2010) Deep *cox1* divergence and hyperdiversity of *Trigonopterus* weevils in a New Guinea mountain range (Coleoptera, Curculionidae). *Zoologica Scripta* 39(1): 63–74. <https://doi.org/10.1111/j.1463-6409.2009.00404.x>
- Riedel A, Sagata K, Suhardjono YR, Tänzler R, Balke M (2013a) Integrative taxonomy on the fast track – towards more sustainability in biodiversity research. *Frontiers in Zoology* 10: 1–15. <https://doi.org/10.1186/1742-9994-10-15>
- Riedel A, Sagata K, Surbakti S, Tänzler R, Balke M (2013b) One hundred and one new species of *Trigonopterus* weevils from New Guinea. *ZooKeys* 280: 1–150. <https://doi.org/10.3897/zookeys.280.3906>
- Riedel A, Tänzler R, Balke M, Rahmadi C, Suhardjono YR (2014) Ninety-eight new species of *Trigonopterus* weevils from Sundaland and the Lesser Sunda Islands. *ZooKeys* 467: 1–162. <https://doi.org/10.3897/zookeys.467.8206>
- Riedel A, Tänzler R (2016) Revision of the Australian species of the weevil genus *Trigonopterus* Fauvel. *ZooKeys* 556: 97–162. <https://doi.org/10.3897/zookeys.556.6126>
- Riedel A, Tänzler R, Pons J, Suhardjono YR, Balke M (2016) Large-scale molecular phylogeny of Cryptorhynchinae (Coleoptera, Curculionidae) from multiple genes suggests American origin and later Australian radiation. *Systematic Entomology* 41: 492–503. <https://doi.org/10.1111/syen.12170>
- Riedel A, Narakusumo RP (2019) One hundred and three new species of *Trigonopterus* weevils from Sulawesi. *ZooKeys* 828: 1–153. <https://doi.org/10.3897/zookeys.828.32200>

- Tänzler R, Sagata K, Surbakti S, Balke M, Riedel A (2012) DNA barcoding for community ecology – how to tackle a hyperdiverse, mostly undescribed Melanesian fauna. *PLoS ONE* 7(1): e28832. <https://doi.org/10.1371/journal.pone.0028832>
- Tänzler R, van Dam MH, Toussaint EFA, Suhardjono YR, Balke M, Riedel A (2016) Macro-evolution of hyperdiverse flightless beetles reflects the complex geological history of the Sunda Arc. *Scientific Reports* 6: e18793. <https://doi.org/10.1038/srep18793>
- Toussaint EFA, Tänzler R, Balke M, Riedel A (2017) Transoceanic origin of microendemic and flightless New Caledonian weevils. *Royal Society Open Science* 4(6): 160546. <https://doi.org/10.1098/rsos.160546>
- Trifinopoulos J, Nguyen L-T, von Haeseler A, Bui QM (2016) W-IQ-TREE: a fast online phylogenetic tool for maximum likelihood analysis, *Nucleic Acids Research* 44 (W1): W232–W235. <https://doi.org/10.1093/nar/gkw256>
- van Dam MH, Laufa R, Riedel A (2016) Four new species of *Trigonopterus* Fauvel from the island of New Britain (Coleoptera, Curculionidae). *ZooKeys* 582: 129–141. <https://doi.org/10.3897/zookeys.582.7709>
- Voris HK (2000) Maps of Pleistocene sea levels in Southeast Asia: shorelines, river systems and time durations. *Journal of Biogeography* 27(5): 1153–1167. <https://doi.org/10.1046/j.1365-2699.2000.00489.x>

A new species of *Ceraeochrysa* Adams (Neuroptera, Chrysopidae), with a key to the species from Mexico

Rodolfo J. Cancino-López¹, Atilano Contreras-Ramos²

1 Posgrado en Ciencias Biológicas, sede Instituto de Biología-UNAM, Cd. Universitaria, 04510 Ciudad de México, Mexico **2** Instituto de Biología-UNAM, Departamento de Zoología, Cd. Universitaria, 04510 Ciudad de México, Mexico

Corresponding author: Atilano Contreras-Ramos (acontreras@ib.unam.mx)

Academic editor: S. Winterton | Received 14 August 2019 | Accepted 9 October 2019 | Published 11 November 2019

<http://zoobank.org/64A28110-F068-4C89-8396-0C23C6A96337>

Citation: Cancino-López RJ, Contreras-Ramos A (2019) A new species of *Ceraeochrysa* Adams (Neuroptera, Chrysopidae), with a key to the species from Mexico. ZooKeys 888: 95–104. <https://doi.org/10.3897/zookeys.888.39064>

Abstract

The genus *Ceraeochrysa* Adams is widely distributed in the New World, from southeastern Canada to Argentina, with 15 out of 61 previously known species recorded in Mexico. In this paper, *Ceraeochrysa tacanensis* **sp. nov.** is described and illustrated from Volcán Tacaná, Chiapas, and an identification key to *Ceraeochrysa* species present in Mexico is provided. The new species is similar to others with swollen and darkened posterior branches of the cubital vein, and it can be separated from these other species by an elongate gonopsis extending from the base of the gonosaccus; the gonopsis is slightly upturned, terminating in a rounded apex with dorsal microteeth. Females of the new species have non-distinctive genitalia morphology. However, they can be associated with males of the species by body color pattern, synchrony, and sympatry.

Keywords

Central American Volcanic Arc, Green lacewings, taxonomy, Volcán Tacaná

Introduction

The Neotropical green lacewing genus *Ceraeochrysa* (Neuroptera, Chrysopidae) was separated from *Chrysopa* by Adams (1982), who based his definition of the genus on male genitalic characters and recognized 24 species. Further studies added several species to this genus (Brooks and Barnard 1990; Penny 1997, 1998, 2002; Tauber et al. 2000; Freitas and Penny 2001; Tauber and De León 2001). *Ceraeochrysa* is the second

most species-rich chrysopid genus in the New World after *Leucochrysa* McLachlan, comprising 61 valid species (Sosa and Freitas 2010, 2011; Tauber and Flint 2010; Tauber and Garland 2014).

This genus is distributed from southeastern Canada to Argentina, and its greatest species richness and abundance is in the tropics (Adams 1982; Brooks and Barnard 1990; Freitas et al. 2009; Tauber et al. 2000; Sosa and Freitas 2010). Currently, countries having the highest species richness of *Ceraeochrysa* include Brazil (33 species), Costa Rica (23), Mexico (15), Panama (14), and Venezuela (12) (Freitas et al. 2009; Sosa and Freitas 2010; Oswald 2018; Martins and Machado 2019). Species of this genus have been reported from dry and open forests and various agroecosystems (Tauber et al. 2000; Freitas et al. 2009). Their larvae are trash-bearers and feed on soft-bodied arthropods such as aphids, diaspidids, thrips, aleyrodids, psyllids, and neonatal larvae of Lepidoptera, which makes them potentially useful for biological control (Tauber et al. 2000; Freitas 2001; Penny 2002; Freitas et al. 2009).

There have been few studies of the Chrysopidae of Mexico, and knowledge of this group is fragmented. The aim of this paper is to describe and illustrate a new species of the genus *Ceraeochrysa* as part of a survey of the lacewings of the Tacaná Volcano, Chiapas across an altitudinal gradient. Also, a key to males of the species of this genus known from Mexico is included, excluding *C. indicata* (Navás) and *C. lateralis* (Guérin-Méneville) for which males are unknown. Due to their potential importance in the biological control of agricultural pests, there is an established need to better describe the green lacewing fauna of Mexico.

Materials and methods

The material examined was obtained during monthly samplings (February 2018–January 2019) in the Tacaná Volcano Biosphere Reserve, Chiapas state, Mexico. Specimens were captured at lights traps and with aerial net on vegetation, kept alive in plastic screw cap vials, then they were pinned as they died, or after being killed by freezing. For dissection of genitalia, the abdomen was cut between the 6th and 7th segments and the apical segments were removed and cleared with solution of 10% potassium hydroxide (KOH) for 15 min at 80 °C in a water bath. The cleared genitalia were stained using Clorazol Black E and then placed in microvials with glycerin. Observations were done under a Discovery V8 Zeiss dissecting microscope. Serial images from different layers were taken with a Zeiss Axio Zoom V16 microscope fitted with an AxioCam MRc5 digital camera and stacked using Zen 2012 (Blue edition). Head width was measured as the distance between the outer margins of the eyes, dorsally. Wing length was measured from the joint region to the apex (Sosa and Freitas 2010). The holotype and allotype, both dissected, are deposited at the Colección Nacional de Insectos (CNIN) of the Instituto de Biología, UNAM, Mexico City; paratypes will be deposited at CNIN, the Colección de Insectos asociados a plantas cultivadas en la Frontera Sur (ECO-TAP-E) and the National Museum of Natural History, Smithsonian Institution (NMNH), Washington, DC. The key was constructed based on Freitas et al. (2009).

Taxonomy

Ceraeochrysa tacanensis Cancino-López & Contreras-Ramos, sp. nov.

<http://zoobank.org/6B20810F-BA84-4838-AF7B-9AD9837497B4>

Figures 1–3

Material examined (20 males, 11 females). *Holotype* (male): MEXICO: Chiapas, Cacahoatán, Ej[ido] Benito Juárez El Plan, 15°05'27.18"N, 92°08'51.06"W, 1479 m, 17.ii.2018, Cancino-López & Luna-Luna, light trap [genitalia dissected] (CNIN). *Allotype*: MEXICO: Chiapas, Unión Juárez, Cantón Chiquihuites, 15°05'46.26"N, 92°05'56.46"W, 2072 m, 16.iv.2018, Cancino-López & Luna-Luna, light trap [genitalia dissected] (CNIN). *Paratypes*: MEXICO: Chiapas, Cacahoatán, Ej[ido] Benito Juárez El Plan, 15°05'27.18"N, 92°08'51.06"W, 1479 m, 17.ii.2018, Cancino-López & Luna-Luna, light trap, 1 male, 1 female [genitalia dissected] (CNIN); same data but, 15°05'13.02"N, 92°08'55.2"W, 1430 m, 16.iii.2018, 2 males [one with genitalia dissected] (CNIN); same data but, 15°05'53.28"N, 92°08'29.88"W, 1705 m, 16.iii.2018, Cancino-López, 1 female, entomological net (CNIN); same data but, 15°05'36.48"N, 92°08'43.92"W, 1553 m, 12.viii.2018, 2 males (CNIN); same data but, 15°05'37.74"N, 92°08'43.26"W, 1572 m, 1 male (CNIN); same data but, 15°05'27.18"N, 92°08'51.06"W, 1479 m, 20.ix.2018, Cancino-López & Luna-Luna, 1 female, light trap (CNIN); same data but, 15°05'41.94"N, 92°08'41.52"W, 1577 m, 06.x.2018, Cancino-López, 1 female, entomological net (NMNH); same data but, 15°05'34.98"N, 92°08'45.42"W, 1541 m, 07.xi.2018, 1 female (NMNH); same data but, 15°05'40.98"N, 92°08'40.8"W, 1567 m, 08.xii.2018, 2 males (CNIN); same data but, 15°05'36.54"N, 92°08'43.8"W, 1549 m, 1 male (CNIN); same data but, 15°05'37.44"N, 92°08'43.68"W, 1564 m, 08.i.2019, 1 male (NMNH); same data but, 15°05'35.22"N, 92°08'44.76"W, 1533 m, 1 male (NMNH); same data but, 15°05'45.66"N, 92°08'40.5"W, 1582 m, 10.i.2019, 1 male, 1 female (ECO-TAP-E). MEXICO: Chiapas, Unión Juárez, Cantón Chiquihuites, 15°05'54.42"N, 92°05'57.96"W, 2157 m, 19.ii.2018, Cancino-López & Luna-Luna, 1 male [genitalia dissected], light trap (CNIN); same data but, 15°05'46.26"N, 92°05'56.46"W, 2076 m, 16.iv.2018, 1 male (CNIN); same data but, 15°05'43.74"N, 92°05'57.6"W, 2060 m, 14.v.2018, 3 males (CNIN); same data but, 15°05'43.79"N, 92°05'57.6"W, 2081 m, 10.ix.2018, 1 male, 1 female (NMNH); same data but, 15°05'43.79"N, 92°05'57.6"W, 08.x.2018, 1 male (CNIN); same data but, 15°06'9.06"N, 92°06'18.42"W, 2430 m, 19.xi.2018, Cancino-López, 1 male, entomological net (NMNH); same data but, Almaraz-Hernández, 1 female (NMNH); same data but, 15°05'43.79"N, 92°05'57.6"W, 2081 m, 14.i.2019, Cancino-López & Luna-Luna, 1 male, light trap (CNIN).

Diagnosis. This species has marks on the pronotum (a discontinuous red lateral stripe) and on the meso- and metanota (two anterior reddish black spots on each) (Fig. 1B) and on the abdominal tergites (orange to dark-brown lateral elongate marks) (Fig. 1D); forewing has the posterior branches of the cubital vein swollen, darkened and edged with dark on the membrane; last tarsal segments are darkened (Fig. 1A). The gonosaccus basally bears gonosetae (Fig. 3A); the arcessus is very long, narrow, straight,



Figure 1. *Ceraeochrysa tacanensis* sp. nov. **A** habitus, lateral **B** head and thorax, dorsal **C** head, frontal **D** abdomen, lateral.

with curved apical point (Fig. 3B); the gonapsis is elongate, its basal section extends internally from the base of gonosaccus and is slightly upturned, terminating anteriorly in a smoothly rounded apex (Fig. 3E), the distal section extends externally and terminates dorsally with microteeth (Fig. 3D); a membranous sac between apices of gonapsis and sternite 9 bears a field of well-developed gonocristae (Fig. 3A).

Description. Measurements, mean (range) ($n = 20$). Male. Head: width 1.3 mm (1.2–1.4 mm). Pronotum: length 0.85 mm (0.7–1 mm), width 0.6 mm (0.4–0.8 mm). Forewing: length 11.7 mm (10–13.4 mm); 4–6 inner and 5–7 outer gradate veins. Hindwing: length 10.2 mm (8.8–11.6 mm); 3–5 inner and 4–6 outer gradate veins. **Female ($n = 11$).** Head: width 1.2 mm (1.1–1.3 mm). Pronotum: length 10 mm (0.9–1.1 mm), width 0.95 mm (0.9–1 mm). Forewing: length 12.4 mm (11.9–12.9 mm); 5–6 inner and 7 outer gradate veins. Hindwing: length 13.5 mm (10.2–11.9 mm); five or six inner and six or seven outer gradate veins.

Head. Front mainly pale (rarely with one brown, irregular transverse-stripe), vertex, clypeus, labrum, gena, maxillary, and labial palpi pale (Fig. 1C). Scape pale with

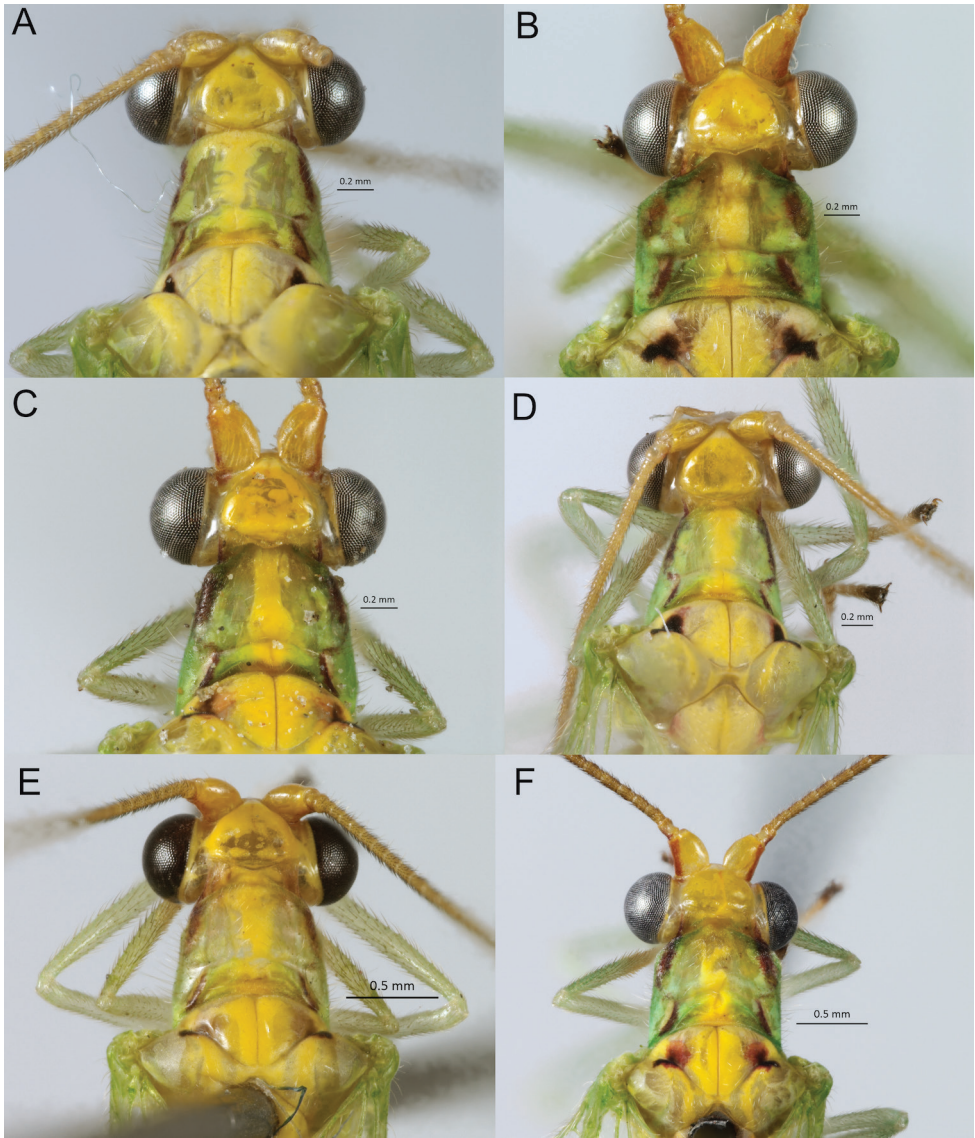


Figure 2. *Ceraeochrysa tacanensis* sp. nov., stripe variation on pronotum **A** discontinuous **B** interrupted **C** thickened **D** narrow **E** pale red **F** dark red.

lateral red stripe and pedicel pale with posterior-lateral red spot; flagellum pale, with 85–90 flagellomeres ($n = 31$).

Thorax. Pronotum greenish with a discontinuous red lateral stripe on each side and a medial, longitudinal yellow band; meso- and metanota greenish, each with a medial, longitudinal yellow band and two anterior reddish-black spots (Fig. 1A), and sometimes with two posterior red or orange spots; pleura pale green. Legs: pale green with yellow

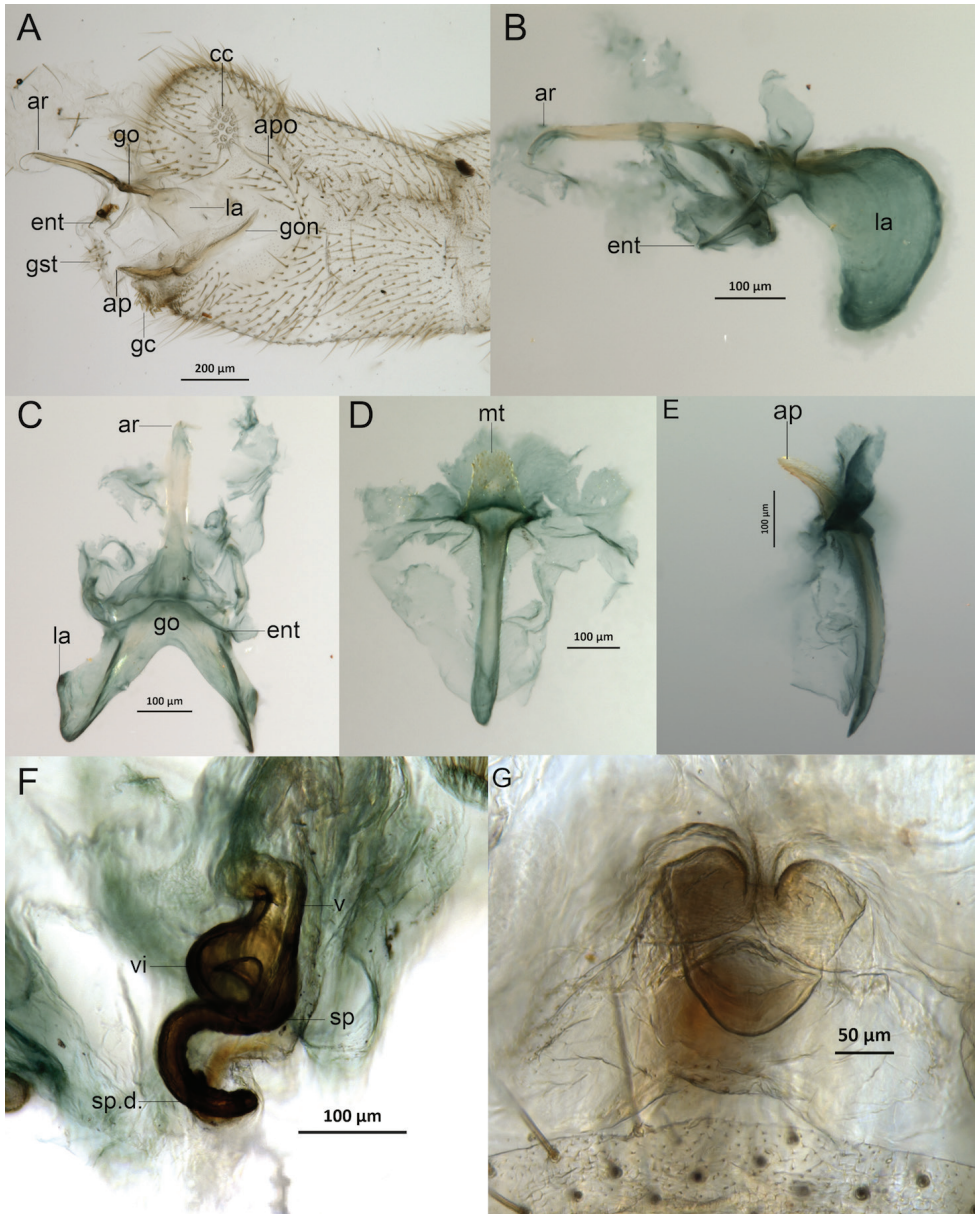


Figure 3. *Ceraeochrysa tacanensis* sp. nov. genitalia: **A** male terminalia, lateral **B** gonarcal complex, lateral **C** gonarcal complex, dorsal **D** gonapsis, dorsal **E** gonapsis, lateral **F** spermathecal complex, dorsolateral **G** female subgenitalia, frontal. Abbreviations: **ap**, apex of gonapsis; **apo**, male apodeme; **ar**, arcessus; **cc**, callus cerci; **ent**, entoprocessus; **gc**, gonocristae; **go**, gonarcus; **gon**, gonapsis; **gst**, gonosetae; **la**, lateral arms; **mt**, microteeth on gonapsis; **sp**, spermatheca; **sp.d.**, spermathecal duct; **v**, vela; **vi**, ventral impression.

tarsi, except one or two dark-brown apical tarsomeres (Fig. 1C). Forewings: venation mostly green, but some crossveins dark; dark markings at apex of 1A, posterior cubitus, and Cua-Cup crossveins form a distinct chevron-shaped mark (Fig. 1D); four to six in-

ner and five to seven outer gradate veins. Hindwing: venation green, with apical section of radius dark; three to five inner and four to six outer gradate veins, all green.

Abdomen. Green, with dorsal, longitudinal yellow band; tergites with orange to dark-brown lateral elongate marks at posterior margin (Fig. 1D). Male apodeme slightly sclerotized and thin, without ventral lobe (Fig. 3A).

Male genitalia. Gonarcus thick with wide and elongate lateral plates (Fig. 3C); entoprocessus elongate, with evenly tapering tips (Fig. 3B); gonocornus lacking. Arcessus very long, narrow, straight, with downward curved apical point (Fig. 3B). Gonosaccus basally with gonosetae (Fig. 3A). Gonapsis elongate, extending from base of gonosaccus, slightly upturned, terminating internally in a smoothly rounded apex (Fig. 3E), with sclerotized microteeth on dorsal side (Fig. 3D); membranous sac between apices of gonapsis and sternite 9 with a field of well-developed gonocristae (Fig. 3A).

Female. Similar to holotype. **Female genitalia.** Female subgenitalia as wide as long, with rounded apex and narrow medial notch (Fig. 3G); spermatheca well sclerotized, with vela broad basally and strongly arched apically; spermathecal duct slightly sinuous before entering oviduct; ventral impression conspicuous (Fig. 3F).

Variation. Lateral stripes of pronotum are variable, for instance whether they are continuous or interrupted (Fig. 2A, B), thickened or narrow (Fig. 2C, D), pale or dark red (Fig. 2E, F); also, dorsolateral marks of the abdomen are generally orange, but may be reddish brown.

Etymology. This species is named after the Tacaná Volcano, located in the state of Chiapas, Mexico, where the specimens were collected.

Ecology. This species is presently known from cloud forest (1,430–1,705 m a.s.l.) and mixed oak-cloud forest (2,060–2,430 m a.s.l.), and with similar collecting techniques and collecting effort, it was not found at lower (661–1,393 m a.s.l.) or higher (2,884–3,246 m a.s.l.) elevation collecting sites. Specimens were found on *Alinus* sp., *Quercus* sp., and *Saurauia* sp., and were collected from February through May, August through December 2018, and January 2019.

Discussion

Ceraeochrysa tacanensis sp. nov. shares the posterior branches of the cubital vein swollen and dark, V-shaped marking with *C. angulata* (Navás), *C. angusta* Freitas & Penny, *C. digitata* Freitas & Penny, *C. elegans* Penny, *C. nigripedis* Penny, and *C. tauberae* Penny. Also, an elongate arcessus is shared with these species (except *C. angulata* and *C. digitata*), plus *C. bitacornua* Freitas & Penny. The new species differs from the former species because it has a discontinuous stripe on the pronotum, while the rest have spots (*C. angulata*, *C. angusta*, *C. elegans*, *C. nigripedis*, and *C. tauberae*) or a continuous stripe (*C. bitacornua* and *C. digitata*). Another species with a discontinuous stripe on the pronotum is *C. pittieri* Sosa & Freitas (Sosa and Freitas 2010: figs 4, 5), however, this species does not share other traits as explained above. In addition, *C. tacanensis* sp. nov. shares marks on the abdominal tergites with *C. elegans*, although the tarsal segments are darkened apically in the new species, as in *C. nigripedis*. Regarding genitalia,

the new species is most similar to *C. nigripedis*, sharing a simple dorsal apodeme, an elongate gonapsis, and the shape of the gonarcal complex. However, the new species has a gonosaccus with gonosetae and a membranous sac with gonocristae between apex of gonapsis and sternite 9, similar to *C. elegans*. The sclerotized microteeth extended on the dorsal side of the gonapsis apex may be a unique trait of the new species (also present in the unrelated *C. sanchezi*), while *C. elegans* has microteeth restricted to the apex.

Key to species of *Ceraeochrysa* of Mexico (Modified from Freitas et al. 2009)

- 1 Pronotum with one or more pairs of lateral spots, or thin, sub-medial stripes 2
- Pronotum with red or brown lateral stripes or no stripes 3
- 2 Last two tarsal segments of legs black; lateral surface of antennal scape red; abdominal tergites with orange spots
..... *Ceraeochrysa tacanensis* Cancino-López & Contreras, sp. nov.
- Tarsal segments of legs pale; lateral surface of antennal scape dark; abdominal tergites with red bands *C. elegans* Penny
- 3 Area of vertex behind antennal bases entirely red *C. smithi* (Navás)
- Area of vertex behind antennal bases pale 4
- 4 Basal flagellar segments pale 5
- Basal flagellar segments dark 9
- 5 Maxillary palpi pale, with dark marks *C. cubana* (Hagen)
- Maxillary palpi pale, without dark marks 6
- 6 Antennal scape with two stripes *C. arioles* (Banks)
- Antennal scape with one stripe 7
- 7 Antennal scape with lateral stripe *C. valida* (Banks)
- Antennal scape with dorsal stripe 8
- 8 Mesonotum with dark marks; male dorsal apodeme with long ventral branch, basally attached; arcessus as broad as long; gonapsis thick and short
..... *C. cornuta* (Navás)
- Mesonotum unmarked; male dorsal apodeme with recurved ventral branch basally attached; arcessus broad; gonapsis long, slender, apically upturned
..... *C. cincta* (Schneider)
- 9 Antennal scape with lateral or dorsolateral stripe/spot 10
- Antennal scape with dorsal stripe *C. claveri* (Navás)
- 10 Genae dark to partially dark 11
- Genae pale yellow to pale brown 13
- 11 Apex of male ectoproct rounded, with simple, thin setae
..... *C. derospogon* Freitas and Penny
- Apex of male ectoproct pointed, with chalazae (thick-based setae) 12
- 12 Male tergite 9 + ectoproct deeply divided; gonosaccus with field of gonocristae; sternite 8 + 9 quadrate with one long chalazate seta at each lateral corner;

- ventral fork of dorsal apodeme not projected caudally beyond ectoproct.....
 *C. berlandi* (Navás)
- Male tergite 9 + ectoproct not deeply divided; gonosaccus lacking field of gonocristae; sternite 8 + 9 rounded with chalazate setae throughout; ventral fork of dorsal apodeme projected ventrocaudally well beyond ectoproct
 *C. effusa* (Navás)
- 13 Arcessus membranous basally with a pair of hooks and two inflated lobes, apex with a medial hook and pair of lateral, decurved and medially curved sclerotized lobes *C. everes* (Banks)
- Arcessus not membranous basally, of triangular-shape; apex with medial decurved point *C. sanchezi* (Navás)

Acknowledgments

We thank Harry Brailovsky (Instituto de Biología-UNAM) and David Bowles (Missouri State University) for providing comments and suggestions on the manuscript. Our appreciation goes to Museo Nacional de Costa Rica, for allowing Adrian Ardila-Camacho to photograph the holotypes of *C. elegans* and *C. nigripedis*, and we also thank Adrian for taking those photos. We thank Susana Guzmán (Laboratorio de Microscopía, IBUNAM) for advice on stereomicroscope photography. Magali Luna-Luna and Johar Almaraz-Hernández provided support during fieldwork, and Yesenia Marquez-López helped with image editing. We are indebted to Beningo Gómez, Reserva de la Biosfera Volcán Tacaná (Francisco J. Jiménez González, director), Cantón Chiquihuites, and Ejido Benito Juárez El Plan, for authorization for fieldwork in the study area. RJCL thanks Consejo Nacional de Ciencia y Tecnología for a doctoral scholarship and Posgrado en Ciencias Biológicas-UNAM, sede Instituto de Biología, for general support through his doctoral program. This study was supported by project IN207517 “Aportaciones a la taxonomía y filogenia del orden Neuroptera (Insecta) en México” funded by “Programa de Apoyo a Proyectos de Investigación e Innovación Tecnológica” (PAPIIT-UNAM).

References

- Adams PA (1982) *Ceraeochrysa*, a new genus of Chrysopinae (Neuroptera) (Studies in New World Chrysopidae, Part II). *Neuroptera International* 2: 69–75.
- Brooks SJ, Barnard PC (1990) The green lacewings of the world: a generic review (Neuroptera: Chrysopidae). *Bulletin of the British Museum of Natural History Entomology* 59: 117–286.
- Freitas S (2001) O uso de crisópídeos no controle biológico de pragas. Funep, Jaboticabal, 66 pp.
- Freitas S, Penny ND (2001) The green lacewings (Neuroptera: Chrysopidae) of Brazilian agroecosystems. *Proceedings of the California Academy of Sciences* 52: 245–395.

- Freitas S, Penny ND, Adams PA (2009) A revision of the New world genus *Ceraeochrysa* (Neuroptera: Chrysopidae). *Proceedings of the California Academy of Sciences* 60: 503–610.
- Martins CC, Machado RJP (2019) Chrysopidae in Catálogo Taxonômico da Fauna do Brasil. PNUD. <http://fauna.jbrj.gov.br/fauna/faunadobrasil/7242> [Accessed on: 2019–10–10]
- Oswald JD (2018) Lacewing digital library. Neuropterida species of the world. <http://lacewing.tamu.edu/Species-Catalogue/index.html> [Accessed on: 2019–10–10]
- Penny ND (1997) Four new species of Costa Rican *Ceraeochrysa* (Neuroptera: Chrysopidae). *Pan-Pacific Entomologist* 73: 61–69.
- Penny ND (1998) New Chrysopinae from Costa Rica (Neuroptera: Chrysopidae). *Journal of Neuropterology* 1: 55–78.
- Penny ND (2002) A Guide to the lacewings (Neuroptera) of Costa Rica. *Proceedings of the California Academy of Sciences* 53: 161–457.
- Sosa F, Freitas S (2010) New Neotropical species of *Ceraeochrysa* Adams (Neuroptera: Chrysopidae). *Zootaxa* 2562: 57–65. <https://doi.org/10.11646/zootaxa.2562.1.4>
- Sosa F, Freitas S (2011) A new synonym, a new male description and new geographical records for three *Ceraeochrysa* species (Neuroptera: Chrysopidae). *Zootaxa* 2913: 47–58. <https://doi.org/10.11646/zootaxa.2913.1.5>
- Tauber CA, Garland JA (2014) *Kymachrysa*, a new genus of Nearctic green lacewings (Neuroptera, Chrysopidae, Chrysopini). *ZooKeys* 437: 87–108. <http://doi.org/10.3897/zookeys.437.7984>
- Tauber CA, Flint Jr OS (2010) Resolution of some taxonomic and nomenclatural issues in a recent revision of *Ceraeochrysa* (Neuroptera: Chrysopidae). *Zootaxa* 2565: 55–67. <https://doi.org/10.11646/zootaxa.2565.1.4>
- Tauber CA, De León T (2001) Systematics of green lacewings (Neuroptera: Chrysopidae): larvae of *Ceraeochrysa* from Mexico. *Annals of the Entomological Society of America* 94: 197–209. [https://doi.org/10.1603/0013-8746\(2001\)094\[0197:SOGLNC\]2.0.CO;2](https://doi.org/10.1603/0013-8746(2001)094[0197:SOGLNC]2.0.CO;2)
- Tauber CA, De León T, Penny N, Tauber MJ (2000) The genus *Ceraeochrysa* (Neuroptera: Chrysopidae) of America north of Mexico: larvae, adults, and comparative biology. *Annals of the Entomological Society of America* 93: 1195–1221. [https://doi.org/10.1603/0013-8746\(2000\)093\[1195:TGCNCO\]2.0.CO;2](https://doi.org/10.1603/0013-8746(2000)093[1195:TGCNCO]2.0.CO;2)

A new species of the genus *Acanthosaura* from Yunnan, China (Squamata, Agamidae)

Shuo Liu¹, Dingqi Rao²

1 Kunming Natural History Museum of Zoology, Kunming Institute of Zoology, Chinese Academy of Sciences, 32 Jiaochang Donglu, Kunming, Yunnan 650223, China **2** Kunming Institute of Zoology, Chinese Academy of Sciences, 32 Jiaochang Donglu, Kunming, Yunnan 650223, China

Corresponding author: Dingqi Rao (raodq@mail.kiz.ac.cn); Shuo Liu (liushuo@mail.kiz.ac.cn)

Academic editor: Thomas Ziegler | Received 24 July 2019 | Accepted 21 October 2019 | Published 11 November 2019

<http://zoobank.org/C454358A-DB07-4BE8-A22A-7B98CE3E6CF9>

Citation: Liu S, Rao D (2019) A new species of the genus *Acanthosaura* from Yunnan, China (Squamata, Agamidae). ZooKeys 888: 105–132. <https://doi.org/10.3897/zookeys.888.38491>

Abstract

A new species of *Acanthosaura* from Yunnan, China is described based on unique morphometric and meristic external characters and a very distinctive color pattern. The fourteenth species recorded of this genus, *Acanthosaura tongbiguanensis* sp. nov., was previously considered *A. lepidogaster* although it more closely resembles *A. crucigera*. It can be separated from all other species of the genus by having different numbers of subdigital lamellae on the fourth finger and toe, and a different shape of the black eye patch. The new species differs genetically from investigated congeners by percentage distance of 14.46% to 23.27% (cytochrome b gene).

Keywords

crucigera, Dehong, *lepidogaster*, Tongbiguan

Introduction

The genus *Acanthosaura* (Gray, 1831) includes thirteen currently recognized species: *A. armata* (Hardwicke & Gray, 1827); *A. lepidogaster* (Cuvier, 1829); *A. capra* (Günther, 1861); *A. coronata* (Günther, 1861); *A. crucigera* Boulenger, 1885; *A. nataliae* Orlov et al., 2006; *A. bintangensis* Wood et al., 2009; *A. titiwangsaensis* Wood et al., 2009; *A. cardamomensis* Wood et al., 2010; *A. brachypoda* Ananjeva et al., 2011; *A. phuketensis* Pauwels et al., 2015; *A. murphyi* Nguyen et al., 2018; and *A. phongdienensis* Nguyen et

al., 2019). It has a very wide distribution, and phylogenetic studies have shown that the genus was in need of revision as it included several undescribed and cryptic species as revealed by molecular data (Kalyabina-Hauf et al. 2004; Ananjeva et al. 2008). Because at least some of its members are difficult to find and similar in appearance, taxonomic research is incomplete, with many species only recognized recently.

During our field research in Dehong Autonomous Prefecture, Yunnan Province, China, we discovered some lizards that looked superficially like *Acanthosaura lepidogaster*. According to Zhao et al. (1999) and Yang et al. (2008), two species of the genus *Acanthosaura* are distributed in China and only *A. lepidogaster* is found in Yunnan Province. Morphological and molecular data show that this population is clearly distinct from all other named species, and we consequently describe and name it herein.

Materials and methods

Specimens were collected by hand. Photographs were taken to document color pattern in life prior to euthanasia. Liver tissues were stored in 99% ethanol and lizards were preserved in 75% ethanol. Specimens were deposited at Kunming Natural History Museum of Zoology, Kunming Institute of Zoology, Chinese Academy of Sciences.

Forty-nine meristic and mensural characters were noted for each adult specimen of the type series, but only meristic characters were noted on juvenile specimens (see Table 3). Measurements were taken to the nearest 0.1 mm with a digital caliper. Paired measurements were made on the left side, as was done in the recent revisions in the *Acanthosaura crucigera* species group (Wood et al. 2009, 2010; Ananjeva et al. 2011). Paired meristic characters are given as left/right. The list and methodology of measurements and meristic counts follow Wood et al. (2010) and Pauwels et al. (2015):

- BEP** presence (1) or absence (0) of a black eye patch;
- CS** number of canthus rostralis-supraciliary scales, counted from the nasal scale to the posterior end of the ridge at the posterior margin of the orbit;
- DIAS** length of the diastema, measured from the posterior end of the nuchal crest to the anterior end of the dorsal crest;
- DIASN** number of scales in the vertebral crest scale diastema, counted from the posterior end of the nuchal crest to the anterior end of the dorsal crest;
- DS** maximum length of the largest spine in the dorsal crest, measured from the base to the tip;
- DSL** longest dorsal scale, measured at the base below the dorsal crest;
- ESBO** presence (1) or absence (0) of elliptical scales below the orbit;
- EYE** eye diameter, measured from the posterior to the anterior edge of the eye;
- FI** number of subdigital lamellae on the fourth finger;
- FOREL** forelimb length, measured from axilla to the proximal edge of the palmar region;
- GP** size of gular pouch, scored as absent (0), small (1), medium (2), large (3) or very large (4);

HD	maximum head height, measured across the parietal region;
HINDL	hindlimb length, measured from groin to the proximal edge of the plantar region;
HL	head length, measured from posterior edge of the lower jaw to the tip of the snout;
HW	head width, maximum head width, the width at the level of the tympanum;
INFRAL	number of infralabials;
LKP	presence (1) or absence (0) of light knee patch;
MH	mental height;
MW	mental width;
NCS	number of scales between the fifth canthals;
ND	presence (1) or absence (0) of a black, diamond shaped, nuchal collar;
NR	number of scales between the nasal and the rostral;
NS	number of scales between the nasals;
NCSL	number of scales from the fifth canthal to the fifth supralabial;
NSL	maximum length of the largest spine in the nuchal crest measured from the base to the tip;
NN	number of nuchal crest spines (in addition to characters abbreviations listed in Pauwels et al. 2015);
NSSLC	number of scales between the seventh supralabial and the sixth canthal;
NSSOS	number of scales surrounding the occipital spine;
NSSPS	number of scales surrounding the postorbital spine (in addition to characters abbreviations listed in Pauwels et al. 2015);
OF	presence (1) or absence (0) of oblique humeral fold;
ORBIT	orbit diameter, measured from the posterior to the anterior edge of the orbit;
OS	length of the occipital spine, measured from the base to the tip;
PM	number of scales bordering the mental;
PS	postorbital spine length, measured from the base to the tip of the spine;
RH	rostral height;
RS	number of scales bordering the rostral scale;
RW	rostral width;
SL	snout length, measured from the anterior edge of the orbit to the tip of the snout;
SUPRAL	number of supralabials;
SVL	snout-vent length, measured from the tip of the snout to the tip of the vent;
TL	tail length, measured from the posterior margin of the vent to the tip of the tail;
TBW	tail base width, maximum width at tail base;
TD	tympanum diameter, measured horizontally from the anterior to the posterior border of the tympanum;
TN	scales absent on tympanum (0) or present (1);
TO	subdigital lamellae on the fourth toe;
VENT	number of ventral scales, counted at the midline from the anterior edge of the shoulders to the edge of the vent;

- WNC** maximum width of the spines in the nuchal crest, measured at the base;
WDS maximum width of the largest dorsal scale below the dorsal crest, measured at the base;
YAS presence (1) or absence (0) of a Y-shaped arrangement of enlarged scales on the snout.

We compared the characters of the new collection with the characters of all currently recognized species of *Acanthosaura* (Pauwels et al. 2015; Nguyen et al. 2018, 2019), see Table 4.

The character DIAS of *Acanthosaura brachypoda* is given both as 4.5 and 1.9 mm in the original description, which is based on a single specimen, so this character is not used here for comparisons. The methodology for taking FOREL and HINDL was insufficiently described in the original description of *A. brachypoda* and thus could not be compared here; CS, NCS, NR, NSCSL, NSSLC and NSSOS were not provided in the original description of *A. brachypoda*; NSSLC, PM, ND, LKP, ESBO and OF were not provided in the original description of *A. murphyi*; SL, ORBIT, WNC, FOREL, HINDL, VENT, OS, NSSOS, CS, RS, NS, NSC, NSCSL, NR, NSSLC, PM, YAS, BEP, ESBO and GP were not provided in the original description of *A. phongdienensis*.

Molecular data were generated for three specimens and all available homologous sequences obtained from GenBank, all new sequences have been deposited in GenBank. According to Ananjeva et al. (2008), the sequences whose GenBank accession numbers are AY572873 to AY572886 belong to *Acanthosaura nataliae*, and the sequences whose GenBank accession numbers are AY572896 to AY572899 belong to *Acanthosaura coronata*. According to Nguyen et al. (2019), it can be inferred that the sequences whose GenBank accession numbers are AY572900, AY572904, AY572905, AY572912 to AY572918, AY572922 and AY572923 probably belong to *Acanthosaura phongdienensis*. According to Pauwels et al. (2015), it can be inferred that the sequences whose GenBank accession numbers are AY572887 and AY572889 to AY572894 probably belong to *Acanthosaura phuketensis*. According to Kalyabina-Hauf et al. (2004) and Ananjeva et al. (2008), the sequences whose GenBank accession numbers are AY572928 to AY572930 belong to some unknown species. Two agamids *Pseudocalotes brevipes* (Werner, 1904) and *Calotes versicolor* (Daudin, 1802) were used as the outgroups based on the results from Kalyabina-Hauf et al. (2004). All the GenBank accession numbers for taxa used in the genetic analysis can be found in Table 1. Total genomic DNA was extracted from liver tissue stored in 99% ethanol. Tissue samples were digested using proteinase K, and subsequently purified following a standard phenol/chloroform isolation and ethanol precipitation (Sambrook et al. 1989). PCR was performed using primers new to this paper TBG-F: ATTCTCGCAATACACTACACAAC and TBG-R: TTTCAAATAATACTTGGGAGGTT. Amplification conditions were as follows: after an initial denaturation at 94 °C for 300 s, 31 cycles followed with a denaturation at 94 °C for 45 s, annealing at 42–45 °C for 45 s, and extension at 70 °C for 120 s; cycle sequencing reactions used a two-step program: 15 cycles followed with denaturation at

Table 1. Sequences (cytb) used in this study.

Species	Locality	Voucher no.	GenBank no.	
<i>Acanthosaura armata</i>	Pulau Pinang, Pinang, Malaysia	PCUM	AY572871	
	Pulau Pinang, Pinang, Malaysia	PCUM	AY572872	
	No data	NSMT-H4595	AB266452	
	No data	No data	NC_014175	
<i>Acanthosaura coronata</i>	Krong Pa, Gia Lai, Vietnam	ROM31985	AY572896	
	Dong Nai, Cat Tien, Dong Nai, Vietnam	ROM42240	AY572897	
	Dong Nai, Cat Tien, Dong Nai, Vietnam	ROM37083	AY572898	
	Dong Nai, Cat Tien, Dong Nai, Vietnam	ROM42241	AY572899	
<i>Acanthosaura crucigera</i>	Bago Division, Bago Yoma, Myanmar	CAS206626	AY572888	
	Bago Division, Bago Yoma, Myanmar	CAS208426	AY572895	
<i>Acanthosaura lepidogaster</i>	Chi Linh, Hia Duong, Vietnam	ROM31954	AY572901	
	Chi Linh, Hia Duong, Vietnam	ROM31957	AY572902	
	Chi Linh, Hia Duong, Vietnam	ROM31960	AY572911	
	Chi Linh, Hia Duong, Vietnam	ROM35038	AY572903	
	Tam Dao, Vinh Phu, Vietnam	ROM30503	AY572906	
	Tam Dao, Vinh Phu, Vietnam	ROM30720	AY572907	
	Tam Dao, Vinh Phu, Vietnam	ROM30694	AY572908	
	Tam Dao, Vinh Phu, Vietnam	ROM30693	AY572927	
	Quang Thanh, Cao Bang, Vietnam	ROM36073	AY572909	
	Quang Thanh, Cao Bang, Vietnam	ROM36075	AY572910	
	Nakai, Khammouane, Laos	FMNH255488	AY572920	
	Nakai, Khammouane, Laos	FMNH255487	AY572921	
	Thaphabat, Bolikhamxay, Laos	FMNH255491	AY572919	
	Hainan, China	MD001	KR092427	
	Sa Pa, Lao Cai, Vietnam	ROM38117	AY572924	
	Sa Pa, Lao Cai, Vietnam	ROM38115	AY572925	
	Sa Pa, Lao Cai, Vietnam	ROM38116	AY572926	
	<i>Acanthosaura nataliae</i>	Krong Pa, Gia Lai, Vietnam	ROM31983	AY572873
		Krong Pa, Gia Lai, Vietnam	ROM32167	AY572874
Krong Pa, Gia Lai, Vietnam		ROM32160	AY572875	
Krong Pa, Gia Lai, Vietnam		ROM31984	AY572876	
Krong Pa, Gia Lai, Vietnam		ROM32154	AY572877	
Krong Pa, Gia Lai, Vietnam		ROM32155	AY572878	
Krong Pa, Gia Lai, Vietnam		ROM32160	AY572879	
Tram Lap, Gia Lai, Vietnam		ROM30627	AY572880	
Tram Lap, Gia Lai, Vietnam		ROM30628	AY572881	
Krong Pa, Gia Lai, Vietnam		ROM32161	AY572882	
Krong Pa, Gia Lai, Vietnam		ROM32152	AY572883	
Krong Pa, Gia Lai, Vietnam		ROM32162	AY572884	
Krong Pa, Gia Lai, Vietnam		ROM32143	AY572885	
Krong Pa, Gia Lai, Vietnam		ROM32166	AY572886	
<i>Acanthosaura cf. phongdienensis</i>		Khe Moi River, Nghe An, Vietnam	ROM26328	AY572900
		Annam, Vu Quang, Ha Tinh, Vietnam	ZISP20753-1	AY572904
		Annam, Vu Quang, Ha Tinh, Vietnam	ZISP20753-2	AY572905
	Boualapha, Khammouane, Laos	FMNH255481	AY572912	
	Con Cuong, Nghe An, Vietnam	FMNH255582	AY572913	
	Con Cuong, Nghe An, Vietnam	FMNH255583	AY572914	
	Tuong Duong, Nghe An, Vietnam	FMNH255585	AY572915	
	Tuong Duong, Nghe An, Vietnam	FMNH255587	AY572916	
	Con Cuong, Nghe An, Vietnam	FMNH255581	AY572917	
	Tuong Duong, Nghe An, Vietnam	FMNH255584	AY572918	
	Vieng Tong, Huaphan, Laos	FMNH255489	AY572922	
	Khao Yoi, Thailand	PCUM	AY572923	

Species	Locality	Voucher no.	GenBank no.
<i>Acanthosaura</i> cf. <i>phuketensis</i>	Kao Yoi, Phetchaburi, Thailand	No data	AY572887
	Khao Lak, TakuaPa, Phang Nga, Thailand	PCUM	AY572889
	Khao Lak, TakuaPa, Phang Nga, Thailand	PCUM	AY572890
	Khao Lak, TakuaPa, Phang Nga, Thailand	PCUM	AY572891
	ThaiMuang, Phang Nga, Thailand	IRSNB15141	AY572892
	Malaysia	No data	AY572893
	Malaysia	No data	AY572894
<i>Acanthosaura</i> sp. 1	Myanmar	HLMD-RA2969	AY572929
<i>Acanthosaura</i> sp. 1	Myanmar	HLMD-RA2970	AY572930
<i>Acanthosaura</i> sp. 2	Ngoc Linh, Kon Tum, Vietnam	ROM37082	AY572928
<i>Calotes versicolor</i>	Vietnam	HLDM57	AY572870
<i>Pseudocalotes brevipes</i>	Pac Ban, Tuyen Quang, Vietnam	ROM30515	AY572869
<i>Acanthosaura tongbiguanensis</i> sp. nov.	Tongbiguan, Dehong, Yunnan, China	KIZL201801	MN604012
	Tongbiguan, Dehong, Yunnan, China	KIZL201802	MN604013
	Tongbiguan, Dehong, Yunnan, China	KIZL201803	MN604014

94 °C for 45 s, annealing at 47–53 °C for 45 s, extension at 70 °C for 60 s, and 15 cycles of denaturation at 94 °C for 45 s and extension at 60 °C for 60 s (Kalyabina-Hauf et al. 2004). We used a ratio of 0.55 H₂O: 0.30 ExoI: 0.15 SAP to clean the PCR product (Hanke et al. 1994). Amplified mitochondrial cytochrome b (cytb) fragments were sequenced in both directions using an ABI PRISM 3730 Automated DNA Sequencer (Applied Biosystems) following the manufacturer's protocol (Nguyen et al. 2019).

Sequences were aligned using CLUSTAL X v1.83 (Thompson et al. 1997) with the default parameters and the alignment revised by eye. Pairwise distances between species were calculated in MEGA 7 (Tamura et al. 2011). The best substitution model HKY+G+I was selected using the Akaike Information Criterion (AIC) in MODEL-TEST v3.7 (Posada and Crandall 1998). Bayesian phylogenetic inference was performed in MRBAYES 3.2.6 (Wang et al. 2009, Ronquist et al. 2012) based on the selected substitution model. Two runs were performed simultaneously with four Markov chains starting from random tree. The chains were run for 1,000,000 generations and sampled every 100 generations. The first 25% of the sampled trees was discarded as burn-in after the standard deviation of split frequencies of the two runs was less than a value of 0.01, and then the remaining trees were used to create a 50% majority-rule consensus tree and to estimate Bayesian posterior probabilities (BPPs). Maximum likelihood analysis was performed in MEGA 7 (Tamura et al. 2011), nodal support was estimated by 1,000 rapid bootstrap replicates.

Results

The obtained sequence alignment is 795 bp in length. Both Bayesian inference and Maximum likelihood analyses recovered this lineage of the new samples as the sister to the clade consisting of *Acanthosaura crucigera* and *A. cf. phuketensis* with weak support (Figures 1, 2). The average uncorrected pairwise distances (p-distance) between other investigated members of *Acanthosaura* ranged from 11.17% to 23.9%, the average

Table 2. Average uncorrected *p*-distances (%) between investigated members of *Acanthosaura* and outgroups calculated from cytb gene sequences.

Species	1	2	3	4	5	6	7	8	9	10	11
1 <i>Acanthosaura tongbiguanensis</i> sp. nov.											
2 <i>A. armata</i>	14.80										
3 <i>A. coronata</i>	23.27	22.20									
4 <i>A. crucigera</i>	15.52	15.11	22.71								
5 <i>A. lepidogaster</i>	15.18	16.11	22.48	16.52							
6 <i>A. nataliae</i>	14.94	14.90	22.15	15.45	13.72						
7 <i>A. cf. phongdienensis</i>	15.88	14.43	22.63	15.23	12.32	14.77					
8 <i>A. cf. phuketensis</i>	14.46	14.83	22.65	11.17	15.35	15.02	14.04				
9 <i>Acanthosaura</i> sp. 1	22.94	21.81	16.18	22.51	23.04	23.77	23.62	23.86			
10 <i>Acanthosaura</i> sp. 2	15.35	14.08	23.90	16.47	14.82	15.82	14.93	15.79	23.78		
11 <i>Pseudocalotes brevipes</i>	22.85	24.43	26.92	24.32	23.66	24.00	24.79	24.44	26.39	24.67	
12 <i>Calotes versicolor</i>	27.25	25.49	28.40	27.60	27.75	27.11	26.39	26.38	28.56	29.33	28.00

uncorrected pairwise distances (*p*-distance) between the new species and investigated congeners ranged from 14.46% to 23.27% (Table 2).

Systematics

***Acanthosaura tongbiguanensis* sp. nov.**

<http://zoobank.org/6E91FE2B-A4E7-4A7E-BD68-A9C883760883>

Figures 3–6, 10

Acanthosaura lepidogaster: Zhao et al. 1999: 82–85.

Acanthosaura lepidogaster: Yang and Rao 2008: 186–187.

Type material. Holotype. KIZL201804, an adult male, 22:18 02 Sept 2018, leg. Shuo Liu, Tongbiguan Township (24°36'51.24"N, 97°35'1.88"E, 1170.24 m elevation), Yingjiang County, Dehong Autonomous Prefecture, Yunnan, China.

Paratypes. KIZL201801, an adult male, 22:53 01 Sept 2018, leg. Shuo Liu, same locality as holotype; KIZL201802 and KIZL201803, two juveniles, 21:00–22:00 02 Sept 2018, leg. Shuo Liu, same locality as holotype; KIZL201805, adult female, 22:40 02 Sept 2018, leg. Shuo Liu, same locality as holotype; 74I0039 and 74I0040, two gravid females, old specimens in the specimen collection room of Kunming Institute of Zoology, Chinese Academy of Sciences, Aug 1974, leg. Longchuan County, Dehong Autonomous Prefecture, Yunnan, China.

Etymology. The name refers to Tongbiguan Nature Reserve, the locality where the new species was found.

Diagnosis. A medium-sized (maximum SVL 115.6 mm) agamid lizard with two pairs of spines: postorbital (supraciliary) spines and spines on occiput between tympanum and nuchal crest; tympanum naked; moderately developed gular pouch; scales on flanks randomly intermixed with medium and large scales; nuchal crest

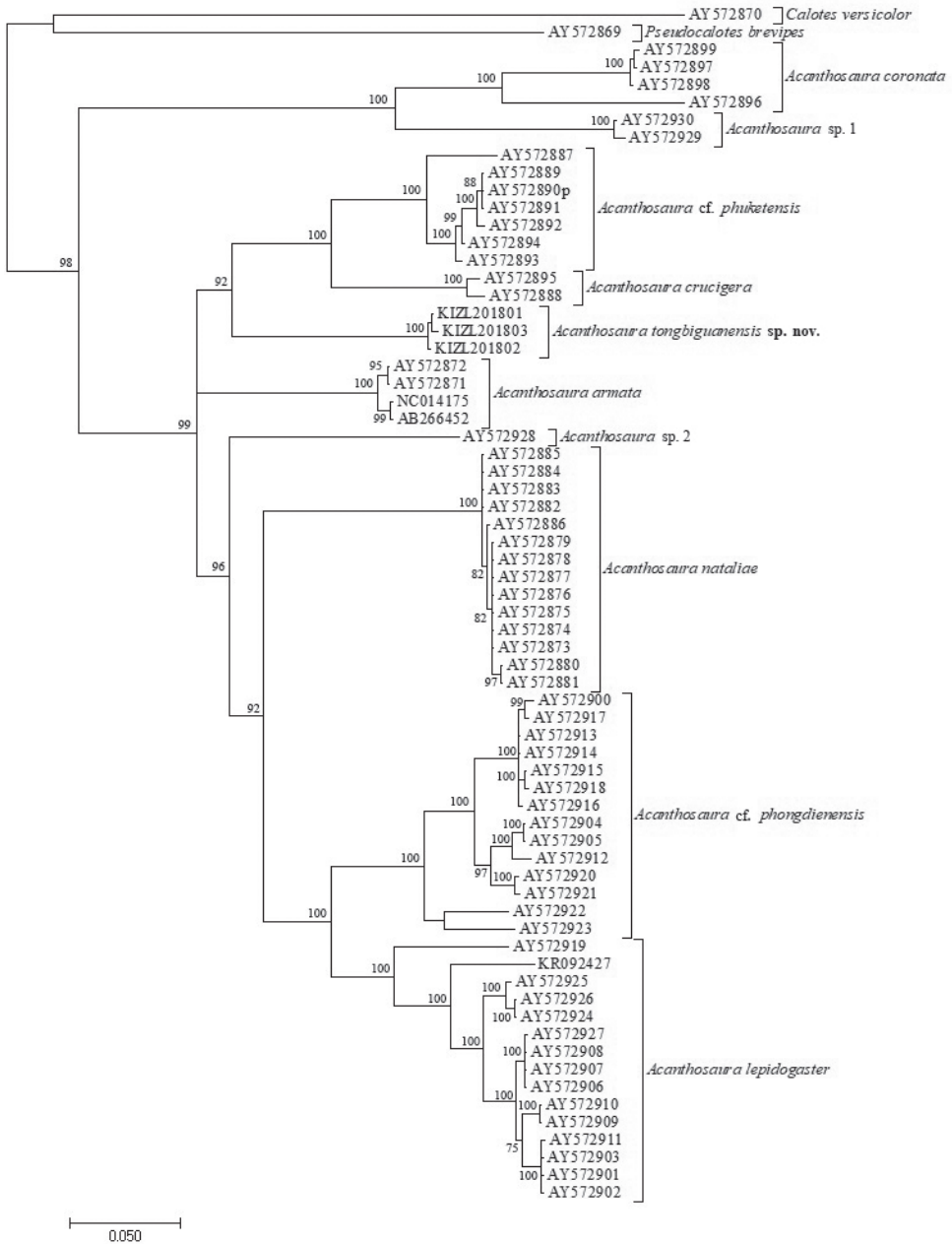


Figure 1. Bayesian phylogram of investigated members of *Acanthosaura* inferred from cytb gene. The nodal numbers are Bayesian posterior probabilities (only values above 70% are shown).

present and strongly developed; diastema between the nuchal and dorsal crests present; dorsal crest slightly developed, composed of enlarged, pointed scales beginning at shoulder region and decreasing regularly in size; tail 1.56–1.85 times SVL; black

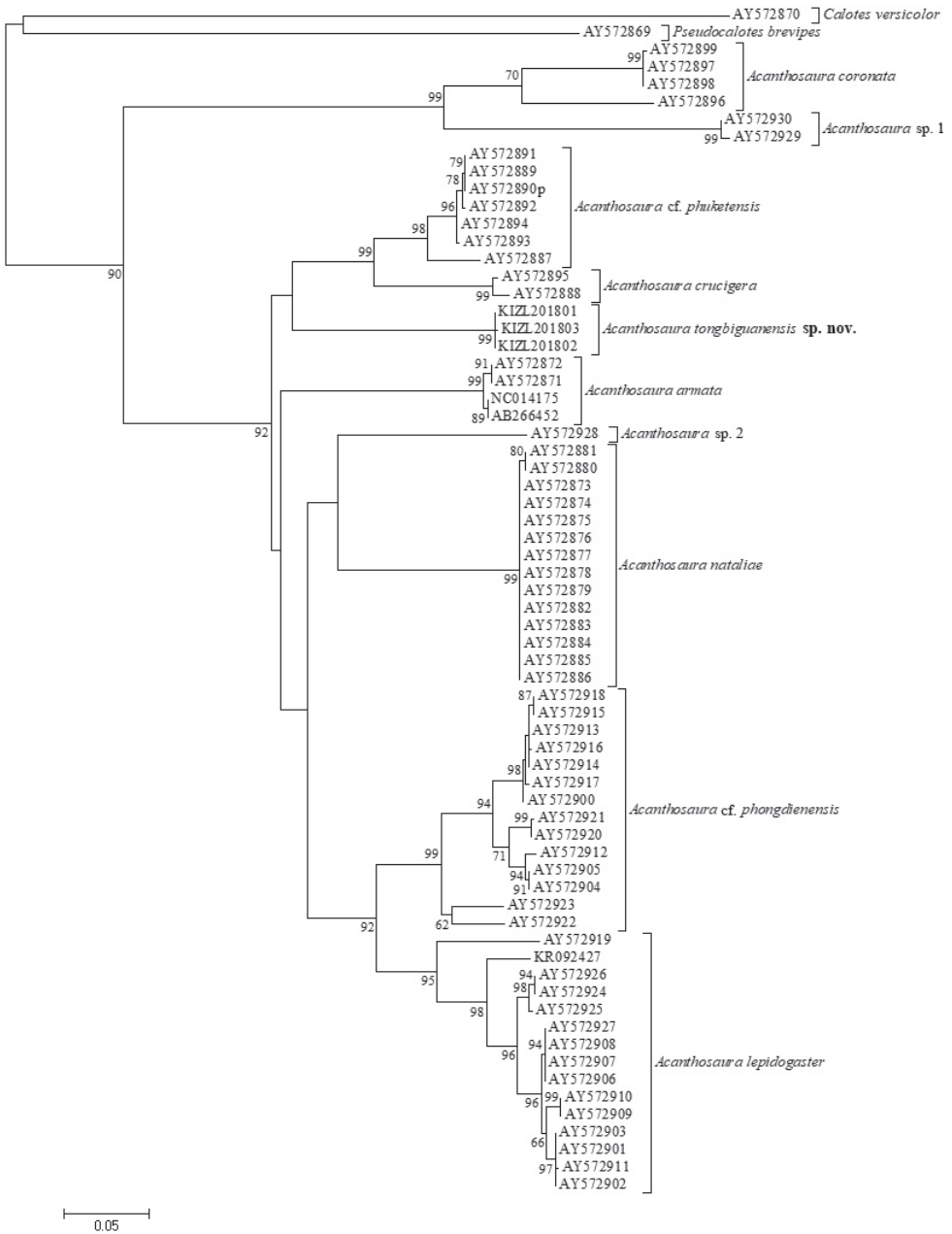


Figure 2. Maximum likelihood phylogram of investigated members of *Acanthosaura* inferred from cytb gene. The nodal numbers are ML bootstrap values (only values above 50% are shown).

nuchal collar present; black eye patch present; black oblique folds anterior to the fore limb insertions present.

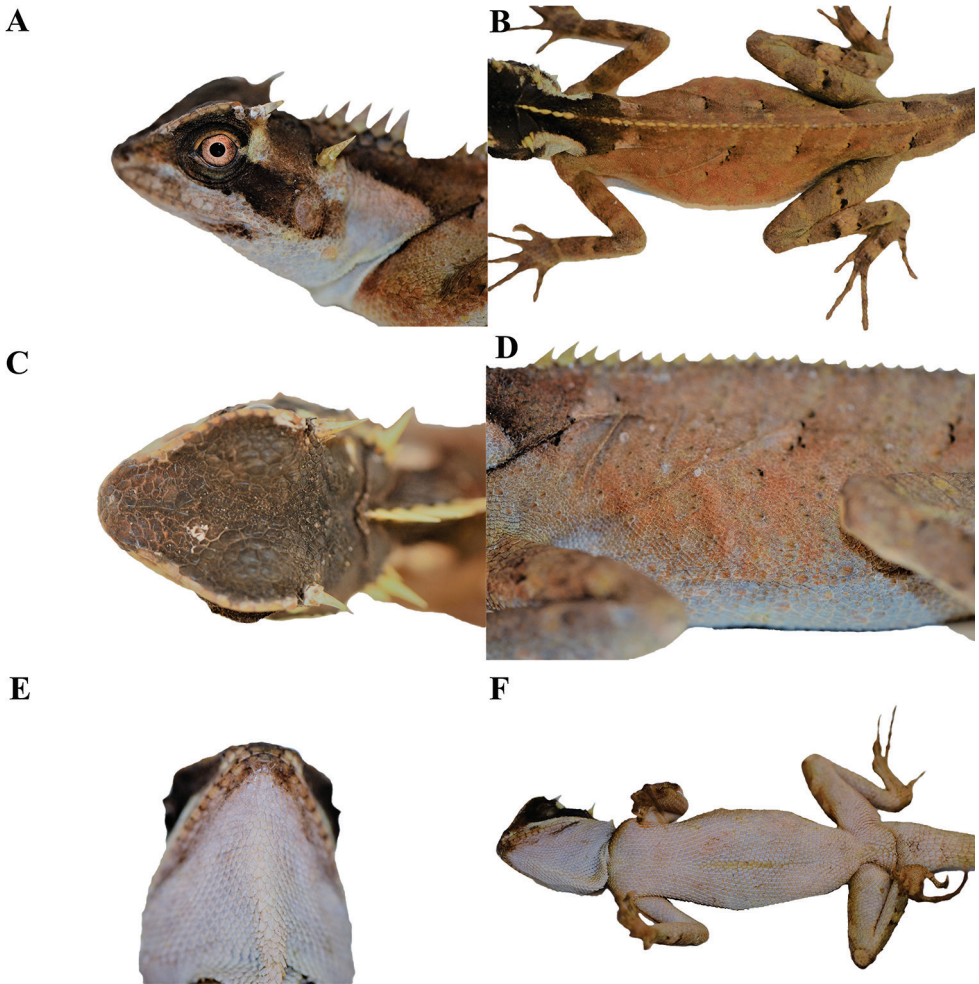


Figure 3. Adult male holotype (KIZL201804) of *Acanthosaura tongbiguanensis* sp. nov. in life **A** lateral view of the head **B** dorsal view of the body **C** dorsal view of the head **D** lateral view of the body **E** ventral view of the head **F** ventral view of the body.

The new species can be separated from all congeners by having different numbers of subdigital lamellae on the fourth finger (19–21) and toe (25–28), and a different shape of the black eye patch, that extends from posterior margin of nostrils through orbit posteriorly and downwards beyond the posterior end of the tympanum but neither meeting the diamond shaped black nuchal collar on nape nor black oblique humeral fold.

Description of the holotype. Adult male. SVL 110.8 mm. TL 205.0 mm, tail complete. Head length 31.1 mm; head moderately long (HL/SVL 28%), somewhat narrow (HW/SVL 18%), not tall (HD/HL 52%), triangular in dorsal and lateral profile. Snout short (SL/HL 31%); interorbital and frontal regions and rostrum wide,

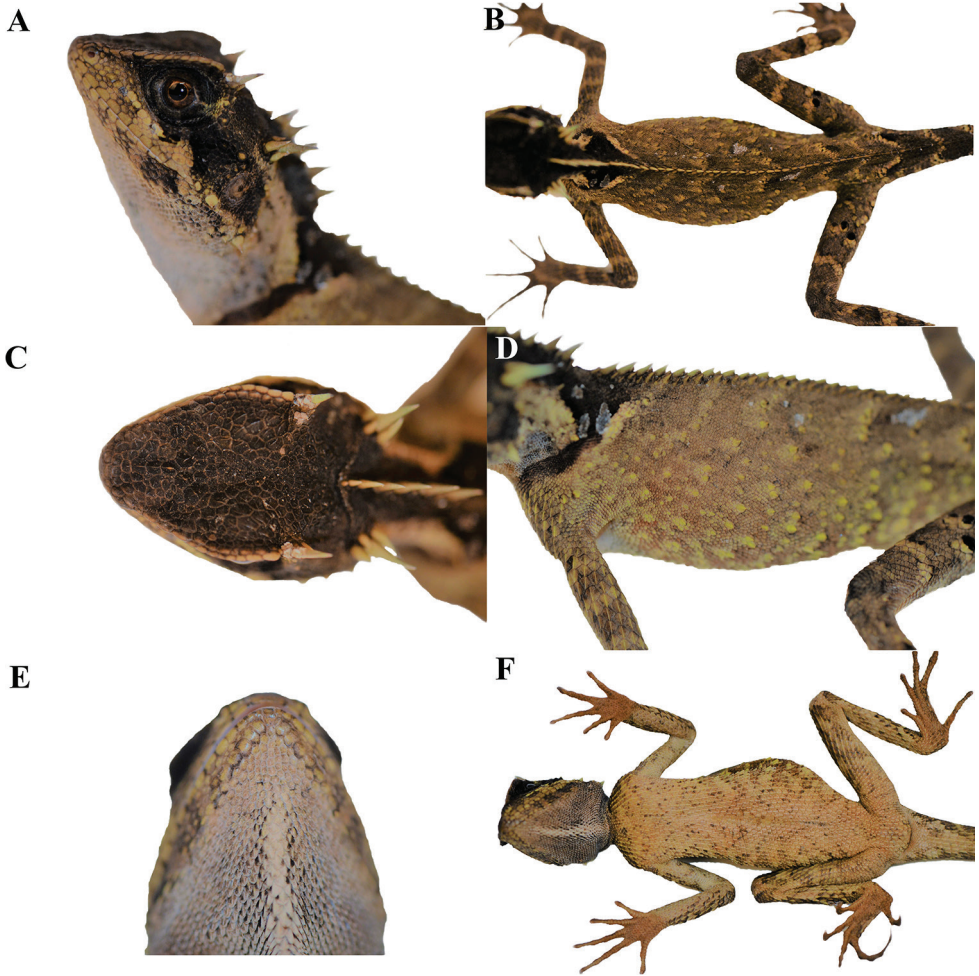


Figure 4. Adult female paratype (KIZL201805) of *Acanthosaura tongbiguanensis* sp. nov. in life **A** lateral view of the head **B** dorsal view of the body **C** dorsal view of the head **D** lateral view of the body **E** ventral view of the head **F** ventral view of the body.

steeply sloping anteriorly. Canthus rostralis prominent, forming a large projecting ridge extending above eye, composed of 11/13 enlarged scales; the ridge terminates with a notch anterior to the postorbital spine. Rostral moderate in size, rectangular; nasal concave, nostrils surrounded by a circular scale. Eye relatively large (EYE/HL 22%), orbit very large (ORBIT/HL 35%). Prefrontal and frontal scales slightly keeled and larger than scales between supralabials; scales on occiput weakly keeled. Moderately elongate epidermal spine above posterior margin of eye, straight, surrounded by 5/4 enlarged scales. A notch present between the supraciliary edge and postorbital spine. Moderately elongate epidermal spine on occipital region, straight, surrounded by a rosette of 5/4 short spiny scales. Tympanum exposed, oblong, surrounded by small

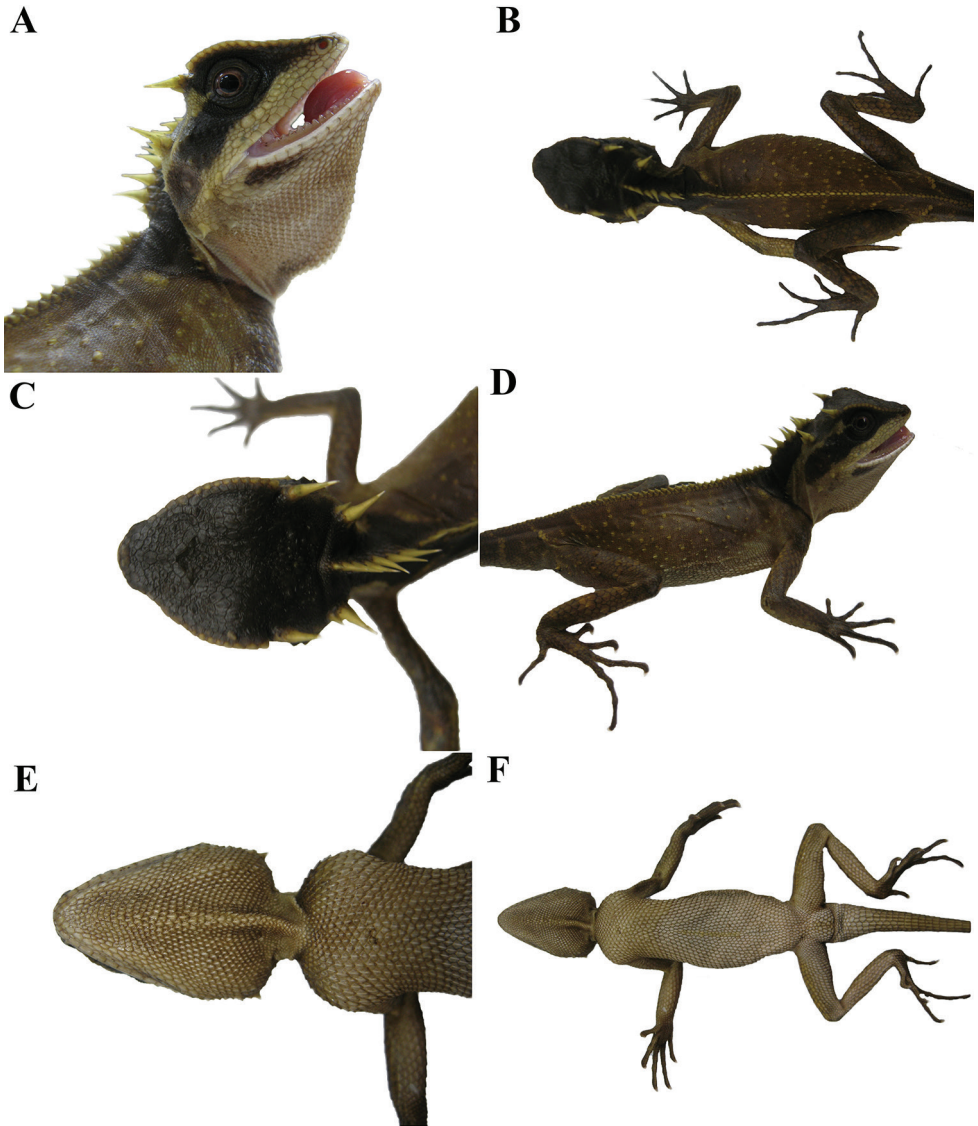


Figure 5. Adult male paratype (KIZL201801) of *Acanthosaura tongbiguanensis* sp. nov. in life **A** lateral view of the head **B** dorsal view of the body **C** dorsal view of the head **D** lateral view of the body **E** ventral view of the head **F** ventral view of the body.

scales. Supralabials 13/13, rectangular, scales in center of series largest; mental squarish above, becoming triangular below, larger than first pair of INFRAL; five scales contacting the mental; infralabials 13/12, rectangular, scales in center of series largest; gulars sharply keeled and spinose. Dewlap extensible, gular pouch moderate. Nuchal crest composed of four very elongate, lanceolate, laterally compressed scales and one moderately elongate, lanceolate, laterally compressed scale bordered on each side by one row of enlarged, spinose scales; nuchal crest followed by a diastema at base of nape. Dorsal



Figure 6. Dorsal view (top) and ventral view (bottom) of type series of *Acanthosaura tongbiguanensis* sp. nov. in preservative. From left to right: male holotype (KIZL201804), female paratype (KIZL201805), male paratype (KIZL201801), female paratype (74I0039), female paratype (74I0040), juvenile paratype (KIZL201802), juvenile paratype (KIZL201803).

body crest slightly developed, extending from posterior margin of diastema onto base of tail; vertebral crest composed of enlarged, epidermal, laterally compressed, spinose scales, bordered by a single row of smaller paravertebral spinose scales; vertebral crest tapers slightly to base of tail, then fades progressively. Body slightly short, triangular in cross-section. Dorsal scales small, mixed with large scales indistinctly arranged in slanted forward and downward rows from the midline of the back, keels projecting posteriorwards; scales of pectoral region and abdomen larger than dorsal scales, keeled, more or less arranged in transverse rows; keeled scales anterior to vent not enlarged. Limbs relatively long (FOREL/SVL 39%, HINDL/SVL 56%); dorsal and ventral scales of forelimbs keeled, spinose, about the same size. Five digits on manus; subdigital scales keeled, subdigital lamellae under fourth finger 20/21. Scales of hind limbs keeled and spinose; postfemoral scales small, interspersed with larger spinose scales. Five digits on pes; subdigital scales keeled, subdigital lamellae under fourth toe 26/27. Tail length 1.85 times SVL, tail covered with keeled spinose scales, keels on subcaudals directed posteriorly; subcaudals much longer than supracaudals; base of tail 13.1 mm wide.

Color of holotype in life. Dorsal surface of head black, dorsal surface of body and limbs orangish brown; black eye patch extending from posterior margin of nostrils through orbit posteriorly and downwards beyond the posterior end of the tympanum but neither meeting the diamond shaped black nuchal collar on nape nor black oblique folds anterior to the fore limb insertions; upper lip white, same as color of lateral and ventral sides of neck, lower lip white with small black speckle at posterior region; iris orangish brown; black nuchal collar extending downward to reach black oblique folds anterior to fore limb insertions, two white patches at lower back of black nuchal collar; gular region white; postorbital spines, occipital spines, nuchal crest spines and ridge of the rostral and orbit cream-colored; tongue and inside of mouth pink; few small black speckles and yellow diagonal stripes from midline of the back, irregular light colored spots on sides of body not obvious; stripes checkered with black and white on dorsal ground of limbs and tail; ventral sides of limbs and body white, front part white and back part dark on ventral side of tail. However, it should be noted that this species can change the color of its body within a certain range like most other members of the genus.

Variations. Morphometric and meristic data for the type series are provided in Table 3. The paratypes resemble the holotype in most aspects except that the male KIZL201801 has a darker dorsal ground of the body with no black speckles in the dorsal pattern, and the number of nuchal crest scales is six. The female KIZL201805 has a much darker dorsal ground of the body and irregular black patterns on the ventral sides of the body, limbs, and tail; light colored spots on the sides of the body are more obvious, the color in the gular region is a bit darker. The juveniles KIZL201802 and KIZL201803 have much shorter postorbital, occipital, and nuchal crest spines, and obvious radial patterns around the eyes; the colors of the bodies are relatively darker, the yellow diagonal stripes from the midline of the back are more obvious; they also have irregular black patterns on the ventral sides of the body, limbs, and tail; nuchal crest scales of KIZL201803 numbers four. The females 74II0039 and 74I0040 were not observed alive but only in preservative: the female 74II0039 has a much more obvious black speckling in the dorsal pattern while the female 74I0039 has no black

Table 4. Comparisons of morphometric (in mm) and meristic data for all currently recognized species of *Acanthosaura* and *Acanthosaura tongbiguanensis* sp. nov., “?” = data not available. (1) *Acanthosaura tongbiguanensis* sp. nov.; (2) *A. armata*; (3) *A. bintangensis*; (4) *A. brachypoda*; (5) *A. capri*; (6) *A. cardamomensis*; (7) *A. coronata*; (8) *A. crucigera*; (9) *A. lepidogaster*; (10) *A. murphyi*; (11) *A. nataliae*; (12) *A. phongdenensis*; (13) *A. phuketensis*; (14) *A. titiwangsaensis*.

	(1)	(2)	(3)	(4)	(5)	(6)	(7)	(8)	(9)	(10)	(11)	(12)	(13)	(14)
SVL	93.0–115.6	72.4–138.0	83.9–142.0	117	94.0–137.9	82–149	66.0–86.1	92.2–127.0	76.5–101.1	103.7–127.3	106.7–158.0	58.5–77.4	69.2–123.5	91.8–118.4
TL	144.9–205.0	96.6–190	112.8–206.0	185.4	133.6–182.1	103–188	86.3–105.0	130.0–174.0	130.6–144.1	159.3–195.8	171.0–287.0	94.6–137.2	107.0–205.6	136.0–174.0
HL	27.5–33.2	6.6–33.7	16.9–25.4	30.3	16.3–38.9	16.3–42.4	14.4–16.3	18.7–23.6	18.9–29.7	29.1–36.8	25.2–43.6	18.6–23.8	19.7–31.4	20.0–24.3
HW	18.6–23.3	15.3–23.0	17.5–23.4	20.6	16.8–27.0	13.6–27.7	13.6–17.5	16.0–22.3	13.4–19.1	20.3–24.6	20.2–27.8	13.1–15.9	14.4–22.8	17.5–23.4
HD	13.9–17.4	12.2–18.9	15.0–19.2	17.2	14.8–24.3	12.6–21.7	11.9–16.8	15.7–22.5	12.0–12.5	18.5–20.6	16.9–24.9	10.4–13.6	10.9–18.6	15.7–20.2
SL	9.2–11.0	6.3–16.6	7.9–11.3	12.2	7.6–16.6	8.6–18.7	6.9–8.4	8.7–12.1	9.3–10.2	10.3–15.3	12.0–19.9	?	6.8–11.0	9.7–12.5
ORBIT	7.7–11.0	5.4–12.2	8.4–12.6	8.3	7.6–11.6	6.0–12.7	6.9–7.5	8.9–10.8	4.7–9.1	9.9–12.3	7.2–10.9	?	6.6–11.2	9.8–13.2
TD	3.2–4.2	2.4–5.2	2.5–3.0	3.6	3.4–5.2	2.5–5.8	1.7–2.8	2.5–3.9	2.2–3.0	3.2–5.2	3.9–7.0	1.78–2.81	3.5–4.7	2.7–4.0
TD/HD	0.21–0.24	0.19–0.28	0.16	0.21	0.21–0.23	0.20–0.27	0.14–0.17	0.14–0.21	0.18–0.24	0.17–0.28	0.23–0.28	0.17–0.22	0.22–0.33	0.17–0.20
TN	0	0	0	0	0	0	0	0	0–1	1	0	0	0	0
PS	3.6–6.3	4.9–9.9	1.9–4.2	3.2	5.2–10.2	3.2–12.7	Absent	1.9–7.8	1.5–2.5	5.6–11.8	7.7–17.8	1.18–2.07	4.6–11.8	3.3–4.4
PS/HL	0.13–0.19	0.22–0.56	0.07–0.19	0.11	0.36	0.14–0.45	0	0.09–0.33	0.06–0.11	0.16–0.34	0.36	0.06–0.09	0.23–0.38	0.14–0.18
NSL	4.0–6.7	5.5–11.2	1.3–4.7	4.7	4.2–14.7	3.8–17.4	0	3.1–8.9	2.9–3.4	7.0–14.9	8.5–23.8	1.24–4.18	4.1–12.2	2.7–4.4
NSL/HL	0.15–0.21	0.22–0.51	0.17–0.21	0.16	0.42–0.43	0.17–0.66	0	0.14–0.38	0.12–0.15	0.24–0.43	0.58	0.07–0.18	0.21–0.39	0.11–0.18
DS	2.4–4.2	4.9–11.3	1.8–2.2	1.9	3.5–6.8	2.0–14.2	Absent	2.0–5.5	1.5–2.7	2.6–10.5	6.0–17.7	0.58–1.65	2.3–8.3	1.7–2.1
DS/HL	0.09–0.13	0.20–0.52	0.08–0.09	0.06	0.16–0.17	0.14–0.45	0	0.09–0.24	0.07–0.12	0.14–0.51	0.44	0.03–0.07	0.11–0.26	0.07–0.09
WNC	1.0–1.5	1.0–2.2	1.6–2.1	1.6	2.3–4.1	1.8–4.2	0	1.3–3.4	1.5	2.9–4.8	3.1–4.8	?	1.4–2.9	1.4–1.6
DIAS	3.9–6.1	1.2–6.8	5.0–7.9	?	2.0–6.7	2.7–8.3	Absent	4.9–8.4	6.3	2.6–4.8	2.5	Absent	3.6–7.6	5.1–7.6
DIASN	6–10	1–8	11–15	7	4–7	6–15	Absent	9–25	10–12	4–8	10	Absent	12–17	10–13
DIAS/SVL	0.03–0.07	0.01–0.06	0.04–0.07	?	0.05	0.03–0.07	Absent	0.04–0.08	0.08	0.02–0.04	0.04	Absent	0.05–0.08	0.05–0.07
FOREL	34.7–43.2	33.7–48.9	33.9–61.5	?	54.2–83.8	31.7–56.8	30.2–35.3	35.6–49.8	33.0–37.1	49.8–56.6	60.0–85.0	?	22.3–42.9	38.0–51.7
HINDL	54.1–63.9	39.0–69.6	43.3–68.6	?	78.5–107.2	42.0–77.1	38.4–47.8	48.8–65.0	49.4–50.4	60.4–68.4	85.0–129.7	?	38.2–60.6	48.5–65.6
SUPRAL	11–14	10–14	12	12–13	10	11–15	12–13	10–13	10–13	12–14	11	9–12	10–12	12–13
INFRAL	10–14	11–12	11–12	11	12–13	10–15	11–13	10–12	9–13	12–14	11–12	10–11	10–12	11–12
VENT	52–66	51–68	51–55	63	55–66	50–65	53–58	55–63	55–61	55–65	64–71	?	57–67	47–57
FI	19–21	13–17	23	24	16–17	15–20	13–14	16–18	17–19	15–18	16–21	14–17	15–17	20–21
TO	25–28	19–26	26–28	24	22–24	20–25	17–19	21–26	22–23	21–23	20–27	19–23	21–24	23–27
TL/SVL	1.56–1.85	1.2–1.6	1.3–1.4	1.58	1.2–1.5	1.2–1.6	0.6–1.0	1.1–1.8	1.6–1.9	1.48–1.54	1.2–1.5	1.5–1.9	1.4–1.7	1.1–1.5
OS	4.5–7.0	4.0–9.4	1.2–2.6	1.0	Absent	4.1–13.3	0	2.5–4.9	3.2–3.4	Absent	Absent	?	2.6–9.5	1.8–2.3
OS/HL	0.16–0.23	0.16–0.38	0.10–0.11	0.03	0	0.24–0.56	0	0.11–0.50	0.14–0.15	0	0	?	0.13–0.30	0.09–0.10

	(1)	(2)	(3)	(4)	(5)	(6)	(7)	(8)	(9)	(10)	(11)	(12)	(13)	(14)
NSSOS	4-5	4-6	6-7	?	Absent	4-6	4-5	4-6	5	Absent	Absent	?	4-5	4-5
CS	10-14	11-15	14-15	?	12-14	11-16	12-15	12-15	10-12	12-14	13	9-13	10-14	14-15
RW	3.3-4.5	1.8-4.5	3.6-5.3	3.5	4.2-4.6	1.7-4.7	0.8-0.9	2.7-4.0	2.8-3.0	3.3-5.1	6.1	2.07-2.65	2.3-3.8	3.6-5.2
RH	1.0-2.0	0.9-1.8	1.7-2.0	2.3	1.8-2.3	1.1-2.2	0.5-0.8	1.3-2.0	1.4-1.5	1.2-2.0	2.6	1.00-1.32	1.1-1.7	1.4-1.8
RS	6-9	5-9	7-9	7	7-8	5-9	5	7-9	5-9	8-9	6	?	5-8	9
NS	8-9	7-10	8	9	9	7-10	7-9	7-9	7-8	7-8	8	?	7-8	8
NCS	10-13	10-17	10-11	?	9	9-17	8-11	9-12	7-10	13-16	14	?	12-13	11-12
NCSL	7-9	6-14	7-8	?	7-8	7-12	5-6	7-11	8	7-10	8	?	8-10	9-11
NR	2	1-2	1	?	1-2	1-2	3-4	1-2	1-2	3-4	1	?	1-2	1-2
NSSLC	9-13	10-22	9-12	?	9-11	10-19	6-11	10-14	10	?	16	?	11-14	11-14
MW	1.4-1.9	0.9-2.0	1.3-1.8	2.9	1.9-2.2	0.2-2.1	0.6-1.5	1.0-1.5	1.2-1.3	1.7-2.2	2.9	0.87-1.52	0.5-1.4	1.4-2.0
MH	1.2-2.0	0.8-2.2	1.4-2.1	2.1	1.7-2.2	0.9-2.0	1.3-1.6	1.1-1.7	1.2-1.3	1.4-2.0	2.0	1.04-1.60	0.6-1.6	1.4-2.4
PM	4-5	3-6	4-5	4	4	4-5	4-5	4	5	?	4	?	4	5
YAS	1	0-1	1	1	1	0-1	0-1	1	1	0-1	1	?	0-1	1
ND	1	0-1	1	1	1	1	0	1	1	?	0	1	1	1
LKP	1	1	0	1	1	1	1	1	1	?	0	1	1	0
BEP	1	0	1	1	1	1	0	1	0-1	0-1	1	?	1	1
ESBO	0	0	1	0	0	0	0	0	0	?	0	?	0	0
GP	1-2	1	3-4	0	3-4	1-4	0	1-2	0-1	4	4	?	0-2	2-4
OF	1	1	1	1	1	1	1	1	1	?	1	?	1	1

speckles, but they both have irregular black patterns on the ventral sides of the body, limbs, and tail; both have six nuchal crest scales.

Distribution. *Acanthosaura tongbiguanensis* sp. nov. is only recorded in Tongbiguan Nature Reserve including Yingjiang County, Longchuan County and Ruili City, the border region with northern Myanmar in western Yunnan, China, so it probably occurs in northern Myanmar.

Natural history. The type series of *Acanthosaura tongbiguanensis* sp. nov. was collected at night while they were asleep on small trees in a primordial forest. However, we suppose that they forage for food on the ground during the day. At the type locality we found four other species of reptiles, namely *Cyrtodactylus khasiensis* (Jerdon, 1870), *Pseudocalotes kakhienensis* (Anderson, 1879); *P. microlepis* (Boulenger, 1887); *Trimeresurus yingjiangensis* Chen et al., 2019; and seven species of amphibians, *Leptobranchella yingjiangensis* (Yang et al., 2018); *Limnonectes longchuanensis* Suwannapoom et al., 2016; *Megophrys feii* Yang et al., 2018; *M. glandulosa* Fei et al., 1990; *Raorchestes longchuanensis* (Yang & Li, 1978); *Theلودerma moloch* (Annandale, 1912); *Zhangixalus smaragdinus* (Blyth, 1852).

Comparisons. Table 4 shows a comparison of morphometric and meristic data for all currently recognized species of *Acanthosaura* and *Acanthosaura tongbiguanensis* sp. nov. It is based mostly on the interspecific comparison tables provided by Pauwels et al. (2015: table 2), Nguyen et al. (2018: table 3) and Nguyen et al. (2019: table 3).

Acanthosaura tongbiguanensis sp. nov. can be distinguished from *A. armata* by having more subdigital lamellae on the fourth finger (19–21 vs. 13–17) and the fourth toe (25–28 vs. 19–26), shorter postorbital spines (3.6–6.3 vs. 4.9–9.9 mm, PS/HL 0.13–0.19 vs. 0.22–0.56) and shorter occipital spines (4.5–7.0 vs. 4.0–9.4 mm, OS/HL 0.16–0.23 vs. 0.16–0.38), much shorter nuchal crest spines (4.0–6.7 vs. 5.5–11.2 mm, NSL/HL 0.15–0.21 vs. 0.22–0.51) and much shorter dorsal crest spines (2.4–4.2 vs. 4.9–11.3 mm, DS/HL 0.09–0.13 vs. 0.20–0.52), a higher number of scales in the diastema between the nuchal and the dorsal crests (6–10 vs. 1–8), a relatively longer tail (TL/SVL 1.56–1.85 vs. 1.2–1.6). *Acanthosaura tongbiguanensis* sp. nov. has a black eye patch (vs. absent) and an obvious black nuchal collar (vs. not obvious or absent); *Acanthosaura tongbiguanensis* sp. nov. has fewer or no spots on the dorsal surface of the body, whereas *A. armata* has more spots on the dorsal surface of the body.

The new species can be distinguished from *Acanthosaura bintangensis* by having a larger tympanum (3.2–4.2 vs. 2.5–3.0 mm, TD/HD 0.21–0.24 vs. 0.16), longer head (27.5–33.2 vs. 16.9–25.4 mm), longer postorbital spines (6.3 vs. 4.2 mm), higher maximal length of spines in the nuchal crest (6.7 vs. 4.7), longer spines in the dorsal crest (2.4–4.2 vs. 1.8–2.2 mm, DS/HL 0.09–0.13 vs. 0.08–0.09), less subdigital lamellae on the fourth finger (19–21 vs. 23), much longer occipital spines (4.5–7.0 vs. 1.2–2.6 mm, OS/HL 0.16–0.23 vs. 0.10–0.11), less scales surrounding the occipital spine (4–5 vs. 6–7), lower number of scales in the diastema between the nuchal and the dorsal crests (6–10 vs. 11–15), presence of a light knee patch (vs. absence), less developed gular pouch (1–2 vs. 3–4), absence of an enlarged row of keeled scales below orbit (vs. presence), absence of large yellow spots edged in blackish-brown arranged on

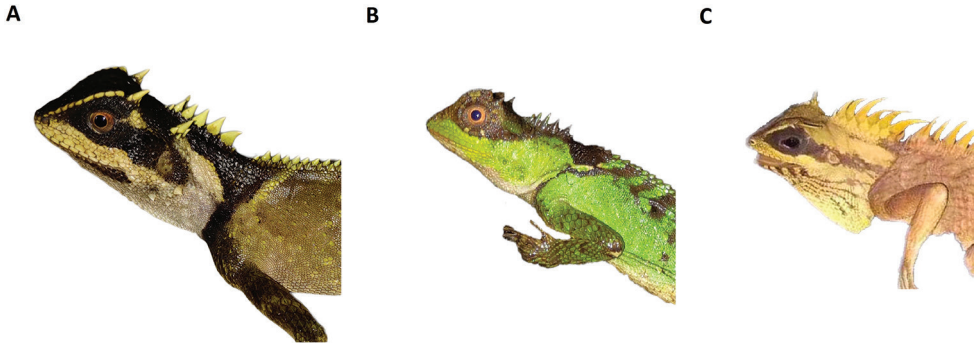


Figure 7. Comparison of three different types of eye patch **A** *Acanthosaura tongbiguanensis* sp. nov. **B** *A. lepidogaster* **C** *A. nataliae*.

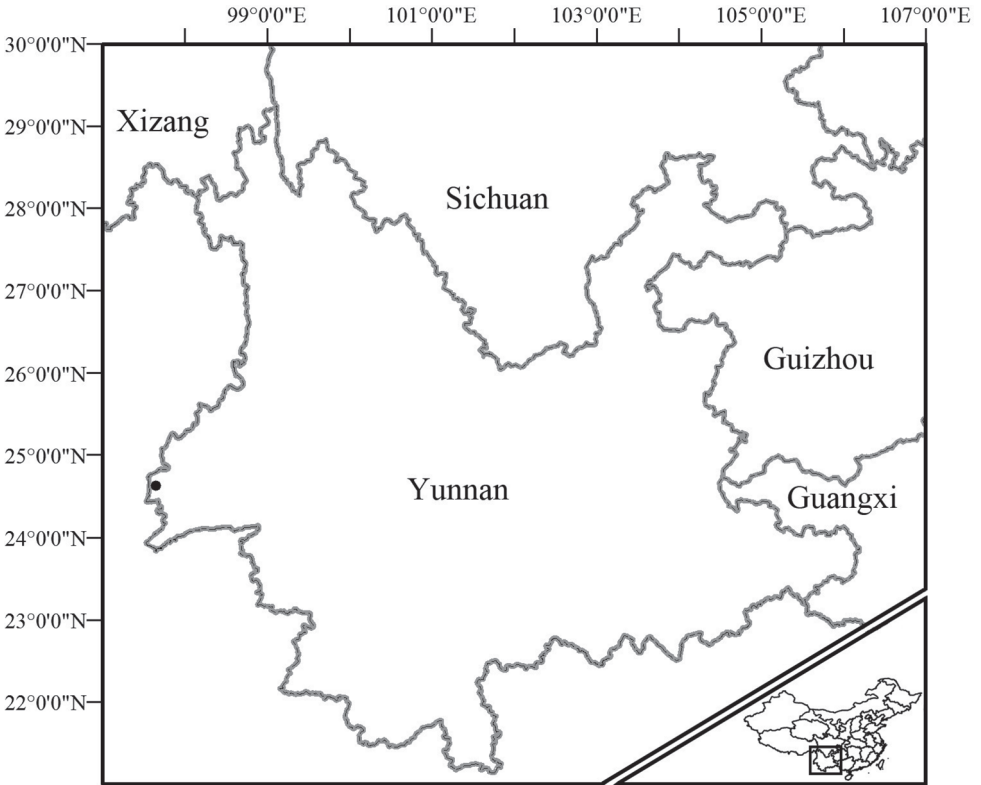


Figure 8. The type locality of *Acanthosaura tongbiguanensis* sp. nov. (black dot) close to the border with Myanmar.

body and base of tail (vs. presence); the black eye patch in *Acanthosaura tongbiguanensis* sp. nov. extends backward and downward beyond the posterior end of the tympanum while it never extends onto the head side in *A. bintangensis* (Wood et al. 2009).



Figure 9. Habitat at the type locality of *Acanthosaura tongbiguanensis* sp. nov., Tongbiguan Township, Yingjiang County, Dehong Autonomous Prefecture, Yunnan, China **A** distant view **B** close view.

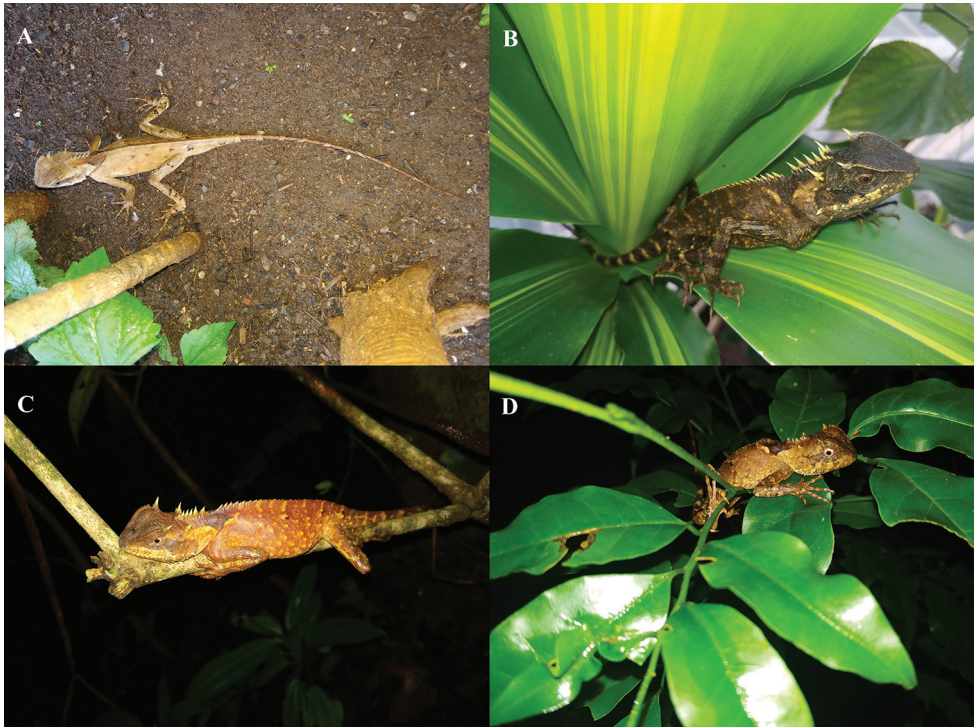


Figure 10. *Acanthosaura tongbiguanensis* sp. nov. **A** live adult male on the ground **B** live adult female on a leaf **C** live adult female asleep on a branch **D** live juvenile asleep on branches and leaves.

From *Acanthosaura brachypoda*, *Acanthosaura tongbiguanensis* sp. nov. can be differentiated by having more subdigital lamellae on the fourth finger (19–21 vs. 18) and the fourth toe (25–28 vs. 24), longer postorbital spines (3.6–6.3 vs. 3.2 mm, PS/HL 0.13–0.19 vs. 0.11) and longer occipital spines (4.5–7.0 vs. 1.0 mm, OS/HL

0.16–0.23 vs. 0.03), much longer spines in the dorsal crest (2.4–4.2 vs. 1.9 mm, DS/HL 0.09–0.13 vs. 0.06), the presence of gular pouch (vs. absence). *Acanthosaura tongbiguanensis* sp. nov. does not have pairs of transverse creamy spots along both sides of spine forming a symmetrical pattern present as in *A. brachypoda*.

Acanthosaura tongbiguanensis sp. nov. can be distinguished from *A. capra* based on its smaller body size (93.0–115.6 vs. 94.0–137.9 mm) but longer tail (144.9–205.0 vs. 133.6–182.1 mm, TL/SVL 1.56–1.85 vs. 1.2–1.5), a higher number of subdigital lamellae on the fourth finger (19–21 vs. 16–17) and the fourth toe (25–28 vs. 22–24), lower maximal length of forelimb (43.2 vs. 83.8 mm) and hindlimb (63.9 vs. 107.2 mm), shorter postorbital spines (3.6–6.3 vs. 5.2–10.2 mm, PS/HL 0.13–0.19 vs. 0.36), nuchal crest spines (4.0–6.7 vs. 4.2–14.7 mm, NSL/HL 0.15–0.21 vs. 0.42–0.43) and dorsal crest spines (2.4–4.2 vs. 3.5–6.8 mm, DS/HL 0.09–0.13 vs. 0.16–0.17), lower width of the nuchal crest spines (1.0–1.5 vs. 2.3–4.1 mm), higher number of scales in the diastema between nuchal and dorsal crests (6–10 vs. 4–7), presence of occipital spines (vs. absence), a smaller gular pouch (1–2 vs. 3–4); the black eye patch in *Acanthosaura tongbiguanensis* sp. nov. extends backward and downward beyond the posterior end of the tympanum, while it usually extends backwards and upwards to reach the nuchal crests in *A. capra*.

From *Acanthosaura cardamomensis*, the new species can be separated based on a higher number of subdigital lamellae on the fourth finger (19–21 vs. 15–20) and the fourth toe (25–28 vs. 20–25), a longer tail (144.9–205.0 vs. 103–188 mm, TL/SVL 1.56–1.85 vs. 1.2–1.6), much shorter postorbital spines (3.6–6.3 vs. 3.2–12.7 mm, PS/HL 0.13–0.19 vs. 0.14–0.45), occipital spines (4.5–7.0 vs. 4.1–13.3 mm, OS/HL 0.16–0.23 vs. 0.24–0.56), nuchal crest spines (4.0–6.7 vs. 3.8–17.4 mm, NSL/HL 0.15–0.21 vs. 0.17–0.66) and dorsal crest spines (2.4–4.2 vs. 2.0–14.2 mm, DS/HL 0.09–0.13 vs. 0.14–0.45), a lower width of nuchal crest spines (1.0–1.5 vs. 1.8–4.2 mm); the black eye patch in *Acanthosaura tongbiguanensis* sp. nov. extends backward and downward beyond the posterior end of the tympanum but never reaches the dark nuchal marking on nape while it does so in *A. cardamomensis* (see species' description and photographs in Wood et al. 2010), besides, *Acanthosaura tongbiguanensis* sp. nov. has fewer or no spots on the dorsal surface of the body, whereas *A. cardamomensis* has more spots on the dorsal surface of the body.

Acanthosaura tongbiguanensis sp. nov. is distinguishable from *A. coronata* based on its much bigger body size (93.0–115.6 vs. 66.0–86.1 mm), much longer tail (144.9–205.0 vs. 86.3–105.0 mm, TL/SVL 1.56–1.85 vs. 0.6–1.0), higher number of subdigital lamellae on the fourth finger (19–21 vs. 17–19) and the fourth toe (25–28 vs. 22–23), relatively larger tympanum (TD/HD 0.21–0.24 vs. 0.14–0.17), bigger rostral (RW 3.4–4.5 vs. 0.8–0.9 mm, RH 1.0–2.0 vs. 0.5–0.8 mm), the presence of postorbital spines, occipital spines, nuchal and dorsal crests (vs. absence or not obvious), a diastema between nuchal crest and dorsal crest (vs. a continuous nuchal and dorsal crest), presence of a black nuchal collar (vs. absence), presence of a black eye patch (vs. absence), and the presence of a gular pouch (vs. absence) (see the original description by Günther 1861 and expanded descriptions by Günther 1864; Boulenger 1885).

Acanthosaura tongbiguanensis sp. nov. can be differentiated from *A. crucigera* by having more subdigital lamellae on the fourth finger (19–21 vs. 16–18) and the fourth toe (25–28 vs. 21–26), a relatively larger tympanum (TD/HD 0.21–0.24 vs. 0.14–0.21), a higher maximal length of tail (205.0 vs. 174.0 mm), a higher maximal length of occipital spines (7.0 vs. 4.9 mm), a lower number of scales in the diastema between the nuchal and the dorsal crests (6–10 vs. 9–25), a larger mental (MW 1.4–1.9 vs. 1.0–1.5 mm, MH 1.2–2.0 vs. 1.1–1.7 mm). Most obvious is the difference in the color pattern: the black eye patch in *Acanthosaura tongbiguanensis* sp. nov. extends back and downwards beyond the posterior end of the tympanum, while it only extends to the anterior edge of the tympanum in *A. crucigera*; additionally, *Acanthosaura tongbiguanensis* sp. nov. has fewer or no spots on the dorsal surface of the body, whereas *A. crucigera* has more spots on the dorsal surface of the body.

Acanthosaura tongbiguanensis sp. nov. can be separated from *A. lepidogaster* based on its higher number of subdigital lamellae on the fourth finger (19–21 vs. 17–19) and the fourth toe (25–28 vs. 22–23), its bigger body size (93.0–115.6 vs. 76.5–101.1 mm), longer postorbital spines (3.6–6.3 vs. 1.5–2.5 mm, PS/HL 0.13–0.19 vs. 0.06–0.11) and longer occipital spines (4.5–7.0 vs. 3.2–3.4 mm, OS/HL 0.16–0.23 vs. 0.14–0.15), longer nuchal crest spines (4.0–6.7 vs. 2.9–3.4 mm, NSL/HL 0.15–0.21 vs. 0.12–0.15) and longer dorsal crest spines (2.4–4.2 vs. 1.5–2.7 mm, DS/HL 0.09–0.13 vs. 0.07–0.12), much higher maximal length of tail (205.0 vs. 144.1 mm), lower number of scales in the diastema between the nuchal and the dorsal crests (6–10 vs. 10–12), much wider rostral (3.3–4.5 vs. 2.8–3.0 mm), and larger gular pouch (1–2 vs. 0–1). The black eye patch in *Acanthosaura tongbiguanensis* sp. nov. extends backwards and downwards beyond the posterior end of the tympanum but never backwards and upwards to reach the black nuchal collar, while it usually does so in *A. lepidogaster*; the black nuchal collar extends downwards to reach the black oblique humeral fold, while it rarely reaches the black oblique humeral fold in *A. lepidogaster*; besides, the tongue and the inside of the mouth are pink in *Acanthosaura tongbiguanensis* sp. nov., while they are bluish-grey or black in *A. lepidogaster*; the postorbital spines, occipital spines, nuchal crest spines, the ridge of the rostralis, and orbit are lighter in color in *Acanthosaura tongbiguanensis* sp. nov., whereas they are darker in color in *A. lepidogaster*.

Acanthosaura tongbiguanensis sp. nov. can be separated from *A. murphyi* based on its smaller body size (93.0–115.6 vs. 103.7–127.3 mm) but relatively longer tail (TL/SVL 1.56–1.85 vs. 1.48–1.54), a higher number of subdigital lamellae on the fourth finger (19–21 vs. 15–18) and the fourth toe (25–28 vs. 21–23), shorter forelimb (34.7–43.2 vs. 49.8–56.6 mm) and hindlimb (54.1–63.9 vs. 60.4–68.4 mm), much shorter postorbital spines (3.6–6.3 vs. 5.6–11.8 mm, PS/HL 0.13–0.19 vs. 0.16–0.34), nuchal crest spines (4.0–6.7 vs. 7.0–14.9 mm, NSL/HL 0.15–0.21 vs. 0.24–0.43) and dorsal crest spines (2.4–4.2 vs. 2.6–10.5 mm, DS/HL 0.09–0.13 vs. 0.14–0.51), much lower width of the nuchal crest spines (1.0–1.5 vs. 2.9–4.8 mm), higher number of scales in the diastema between nuchal and dorsal crests (6–10 vs. 4–8), presence of occipital spines (vs. absence), a smaller gular pouch (1–2 vs. 4); the black eye patch in *Acanthosaura tongbiguanensis* sp. nov. extends backward and downward beyond the posterior

end of the tympanum, while it usually extends backwards and upwards to reach the nuchal crests in *A. murphyi* (see species' photographs in Nguyen et al. 2018).

Acanthosaura tongbiguanensis sp. nov. can be separated from *A. nataliae* by its smaller body size (93.0–115.6 vs. 106.7–158.0 mm) and a lower maximal tail length (205.0 vs. 287.0 mm) but a relatively longer tail (TL/SVL 1.56–1.85 vs. 1.2–1.5), much shorter length of postorbital spines (3.6–6.3 vs. 7.7–17.8 mm, PS/HL 0.13–0.19 vs. 0.36), nuchal crest spines (4.0–6.7 vs. 8.5–23.8 mm, NSL/HL 0.15–0.21 vs. 0.58) and dorsal crest spines (2.4–4.2 vs. 6.0–17.7 mm, DS/HL 0.09–0.13 vs. 0.44), a lower width of the nuchal crest spines (1.0–1.5 vs. 3.1–4.8 mm), lower width of mental (1.4–1.9 vs. 2.9 mm), a lower number of ventral scales (52–66 vs. 64–71), lower maximal length of forelimb (43.2 vs. 85.0 mm) and hindlimb (63.9 vs. 129.7 mm), presence of occipital spines (vs. absence), much lesser development of gular pouch (1–2 vs. 4), presence of light knee patch (vs. absence) and presence of a black nuchal collar (vs. absence); the black eye patch in *Acanthosaura tongbiguanensis* sp. nov. extends backward and downward beyond the posterior end of the tympanum but never continues backward to reach the black oblique folds anterior to the fore limb insertions while it usually does so in *A. nataliae* (see species' description and photographs in Orlov et al. 2006).

Acanthosaura tongbiguanensis sp. nov. is distinguishable from *A. phongdienensis* based on its bigger body size (93.0–115.6 vs. 58.5–77.4 mm), longer tail (144.9–205.0 vs. 94.6–137.2 mm), higher number of subdigital lamellae on the fourth finger (19–21 vs. 14–17) and the fourth toe (25–28 vs. 19–23), longer postorbital spines (3.6–6.3 vs. 1.18–2.07 mm, PS/HL 0.13–0.19 vs. 0.06–0.09), longer nuchal crest spines (4.0–6.7 vs. 1.24–4.18 mm, NSL/HL 0.15–0.21 vs. 0.07–0.18) and longer dorsal crest spines (2.4–4.2 vs. 0.58–1.65 mm, DS/HL 0.09–0.13 vs. 0.03–0.07), a diastema between nuchal crests and dorsal crests (vs. a continuous nuchal and dorsal crest); the black eye patch in *Acanthosaura tongbiguanensis* sp. nov. extends backwards and downwards beyond the posterior end of the tympanum but never backwards and upwards to reach the black nuchal collar, while it does so in male *A. phongdienensis* (see species' description and photographs in Nguyen et al. 2019), the postorbital spines, occipital spines, nuchal crest spines, the ridge of the rostralis and orbit are lighter in color in *Acanthosaura tongbiguanensis* sp. nov., whereas they are darker in color in *A. phongdienensis*.

Acanthosaura tongbiguanensis sp. nov. can be differentiated from *A. phuketensis* by having a higher number of subdigital lamellae on the fourth finger (19–21 vs. 15–17) and the fourth toe (25–28 vs. 21–24), a relatively longer tail (TL/SVL 1.56–1.85 vs. 1.4–1.7), much shorter postorbital spines (3.6–6.3 vs. 4.6–11.8 mm, PS/HL 0.13–0.19 vs. 0.23–0.38), nuchal crest spines (4.0–6.7 vs. 4.1–12.2 mm, NSL/HL 0.15–0.21 vs. 0.21–0.39) and dorsal crest spines (2.4–4.2 vs. 2.3–8.3 mm, DS/HL 0.09–0.13 vs. 0.11–0.26), a lower width of nuchal crest spines (1.0–1.5 vs. 1.4–2.9 mm), a lower maximal length of occipital spines (7.0 vs. 9.5 mm), a lower number of scales in the diastema between the nuchal and the dorsal crests (6–10 vs. 12–17), a bigger mental (MW 1.4–1.9 vs. 0.5–1.4 mm, MH 1.2–2.0 vs. 0.6–1.6 mm); the black

eye patch in *Acanthosaura tongbiguanensis* sp. nov. never extends backward to reach the nuchal crest while it does so in male *A. phuketensis* (see species' original description by Pauwels et al. 2015) and *Acanthosaura tongbiguanensis* sp. nov. has fewer or no spots on the dorsal surface of the body, whereas *A. phuketensis* has more spots on the dorsal surface of the body.

From *Acanthosaura titiwangsaensis*, the new species can be distinguished by its relatively larger tympanum (TD/HD 0.21–0.24 vs. 0.17–0.20), its longer tail (144.9–205.0 vs. 136.0–174.0mm, TL/SVL 1.56–1.85 vs. 1.1–1.5), higher maximal length of postorbital spines (6.3 vs. 4.4 mm) and nuchal crest spines (6.7 vs. 4.4 mm), higher length of dorsal crest spines (2.4–4.2 vs. 1.7–2.1 mm, DS/HL 0.09–0.13 vs. 0.07–0.09), much longer occipital spines (4.5–7.0 vs. 1.8–2.3 mm, OS/HL 0.16–0.23 vs. 0.09–0.10), lower number of scales in the diastema between the nuchal and the dorsal crests (6–10 vs. 10–13), presence of a light knee patch (vs. absence), less developed gular pouch (1–2 vs. 2–4), absence of medium-sized light orange spots edged in a faded black color on body and base of tail (vs. presence); the black eye patch in *Acanthosaura tongbiguanensis* sp. nov. extends backward and downward beyond the posterior end of the tympanum while it is restricted to the orbit and not extends into the postorbital region in *A. titiwangsaensis* (Wood et al. 2009).

Discussion

Although *Acanthosaura* collections from Myanmar and other Southeast Asian countries were not available for comparative analyses, we could demonstrate that *Acanthosaura tongbiguanensis* sp. nov. is a distinct species using data available from literature (Hardwicke and Gray 1827; Cuvier 1829; Günther 1861; Boulenger 1885; Orlov et al. 2006; Manthey 2008; Wood et al. 2009, 2010, Ananjeva et al. 2011; Grismer 2011; Pauwels et al. 2015; Nguyen et al. 2018; Nguyen et al. 2019).

Several morphometric characters of *Acanthosaura tongbiguanensis* sp. nov. overlap with some characters of other species in this genus, however, the new species can be differentiated from all other species of *Acanthosaura* by the black eye patch extending from the posterior margin of the nostrils through the orbit backwards and downwards to beyond the posterior end of the tympanum but neither meeting black nuchal collar nor the black oblique humeral fold (see Fig. 7).

The *Acanthosaura crucigera* group is wide ranging and its morphological variation is conserved, it is not surprising to find cryptic diversity within the *A. crucigera* complex (Wood et al. 2010). *Acanthosaura tongbiguanensis* sp. nov. was previously considered to represent *A. lepidogaster* (Yang et al. 2008) although it more closely resembles *A. crucigera*, however the numbers of subdigital lamellae on the fourth finger and toe of *Acanthosaura tongbiguanensis* sp. nov. are significantly different from *A. lepidogaster* and *A. crucigera*, and the molecular analyses also revealed them distinct taxa. Together with the species described herein *Acanthosaura* currently comprises 14 species in total.

Acknowledgements

We would like to thank Decai Ouyang and Lei Ouyang for assistance in the field. Thanks also to our workmates for their help and advice. Thanks to the manager of the collection room of the Institute of Zoology, Chinese Academy of Sciences for helping to find specimens. We also thank the reviewers for their valuable comments on the manuscript. We owe thanks to the curator Weiwei Li for giving us the opportunity to conduct the field investigation; this work was supported by Kunming Natural History Museum of Zoology, Kunming Institute of Zoology, Chinese Academy of Sciences.

References

- Ananjeva NB, Guo XG, Wang YZ (2011) Taxonomic diversity of agamid lizards (Reptilia, Sauria, Acrodonta, Agamidae) from China: a comparative analysis. *Asian Herpetological Research* 2(3): 117–128. <https://doi.org/10.3724/SP.J.1245.2011.00117>
- Ananjeva NB, Orlov NL, Kalyabina-Hauf SA (2008) Species of *Acanthosaura* Gray, 1831 (Agamidae: Sauria, Reptilia) of Vietnam: results of Molecular and Morphological study. *Biology Bulletin* 35(2): 178–186. <https://doi.org/10.1134/S106235900802012X>
- Ananjeva NB, Orlov NL, NguyenTQ (2007) Agamid lizards (Agamidae, Acrodonta, Sauria, Reptilia) of Vietnam. *Mitteilungen aus dem Museum für Naturkunde in Berlin, Zoologische Reihe* 83(2007): 13–21. <https://doi.org/10.1002/mmzn.200600021>
- Ananjeva NB, Orlov NL, Nguyen TT, Ryabov SA (2011b) A new species of *Acanthosaura* (Agamidae, Sauria) from northwest Vietnam. *Russian Journal of Herpetology* 18(3): 195–202.
- Anderson J (1879) Reptilia and amphibia. In: Quarich B (Ed.) *Comprising an Account of the Zoological Results of the Two Expeditions to Western Yunnan in 1868 and 1875. Anatomical and Zoological Research (Vol. I)*. London, 705–860. <https://doi.org/10.5962/bhl.title.50434>
- Annandale N (1912) Zoological results of the Abor Expedition, 1911–1912. I Batrachia. *Records of the Indian Museum* 8: 7–36. <https://doi.org/10.5962/bhl.part.1186>
- Blyth E (1852) Report of Curator, Zoological Department. *Journal of the Asiatic Society of Bengal* 21: 341–358.
- Boulenger GA (1885) *Catalogue of the lizards in the British Museum (Natural History)*. Second edition (Vol. I). Geckonidae, Eublepharidae, Uroplatidae, Pygopodidae, Agamidae. British Museum (Natural History), London, 436 pp.
- Boulenger GA (1887) An account of the reptiles and batrachians obtained in Tenasserim by M. L. Fea, of the Genova Civic Museum. *Annali del Museo Civico di Storia Naturale da Genova* 5: 474–486.
- Boulenger GA (1908) A revision of the Oriental pelobatid batrachians (genus *Megalophrys*). *Proceedings of the Zoological Society of London* 1908: 407–430. <https://doi.org/10.1111/j.1096-3642.1908.tb01852.x>
- Chan-ard T, Grossmann W, Gumprecht A, Schulz K-D (1999) Amphibians and reptiles of Peninsular Malaysia and Thailand. *An Illustrated Checklist*. [Amphibien und reptilien der

- Halbinsel Malaysia und Thailand. Eine illustrierte Checkliste] Bushmaster Publications, Würselen, Germany, 240 pp.
- Chen ZN, Zhang L, Shi JS, Tang YZ, Guo YH, Song ZB, Ding L (2019) A New Species of the Genus *Trimeresurus* from Southwest China (Squamata: Viperidae). *Asian Herpetological Research* 10(1): 13–23. <http://doi.org/10.16373/j.cnki.ahr.180062>
- Cuvier GJLNF (1829) *Le Règne Animal Distribué, d'après son Organisation, pur servir de base à l'Histoire naturelle des Animaux et d'introduction à l'Anatomie Comparée*. Nouvelle Edition [2^{ème} ed] (Vol. 2). Les Reptiles. Déterville, Paris, 406 pp.
- Daudin FM (1802) *Histoire Naturelle, Générale et Particulière des Reptiles; ouvrage faisant suite à l'Histoire naturelle générale et particulière, composée par Leclerc de Buffon; et rédigée par CS Sonnini, membre de plusieurs sociétés savantes (Tome 4)*. F Dufart, Paris. <https://doi.org/10.5962/bhl.title.60678>
- Fei L, Ye CY, Huang YZ (1990) *Key to Chinese Amphibians*. Publishing House for Scientific and Technological Literature, Chongqing, 364 pp.
- Gray JE (1831) A synopsis of the species of the Class Reptilia. In: Griffiths E, Pidgeon E (Ed.) *The Animal Kingdom Arranged in Conformity with its Organization by the Baron Cuvier with Additional Descriptions of all the Species Hitherto Named and of Many not Before Noticed (Vol. 9)*. The class Reptilia arranged by the Baron Cuvier with specific descriptions. Whittaker, Treacher and Co., London, 483–600.
- Grismer LL (2011) *Lizards of Peninsular Malaysia, Singapore and Their Adjacent Archipelagos*. Edition Chimaira, Frankfurt am Main, 728 pp.
- Grismer LL, Pan KA (2008) Diversity, endemism, and conservation of the amphibians and reptiles of southern Peninsular Malaysia and its offshore islands. *Herpetological Review* 39(3): 270–281.
- Günther ACLG (1858) Neue Batrachier in der Sammlung des britischen Museums. *Archiv für Naturgeschichte* 24: 319–328. <https://doi.org/10.5962/bhl.part.5288>
- Günther ACLG (1861) Second list of Siamese reptiles. *Proceedings of the Zoological Society of London* 1861(10): 187–189.
- Günther ACLG (1864) *The Reptiles of British India*. The Ray Society, London, 452 pp.
- Hallermann J (2000) The taxonomic status of *Acanthosaura frubstorferi* Werner, 1904 and *Calotes brevipes* Werner, 1904 (Squamata, Agamidae). *Mitteilungen aus dem Museum für Naturkunde in Berlin, Zoologische Reihe* 76(1): 143–150. <https://doi.org/10.1002/mmzn.20000760113>
- Hanke M, Wink M (1994) Direct DNA sequencing of PCR-amplified vector inserts following enzymatic degradation of primer and dNTPs. *Biotechniques* 17(5): 858–860.
- Hardwicke T, Gray JE (1827) A synopsis of the species of saurian reptiles, collected in India by Major-General Hardwicke. *Zoological Journal* 3: 214–229.
- Jerdon TC (1870) Notes on Indian Herpetology. *Proceedings of the Asiatic Society of Bengal* 1870: 66–85.
- Kalyabina-Hauf S, Ananjeva NB, Joger U, Lenk P, Murphy RW, Stuart BL, Orlov NL, Ho CT, Wink M (2004) Molecular phylogeny of the genus *Acanthosaura* (Agamidae). *Current Herpetology* 23(1): 7–16. <https://doi.org/10.5358/hsj.23.7>

- Manthey U (2008) *Agamid Lizards of Southern Asia – Agamen des südlichen Asien – Draconinae 1. Terralog* (Vol. 7a). Edition Chimaira, Frankfurt am Main, 160 pp.
- Nguyen LT, Do DT, Hoang HV, Nguyen TT, McCormack TEM, Nguyen TQ, Orlov NL, Nguyen VDH, Nguyen SN (2018) A new species of the genus *Acanthosaura* Gray, 1831 (Reptilia: Agamidae) from Central Vietnam. *Russian Journal of Herpetology* 25(4): 259–274.
- Nguyen SN, Jin JQ, Dinh BV, Nguyen LT, Zhou WW, Che J, Murphy RW, Zhang YP (2019) A new species of *Acanthosaura* Gray 1831 (Reptilia: Agamidae) from Central Vietnam. *Zootaxa* 4612(4): 555–565. <https://doi.org/10.11646/zootaxa.4612.4.7>
- Orlov NL, Nguyen TQ, Nguyen VS (2006) A new *Acanthosaura* allied to *A. capra* Günther, 1861 (Agamidae, Sauria) from central Vietnam and southern Laos. *Russian Journal of Herpetology* 13(1): 61–76.
- Pauwels OSG, Sumontha M, Kunya K, Nitikul A, Samphanthamit P, Wood PL Jr, Grismer LL (2015) *Acanthosaura phuketensis* (Squamata: Agamidae), a new long-horned tree agamid from southwestern Thailand. *Zootaxa* 4020(3): 473–494. <https://doi.org/10.11646/zootaxa.4020.3.4>
- Posada D, Crandall KA (1998) Modeltest: testing the model of DNA substitution. *Bioinformatics* 14(9): 817–818. <https://doi.org/10.1093/bioinformatics/14.9.817>
- Ronquist F, Teslenko M, van der MP, Ayres DL, Darling A, Höhna S, Larget B, Liu L, Suchard MA, Huelsenbeck JP (2012) MrBayes 3.2: Efficient Bayesian phylogenetic inference and model choice across a large model space. *Systematic biology* 61(3): 539–542. <https://doi.org/10.1093/sysbio/sys029>
- Sambrook J, Fritsch EF, Maniatis T (1989) *Molecular Cloning: A Laboratory Manual*. Cold Spring Harbor Laboratory Press, New York, 1546 pp.
- Stuart BL, Sok K, Neang T (2006) A collection of amphibians and reptiles from hilly eastern Cambodia. *The Raffles Bulletin of Zoology* 54(1): 129–155.
- Stuart BL, Rowley JJJ, Neang T, Emmett DA, Sitha S (2010) Significant new records of amphibians and reptiles from Virachey National Park, northeastern Cambodia. *Cambodian Journal of Natural History* 2010(1): 38–47.
- Suwannapoom C, Yuan ZY, Chen JM, Hou M, Zhao HP, Wang LJ, Nguyen TS, Nguyen TQ, Murphy RW, Sullivan J, McLeod DS, Che J (2016) Taxonomic revision of the Chinese *Limnonectes* (Anura, Dicroglossidae) with the description of a new species from China and Myanmar. *Zootaxa* 4093: 181–200. <https://doi.org/10.11646/zootaxa.4093.2.2>
- Tamura K, Peterson D, Peterson N, Stecher G, Nei M, Kumar S (2011) MEGA5: molecular evolutionary genetics analysis using maximum likelihood, evolutionary distance, and maximum parsimony methods. *Molecular Biology and Evolution* 28(10): 2731–2739. <https://doi.org/10.1093/molbev/msr121>
- Thompson JD, Gibson TJ, Plewniak F, Jeanmougin J, Higgins DG (1997) The CLUSTAL_X windows interface: flexible strategies for multiple sequence alignment aided by quality analysis tools. *Nucleic Acids Research* 25(24): 4876–4882. <https://doi.org/10.1093/nar/25.24.4876>
- Wang Y, Cheng KP, Yao Q (2009) An introduction to the operation method of phylogenetic analysis program MrBayes 3.1. *Journal of Anhui Agricultural Sciences* 37(33): 16665–16669.

- Werner F (1904) Beschreibung neuer Reptilien aus den Gattungen *Acanthosaura*, *Calotes*, *Gastropholis* und *Typhlops*. Zoologischer Anzeiger 27: 461–464.
- Wood Jr PL, Grismer JL, Grismer LL, Norhayati A, Chan K-O, Bauer AM (2009) Two new montane species of *Acanthosaura* Gray, 1831 (Squamata: Agamidae) from Peninsular Malaysia. Zootaxa 2012: 28–46. <https://doi.org/10.11646/zootaxa.2012.1.2>
- Wood Jr PL, Grismer LL, Grismer JL, Neang T, Chav T, Holden J (2010) A new cryptic species of *Acanthosaura* Gray, 1831 (Squamata: Agamidae) from Thailand and Cambodia. Zootaxa 2488: 22–38. <https://doi.org/10.11646/zootaxa.2488.1.2>
- Yang DT, Rao DQ (2008) Amphibia and Reptilia of Yunnan. Yunnan Publishing Group Corporation, Yunnan Science and Technology Press, Kunming, 411 pp.
- Yang DT, Su CY, Li SM (1978) Amphibians and Reptiles of Gaoligongshan. Compilation of Scientific Research Work 1978: 1–94.
- Yang JH, Wang J, Wang YY (2018) A new species of the genus *Megophrys* (Anura: Megophryidae) from Yunnan Province, China. Zootaxa 4413: 325–338. <https://doi.org/10.11646/zootaxa.4413.2.5>
- Yang JH, Zeng ZC, Wang YY (2018) Description of two new sympatric species of the genus *Leptolalax* (Anura: Megophryidae) from western Yunnan of China. PeerJ 6: e4586. <https://doi.org/10.7717/peerj.4586>
- Zhao EM, Jiang YM, Huang QY, Zhao H, Zhao KT, Zhou KY, Liu YZ, Liu MY, Li DJ, Zhang YX (1999) Fauna Sinica (Reptilia 2): Squamata (Lacertilia). Science Press, Beijing, 394 pp.

Who are you, Griselda? A replacement name for a new genus of the Asiatic short-tailed shrews (Mammalia, Eulipotyphla, Soricidae): molecular and morphological analyses with the discussion of tribal affinities

Anna A. Bannikova^{1*}, Paulina D. Jenkins^{2*}, Evgeniya N. Solovyeva³,
Svetlana V. Pavlova⁴, Tatiana B. Demidova⁴, Sergey A. Simanovsky⁴,
Boris I. Sheftel⁴, Vladimir S. Lebedev³, Yun Fang⁵,
Love Dalen⁶, Alexei V. Abramov⁷

1 Department of Vertebrate Zoology, Lomonosov Moscow State University, Vorobievy Gory, 1/12, Moscow, Russia **2** The Natural History Museum, Cromwell Road, London SW7 5BD, UK **3** Zoological Museum of Lomonosov Moscow State University, B. Nikitskaya 6, Moscow, Russia **4** A.N. Severtsov Institute of Ecology and Evolution, Russian Academy of Sciences, Leninskii pr. 33, Moscow, Russia **5** Institute of Zoology, Chinese Academy of Science, Beijing 100101, China **6** Department of Bioinformatics and Genetics of Swedish Museum of Natural History, Stockholm, Sweden **7** Zoological Institute, Russian Academy of Sciences, Universitetskaya nab. 1, Saint-Petersburg 199034, Russia

Corresponding author: Anna A. Bannikova (hylomys@mail.ru)

Academic editor: R. López-Antoñanzas | Received 4 July 2019 | Accepted 21 October 2019 | Published 11 November 2019

<http://zoobank.org/C32A9617-E290-4723-B21E-7C413199F4E7>

Citation: Bannikova AA, Jenkins PD, Solovyeva EN, Pavlova SV, Demidova TB, Simanovsky SA, Sheftel BI, Lebedev VS, Fang Y, Dalen L, Abramov AV (2019) Who are you, Griselda? A replacement name for a new genus of the Asiatic short-tailed shrews (Mammalia, Eulipotyphla, Soricidae): molecular and morphological analyses with the discussion of tribal affinities. ZooKeys 888: 133–158. <https://doi.org/10.3897/zookeys.888.37982>

Abstract

The first genetic study of the holotype of the Gansu short-tailed shrew, *Blarinella griselda* Thomas, 1912, is presented. The mitochondrial analysis demonstrated that the type specimen of *B. griselda* is close to several recently collected specimens from southern Gansu, northern Sichuan and Shaanxi, which are highly distinct from the two species of Asiatic short-tailed shrews of southern Sichuan, Yunnan, and Vietnam, *B. quadraticauda* and *B. wardi*. Our analysis of four nuclear genes supported the placement of *B. griselda* as sister to *B. quadraticauda* / *B. wardi*, with the level of divergence between these two clades corresponding

* These authors contributed equally to this work and should be considered as co-first authors.

to that among genera of Soricinae. A new generic name, *Parablarinella*, is proposed for the Gansu short-tailed shrew. Karyotypes of *Parablarinella griselda* ($2n = 49$, $NFa = 50$) and *B. quadraticauda* ($2n = 49$, $NFa = 62$) from southern Gansu are described. The tribal affinities of Blarinellini and Blarinini are discussed.

Keywords

Blarinini, Blarinellini, karyotypic variation, molecular phylogeny, *Parablarinella*

Introduction

Asiatic short-tailed red-toothed shrews are commonly referred to the genus *Blarinella* Thomas, 1911. The composition of the genus *Blarinella* has been disputed for a long time. The holotype of *Sorex quadraticauda* Milne Edwards, 1872 was described from Moupin (now Baoxing) in Sichuan Province, China. Thomas (1911) considered that this species was more closely allied to the New World genus *Blarina* rather than to any Old World genus of shrews and assigned the Asian short-tailed shrews to a separate genus, *Blarinella*. In the following few years Thomas described two further species: *Blarinella griselda* Thomas, 1912 (type locality: “42 miles S.E. of Tao-chou”, = Lintan, Gansu, China) and *B. wardi* Thomas, 1915 (North Burma, “Hpimaw, Upper Burma...” = Pianma, Yunnan, China), so recognizing three species of *Blarinella*. Some subsequent authors disagreed with the species status of *griselda* and *wardi*, and regarded them either as subspecies or synonyms of *B. quadraticauda* (Allen 1938; Ellerman and Morrison-Scott 1951; Corbet 1978; Hoffmann 1987; Corbet and Hill 1992), while Hutterer (1993) considered *griselda* as a synonym of *B. quadraticauda* but *B. wardi* as a distinct species. Based on a multivariate analysis of cranial measurements, *B. griselda* and *B. wardi* were again raised to species rank (Jiang et al. 2003; Lunde et al. 2003). This treatment of *Blarinella* was accepted in MSW3 (Hutterer 2005) and other monographs (e.g. Hoffmann and Lunde 2008). The results by Jiang et al (2003) further suggested that *B. quadraticauda* is limited to west-central Sichuan and *B. wardi* is distributed from the mountains of northern Myanmar and Yunnan to the southwest of Sichuan, while *B. griselda* ranged widely from southern Gansu Province to northern Vietnam and from northwestern Yunnan to northwestern Hubei.

The analysis of one nuclear (*ApoB*) and two mitochondrial (*cytb*, *16S rRNA*) genes confirmed the distinct position of *B. wardi*, but the sequences assigned to *B. quadraticauda* (including those from the type locality in Baoxing) form a clade close to a haplogroup of the polymorphic *B. griselda* (Chen et al. 2012). Among various scenarios these authors suggested that *B. quadraticauda* is only a subspecies of *B. griselda*; however, because of the Principle of Priority within the rules of the International Commission on Zoological Nomenclature (ICZN 1999) this would be incorrect as the junior name, *B. griselda*, should be treated as a subspecies of the senior name, *B. quadraticauda*.

Recently, Bannikova et al. (2017) analyzed the genetic diversity of the genus *Blarinella* using the complete sequence of the mitochondrial gene *cytb* and four nuclear genes (*ApoB*, *BRCA2*, *RAG2*, and *IRBP*). The results of the molecular genetic analysis

of samples of specimens of *Blarinella* from various locations in China and Vietnam showed that the *Blarinella* specimen from southern Gansu stands apart from the other representatives of the genus and could not be assigned to a known species based on the molecular data available at that time. This individual (ZMMU S-195179, ID Chi111) was karyotyped and its chromosome set ($2n = 49$, $NFa = 50$) was described in Sheftel et al. (2018) without an illustration. Previously only two karyotypes of Asiatic short-tailed shrews have been described: *B. wardi* ($2n = 32$, $NFa = 58$) from Yunnan Province (Moribe et al. 2007) and *B. "griselda"* ($2n = 44$) (Ye et al. 2006) also from Yunnan Province, Nanjian County (Dr Chen Zhongzheng pers. comm. 2016).

The distinct position of the Gansu specimen led us to continue with further studies to re-evaluate the taxonomic status of the Asiatic short-tailed shrews from China and Vietnam. In the meantime, a new generic name was proposed based on the previously published data of our specimen from Gansu and additional specimens from Shaanxi (He et al. 2018). The new genus was named as *Pantherina* He, 2018 with *Blarinella griselda* Thomas, 1912 as the type species. Unfortunately, the authors made a nomenclatural error, since the name *Pantherina* He, 2018 is preoccupied by *Pantherina* Curletti, 1998, which was proposed as a subgeneric name for the African beetles (Coleoptera, Buprestidae, *Agrius*) (see Curletti 1998). According to the ICZN (1999) a new name should be proposed for the Asiatic short-tailed shrew from Gansu.

Another question arises over the attribution of the new name to *B. griselda* Thomas, 1912 from Gansu, because no direct comparison with the type specimen was made by He et al. (2018). None of the previous studies (Jiang et al. 2003; Chen et al. 2012; He et al. 2018) analyze the holotype of *B. griselda*. The only shrew from Gansu included in the molecular analysis by He et al. (2018) was represented by previously published *cytb* sequence of the specimen ZMMU S-195179 from Bannikova et al. (2017). The only shrew from Gansu included in their craniometric analysis was specimen AMNH M-60499 (labeled as "Kansu") using data retrieved from the paper of Jiang et al. (2003). However, this specimen was never sequenced and the skull of this specimen from the American Museum of Natural History (AMNH) was lost a long time ago (Dr Ross MacPhee pers. comm. April 2016). According to their craniometric data this specimen falls into the same morphological cluster together with *B. quadrata-cauda* and "*Pantherina*" specimens from Shaanxi Province. Therefore, as neither the holotype specimen nor topotypes of *B. griselda* were included by He et al. (2018) for the morphological diagnosis of the newly described genus, their diagnosis was based on the specimens from Shaanxi Province.

This current study presents the first molecular study of the holotype of *B. griselda* and includes new data on additional specimens of this rare species from Gansu and northern Sichuan. The new name for this taxon is provided below.

Allen (1938) disagreed with Thomas (1911) about the supposed relationship of *Blarinella* with *Blarina* and, based on external, cranial and dental morphology, was of the opinion that *Blarinella* was more closely related to *Sorex*. Reppening (1967) shared this view and in his division of the Soricinae into three tribes, he placed *Blarinella* in the tribe Soricini, with *Blarina* and *Cryptotis* in the tribe Blarinini. Reumer (1998)

considered that *Blarinella* and eight related fossil genera should be separated from the Soricini and placed in a new tribe, the Blarinellini. This useful tribal arrangement based entirely on morphology has been accepted and widely followed; however, some of the results of recent molecular studies (Dubey et al. 2007) have suggested that the tribal arrangement may not be so well defined and is in need of revision. Thus, on the basis of our new data, another task was to revise the arrangement of the Blarinini/Blarinellini tribes.

Material and methods

Taxon sampling and tissue collection

The specimens of Asiatic short-tailed shrews were collected during the surveys of small mammals conducted by the Russian Academy of Sciences and the Chinese Academy of Sciences in Gansu and Sichuan provinces of China. Voucher specimens are deposited in the Zoological Museum of Lomonosov Moscow State University (ZMMU). These specimens were compared with the Asiatic short-tailed shrews kept in the collection of the Natural History Museum, London, UK (NHMUK) and the Zoological Institute of the Russian Academy of Sciences, Saint Petersburg, Russia (ZIN). Among them, the holotype of *B. griselda* (NHMUK 1912.8.5.23) was genetically studied for the first time. On the whole, we obtained 23 new sequences from 11 specimens of *Blarinella* and two specimens of *Chodsigoa hypsibia* (Table 1). For the phylogenetic analysis, 47 mitochondrial and nuclear sequences of *Blarinella*, *Blarina*, *Chodsigoa*, *Chimarrogale*, *Neomys*, *Anourosorex*, and *Sorex* from our previous studies (Abramov et al. 2017b; Bannikova and Lebedev 2010; Bannikova et al. 2015, 2017, 2018) and additional 116 sequences of different genera of Soricinae as well as Crocidurina (*Crocidura fuliginosa*) from GenBank were used (see Suppl. material 1: Table S1).

DNA extraction, PCR amplification, and sequencing

Genomic DNA from ethanol-preserved tissues of the recent specimens was extracted using a standard protocol of proteinase K digestion, phenol-chloroform deproteinisation and isopropanol precipitation (Sambrook et al. 1989). We sequenced the complete mitochondrial cytochrome *b* (*cytb*) gene and fragments of four nuclear loci: apolipoprotein B (*ApoB*), exon 11 of the breast cancer type 1 susceptibility protein (*BRCA1*), recombination activating gene 2 (*RAG2*), and the interphotoreceptor retinoid binding photoreceptor (*IRBP*). Primers and polymerase chain reaction protocols for nuclear loci (*ApoB*, *BRCA1*, *IRBP* and *RAG2*) are described in Abramov et al. (2017a) and Bannikova et al. (2018). New primers were designed specifically for amplification and sequencing the complete *cytb* gene and its short fragments from the historical museum specimen, the holotype of *B. griselda* (Suppl. material 1: Table S2). General methods for the amplification and sequencing of *cytb* from recent samples are described in Ban-

Table 1. List of the original material used in the molecular study and specimens examined in the morphological analysis: species, specimen ID, collection and geographic origin. Samples are stored in the following collections: ZMMU – Zoological Museum of Moscow State University, Russia; ZIN – Zoological Institute of Russian Academy of Sciences, St.-Petersburg, Russia; NHMUK – Natural History Museum, London, UK. All specimens in the phylogenetic analysis were also included in the morphological analysis, with the exception of those marked thus – #.

Species	Specimen code in phylogenetic analysis (Figs. 2, 3, Suppl. material 1: Figure S1)	Museum catalogue number and/or field collection code (in brackets)	Collecting locality (country, province and closest city)
<i>"Blarinella" griselda</i>	NHMUK	NHMUK 1912.8.5.23 Holotype	China, Gansu, 68 km SE Taochou (Lintan), Tsingling (Qinling) Mountains, 34°40'N, 103°35'E
	Chi111	ZMMU S-195179	China, S. Gansu, Taizhishan NR, 35°16'N, 103°26'E
		ZMMU S-199245	China, S. Gansu, Taizhishan NR, 35°16'N, 103°26'E
	G17-87	ZMMU G17-87	China, N. Sichuan, Ruoergai (Zoige), 33°35'N, 103°09'E
<i>B. quadraticauda</i>	G18-252	ZMMU G18-252	China, N. Sichuan, Songpan, 32°30'N 103°35'E
	Bl-1	ZIN 91211 (36) #	Vietnam, Lao Cai, Van Ban, 21°58'N, 104°02'E
	Bl-2	ZIN 96272 (42) #	Vietnam, Lao Cai, Sa Pa, 22°21'N, 103°46'E
	Bl-3	ZIN 96273 (43) #	Vietnam, Lao Cai, Sa Pa, 22°21'N, 103°46'E
		ZIN 98268	Vietnam, Lao Cai, Sa Pa, 22°21'N, 103°46'E
		ZIN 99935	Vietnam, Lao Cai, Sa Pa, 22°21'N, 103°46'E
	Bl-5	ZIN 97788 (136)	Vietnam, Lao Cai, Sa Pa, 22°21'N, 103°46'E
	V12-40	ZIN 101574	Vietnam, Lao Cai, Sa Pa, 22°21'N, 103°46'E
V12-61	ZIN 101575	Vietnam, Lao Cai, Sa Pa, 22°21'N, 103°46'E	
<i>B. cf. quadraticauda</i>	G17-12	ZMMU G17-12	China, S. Gansu, Huixian, 33°40'N 106°15'E
<i>B. quadraticauda</i>		NHMUK 1911.9.8.56	China, S. Sichuan, Omi-San (Emei Shan), 29°30'N, 103°18'E
		NHMUK 1911.9.8.57	China, S. Sichuan, Omi-San (Emei Shan), 29°30'N, 103°18'E
		NHMUK 1911.9.8.58	China, S. Sichuan, Omi-San (Emei Shan), 29°30'N, 103°18'E
		NHMUK 1911.9.8.59	China, S. Sichuan, Omi-San (Emei Shan), 29°30'N, 103°18'E
		NHMUK 1911.9.8.25	China, S. Sichuan, Nan-chwan (Nanchuan), 29°07'N, 107°16'E
<i>B. wardi</i>		NHMUK 1915.2.1. Holotype	China, Yunnan, Hpimaw, [formerly Upper Burma / Myanmar] (Pianma), 26°N, 98°35'E (26°00'N, 98°37'E)
		NHMUK 1932.11.1.33	Myanmar, Adung Valley, 28°15'N, 97°40'E
		NHMUK 1922.9.1.26	China, Yunnan, Mekong – Salwin (Salween) Divide, 28°N (c. 27°30'N 98°56'E / 28°20'N 98°44'E)
		NHMUK 1922.9.1.27	China, Yunnan, Kiu-Kiang – Salwin Divide, 28°N (c. 28°40'N 98°15'E)
<i>Chodsigoa hypsibia</i>	Chi11-72	ZMMU S-195190	China, S. Gansu, Lianhuashan NR, 34°56'N, 103°44'E
	G17-13	ZMMU G17-13	China, S. Gansu, Huixian, 33°40'N 106°15'E

nikova et al. (2010). PCR products were sequenced on the autosequencing system ABI 3100-Avant using ABI PRISM BigDye™ Terminator v. 3.1 (Applied Biosystems, Foster City, CA, USA).

Molecular analysis of the holotype of *B. griselda*

Molecular analysis (DNA extraction and PCR preparation) of the holotype of *B. griselda* NHMUK1912.8.5.23 was performed in the laboratories of Department of Bioinformatics and Genetics of the Swedish Museum of Natural History in the

special laboratory for historical museum samples. DNA was extracted from a ~1.5 mm × 1.5 mm skin sample that was washed in ethanol prior to initiating the extraction procedure.

Extraction of DNA was performed using Qiagen QIAamp DNA Micro Kit following the protocol “Isolation of Genomic DNA from Tissues” with some changes: (1) additional 5 µl of Proteinase K after overnight lysis and incubation at room temperature for 30 min; (2) two steps of elution with AE buffer, each with 20 µl of buffer and 5 min of incubation at room temperature. Amplification of *cytb* fragments was performed in 25 µl reaction volume containing 1–2 µl DNA, 2.5 µl 10× buffer, 1 µl of each primer (10 pmol/µl), 0.5 µl of dNTP mix, 1 µl MgCl₂, 2.5 µl BSA, and 0.4 µl Taq polymerase. Extraction was performed twice, the second time with blank as a negative control. Double-stranded polymerase chain reaction entailed 50-thermal cycles and was performed as follows: 95 °C for 10 min, (94 °C for 30 sec, 52 °C for 30 sec, 72 °C for 30 sec) ×50 cycles, 72 °C for 7 min, 12 °C for forever. Negative controls were used both for DNA and PCR mix. PCR products were verified on 1% agarose gels stained with Gel Green. Primer pairs which resulted in bands on the gel and empty negative controls: L467x – H601x, L240a – H400a, L62x – H190x, L170ax – H330x, L580x – H670x. Amplicons were sequenced directly by Sanger sequencing on Applied Biosystems 3130xl Genetic Analyzer. Each fragment was sequenced several times to ensure the authenticity of the sequence.

It is known that DNA undergoes degradation over time (Hofreiter et al. 2001), such that mtDNA sequences from even relatively recent museum specimens can exhibit sequencing artifacts (Sefc et al. 2007). Most errors involves C→T changes, presumably due to the deamination of cytosine bases in the template (Hofreiter et al. 2001). Here, neither clear double C/T peaks nor an excess of C→T transitions were observed in the *cytb* sequences obtained from the historical *Blarinella* sample relative to modern samples, suggesting that the holotype sequences are authentic.

The sequences obtained in this study can be accessed via GenBank (accession numbers: MN199101 to MN199123, Suppl. material 1:Table S1).

Alignment, partitioning, and phylogenetic tree reconstruction

All sequences were aligned by eye using Bioedit v. 7.0.9.0 (Hall 1999). Heterozygous positions in nuclear genes were coded using the IUB ambiguity codes and sequences were used as unphased genotypes. The ModelFinder routine (Kalyaanamoorthy et al. 2017) as implemented in IQTREE v. 1.6 (Nguyen et al. 2015) was used to determine the optimum partitioning scheme and the best-fit substitution models for each subset under the BIC criterion.

Phylogenetic reconstructions were performed with each nuclear gene separately and all nuclear genes combined. Phylogenetic trees were reconstructed from nuclear concatenation under Maximum Likelihood (ML) and Bayesian criteria. Maximum

likelihood reconstructions were conducted in IQTREE v. 1.6 (Nguyen et al. 2015). Clade stability was tested using Ultrafast Bootstrap (Minh et al. 2013) with 10 000 replicates. Bayesian tree reconstructions were performed in MrBayes v. 3.2 (Ronquist et al. 2012). Models with either two or six rate matrix parameters were selected for each subset using ModelFinder. For most parameters, default priors were used. Compound Dirichlet priors for branch lengths combined with gamma prior on the tree length were invoked. All parameters except branch lengths were unlinked across partitions. The analysis included two independent runs of four chains with the default heating scheme. The chain length was set at 20 million generations with the sampling of every 10 000 generation. Tracer v. 1.6 software (Rambaut and Drummond 2003) was used to check for convergence and to determine the necessary burn-in fraction, which was 10% of the chain length. The effective sample size exceeded 200 for all estimated parameters.

The mitochondrial phylogeny of *Blarinella* was generated from the *cytb* alignment containing 46 sequences of Asiatic short-tailed shrews including the partial sequence of the holotype of *Blarinella griselda*. The ML and Bayesian trees were reconstructed as described above and rooted using *Blarina* and *Cryptotis* as the outgroups. In addition, we performed the analyses of the extended set of taxa of Soricinae with the aim to examine more thoroughly the relationships among taxa of the Blarinini-Blarinellini clade and other soricine genera. The *p*-distances were calculated in PAUP* v. 4.0b10 (Swofford 2003).

Molecular dating

Molecular dating was performed in BEAST v. 1.84 based on the nuclear dataset. The optimum partitioning scheme and substitution model were determined separately for each gene in ModelFinder (Kalyaanamoorthy et al. 2017). Based on the results of the hierarchical likelihood ratio tests performed in PAUP* v. 4.0b10 (Swofford 2003) strict clock models were employed. The analysis was conducted using birth-death tree shape prior. The chain length was set at 100 million generations, the effective sample size exceeded 200 for all estimated parameters after the 10% burn-in fraction was discarded. The tree was calibrated using a secondary calibration point corresponding to the time of divergence of Blarinini and Blarinellini (normal distribution with 15.38 million years (My) as the mean and 2.34 My as the standard deviations). In addition, an informative prior for the *ApoB* clock rate was employed (lognormal distribution with 2.42 E^{-3} as the mean and 2.59 E^{-4} as the standard deviations). The parameters of these prior densities are equivalent to those of the posterior distribution produced by the Bayesian molecular clock analysis of the multilocus data on Soricinae (Bannikova et al. 2018). Taking into account potential ambiguity in interpretation of fossil data on Blarinini and Blarinellini (Doby 2015) the dataset of Bannikova et al. (2018) was re-analyzed omitting the calibration concerning the latter two taxa.

Morphology

Specimens sampled for the phylogenetic analysis and included in the morphological analysis were compared with historical material of all three taxa in the NHMUK collection (Table 1). For the historical material, place names and their coordinates were determined from field notes in combination with information obtained from the United States Board on Geographic Names (**USBGN**), the GEOnet Names Server (**GNS**) (<http://geonames.nga.mil/gns/html/>) and Google Earth (<http://earth.google.com>).

External measurements of historical specimens are those recorded by collectors on specimen labels. Recently collected specimens and the crania of all specimens were measured in millimetres using digital callipers. Cranial and dental nomenclature follows that of McDowell (1958), Meester (1963), Mills (1966), Repenning (1967), Butler and Greenwood (1979), Reumer (1984), and Dannelid (1998). Abbreviations used in the text for the dental nomenclature are incisor (I/i), unicuspid (Un), lower antemolar (a), premolar (P/p), and molar (M/m), with premaxillary and maxillary teeth denoted by uppercase and mandibular teeth by lowercase letters.

Karyotyping

Karyotypes of two Asiatic short-tailed shrews, a male ZMMU S-195179 (ID Chi111) from southern Gansu, Taizishan and a female G17-12 from southern Gansu, Huixian were examined. Mitotic chromosome preparations were made in the field from both bone marrow and spleen after colchicine treatment *in vivo* following Ford and Hamerton (1956) with some modifications (Bulatova et al. 2009).

In case of the male, preparations were made from spleen using a simple technique without centrifugation proposed by Krysanov et al. (2009). Briefly, after colchicine treatment *in vivo* an incised spleen incubates with 5 mL of KCl hypotonic solution (0.07 M) for 20–30 min at room temperature, and fix with 5 mL of freshly prepared glacial acetic-methanol (1:3) for 5 min twice. Such samples can be stored at -10°C up to 6 months. To prepare air-dried slides a fixed tissue incubates with 200 μl of 50% glacial acetic acid for 3–4 min, resuspends, and then drops suspension onto a hot slide (30 min at 90°C). After drying, a slide incubates with pure methanol for 5 min, and then dried again. Air-dried chromosome spreads of both specimens were stained conventionally with 4% Giemsa for 8 min.

CBG-banding was performed using the standard technique (Sumner 1972) to determine C-heterochromatin blocks (for the female karyotype only).

Results

Alignment and partitioning

The total matrix used in the *cytb* analysis (74 sequences, 1140 bp) contained 46 specimens of *Blarinella* and 28 specimens of other soricids. Models for the *cytb* gene esti-

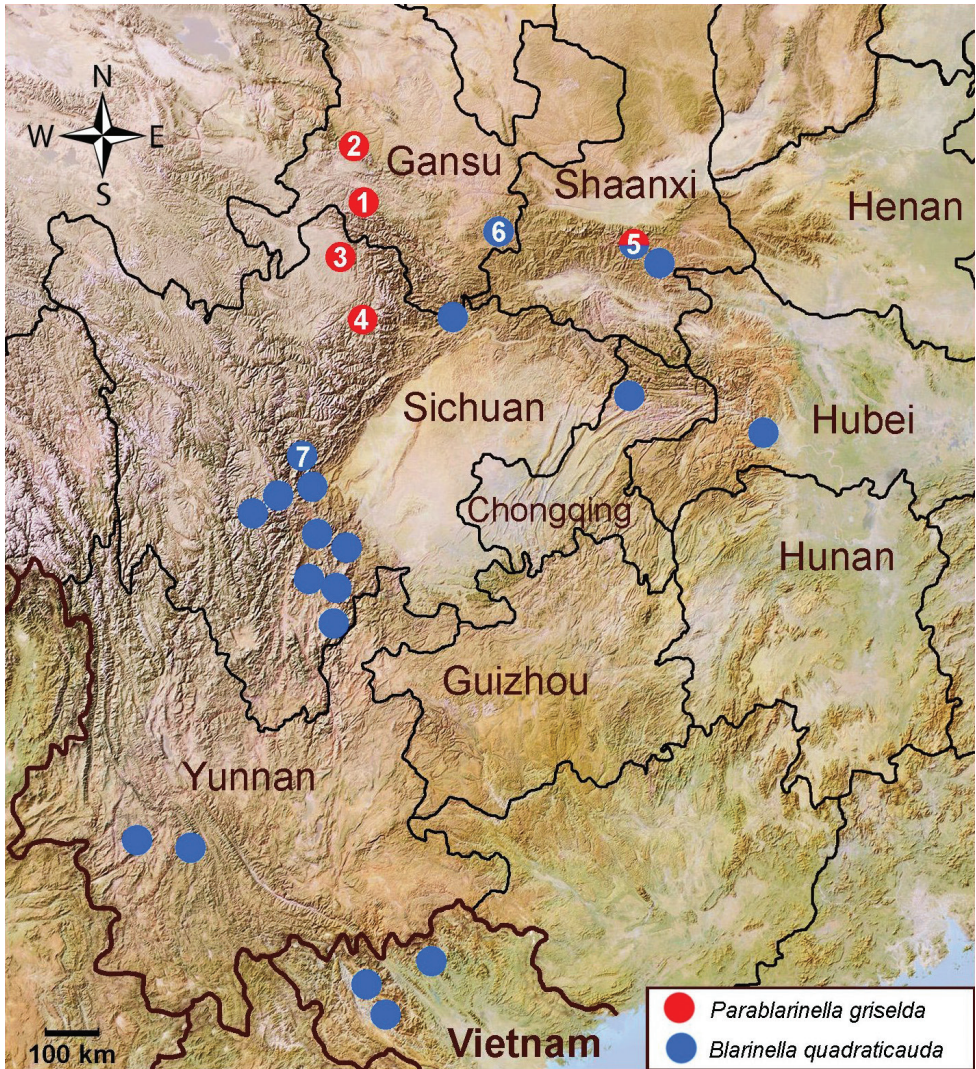


Figure 1. Sample localities of specimens used for molecular analyses **1** China, Gansu, Lingtan County (NHMUK 12.8.5.23, holotype of *Blarinella griselda* Thomas, 1912) **2** China, Gansu, Taizishan NR (ZMMU S-195179) **3** China, Sichuan, Ruergai (Zoige) (ZMMU G17-87) **4** China, Sichuan, Songpan (ZMMU G18-252) **5** China, Shaanxi, Mt.Qinling (after He et al. 2018) **6** China, Gansu, Huixian (ZMMU G17-12) **7** China, Sichuan, Baoxing (type locality of *Blarinella quadraticauda* (Milne-Edwards, 1872)). Unnumbered localities based on the GenBank data.

mated by IQTREE and employed in the Maximum likelihood analysis were as follows: 1st codon position TIM2e+I+G4, 2nd codon position TIM3+F+I+G4, and 3rd codon position TIM2+F+I+G4.

In the combined analyses of four nuclear genes, the final alignment consisted of 2914 nucleotide positions, including 472 bp of *ApoB*, 840 bp of *BRCA1*, 741 bp of *RAG2*, and 861 bp of *IRBP*. In total, the nuclear dataset contained 34 specimens, in-

cluding 19 outgroups. We also performed a separate analysis of the extended *ApoB* data (44 sequences, 472 bp) because this nuclear gene is represented by the largest number of *Blarinella* sequences in GenBank. The best-fit substitution models employed for each of the five partitions found by IQTREE are given in Suppl. material 1: Table S3.

Position of the holotype of *B. griselda* on the mitochondrial *cytb* tree

As a result of the genetic analysis of the type specimen of *B. griselda*, we obtained sequences of three fragments of *cytb*: 90, 160 and 120 bp. The analysis of these fragments showed that the holotype of *griselda* is very close to our specimen from southern Gansu, two other specimens from northern Sichuan and three specimens from Shaanxi named as *Pantherina* in He et al. (2018) (Fig. 2; Suppl. material 1: Fig. S1). Together all seven specimens form a clade which appears distinctly separate from all the species of *Blarinella* (*p*-distance ~19%).

Overall, three clades of the species of *Blarinella* may be recognized in the *cytb* tree: (I) the first clade consists of *B. wardi* (described from Myanmar and found also

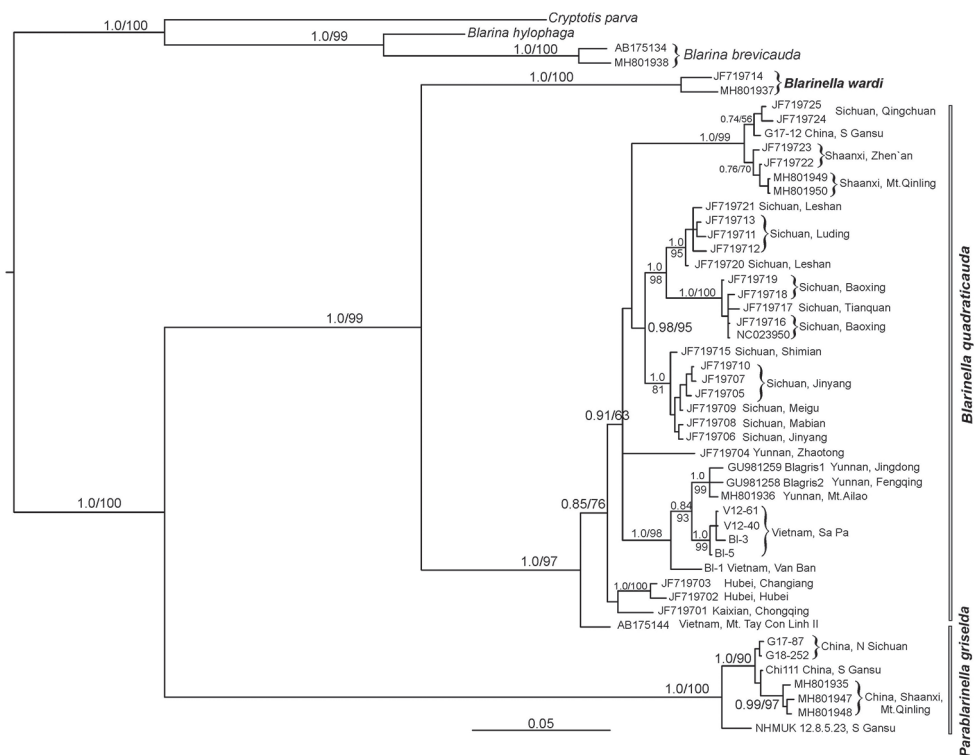


Figure 2. The phylogenetic relationships in *Blarinella* as reconstructed in MrBayes based on *cytb* data. Numbers above or below branches correspond to Bayesian posterior probabilities and ML bootstrap values (>50%) generated using fast bootstrap algorithm in IQTREE. The genera *Blarina* and *Cryptotis* are used as outgroups.

in western Yunnan); (II) the second one corresponds to *B. quadraticauda*: these are specimens previously identified as *B. griselda* from different localities in China and northern Vietnam and *B. quadraticauda* from Sichuan Province, including specimens from Baoxing (the type locality of *B. quadraticauda*); this clade stands as a sister branch to *B. wardi*; (III) the third clade contains the holotype of *griselda*, one specimen from southern Gansu, two specimens from northern Sichuan and three specimens from Shaanxi; it is highly divergent from clades I and II. Based on these data combined with morphological and nuclear results presented below, we consider this third clade rather as a separate genus, hereinafter referred to as *Parablarinella*. A detailed justification of this decision and the description of the new taxon is given in the Discussion.

Phylogenetic analysis of the species based on nuclear genes and molecular time estimation

Phylogenetic analysis of the relationships of the species of *Blarinella* based on nuclear genes (Fig. 3; Suppl. material 1: Fig. S2) supported the separate position of the specimens that were close to the holotype of *B. griselda* on the mitochondrial tree

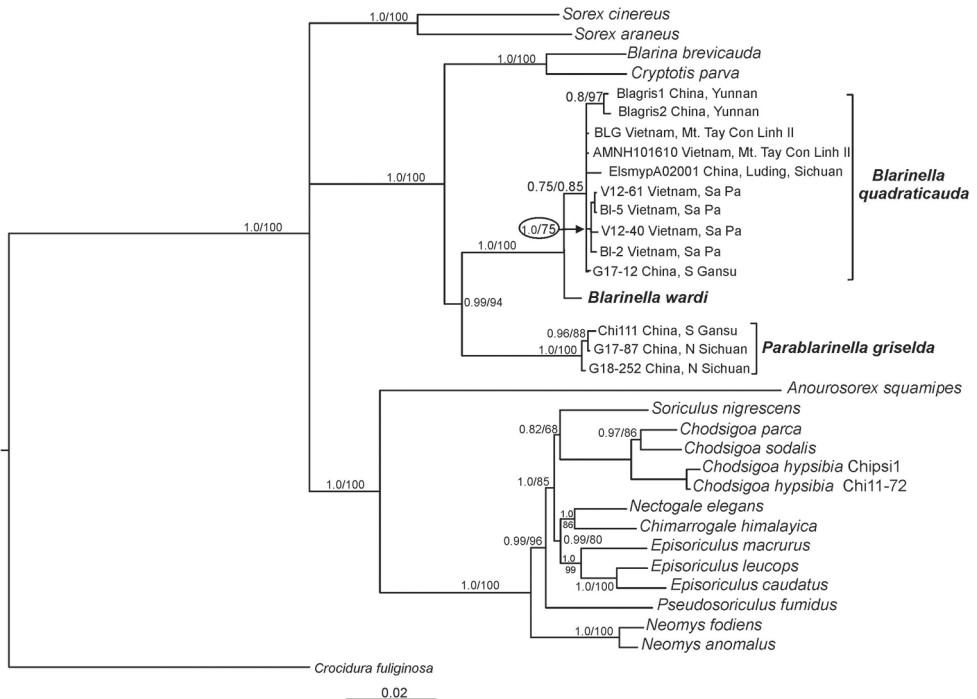


Figure 3. MrBayes tree of Soricinae genera as inferred from the concatenation of four nuclear genes. Numbers above or below branches correspond to Bayesian posterior probabilities and ML bootstrap values (>50%) generated using fast bootstrap algorithm in IQTREE. *Crocidura fuliginosa* is used as outgroup.

(Fig. 2). This clade occupied the sister position to all the remaining species of *Blarinella* (0.99/94). This pattern is consistent with the previous results by Bannikova et al. (2017) and He et al. (2018). The genetic distance between the *B. griselda* clade (*Parablarinella*) and the *B. quadraticauda* clade is higher than that between the genera *Blarina* and *Cryptotis* (*p*-distance ~0.5% and 0.038% accordingly). The specimens of *B. quadraticauda* formed a single clade sister to *B. wardi* (1.0/100).

The relatively close relationship of the *Blarina* / *Cryptotis* clade to the *Blarinella* / *Parablarinella* clade is clearly shown in Figure 3, demonstrating that these taxa form a clade separate from the other sorcid outgroups. Divergence times as inferred from nuclear concatenated data using BEAST (Table 2) are nearly half of those obtained in He et al. (2018) based on mitogenomic data, which is likely explained by a bias due to saturation in the fast evolving mitochondrial DNA. The estimated divergence time between *Parablarinella griselda* and *Blarinella* proper is 9.61 My (95% HPD = 6.87–12.74), that is ~1.5 times higher than the most recent common ancestor (tmrca) of Blarinini. The tmrca of *B. quadraticauda* and *B. wardi* was estimated at 1.68 My (95% HPD = 0.71–3.25).

Morphology

The three species are very similar in external appearance; the tail is approximately half the length of the head and body (48–63% in *B. quadraticauda*, 50–61% in *B. wardi* and 47–51% in *B. griselda*). The eyes are small, the ears small and almost completely concealed in the pelage, the claws on all feet are moderately large, and a gland is indicated on the mid-ventral surface of males.

Despite the marked genetic divergence between “*B. griselda*” (*Parablarinella*) and the other two species, differences in cranial and dental morphology are comparatively limited and not as great as might be expected to distinguish genera, and for some characters there is equal variation between *B. quadraticauda* and *B. wardi* as between either one of these species and *Parablarinella*. In their description of the new genus, He et al. (2018) presented characters to separate *B. griselda* from the other two species. Here, based on historical material and the recently acquired specimens available to us, we elaborate on these characters and provide additional ones. The craniodental characters that in combination serve to distinguish the three taxa, and those that separate the two genera, are shown in Table 3 and Figures 4–6.

Table 2. Approximate node age estimates (My) in Blarinellini based on nuclear data.

Node of species, clades or subclades	Age (My)	95% HPD
Blarinini/Blarinellini	12.39	9.29–15.93
Tmrca Blarinini (<i>Blarina</i> / <i>Cryptotis</i>)	5.99	3.81–8.12
Tmrca Blarinellini (<i>Parablarinella</i> / <i>Blarinella</i>)	9.61	6.87–12.74
Tmrca <i>Blarinella</i> (<i>B. wardi</i> / <i>B. quadraticauda</i>)	1.68	0.71–3.25
Tmrca <i>B. quadraticauda</i>	1.11	0.71–3.25
Tmrca <i>Parablarinella griselda</i>	0.45	0.16–0.89

Table 3. Comparison of dental and cranial morphology of *Blarinella quadraticauda*, *B. wardi* and *Parablarinella griselda*.

Character	<i>Parablarinella griselda</i>	<i>Blarinella quadraticauda</i>	<i>Blarinella wardi</i>
I1 angle of principal to posterior cusp	Moderately shallow > 90°	Moderately acute, approaching or < 90°	Moderately acute
Relative size of unicuspid (Fig. 4)	Un1>Un2>Un3>>Un4>Un5	Un1>Un2>>Un3>>Un4>Un5 or Un1>Un2>>Un3>>Un4>>Un5	Un1>Un2>>Un3>>Un4>Un5 or Un1>Un2>>Un3>>Un4sub=Un5
Size of Un3	Un3 smaller than Un2	Un3 markedly smaller than Un2	Un3 markedly smaller than Un2
	Height c. 0.6 – 0.75, volume c 0.7 – 0.75 of Un2	Height c 0.45 – 0.6, volume c 0.5 – 0.6 of Un2	Height 0.5 – 0.6, volume 0.5 – 0.6 of Un2
Size of Un4	Height c 0.4 – 0.45, volume c 0.33 – 0.6 of Un3	Height c 0.5 – 0.75, volume c 0.5 – 0.75 of Un3.	Height c 0.6, volume c 0.5 – 0.75 of Un3.
P4 shape	Lingual margin of tooth curved. Ratio of anterior to posterior width moderate, tooth noticeably broader posteriorly than anteriorly. Hypocone absent; narrow trough between anterior of cingulum and protocone. Lingual cingulum forms a shallow semi-circle; postero-lingual margin projects beyond antero-lingual border of M1.	Lingual margin of tooth sub-angular. Ratio of anterior to posterior width relatively low, tooth quadrangular in shape. Hypocone low but distinct, broad trough between hypocone and protocone. Lingual cingulum shallowly curved, postero-lingual margin more or less in line with antero-lingual border of M1.	Lingual margin of tooth shallowly curved. Ratio of anterior to posterior width slightly greater than that of <i>B. quadraticauda</i> , tooth sub-quadrangular in shape. Hypocone low but distinct; broad trough between hypocone and protocone; cingulum from hypocone to posterior short and shallowly curved; postero-lingual margin projects slightly beyond antero-lingual border of M1.
Number cuspid on i1 posterior to principal cusp in unworn dentition	Bicuspid.	Tricuspid.	Tricuspid, one specimen bicuspid.
Talonid of m1 and m2 (Fig. 5)	Talonid complete: low distinct mesoconid with oblique crest to hypoconid; low distinct hypoconulid; separate, distinct entoconid with a very low indistinct entoconid crest, scarcely linking to the metaconid.	Talonid with indistinct mesoconid as oblique crest to hypoconid, low hypoconulid, low but distinct entoconid linked by entoconid crest to metaconid. Entoconid in usually more evident on m1 than m2.	Talonid reduced: low mesoconid with low oblique crest to hypoconid, low but distinct hypoconulid but entoconid absent with a low indistinct trace of entoconid crest.
Talonid of m3 (Fig. 5)	Talonid incomplete: small but distinct mesoconid with oblique crest to hypoconid.	Talonid incomplete: elements comprise oblique crest to hypoconid.	Talonid incomplete: trace of mesoconid as oblique crest to low hypoconid.
Position of Foramen Ovale on Inferior Articular Facet (Fig. 4)	Central. Opens onto the inferior articular facet with a shallow depression towards the anterior.	Anterior. Opens anteriorly into the orbital region; antero-lateral roof formed by the pterygoid.	Anterior. Opens anteriorly into the orbital region; antero-lateral roof formed by the pterygoid.
Small foramen on rostrum anterior to infraorbital canal	Above P4, posterior to rostral fossa, within depression leading to infraorbital canal. One specimen with an additional foramen in the antorbital fossa above the junction of Un2 and Un3.	In rostral fossa above junction of P4 and Un4.	In rostral fossa above junction of P4 and Un4.
Extent of reticulation area of the wall of the mesopterygoid fossa	Extends to the base of the mesopterygoid fossa at the level of the hamular processes of the pterygoids and extends posteriorly well beyond hamular processes and close to the level of the vidian foramina.	Area of reticulation smaller than in <i>Parablarinella</i> , not extending to the base of the mesopterygoid fossa, barely posterior to hamular processes and far short of the vidian foramina.	Area of reticulation not extending to the base of the mesopterygoid fossa, nor extending posteriorly far beyond the level of the hamular processes and far short of the vidian foramina
Mandibular Foramen (MF) opens posteriorly leads anteriorly into the mandibular corpus and is ventral to the Ramal Foramen (RF) which opens dorsally into the postero-internal ramal fossa (or temporal fossa) (Fig. 6)	Mandibular foramen well separated from ramal foramen and clearly visible in lingual view. Ramal foramen posterodorsally positioned, largely concealed within the ventral border of the temporal fossa, not or barely visible in lingual view.	Mandibular foramen and ramal foramen occupy a shared fossa. Mandibular foramen not or barely visible in lingual view. Ramal foramen large and clearly visible in lateral view.	Mandibular foramen and ramal foramen in shared fossa but well separated. Ramal foramen small, posterodorsally positioned and visible in lingual view.
Coronoid spicule on buccal face of coronoid process	Prominent, projects posteriorly.	Moderately prominent not projecting far posteriorly.	Stout, not very prominent.



Figure 4. Skulls from left to right of the holotype of *Parablarinella griselda* NHMUK 1912.8.5.23; *Blarinella quadraticauda* NHMUK 1911.2.1.59; the holotype of *Blarinella wardi* NHMUK 1915.2.1.3 (please note that the number written incorrectly as 12.2.1.3 on the skull of this species should read 15.2.1.3). Top row: dorsal view; middle row: ventral view; lower row: left lateral view.

Karyotype structure

The karyotyped specimens were assigned to *B. quadraticauda* and “*B. griselda*” (*Parablarinella*) based on the combination of molecular and morphological traits.

***Blarinella quadraticauda*.** The diploid chromosome number of the studied female (G17-12) was $2n = 49$, and the fundamental autosome number (NF_a) was 62 (Fig. 7A). The autosomal complement was represented by the largest polymorphic metacentric pair (# 1), three pairs of large submetacentrics (# 2–4), one medium-sized (#5) submetacentric pair, three medium-sized (#6–8) metacentric pairs, and 15 pairs of medium-sized to small acrocentrics (#9–23). The X chromosomes were medium-sized submetacentrics.

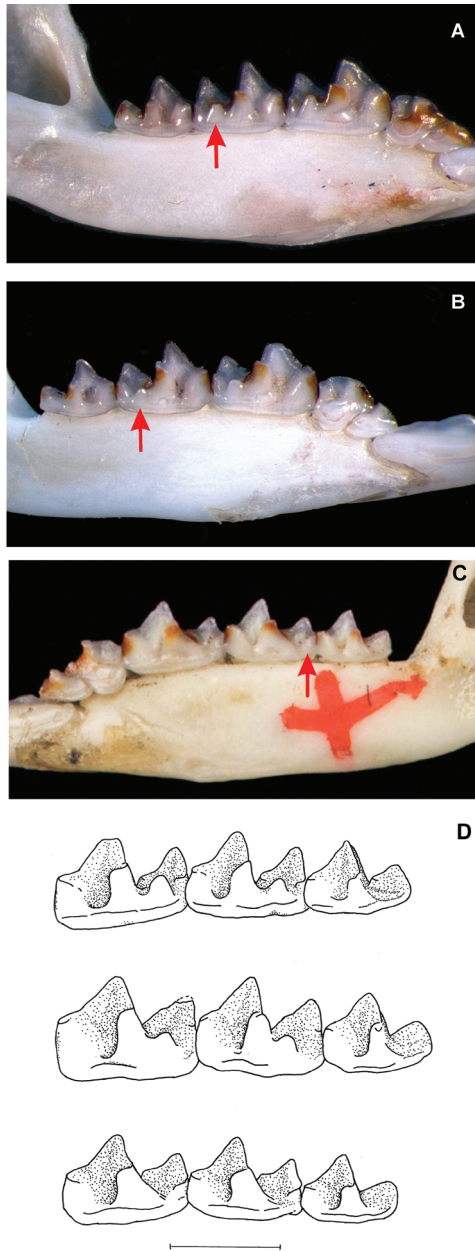


Figure 5. Variation in morphology of the talonid of the lower molars **A** lingual view of left mandibular ramus of *Parablarinella griselda* ZMMU G18-252 **B** lingual view of left mandibular ramus of *Blarinella quadraticauda* ZMMU G17-12 **C** lingual view of right mandibular ramus of holotype of *Blarinella wardi* NHMUK 1915.2.1.3 **D** comparison of right lower molars to show variation in development of the entoconid and entoconid crest on m1 and m2 and the talonid of m3. Above holotype of *Parablarinella griselda* NHMUK 1912.8.5.23, middle *Blarinella quadraticauda* NHMUK 1911.2.1.57, below holotype of *Blarinella wardi* NHMUK 1915.2.1.3. The arrows indicate the entoconid and entoconid crest on m2. Scale bar: 1 mm.

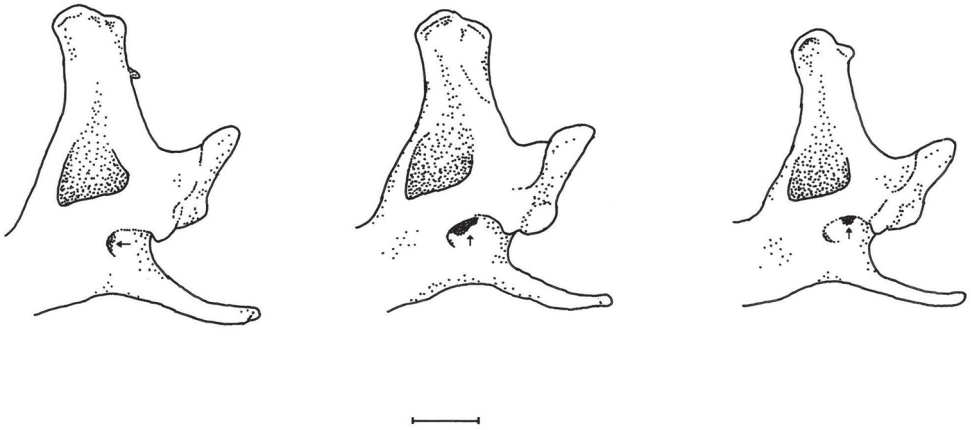


Figure 6. Comparison of lingual view of posterior region of right mandible to show variation in mandibular and ramal foramina. Mandibular foramen: horizontal arrow; ramal foramen: vertical arrow. From left to right: holotype of *Parablarinella griselda* NHMUK 1912.8.5.23; *Blarinella quadraticauda* NHMUK 1911.2.1.59; holotype of *Blarinella wardi* NHMUK 1915.2.3. Scale bar: 1 mm.

C-heterochromatic blocks (Fig. 7B) were revealed in the pericentric regions of all acrocentric autosomes (#9–23) as well as in four pairs of bi-armed autosomes (#4 and 6–8). Several C-blocks found in one submetacentric pair (#3) were localized interstitially and at telomeric region of the short arm. The polymorphic pair (#1) shown C-positive blocks in pericentric regions of both acrocentrics while the homologous metacentric was C-negative. Two pairs of medium-sized submetacentrics (#2 and 5) were C-negative. The X chromosomes had C-positive short arms.

***Parablarinella griselda*.** A short description of chromosome set of this male ($2n = 49$; $NFa = 50$; ZMMU S-195179) was previously reported in Sheftel et al. (2018) under the name *Blarinella cf. griselda*. Here we describe this karyotype in more details and present a karyogram of this specimen for the first time (Fig. 8). The studied male (ZMMU S-195179) had $2n = 49$; $NFa = 50$. The autosomal part of the karyotype consisted of one largest metacentric pair (#1), one large polymorphic submetacentric pair (#2) and 21 pairs of medium-sized to small acrocentrics (#3–23). The X chromosome was the medium-sized submetacentric and the Y was a small acrocentric. Only conventional Giemsa staining was applied for this specimen because of a poor quality of chromosome suspension.

Discussion

Systematics and nomenclature

There is no doubt from the results of the current study that the clade comprising the holotype of *Blarinella griselda* and a few other specimens from southern Gansu, north-

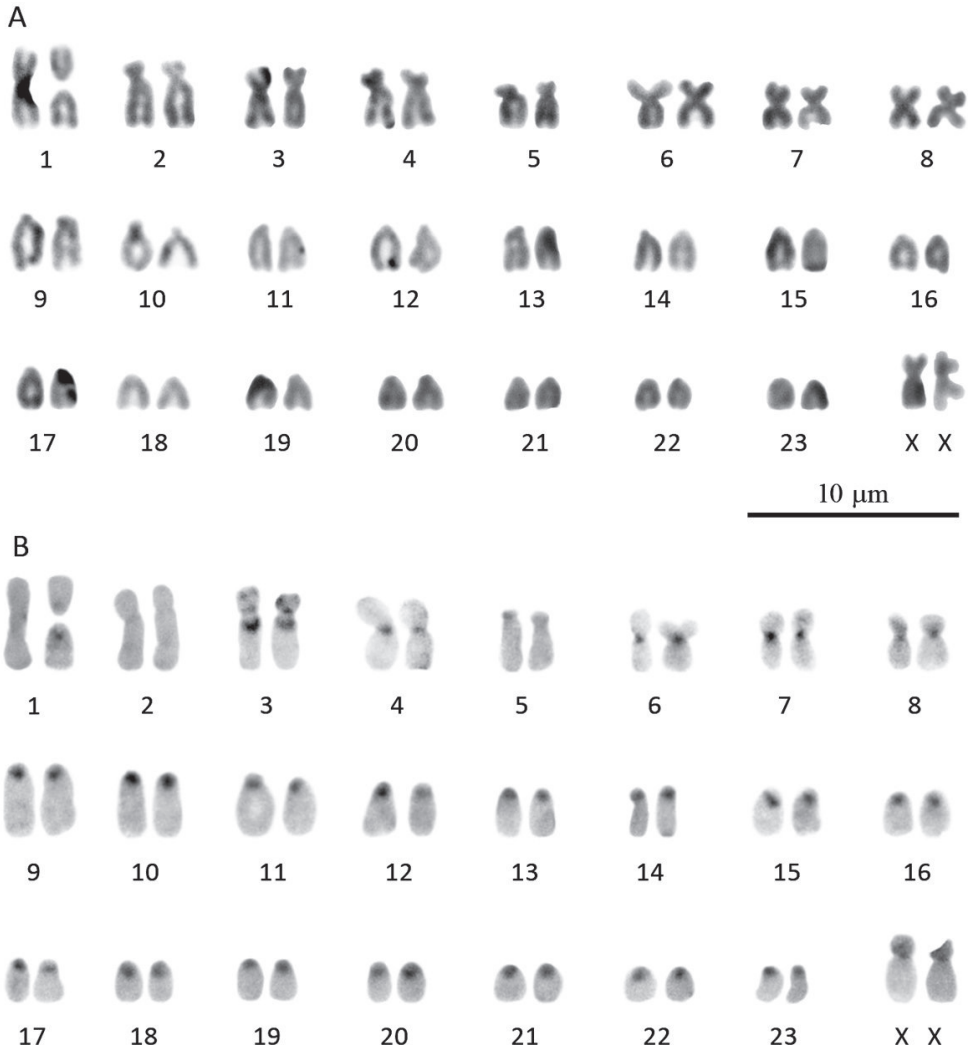


Figure 7. The female karyotype of *Blarinella quadraticauda* (G17-12) with $2n = 49$, $NFa = 62$: routine Giemsa staining **A** and CBG-banding **B**.

ern Sichuan and Shaanxi is the true *griselda* clade, which is highly divergent from the *B. quadraticauda* + *B. wardi* clade. We believe that *griselda* should be attributed to a separate genus because the age of divergence corresponds to that among recognized genera in the Soricinae (Dubey et al. 2007; He et al. 2010; our data). Recently, He et al. (2018) suggested the same taxonomic decision. However, without including comparisons with the holotype or topotypical material they had insufficient evidence for their attribution of the new name to *B. griselda* Thomas, 1912, and unfortunately the name *Pantherina* that they chose is already preoccupied by the same name for a sub-genus of African beetles (*Agrilus* (*Pantherina*) Curletti, 1998). Thus, we provide a new

replacement name for this genus: *Parablarinella* nom. nov. While some of the specific morphological traits of the new genus are highlighted in the description by He et al. (2018), a more detailed account is warranted and an enhanced diagnosis of the new genus is provided.

Family Soricidae Fischer, 1817

Subfamily Soricinae Fischer, 1817

Tribe Blarinini Stirton, 1930

Parablarinella nom. nov.

Pantherina He in He et al. 2018, not *Pantherina* Curletti, 1998 (Coleoptera).

Type species. *Blarinella griselda* Thomas, 1912.

Distribution. Endemic to China. Known from a few specimens from southern Gansu, north-western Sichuan and southern Shaanxi.

Etymology. The name of the new genus is derived from the Greek word παρά “para” (near) and the generic name *Blarinella* previously attributed to this taxon. Gender is feminine.

Amplified diagnosis. A medium-sized shrew, externally similar in appearance to *Blarinella*. Genetically and karyotypically distinct from that genus and distinguished by a combination of the following craniodental characters. Angle of principal to posterior cusp of I1 moderately shallow, greater than 90°; Un3 smaller than Un2 but not markedly so; lingual margin of P4 curved, hypocone absent; talonid of m1 and m2 with a low distinct mesoconid and a separate, distinct entoconid with a very low indistinct entoconid crest scarcely linking to the metaconid; talonid of m3 with a small but distinct mesoconid. The foramen ovale is centrally positioned on the inferior articular facet; small foramen present on rostrum above P4, posterior to the rostral fossa, within depression leading to the infraorbital canal; reticulation of the wall of the mesopterygoid fossa extends to the base of the fossa and posteriorly beyond the hamular processes and close to the level of the vidian foramina; mandibular foramen well separated from ramal foramen and clearly visible in lingual view; ramal foramen posterodorsally positioned, largely concealed within the ventral border of the temporal fossa, not or barely visible in lingual view.

Comparison of karyotypes

Up to date, only three different karyotypes of Asiatic short-tailed shrews have been known – *Blarinella wardi* with $2n = 32$, $NFa = 58$ (Moribe et al. 2007), *Blarinella* cf. *quadraticauda* (authors named this specimen *B. griselda*) with $2n = 44$, $NFa = 56$ (Ye et al. 2006), and *Parablarinella griselda* (specimen ZMMU S-195179) karyo-

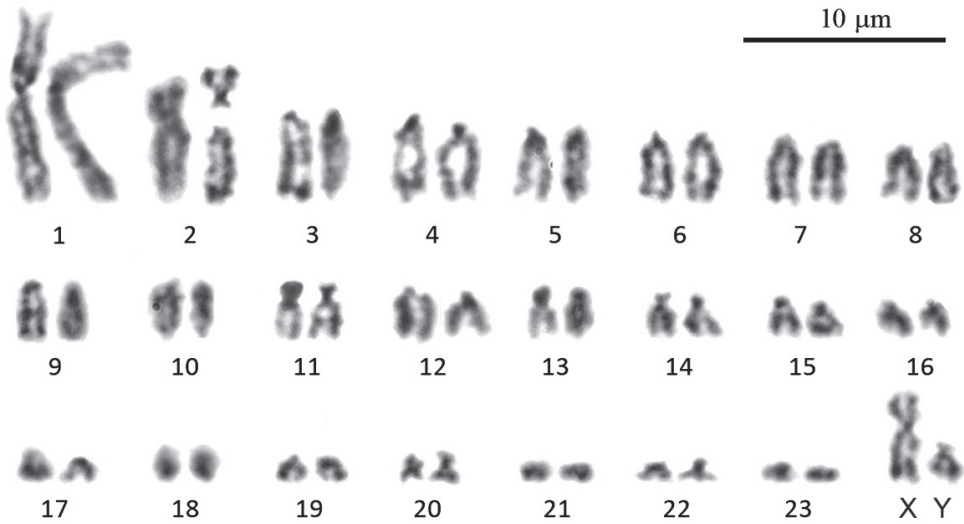


Figure 8. The male karyotype of *Parablarinella griselda* (ZMMU S-195179) with $2n = 49$; $NFa = 50$.

type ($2n = 49$; $NFa = 50$) described by Sheftel et al. (2018) under the name *Blarinella* cf. *griselda* without a karyogram. In this study we present for the first time the fourth karyotypic variant found among Asiatic short-tailed shrews species and belonging to *Blarinella quadraticauda*, as well as the karyogram of the specimen ZMMU S-195179 of *P. griselda*. Both studied specimens have an odd number of chromosomes because of a polymorphism of one of the autosomes, the first largest metacentric pair in the case of *B. quadraticauda* and the second bi-armed submetacentric pair in *P. griselda*. In spite of the same number of chromosomes ($2n = 49$), the karyotype structure of these two individuals differs substantially from each other. The *B. quadraticauda* karyotype contains eight pairs of bi-armed and 15 pairs of single-armed (acrocentric) chromosomes while *P. griselda* has only two pairs of bi-armed chromosomes and 21 pairs of acrocentrics. However, there is little difference in karyotype structure between *B. quadraticauda* from Gansu studied here and the specimen from Yunnan described in Ye et al. (2006). The latter has the same number of bi-armed (eight pairs) and 13 pairs of acrocentric chromosomes. Unfortunately, we were not able to apply GTG-banding for the studied specimen to determine the type of chromosomal rearrangements.

The karyotype of *B. wardi* has the lowest number of chromosomes ($2n = 32$) among all the Asiatic short-tailed shrews examined. The autosomal complement consists only of bi-armed chromosomes excluding the one single-armed pair of the smallest acrocentrics. Up to now there is no data about any differential staining for this species which could allow one to reveal structural rearrangements contributing to the karyotype divergence in this group. We conclude that the three species of Asiatic short-tailed shrews (*P. griselda*, *B. quadraticauda*, and *B. wardi*) demonstrate quite different karyotypic structure and chromosome morphology.

Distribution of Asiatic short-tailed shrews

The available genetic data suggest that most of the specimens of Asiatic short-tailed shrews from China and Vietnam previously recorded as *B. griselda* (Jiang et al. 2003; Lunde et al. 2003; Abramov et al. 2007; Hoffmann and Lunde 2008; Chen et al. 2012) and *B. cf. quadraticauda* (He et al. 2018) belong to the widespread and polymorphic species *B. quadraticauda*. This species may be sympatric with *B. wardi* in western Yunnan and northern Myanmar (Chen et al. 2012; Bannikova et al. 2017).

Our research not only proved the conspecificity of the holotype of *B. griselda* with specimens from southern Gansu and Sichuan, but also demonstrated that true *griselda* is more widespread than was suggested by He et al. (2018). Only two specimens of Asiatic short-tailed shrews were known from Gansu Province before this study. These include the holotype of *B. griselda* (NHMUK 1912.8.5.23, skull, skin) and specimen AMNH M-60449 (skin only, skull lost). The former was collected from “42 miles S.E. of Tao-chou, Tsin-ling Mountains, Kansu, 10000 feet” [68 km S.E. of Lintan, Qinling Mountains, Gansu, 3048 m] (in Lintan County, Gannan Prefecture) (Fig. 1, loc. 1), the latter has no exact locality, just “Kansu”.

Bannikova et al. (2017) listed the specimen of *Parablarinella* (ZMMU Chi-111) from the Taizishan National Reserve in southern Gansu, which on current knowledge appears to be the northernmost point of the range of *Parablarinella*. He et al. (2018) listed three specimens of the new genus from an unspecified locality in Qinling Mountains, southern Shaanxi (Fig. 1, loc. 5) where it is sympatrically distributed with “*B. cf. quadraticauda*”. The Qinling Mountains are an extensive mountain range, extending from Gansu in the west, the site of the type locality of *P. griselda*, to Shaanxi in the east, the location of the specimens recorded by He et al. (2018). The authors also noted that this species was not found in Chongqing, Hubei, or northwestern Sichuan. Recently however, this species was collected in two localities in northwestern Sichuan (G17-87, Zoigê and G18-252, Songpan; Fig. 1). As in Shaanxi, *P. griselda* may also occur here with *B. quadraticauda*; however, no data support this to date. It is possible that the two species prefer different elevational zones. All our specimens of *P. griselda* were collected in conifer and mixed forests at an altitude of 2800–3400 m, where they were trapped in the riparian growth along streams, while *B. cf. quadraticauda* (at one of its northernmost points in south-eastern Gansu, Huixian County, specimen G17-12) was found in the broadleaf (subtropical) forest at an altitude of ~1500 m. In Vietnam, this species is reported to occur in bamboo forests between 1500 and 1700 m elevation. However, typical *B. quadraticauda* from western Sichuan is also known to inhabit mountain conifer forests and the alpine zone (Hoffmann and Lunde 2008), thus, suggesting potential ecological plasticity of this species.

Phylogenetic position of *Parablarinella*

The molecular data clearly indicate that *Parablarinella* and *Blarinella* are phylogenetically close to *Blarina* and *Cryptotis* (Ohdachi et al. 2006; Dubey et al. 2007; He et al.

2018; this study). Although Thomas (1911) emphasized the similarity between *Blarina* and *Blarinella*, this view was discounted by Allen (1938) who considered that *Blarinella* was more closely related to *Sorex*. In his meticulous study of fossil Soricidae, Repenning (1967) divided the Soricinae into three tribes: the Soricini, to which *Blarinella* was assigned; the Blarinini, to which *Blarina* and *Cryptotis* were assigned; and the Neomyiinae. The mandibular condyle with a broad interarticular area occurs in both the Soricini and Blarinini (as opposed to the narrow interarticular area in the Neomyiini) but the Soricini (as in the Neomyiini) were defined by the presence of an entoconid crest on the first two lower molars (m1 and m2), whereas the entoconid crest is absent in the Blarinini. In his classification of fossil and Recent shrews Reumer (1998), erected a separate tribe Blarinellini, for *Blarinella* and eight North American and Eurasian fossil genera, which was diagnosed by a combination of characters to separate this tribe from the other six tribes that he recognised. When the characters for the tribes Blarinellini and Blarinini are compared as in Table 4 it may be seen that the only substantive character to distinguish recent genera belonging to the two tribes is that in Blarinellini the entoconid on m1 and m2 is close to the metaconid and an entoconid crest is present, whereas in Blarinini the entoconid is separate from the metaconid and the entoconid crest is absent. However, based on molecular data, Dubey et al. (2007) suggested that *Blarinella* should be allocated to Blarinini. We concur with this view taking into account the level of genetic divergence between *Blarinella* and *Blarina* recovered in our study. It remains to be established which morphological characters should be regarded as synapomorphies for Blarinini in the wider sense. It is noteworthy that *Parablarinella* is characterized by a prominent entoconid with an indistinct entoconid crest, which is a condition considered to be synapomorphy of Blarinini by Reumer (1998), while in *B. wardi* both the entoconid and entoconid crest are reduced. Consequently, *Blarinella* and *Parablarinella* should be considered as members of the tribe Blarinini Stirton, 1930

Table 4. Compilation of characters used by Reumer (1998) for definition of the tribes Blarinellini and Blarinini. Distinctive characters are indicated by bold typeface.

Blarinellini (<i>Blarinella</i>, <i>Parablarinella</i>)	Blarinini (<i>Blarina</i>, <i>Cryptotis</i>)
Horizontal ramus of mandible short and high, making the lower dentition compressed anteroposteriorly and giving the loph and lophids a compressed W-shaped appearance ^a	Lower molars W-shaped*
Mandible with a broad interarticular area ^a	Mandible with a broad interarticular area ^a
Mandibular condyle with its articular facets separated*	Mandibular condyle with its articular facets separated ^a
Coronoid spicule well developed ^a	Coronoid spicule present*
Internal temporal fossa of moderate size*	Internal temporal fossa of moderate size ^a
Lower molars with the entoconid close to the metaconid so that the entoconid crest is short and high (N.B. specific variation)	Lower molars with the entoconid separate from the metaconid and* lacking the entoconid crest
M3 with a reduced talonid ^a	M3 with a reduced talonid*
Teeth heavily pigmented ^a	Pigmented ^a
Upper incisor protruding but not fissident ^a	Upper incisor not fissident ^a
Upper molariform teeth with a reduced posterior emargination, showing a tendency to develop a continuous endoloph ^a	Slight emargination*
Occlusal surface of M1 nearly square ^a	Variable sub-square or oblong*

^a Characters specified by Reumer (1998)

* Character state not mentioned in Reumer (1998) but observed in specimens of *Blarinella*, *Parablarinella*, *Blarina* and *Cryptotis* in this study

instead of Blarinellini Reumer, 1998. In this respect, the molecular results are consistent with the fossil data, which reveal parallelisms in reduction of the entoconid crest in several fossil genera attributed to Blarinini and Blarinellini (Doby 2015). However, a detailed analysis of relationships among Neogene lineages deserves a separate study.

Acknowledgements

We thank Dr Ross MacPhee (AMNH, New York, USA) and Dr Chen Zhongzheng (Kunming Institute of Zoology of CAS, China) for the collection of information. This work was funded by the Russian Foundation for Basic Research, projects 17-04-00065a (genetic studies, phylogenetic analysis and the processing of the paper) and 17-54-53085-GFEN-a (collection of material).

References

- Abramov AV, Rozhnov VV, Shchinov AV, Makarova OV (2007) New records of the Asiatic short-tailed shrew *Blarinella griselda* (Soricidae) from Vietnam. *Mammalia* 71(4): 181–182. <https://doi.org/10.1515/MAMM.2007.035>
- Abramov AV, Bannikova AA, Chernetskaya DM, Lebedev VS, Rozhnov VV (2017a) The first record of *Episoriculus umbrinus* from Vietnam, with notes on the taxonomic composition of *Episoriculus* (Mammalia, Soricidae). *Russian Journal of Theriology* 16: 117–128. <https://doi.org/10.15298/rusjtheriol.16.2.01>
- Abramov AV, Bannikova AA, Lebedev VS, Rozhnov VV (2017b) Revision of *Chimarrocale* (Lipotyphla: Soricidae) from Vietnam with comments on taxonomy and biogeography of Asiatic water shrews. *Zootaxa* 4232: 216–230. <https://doi.org/10.11646/zootaxa.4232.2.5>
- Allen GM (1938) The mammals of China and Mongolia. Part 1. American Museum of Natural History, New York, 620 pp. <https://doi.org/10.5962/bhl.title.12195>
- Bannikova AA, Dokuchaev EN, Yudina EV, Bobretzov AV, Sheftel BI, Lebedev VS (2010) Holarctic phylogeography of the tundra shrew (*Sorex tundrensis*) based on mitochondrial genes. *Biological Journal of the Linnean Society* 101: 721–746. <https://doi.org/10.1111/j.1095-8312.2010.01510.x>
- Bannikova AA, Lebedev VS (2010) Genetic heterogeneity of the Caucasian shrew *Sorex satunini* (Mammalia, Lipotyphla, Soricidae) inferred from the mtDNA markers as a potential consequence of ancient hybridization. *Molecular Biology* 44: 658–662. <https://doi.org/10.1134/S0026893310040230>
- Bannikova AA, Zemlemerova ED, Lebedev VS, Aleksandrov DYU, Fang Y, Sheftel BI (2015) Phylogenetic position of the Gansu mole *Scapanulus oweni* Thomas, 1912 and the relationships between strictly fossorial tribes of the family Talpidae. *Doklady Biological Sciences* 464: 230–234. <https://doi.org/10.7868/S0869565215260266>
- Bannikova AA, Abramov AV, Lebedev VS, Sheftel BI (2017) Unexpectedly high genetic diversity of the Asiatic short-tailed shrews *Blarinella* (Mammalia, Lipotyphla, Soricidae). *Doklady Biological Sciences* 474: 93–97. <https://doi.org/10.1134/S0012496617030012>

- Bannikova AA, Chernetskaya D, Raspopova A, Alexandrov D, Fang Y, Dokuchaev N, Sheftel B, Lebedev V (2018) Evolutionary history of the genus *Sorex* (Soricidae, Eulipotyphla) as inferred from multigene data. *Zoologica Scripta* 47: 518–538. <https://doi.org/10.1111/zsc.12302>
- Bulatova NSh, Searle JB, Nadjafova RS, Pavlova SV, Bystrakova NV (2009) Field protocols for the genomic era. *Comparative Cytogenetics* 3: 57–62. <https://doi.org/10.3897/compcytogen.v3i1.9>
- Butler PM, Greenwood M (1979) Soricidae (Mammalia) from the early Pleistocene of Olduvai Gorge, Tanzania. *Zoological Journal of the Linnaean Society* 67: 329–379. <https://doi.org/10.1111/j.1096-3642.1979.tb01119.x>
- Chen S, Liu S, Liu Y, He K, Chen W, Zhang X, Fan Z, Tu F, Jia X, Yue B (2012) Molecular phylogeny of Asiatic short-tailed shrews, genus *Blarinella* Thomas, 1911 (Mammalia: Soricomorpha: Soricidae) and its taxonomic implications. *Zootaxa* 3250: 43–53. <https://doi.org/10.11646/zootaxa.3250.1.3>
- Corbet GB (1978) *The Mammals of the Palaearctic Region: a Taxonomic Review*. Cornell University Press, London, 314 pp.
- Corbet GB, Hill JE (1992) *The Mammals of the Indomalayan Region: a Systematic Review*. Natural History Museum Publications, Oxford University Press, Oxford, 488 pp.
- Curletti G (1998) Notes on metatarsal morphology in the genus *Agrilus* and a proposed redefinition of its subgenera in the Afrotropical region (Coleoptera Buprestidae). *Bollettino Società Entomologica Italiana* 130: 125–134. https://www.researchgate.net/profile/Gianfranco_Curletti/publication/233758814
- Dannelid E (1998) Dental adaptations in shrews. In: Wójcik JM, Wolsan M (Eds) *Evolution of Shrews*. Mammal Research Institute Polish Academy of Sciences, Białowieża, 157–174.
- Doby J (2015) A systematic review of the soricimorph Eulipotyphla (Soricidae: Mammalia) from the Gray Fossil Site (Hemphillian), Tennessee. *Electronic Theses and Dissertations*. Paper 2526. East Tennessee State University. <https://dc.etsu.edu/etd/2526>
- Dubey S, Salamin N, Ohdachi SD, Barriere P, Vogel P (2007) Molecular phylogenetics of shrews (Mammalia: Soricidae) reveal timing of transcontinental colonizations. *Molecular Phylogenetics and Evolution* 44: 126–137. <https://doi.org/10.1016/j.ympev.2006.12.002>
- Ellerman JR, Morrison-Scott TCS (1951) *Checklist of Palaearctic and Indian Mammals, 1758 to 1946*. Trustees of the British Museum (Natural History), London, 810 pp.
- Ford CE, Hamerton JL (1956) A colchicine, hypotonic citrate, squash sequence for mammalian chromosomes. *Stain Technology* 31: 247–251. <https://doi.org/10.3109/10520295609113814>
- Hall TA (1999) BioEdit: a user-friendly biological sequence alignment editor and analysis program for Windows 95/98/NT. *Proceedings of the Conference held in Nucleic acids symposium series* 41: 95–98. <http://jwbrown.mbio.ncsu.edu/JWB/papers/1999Hall1.pdf>
- He K, Li Y-J, Brandley MC, Lin L-K, Wang Y-X, Zhang Y-P, Jiang X-L (2010) A multi-locus phylogeny of Nectogalini shrews and influences of the paleoclimate on speciation and evolution. *Molecular Phylogenetics and Evolution* 56: 734–746. <https://doi.org/10.1016/j.ympev.2010.03.039>
- He K, Chen X, Chen P, He S-W, Chen F, Jiang X-L, Campbell KL (2018) A new genus of Asiatic short-tailed shrew (Soricidae, Eulipotyphla) based on molecular and morphological comparisons. *Zoological Research* 39(5): 309–323. <https://doi.org/10.24272/j.issn.2095-8137.2018.058>

- Hoffmann RS (1987) A review of the systematics and distribution of Chinese red-toothed shrews (Mammalia: Soricinae). *Acta Theriologica Sinica* 7: 100–139. http://en.cnki.com.cn/Article_en/CJFDTotal-SLXX198702004.htm
- Hoffmann RS, Lunde D (2008) Order Erinaceomorpha, Order Soricomorpha. In: Smith AT, Xie Y (Eds) *A Guide to the Mammals of China*. Princeton University Press, Princeton, 292–327.
- Hofreiter M, Jaenicke V, Serre D, von Haeseler A, Pääbo S (2001) DNA sequences from multiple amplifications reveal artifacts induced by cytosine deamination in ancient DNA. *Nucleic Acids Research* 29: 4793–4799. <https://doi.org/10.1093/nar/29.23.4793>
- Hutterer R (1993) Order Insectivora. In: Wilson DE, Reeder DM (Eds) *Mammal Species of the World: a Taxonomic and Geographical Reference* (2nd edn). Smithsonian Institution Press, Washington/London, 69–130.
- Hutterer R (2005) Order Erinaceomorpha, Order Soricomorpha. In: Wilson DE, Reeder DM (Eds) *Mammal Species of the World. A Taxonomic and Geographic Reference* (3rd edn). John Hopkins Press, Baltimore, 212–311.
- International Commission on Zoological Nomenclature (1999) *International code of zoological nomenclature* (4th edn). London: The International Trust for Zoological Nomenclature.
- Jiang X-L, Wang Y-X, Hoffmann RS (2003) A review of the systematics and distribution of Asiatic short-tailed shrews, genus *Blarinella* (Mammalia: Soricidae). *Mammalian Biology* 68: 193–204. <https://doi.org/10.1078/1616-5047-00085>
- Kalyaanamoorthy S, Minh BQ, Wong TKF, von Haeseler A, Jermini LS (2017) ModelFinder: Fast Model Selection for Accurate Phylogenetic Estimates. *Nature Methods* 14: 587–589. <https://doi.org/10.1038/nmeth.4285>
- Krysanov EYu, Demidova TB, Sheftel BI (2009) A simple technique for making of small mammalian chromosome preparations. *Zoologicheskii Zhurnal* 88: 234–238. [in Russian]
- Lunde DP, Musser GG, Nguyen TS (2003) A survey of small mammals from Mt. Tay Con Linh II, Vietnam, with the description of a new species of *Chodsigoa* (Insectivora: Soricidae). *Mammal Study* 28: 31–46. <https://doi.org/10.3106/mammalstudy.28.31>
- McDowell SB (1958) The greater Antillean insectivores. *Bulletin of the American Museum of Natural History* 115: 113–214. <http://hdl.handle.net/2246/1199>
- Meester J (1963) A systematic revision of the shrew genus *Crocidura* in southern Africa. *Transvaal Museum Memoir* 13: 1–127.
- Mills JRE (1966) The functional occlusion of the teeth of Insectivora. *Journal of the Linnaean Society Zoology* 46: 1–25. <https://doi.org/10.1111/j.1096-3642.1966.tb00081.x>
- Milne Edwards A (1872) *Memoire sur la faune mammalogique du Tibet oriental et principalement de la Principaute de Moupin*. In: Milne-Edwards H (Ed.) *Recherches Pour Servir a L'histoire Naturelle des Mammifères*. Libraire de l'Academie de Medecine, Paris, 231–304.
- Minh BQ, Nguyen MAT, von Haeseler A (2013) Ultrafast approximation for phylogenetic bootstrap. *Molecular Biology and Evolution* 30: 1188–1195. <https://doi.org/10.1093/molbev/mst024>
- Moribe J, Li S, Wang YX, Kobayashi S, Oda SI (2007) Karyological notes on the southern short-tailed shrew, *Blarinella wardi* (Mammalia, Soricidae). *Cytologia* 72: 323–327. <https://doi.org/10.1508/cytologia.72.323>

- Nguyen L-T, Schmidt HA, von Haeseler A, Minh BQ (2015) IQTREE: A fast and effective stochastic algorithm for estimating maximum likelihood phylogenies. *Molecular Biology and Evolution* 32: 268–274. <https://doi.org/10.1093/molbev/msu300>
- Ohdachi SD, Hasegawa M, Iwasa MA, Vogel P, Oshida T, Lin LK, Abe H (2006) Molecular phylogenetics of soricid shrews (Mammalia) based on mitochondrial cytochrome *b* gene sequences: with special reference to the Soricinae. *Journal of Zoology* 270: 177–191. <https://doi.org/10.1111/j.1469-7998.2006.00125.x>
- Repenning CA (1967) Subfamilies and Genera of the Soricidae. Classification, Historical Zoogeography, and Temporal Correlation of the Shrews. Geological Survey Professional Paper 565. United States Government Printing Office, Washington, 74 pp. <https://doi.org/10.3133/pp565>
- Reumer JWF (1984) Ruscinian and early Pleistocene Soricidae (Insectivora, Mammalia) from Tegelen (The Netherlands) and Hungary. *Scripta Geologica* 73: 1–173. <https://www.repositorio.naturalis.nl/document/148756>
- Reumer JWF (1998) Classification of the fossil and recent shrews. In: Wojcik JM, Wolsan M (Eds) *Evolution of Shrews*. Mammal Research Institute, Polish Academy of Science, Bialowieza, 5–21.
- Ronquist F, Teslenko M, van der Mark P, Ayres DL, Darling A, Höhna S, Larget B, Liu L, Suchard MA, Huelsenbeck JP (2012) MrBayes 3.2: efficient Bayesian phylogenetic inference and model choice across a large model space. *Systematic Biology* 61: 539–542. <https://doi.org/10.1093/sysbio/sys029>
- Rambaut A, Drummond A (2003) Tracer. A program for Analysing Results from Bayesian MCMC Programs Such as BEAST and MrBayes. University of Edinburgh, UK. Version 1.6. <http://beast.bio.ed.ac.uk/>
- Sambrook J, Fritsch EF, Maniatis T (1989) *Molecular Cloning: a Laboratory Manual*. Cold Spring Harbor Laboratory Press, New York. 1546 pp.
- Sheftel BI, Bannikova AA, Fang Y, Demidova TB, Alexandrov DYU, Lebedev VS, Sun Y-H (2018) Notes on the fauna, systematics, and ecology of small mammals in Southern Gansu, China. *Biology Bulletin* 45: 110–124. <https://doi.org/10.1134/S1062359018080150>
- Sefc KM, RB Payne, MD (2007) Sorenson Single base errors in PCR products from avian museum specimens and their effect on estimates of historical genetic diversity. *Conservation Genetics* 8: 879–884. <https://doi.org/10.1007/s10592-006-9240-8>
- Sumner AT (1972) A simple technique for demonstrating centromeric heterochromatin. *Experimental Cell Research* 75: 304–306. [https://doi.org/10.1016/0014-4827\(72\)90558-7](https://doi.org/10.1016/0014-4827(72)90558-7)
- Swofford DL (2003) PAUP*: phylogenetic analysis using parsimony, version 4.0 b10. <http://www.citeulike.org/group/894/article/2345226>
- Thomas O (1911) The Duke of Bedford's zoological exploration of eastern Asia. XIII. On mammals from the provinces of Kan-su and Szechwan, western China. *Proceedings of the Zoological Society of London* 82(1): 158–180. <https://doi.org/10.1111/j.1469-7998.1912.tb07008.x>
- Thomas O (1912) On a collection of small mammals from the Tsin-ling Mountains, Central China, presented by Mr. G. Fenwick Owen to the National Museum. *Annals and Magazine of Natural History, Ser. 8*, 10(58): 395–403. <https://doi.org/10.1080/00222931208693252>

- Thomas O (1915) A new shrew of the genus *Blarinella* from Upper Burma. Annals and Magazine of Natural History, Ser. 8, 15(87): 335–336. <https://doi.org/10.1080/00222931508693646>
- Ye J, Biltueva L, Huang L, Nie W, Wang J, Jing M, Su W, Vorobieva N, Jiang X, Graphodatsky A, Yang F (2006) Cross-species chromosome painting unveils cytogenetic signatures for the Eulipotyphla and evidence for the polyphyly of Insectivora. Chromosome Research 14: 151–159. <https://doi.org/10.1007/s10577-006-1032-y>

Supplementary material 1

Figures S1, S2; Tables S1–S3

Authors: Anna A. Bannikova, Paulina D. Jenkins, Evgeniya N. Solovyeva, Svetlana V. Pavlova, Tatiana B. Demidova, Sergey A. Simanovsky, Boris I. Sheftel, Vladimir S. Lebedev, Yun Fang, Love Dalen, Alexei V. Abramov

Explanation note: **Figure S1.** The phylogenetic relationships in *Blarinella* as reconstructed in MrBayes based on the extended alignment of *cytb*. **Figure S2.** The phylogenetic relationships in *Blarinella* as reconstructed in MrBayes based on the alignment of *ApoB*. **Table S1.** GenBank accession numbers of sequences retrieved from GenBank and newly collected sequences used in the study (marked in bold). **Table S2.** Primers for *cytb* amplification and sequencing. **Table S3.** The best-fit substitution models employed for each of the five partitions found by IQTREE.

Copyright notice: This dataset is made available under the Open Database License (<http://opendatacommons.org/licenses/odbl/1.0/>). The Open Database License (ODbL) is a license agreement intended to allow users to freely share, modify, and use this Dataset while maintaining this same freedom for others, provided that the original source and author(s) are credited.

Link: <https://doi.org/10.3897/zookeys.88.37982.suppl1>